Immune Responses of Carp

A molecular and cellular approach to infections

Maria Forlenza

Thesis committee

Thesis supervisors
Prof. Dr. Ir. Huub F.J. Savelkoul
Professor of Cell Biology and Immunology
Wageningen University

Dr. Ir. Geert F. Wiegertjes
Associate Professor, Cell Biology and Immunology Group
Wageningen University

Other members:
Prof. Dr. Giuseppe Scapigliati (University of Tuscia, Italy)
Prof. Dr. Chris J. Secombes (University of Aberdeen, Scotland)
Prof. Dr. Ir. Stefan Magez (Vrije Universiteit Brussel, Belgium)
Prof. Dr. Ir. Jaap Keijer (Wageningen University, The Netherlands)

Immune Responses of Carp

A molecular and cellular approach to infections

Maria Forlenza

To my father.
He would have been proud

Contents

CHAPTER

1

General Introduction:
Parasitic infections revisited

Geert F. Wiegertjes, Maria Forlenza,
Maaike Joerink and Jörn Scharsack

ELSEVIER

Review

Parasite infections revisited

Geert F. Wiegertjes*, Maria Forlenza, Maaike Joerink, Jörn P. Scharsack

Cell Biology and Immunology Group, Department of Animal Sciences, Wageningen Institute of Animal Sciences, Wageningen University, P.O. Box 338, Wageningen AH 6700, The Netherlands

Abstract

Studying parasites helps reveal basic mechanisms in immunology. For long this has been recognized for studies on the immune system of mice and man. But it is not true for immunological studies on fish. To support this argument we discuss selected examples of parasite infections not only in warm-blooded but also in cold-blooded vertebrates. We point out that parasite infections deserve more attention as model systems in comparative immunology.
© 2005 Elsevier Ltd. All rights reserved.

Keywords: Parasites; Immunology; Fishes

Contents

1. Introduction

Parasite infections of cold-blooded vertebrates certainly deserve their place in comparative immunological studies, not just to solve problems in, e.g. aquaculture but to exploit these infections as models for a better understanding of immunological concepts. After all, despite all molecular analyses and studies on cellular responses to well-described antigens and mitogens, whole animal infection experiments remain essential for a true understanding of the immune system of all vertebrates. Here, we

* Corresponding author. Tel.: +31 317 482732; fax: +31 317 483955.
E-mail address: geert.wiegertjes@wur.nl (G.F. Wiegertjes).

highlight only some of the exciting new developments in the comparative immuno-parasitological research area.

Comparative immunology is advancing rapidly but progress is definitely hampered by the fact that frequently, different laboratories study different animal (often fish) species. In fact, when realizing that fish species belonging to the Salmonidae, Cyprinidae, Ictaluridae or Gadidae should be considered evolutionarily distant, it is surprising that the research area is progressing as rapidly as it is today. This can for a large part be ascribed to selected genome initiatives in puffer fish (*Fugu rubripes*) and zebra fish (*Danio rerio*) that brought a wealth of information on immuno-regulatory genes. Database mining and the design of degenerate primers based on conserved regions in immuno-regulatory genes has allowed for a rapid expansion of gene information for fish.

Parasite biology can be enormously complex, eukaryote parasite life cycles often involve multiple hosts. Vertebrates can act as the definitive host, i.e. the host in which the parasite reproduces sexually, such as with schistosome parasites. Here, invertebrate snails act as intermediate hosts, i.e. the host in which larval or asexual stages of the parasite develop. But in other cases vertebrates can act as intermediate hosts. This is true for the malaria parasite which completes its sexual stages in mosquitoes. And last but not necessarily least, they may be just one host in the cycle of an organism which does not show sexual reproduction as such Trypanosomes and *Leishmania*, e.g. need to undergo sequential developmental changes in the bodies of at least two different species. This complexity of host–parasite interactions may be one explanation for the relatively limited number of research groups that study the immune responses to fish parasites. This certainly does not mean, however, that such studies are not worth undertaking.

Although the present review focuses on parasite infections of vertebrate hosts it is good to realize the emerging interest of comparative immunologists in studying insect parasites. The malaria (e.g. *Plasmodium falciparum*) parasite interacts with two different hosts: the intermediate vertebrate and the final mosquito (e.g. *Anopheles gambiae*) host. Mosquitoes have for long been considered mere intermediates in the route to infection of humans, but are now recognized as highly informative model organisms.

This is mainly because many novel molecular technological developments (such as genome sequencing projects and production of micro-arrays) are now being applied not only to the parasite but also to the mosquito [1–4]. This allows for a better understanding of the molecular mechanisms mediating the physiological responses of insects to parasite invasion [5]. Thus, at present, the mosquito as a model organism for directly studying antiparasitic innate immune responses in insects, complements studies of defense reactions against bacteria and fungi in the fruit fly, *Drosophila melanogaster* [6].

We do not aim at an extensive overview of the immune defense reactions to all parasite infections in vertebrates. For recent overviews of the immune responses to well-known parasites of warm- and cold-blooded vertebrates and of invertebrates, the reader is referred to some excellent reviews [7–10,3]. Instead we discuss selected examples of parasite infections with a special interest to immunologists with an evolutionary focus. We argue that these studies are bringing us a wealth of information on the functioning of the immune system in vertebrates and that therefore, parasite infections deserve immediate attention as model systems in comparative immunology.

2. Parasite infection models have defined the current paradigm

At present, laboratories interested in comparative immunology strongly focus on molecular immunological research, sometimes extending to cellular immunology. But, with the progression of the genomics era into a proteomics era, it is the concept of studying whole animals in vivo that deserves renewed interest. This is true for endothermic vertebrates, where a large research effort goes into studies on the laboratory mouse, but no less true for ectothermic vertebrates. High quality infection models, of which some clearly have paved the way for much of modern immunology, require well-designed animal experiments. This has been achieved through the use of genetically well-defined animals such as inbred and knock-out mice. But it is important to realize that investigations on mice usually are models for investigations on humans. Often these animal models do not describe natural host–pathogen

combinations, where the pathogen's host specificity has arisen from progressive selection over thousands of years. Typically, the natural situation is characterized by chronic infection with low pathogen loads to ensure survival of both host and parasite. Experimental models, however, frequently have death as an outcome. Most comparative parasite infection models do not suffer from this disadvantage because these infections are studied in the target animal species. Also, sometimes the mouse model systems have been used simply because they had been in use for many years already, defining the current paradigm. Or just because they are easy to work with [11]. Of course, the mere fact that certain mouse model systems define a paradigm demonstrates the enormous scientific impact the use of inbred mouse lines have had as model systems.

It is often not well appreciated how much of our present understanding of the immune system has come from studying host–parasite interactions. For example, the murine model of infection with *Leishmania major* (Protozoa, Kinetoplastida) provided the first in vivo correlation between protective immunity and an expansion of CD4+ T helper 1 (Th1) lymphocytes and between progressive disease and the development of a Th2 response [9]. Although Th cell differentiation in human infection with *Leishmania* is not always as clear as in mice infected with *L. major*, the description of the molecular mechanisms necessary for polarization of Th responses in mice did bring a wealth of information on the vertebrate immune response to pathogens.

Variation between individuals often disturbs the outcome of our experiments. Scientists working with warm-blooded vertebrates have found the answer to genetic variation in focusing on inbred strains of mice. Comparative immunologists, however, have even been suffering from the lack of focus on a single common species. They have chosen to study invertebrates, or fish. Frequently these (commercial) fish species have relatively long generation intervals. This severely reduce the possibilities to produce inbred strains via mating of close relatives, for which approximately 20 generations are needed. The exception to the rule, of course, is zebra fish (*D. rerio*). Zebra fish do have the advantage of a short generation time allowing for the development of genetically uniform strains by classical inbreeding, while also

haploid and diploid androgenetic or gynogenetic fish are available [12]. As a result, zebra fish have gained broad utility over the last 10–20 years. Considered a representative vertebrate developmental model, large-scale mutagenesis screens have created thousands of mutant zebra fish lines for developmental studies [13]. In addition, antisense morpholinos have proven specific and highly effective translational inhibitors to study targeted gene-knock down in zebra fish [14]. As a consequence, to date, zebra fish are becoming increasingly attractive for immunological studies, also because of the recognition that zebra fish share many orthologous genes or regions with the human genome [15].

Although the small size of zebra fish limits their use for cellular assays, considerable progress is made also towards a functional analysis of immune-relevant genes. For example, recently in zebra fish 19 putative TOLL-like receptor (TLR) variants were described, of which two are homologous to TLR4, showing that the lack of TLR4 as reported for the puffer fish [16] is not general for fish [17]. In addition, expression analysis showed that a subset, including TLR1 and TLR2 are expressed at higher levels following infection of zebra fish with *Mycobacterium marinum* [18]. Clearly, with renewed interest in innate immunity and associated pattern recognition receptors (PRRs) such as the TLRs, fish increasingly prove to be a highly interesting animal species for comparative immunological studies. Unfortunately, although zebra fish are natural hosts to a number of parasites, including nematodes, microsporidians and dinoflagellates [15], none of these infections are presently exploited as parasite infection models for fish.

3. Infections with schistosomes

A parasite infection model that has enormously increased our understanding of the immune system is infection of mice with *Schistosoma mansoni* (Platyhelminthes, Digenea). Schistosomes (e.g. *S. mansoni*) infect their mammalian hosts as aquatic cercariae released from snails (often *Biomphalaria glabrata*). Relatively little genetic information is available on the snail as the intermediate host or its immune defense against schistosome although snails certainly

are interesting from a comparative immunological point of view [19].

Following their production in the sporocyst stages, in the snail intermediate host, cercariae actively penetrate the skin of vertebrates. Eggs laid by female worms finally become entrapped in, e.g. the liver where they are not easily cleared by phagocytic cells. As a reaction granulomas are formed around the schistosome eggs. Often macrophages fuse to form giant cells recruiting T cells from a systemically activated T cell pool to the granuloma. Interleukin (IL)-4 operates as the key cytokine driving the Th2 response to schistosome eggs, including an alternative activation of macrophages [20]. In the absence of IL-4 or IL-10 an overproduction of pro-inflammatory mediators including interferon (IFN)-γ, tumor necrosis factor (TNF)-α and nitric oxide (NO) cause excessive liver damage. Also, schistosome granulomas produce IL-12 and transforming growth factor (TGF)-β both of which have an important role in controlling IFN-γ synthesis [21]. Typically, granulomas containing schistosome eggs represent a localized Th2 response, whereas granulomas containing, e.g. Mycobacteria represent a clear Th1 response. As such, granulomas represent unique models for immunological research [20].

The present interest in innate immunity and its recognition receptors lead to an increased research focus on pathogen associated molecular patterns (PAMPS) in parasites, able to stimulate these receptors [22]. Studies on *S. mansoni* have shown the importance of the surface syncytial layer in the survival of this parasite in the mammalian host [23]. Several of these surface layer components are candidates for protective capacity, including the large subunit of calpain, Sm-p80. DNA immunization protocols using Sm-p80 alone or with plasmids encoding granulocyte-macrophage colony-stimulating factor (GM-CSF) and IL-4 [24] or a combination of IL-2 and IL-12 [25] suggest that Sm-p80 is an excellent vaccine candidate. Interestingly, these studies [24,25] suggest that the balance between Th1/Th2 responses to this antigen can be influenced by the different cytokines included in the vaccine. This clearly shows the potential of DNA vaccines to not only induce protection against parasite infections but also to be included in studies on type I and type II immune responses. With the current success of DNA

vaccines in protecting fish against viruses [26] in mind, this opens up new research areas for studying the fish immune response to DNA vaccination against parasites.

Fish can be infected with blood flukes of the family Sanguinicolidae, a model which is much under-appreciated for comparative immunological studies since the fish host immune reaction shows clear analogies to the mouse's reactions to schistosome infections. Snails (*Lymnaea peregra*) host *Sanguinicola inermis*, a blood fluke pathogenic to common carp, and release cercariae that penetrate the fish skin [27]. The eggs become entrapped in a number of organs including the gills and mesonephros, leading to local granuloma formation. Eggs are encapsulated by different types of phagocytic cells [28]. The fish host immune reaction to this parasite has not been studied in great detail. Most studies describe cellular changes following in vivo infection [28–31], some show in vitro polarisation of lymphocytes in response to this parasite [32]. The most recent studies focused on the humoral C-reactive protein response to *S. inermis* [33]. This parasite model in fish certainly deserves further immunological characterization. Especially now that several of the chemical messengers involved in the Th2 response in warm-blooded vertebrates, such as IL-10 and TGF-β have been described for fish, this model holds great potential for studying a putative type II response in cold-blooded vertebrates.

4. Infections with trypanosomes

Studies on infections with kinetoplastid parasites have brought much understanding of host–parasite interactions. Antigenic variation (e.g. *Trypanosoma brucei*) as well as intracellular hiding (e.g. *Trypanosoma cruzi*) have become schoolbook examples of parasite adaptations to the host. At present, emerging insecticide resistance in vectors and drug resistance in parasites have led to a renewed research interest in these infections models. As a consequence, to date many of the state-of-the-art molecular techniques are being applied to both parasite (e.g. *T. brucei*) [34] and vector (e.g. tsetse fly) [35], bringing a wealth of genetic information.

The Kinetoplastida, Protozoa with a kinetoplastid organelle containing the mitochondrial DNA, are

sub-divided into two suborders. The Trypanosomatina contain the important mammalian trypanosome parasites with a single flagellum, whereas the parasites in the second suborder (Bodonina) have two flagella. Often, the Trypanosomatina are sub-divided into salivarian parasites (transmitted via saliva) such as *T. brucei* and stercorarian (transmitted via faeces) parasites such as *T. cruzi*. The two groups diverged some 200–300 million years ago [36]. In fish representatives of both suborders are studied. *Trypanosoma danilewskyi* (syn. *Trypanosoma carassii*) (infects cyprinids) belongs to the 'aquatic clade' within the Trypanosomatina [36] while *Trypanoplasma borreli* (cyprinids) and *Cryptobia salmositica* (salmonids) both belong to the Bodonina.

Most of our present understanding of immune reactions to trypanosomiasis has been obtained from infections of mice which are not a natural host to the tsetse-transmitted trypanosomes. This clearly is not the case for the kinetoplastid parasites that infect fish since they all represent natural parasite–host interactions. In the aqueous environment, blood-sucking leeches act as vectors between fishes for transmitting kinetoplastid parasites. A disadvantage of the fish host–parasite model is that little is known about the leech vector. For some fish kinetoplastid parasites, leeches just act as a vector while for others they are obligatory intermediate hosts [37]. Like the Salivaria, fish kinetoplasts are believed to be exclusively extra cellular, and are found in the blood and tissue fluids of their fish hosts [38,39]. The African trypanosomes show antigenic variation of the variant surface glycoprotein (VSG), their counterparts in fish do not show evidence of antigenic variation [38]. Although different in this respect, analogies of the fish' immune response to kinetoplasts with the mouse immune response to the extracellular blood stage of trypanosomes can be found. For example, peritoneal macrophages from *T. brucei* infected mice produce trypanostatic NO radicals in the presence of L-arginine in vitro [40], although in vivo parasites proliferate in the vicinity of macrophages. In these mice, the role of parasite-specific antibodies may be crucial by mediating the attachment of trypanosomes to activated macrophages, thereby facilitating NO-mediated trypanolysis [41]. In carp, similarly, *T. borreli* induces the production of trypanostatic concentrations of NO in vitro [42] but non-effective or

even immuno-suppressive concentrations in vivo [43]. The effect of parasite-specific antibodies mediating attachment of these parasites to activated carp macrophages, facilitating NO-mediated effects on *T. borreli*, could be similar to those seen in mice, and are presently under investigation in our laboratory. The glycosylphosphatidylinositol (GPI) anchors found in protozoa are PAMPs that are recognized as foreign [44], with divergent GPIs having evolved to the advantage of the parasites to manipulate the endogenous signaling pathways of the host [45].

The non-Salivarian trypanosomes are characterized by surfaces dominated by carbohydrate-rich coats of GPI-anchored mucin-like glycoproteins, which are not subject to antigen variation. The fish trypanosomes (*T. danilewskyi*) and probably also the Bodonina (*T. borreli*) have a surface coat highly comparable to that of the non-Salivaria [46]. It has been confirmed for *T. danilewskyi* that the carbohydrate moiety of the mucins contains sialic acid, a monosaccharide that in other trypanosomes is transferred from host glycoconjugates to parasite surface molecules by trans-sialidase (TS). TS has recently been detected in the fish trypanosome *T. danilewskyi* [47]. Sialylated mucins are considered to be essential for the survival of the parasite in the host. These PAMPs in *T. danilewskyi* seem to provide a protective layer against initial attack by the alternative complement pathway while specific antibodies against these PAMPs may be needed for antibody-mediated lysis [48]. For *T. borreli* infections in carp, a heat-labile fraction that could be GPI-anchored proteins is one of the PAMPs responsible for the induction of NO in vitro [49].

A particular trypanosome PAMP has been shown responsible for the activation of murine macrophages: the cysteine protease cruzipain from *T. cruzi*. This protease is found in every developmental form of the parasite as a glycoprotein of about 52–58 KDa with a highly mannose glycosylated C-terminal domain. For *C. salmositica*, a close relative of *T. borreli*, a cysteine protease with chemical properties similar to that of cruzipain has been described [50]. Interestingly, cruzipain when injected into mice, induces an increase of urea associated with a decrease in nitrate levels, suggesting a preferential up-regulation of the arginase pathway associated with alternatively activated macrophages [51]. It could therefore, be of great

interest to study fish macrophage activation by the cysteine protease of *C. salmositica*.

Macrophages play an essential role in trypanolytic events. These versatile cells are able to respond to a variety of micro-environmental signals including PAMPs and many cytokines. Typical intracellular parasites such as *Leishmania* spp. and *T. cruzi* have brought much understanding of what is presently re-named the 'classical' activation of macrophages. This particular activation integrates the cytokines tumor necrosis factor alpha (TNF-α) and gamma interferon (IFN-γ), among others, in the type I response. More recently, it has been recognized that particular cytokines from Th2 cells can induce an 'alternative' activation of macrophages that induces distinct functional activities as part of the type II response [52–55]. It is evident that an effective immune response against a particular parasite requires a balanced differentiation between classically activated macrophages (type I response) and alternatively activated macrophages (type II response). In fact, mouse resistance to *T. brucei* is dependent on their ability to produce IFN-γ, TNF-α but also NO (type I response) early during infection and the production of IL-4 and IL-10 (type II response) during the chronic phase. Imbalance induces tissue damage (over stimulation of classically activated macrophages) or a failure to control early pathogen replication [56]. In a similar manner, in fish, the high production of NO during *T. borreli* infection of carp [57] and related immuno-suppression could explain part of the pathology associated with these infections [58]. The potential role of TNF-α, which has also been described for fish, in inducing tissue damage after *T. borreli* infection is still unclear and remains to be investigated. What is clear, however, is that the concept of classically versus alternatively activated macrophages deserves more attention as a concept of type I versus type II responses in fish. Conveniently, both inducible nitric oxide synthase and arginase activities can be measured in fish macrophages [42,59].

5. Parasite-driven immunogenetic diversity

The Major Histocompatibility Complex (MHC) genes, at least in humans, are the most polymorphic genes known to date, and the MHC consists of a single region of 4 Mb comprising the MHC class I and class II but also other immunologically relevant genes [60]. A number of genes within the MHC code for the peptide binding region (PBR), which is the most polymorphic portion of the MHC class I and class II molecules. In this area, non-synonymous mutations occur at a higher rate than can be expected by random events, suggesting there must be a selective pressure affecting these genes. Since the PBR interacts with pathogen-derived molecules, pathogens must have driven MHC selection, most likely through mechanisms such as heterozygote advantage and balancing selection [61].

In humans, many studies have tried to establish possible associations between infectious disease and MHC polymorphisms, but firm conclusions have been obscured by the MHC redundancy (multiple co-dominantly expressed genes) and a confounding pattern of linkage (class I and class II genes in a complex). In fact, the most compelling evidence has come from chickens infected with a viral pathogen, Mareks disease virus [62]. Chickens possess a relatively simple MHC with single dominantly expressed class I and class II loci [63], which may be the reason for the clear association between the presence of particular MHC haplotypes and resistance to Mareks disease. The organization of the MHC in teleosts is different from that in mammals or chicken. Interestingly, fishes do not follow the paradigm of one complex of genes on a single chromosome but have taken an evolutionary route where the MHC class I and class II genes are located on different linkage groups [64,65]. This aspect, unique to teleost fishes, allows for studies on associations of MH class I and class II polymorphisms and disease resistance without the confounding pattern of linkage found in warm-blooded vertebrates [66].

Studies in Atlantic salmon (*Salmo salar*) indeed have shown an association between MH polymorphism and resistance to the bacterium *Aeromonas salmonicida* [67]. Using denaturing gradient gel electrophoresis to identify alleles, at least one MH class II β allele was significantly more prevalent in resistant families. The relative importance of this particular allele in conferring resistance of Atlantic salmon to *A. salmonicida* has been confirmed by Grimholt et al. [68] using sequence-based typing to identify alleles. In addition, using the same strategy, these authors identified two class I α and two class II α

alleles associated with increased resistance of Atlantic salmon to infectious salmon anaemia virus. There are not many studies in fish that have focused on associations between MH polymorphisms and resistance to parasite infections, however.

One of the reasons that associations between MH polymorphisms in fish and resistance to parasites have not often been studied may be the recognized complexity of parasite biology. Another reason may be that few parasite infections in teleosts have had enough economic impact to drive research towards investigating an immunogenetic approach. Although this is not true for the salmon louse (e.g. *Lepeophtheirus salmonis*), which has detrimental effects (including economic ones) on farmed Atlantic salmon, to our knowledge, no data in this species have been published so far. One of the few published studies is on simultaneous infections from multiple parasite species in three-spined sticklebacks (*Gasterosteus aculeatus*). These fish are particularly suited to test for optimal rather than maximal MH diversity because their class II genotypes can differ markedly in the number of class II B alleles. These studies have demonstrated a consistent relationship between parasite diversity among different habitats and MH diversity and fitness [69,70] and are a good example of how parasite models in fish can help to resolve fundamental scientific questions.

6. Future perspective

Now that, at least for fish, the molecular characterization of several messengers potentially involved in type I (IFN, IL-1, TNF) or type II (IL-10, TGF) immune responses is rapidly bridging the gap with mammalian immunology, the rationale for a subsequent functional analysis is stronger than ever. Alternative macrophage activation routes seem to offer new opportunities for analyzing type II immune responses in fish. The need for well-defined parasite infection models in fish becomes even more evident taking into account that parasites (e.g. *L. major*, *S. mansoni*) especially, have contributed so much to the understanding of the Th1/Th2 concept in warm-blooded vertebrates.

There are at least two infection models in fish that hold a great promise in that they seem to induce

immune responses in fish with clear similarities to the immune responses of mammals. *S. inermis* is a parasite of carp that induces granuloma formation comparable to what is seen in the mammalian response to schistosomes. Also, the fish' immune response to trypanosomes shows clear similarities to the mammalian immune response to extra cellular stages of mammalian trypanosomes. Therefore, these parasite models provide unique opportunities for comparative immunologists.

There are several parasite infection models, such as infection of fish with *Ichthyophthirius multifiliis*, that have not been discussed here. This particular parasite model has proven highly informative for studies on GPI-anchored membrane proteins [71] and certainly holds a future potential as model system for studying mucosal immunity. We did not aim at an extensive overview of all immune defense reactions to parasites in teleosts. Instead we have pointed out that these studies are bringing us a wealth of information on the functioning of the immune system in both warm- and cold-blooded vertebrates and that therefore, parasite infections deserve immediate attention as model systems in comparative immunology.

Acknowledgements

References

[1] Ghosh A, Srinivasan P, Abraham EG, Fujioka H, Jacobs-Lorena M. Molecular strategies to study Plasmodium-mosquito interactions. Trends Parasitol 2003;19(2):94–101.

[2] Craig A, Kyes S, Ranson H, Hemingway J. Malaria parasite and vector genomes: partners in crime. Trends Parasitol 2003; 19(8):356–62.

[3] Blandin S, Levashina EA. Mosquito immune responses against malaria parasites. Curr Opin Immunol 2004;16(1): 16–20.

[4] Dimopoulos G, Christophides GK, Meister S, Schultz J, White KP, Barillas-Mury C, et al. Genome expression analysis

of *Anopheles gambiae*: responses to injury, bacterial challenge, and malaria infection. Proc Natl Acad Sci USA 2002; 99(13):8814–9.

[5] Land KM. The mosquito genome: perspectives and possibilities. Trends Parasitol 2003;19(3):103–5.

[6] Dimopoulos G, Müller H-M, Levashina EA, Kafatos FC. Innate immune defense against malaria infection in the mosquito. Cun Opin Immunol 2001;13(1):79–88.

[7] Carton, Y, Nappi, AJ, Poirie, M. Genetics of anti-parasite resistance in invertebrates. Dev Comp Immunol 2005;29:9–32.

[8] Maizels RM, Yazdanbakhsh M. Immune regulation by helminth parasites: cellular and molecular mechanisms. Nat Rev Immunol 2003;3(9):733–44.

[9] Gumy A, Louis JA, Launois P. The murine model of infection with *Leishmania major* and its importance for the deciphering of mechanisms underlying differences in Th cell differentiation in mice from different genetic backgrounds. Int J Parasitol 2004;34(4):433–44.

[10] Jones SRM. The occurrence and mechanisms of innate immunity against parasites in fish. Dev Comp Immunol 2001;25(8–9):841–52.

[11] Druilhe P, Hagan P, Rook GAW. The importance of models of infection in the study of disease resistance. Trends Microbiol 2002;10(10 Suppl.):S38–S46.

[12] Brandhorst BP, Corley-Smith GE. Production of haploid and diploid androgenetic zebrafish. Methods Mol Biol 2004;254: 255–70.

[13] Yeh J-RJ, Crews CM. Chemical genetics: adding to the developmental biology toolbox. Dev Cell 2003;5(1):11–19.

[14] Nasevicius A, Ekker SC. Effective targeted gene 'knockdown' in zebrafish. Nat Genet 2000;26(2):216–20.

[15] Yoder JA, Nielsen ME, Amemiya CT, Litman GW. Zebrafish as an immunological model system. Microbes Infect 2002; 4(14):1469–78.

[16] Oshiumi H, Tsujita T, Shida K, Matsumoto M, Ikeo K, Seya T. Prediction of the prototype of the human Toll-like receptor gene family from the pufferfish, *Fugu rubripes*, genome. Immunogenetics 2003;54(11):791–800.

[17] Jault C, Pichon L, Chluba J. Toll-like receptor gene family and TIR-domain adapters in *Danio rerio*. Mol Immunol 2004; 40(11):759–71.

[18] Meijer AH, Gabby Krens SF, Medina Rodriguez IA, He S, Bitter W, Snaar-Jagalska BE, Spaink HP. Expression analysis of the Toll-like receptor and TIR domain adaptor families of zebrafish. Mol Immunol 2004;40(11):773–83.

[19] Raghavan N, Miller AN, Gardner M, FitzGerald PC, Kerlavage AR, Johnston DA, Lewis FA, Knight M. Comparative gene analysis of *Biomphalaria glabrata* hemocytes pre- and post-exposure to miracidia of *Schistosoma mansoni*. Mol Biochem Parasitol 2003;126(2):181–91.

[20] Sandor M, Weinstock JV, Wynn TA. Granulomas in schistosome and mycobacterial infections: a model of local immune responses. Trends Immunol 2003;24(1):44–52.

[21] Rakasz E, Blum AM, Metwali A, Elliott DE, Li J, Ballas ZK, Qadir K, Lynch R, Weinstock JV. Localization and regulation of IFN-gamma production within the granulomas of murine schistosomiasis in IL-4-deficient and control mice. J Immunol 1998;160(10):4994–9.

[22] Medzhitov R, Janeway Jr CA. Innate immunity: impact on the adaptive immune response. Curr Opin Immunol 1997;9(1):4–9.

[23] Siddiqui AA, Podesta RB, Clarke MW. *Schistosoma mansoni*: characterization and identification of calcium-binding proteins associated with the apical plasma membrane and envelope. Exp Parasitol 1991;72(1):63–8.

[24] Siddiqui AA, Phillips T, Charest H, Podesta RB, Quinlin ML, Pinkston JR, Woyd JD, Paz M, Villalovos RM, Pampa J. Induction of protective immunity against *Schistosoma mansoni* via DNA priming and boosting with the large subunit of calpain (Sm-p80): adjuvant effects of granulocyte-macrophage colony-stimulating factor and interleukin-4. Infect Immun 2003;71(7):3844–51.

[25] Siddiqui AA, Phillips T, Charest H, Podesta RB, Quinlin ML, Pinkston JR, Woyd JD, Pompa J, Villalovos RM, Paz M. Enhancement of Sm-p80 (large subunit of calpain) induced protective immunity against *Schistosoma mansoni* through co-delivery of interleukin-2 and interleukin-12 in a DNA vaccine formulation. Vaccine 2003;21(21–22):2882–9.

[26] Lorenzen N, Lorenzen E, Einer-Jensen K, LaPatra SE. DNA vaccines as a tool for analysing the protective immune response against rhabdoviruses in rainbow trout. Fish Shellfish Immunol 2002;12(5):439–53.

[27] Kirk RS, Lewis JW. Histopathology of *Sanguinicola inermis* infection in carp *Cyprinus carpio*. J Helminthol 1998;72(1): 33–8.

[28] Richards DT, Hoole D, Lewis JW, Ewens E, Arme C. Ultrastructural observations on the cellular response of carp, *Cyprinus carpio* L., to eggs of the blood fluke *Sanguinicola inermis* Plehn, 1905 (Trematoda: Sanguinicolidae). J Fish Dis 1994;17:439–46.

[29] Richards DT, Hoole D, Lewis JW, Ewens E, Arme C. Changes in the cellular composition of the spleen and pronephros of carp *Cyprinus carpio* infected with the blood fluke *Sanguinicola inermis* (Trematoda: Sanguinicolidae). Dis Aquat Organ 1994;19:173–9.

[30] Richards DT, Hoole D, Lewis JW, Ewens E, Arme C. Stimulation of carp *Cyprinus carpio* lymphocytes by the blood fluke *Sanguinicola inermis* (Trematoda: Sanguinicolidae). Dis Aquat Organ 1996;25:87–93.

[31] Richards DT, Hoole D, Lewis JW, Ewens E, Arme C. In vitro polarization of carp leucocytes in response to the blood fluke *Sanguinicola inermis* Plehn, 1905 (Trematoda: Sanguinicolidae). Parasitology 1996;112(Pt 5):509–13.

[32] Richards DT, Hoole D, Lewis JW, Ewens B, Arme C. Adherence of carp leucocytes to adults and cercariae of the blood fluke *Sanguinicola inermis*. J Helminthol 1996;70: 63–7.

[33] Hoole D, Lewis JW, Schuwerack PM, Chakravarthy C, Shrive AK, Greenhough TJ, Cartwright JR. Inflammatory interactions in fish exposed to pollutants and parasites: a role for apoptosis and C reactive protein. Parasitology 2003; 126(Suppl.):S71–S85.

[34] Davilá AMR, Majiwa PAO, Grisard EC, Aksoy S, Melville SE. Comparative genomics to uncover the secrets of tsetse and livestock-infective trypanosomes. Trends Parasitol 2003;19(10):436–9.

[35] Butler D. African labs win major role in tsetse-fly genome project. Nature 2004;427(6973):384.

[36] Stevens JR, Noyes HA, Schofield CJ, Gibson W. The molecular evolution of Trypanosomatidae. Adv Parasitol 2001;48:1–56.

[37] Joerink M, Saeij JPJ, Stafford JL, Belosevic M, Wiegertjes GF. Animal models for the study of innate immunity: protozoan infections in fish. In: Wiegertjes GF, Flik G, editors. Host–parasite interactions. Abingdon, UK: BIOS Sci Publ; 2004. p. 67–89.

[38] Overath P, Haag J, Mameza MG, Lischke A. Freshwater fish trypanosomes: definition of two types, host control by antibodies and lack of antigenic variation. Parasitology 1999;119(Pt 6):591–601.

[39] Woo PTK. Cryptobia (Trypanoplasma) salmositica and salmonid cryptobiosis. J Fish Dis 2003;26(11–12):627–46.

[40] Kaushik RS, Uzonna JE, Gordon JR, Tabel H. Innate resistance to Trypanosoma congolense infections: differential production of nitric oxide by macrophages from susceptible BALB/c and resistant C57Bl/6 mice. Exp Parasitol 1999; 92(2):131–43.

[41] Gobert AP, Daulouede S, Lepoivre M, Boucher JL, Bouteille B, Buguet A, et al. L-Arginine availability modulates local nitric oxide production and parasite killing in experimental trypanosomiasis. Infect Immun 2000;68(8): 4653–7.

[42] Saeij JPJ, Stet RJM, Groeneveld A, Verburg-van Kemenade BM, van Muiswinkel WB, Wiegertjes GF. Molecular and functional characterization of a fish induci-ble-type nitric oxide synthase. Immunogenetics 2000;51(4–5):339–46.

[43] Saeij JPJ, van Muiswinkel WB, Groeneveld A, Wiegertjes GF. Immune modulation by fish kinetoplastid parasites: a role for nitric oxide. Parasitology 2002;124(Pt 1):77–86.

[44] Tachado SD, Gerold P, Schwarz R, Novakovic S, McConville M, Schofield L. Signal transduction in macro-phages by glycosylphosphatidylinositols of Plasmodium, Trypanosoma, and Leishmania: activation of protein tyrosine kinases and protein kinase C by inositolglycan and diacylgly-cerol moieties. Proc Natl Acad Sci USA 1997;94(8):4022–7.

[45] Tachado SD, Mazhari-Tabrizi R, Schofield L. Specificity in signal transduction among glycosylphosphatidylinositols of Plasmodium falciparum, Trypanosoma brucei, Trypanosoma cruzi and Leishmania spp. Parasite Immunol 1999;21(12): 609–17.

[46] Overath P, Haag J, Lischke A, O'HUigin C. The surface structure of trypanosomes in relation to their molecular phylogeny. Int J Parasitol 2001;31(5–6):468–71.

[47] Agüero F, Campo V, Cremona L, Jäger A, Di Noia JM, Overath P, Sánchez DO, Carlos Frasch A. Gene discovery in the freshwater fish parasite Trypanosoma carassii: identifi-cation of trans-sialidase-like and mucin-like genes. Infect Immun 2002;70(12):7140–4.

[48] Lischke A, Klein C, Stierhof Y-D, Hempel M, Mehlert A, Almeida IC, Ferguson MAJ, Overath P. Isolation and characterization of glycosylphosphatidylinositol-anchored, mucin-like surface glycoproteins from bloodstream forms of the freshwater-fish parasite Trypanosoma carassii. Biochem J 2000;345(Pt 3):693–700.

[49] Saeij JPJ, de Vries BJ, Wiegertjes GF. The immune response of carp to Trypanoplasma borreli: kinetics of immune gene expression and polyclonal lymphocyte activation. Dev Comp Immunol 2003;27(10):859–74.

[50] Zuo X, Woo PTK. Characterization of purified metallo- and cysteine proteases from the pathogenic haemoflagellate Cryptobia salmositica Katz 1951. Parasitol Res 1998;84(6): 492–8.

[51] Giordanengo L, Guinazu N, Stempin C, Fretes R, Cerban F, Gea S. Cruzipain, a major Trypanosoma cruzi antigen, conditions the host immune response in favor of parasite. Eur J Immunol 2002;32(4):1003–11.

[52] Mills CD. Macrophage arginine metabolism to ornithine/urea or nitric oxide/citrulline: a life or death issue. Crit Rev Immunol 2001;21(5):399–425.

[53] Gordon S. Alternative activation of macrophages. Nat Rev Immunol 2003;3(1):23–35.

[54] Mantovani A, Sozzani S, Locati M, Allavena P, Sica A. Macrophage polarization: tumor-associated macrophages as a paradigm for polarized M2 mononuclear phagocytes. Trends Immunol 2002;23(11):549–55.

[55] Noel W, Raes G, Hassanzadeh Ghassabeh G, De Baetselier P, Beschin A. Alternatively activated macro-phages during parasite infections. Trends Parasitol 2004; 20(3):126–33.

[56] Baetselier PD, Namangala B, Noel W, Brys L, Pays E, Beschin A. Alternative versus classical macrophage activation during experimental African trypanosomosis. Int J Parasitol 2001;31(5–6):575–87.

[57] Saeij JPJ, Van Muiswinkel WB, Groeneveld A, Wiegertjes GF. Immune modulation by fish kinetoplastid parasites: a role for nitric oxide. Parasitology 2002;124(Pt 1):77–86.

[58] Bunnajirakul S, Steinhagen D, Hetzel U, Körting W, Drommer W. A study of sequential histopathology of Trypanoplasma borreli (Protozoa: Kinetoplastida) in suscep-tible common carp Cyprinus carpio. Dis Aquat Organ 2000; 39(3):221–9.

[59] Wiegertjes GF, Joerink M. Macrophage polarization in the immune response to parasites. Bull Eur Assoc Fish Pathol 2004;24(1):5–10.

[60] Beck S, Trowsdale J. The human major histocompatability complex: lessons from the DNA sequence. Annu Rev Genomics Hum Genet 2000;1:117–37.

[61] Parham P, Ohta T. Population biology of antigen presen-tation by MHC class I molecules. Science 1996;272(5258): 67–74.

[62] Kaufman J, Salomonsen J. The 'minimal essential MHC' revisited: both peptide-binding and cell surface expression level of MHC molecules are polymorphisms selected by pathogens in chickens. Hereditas 1997;127(1–2):67–73.

[63] Kaufman J, Milne S, Gobel TW, Walker BA, Jacob JP, Auffray C, et al. The chicken B locus is a minimal essential major histocompatibility complex. Nature 1999;401(6756):923–5.

[64] Bingulac-Popovic J, Figueroa F, Sato A, Talbot WS, Johnson SL, Gates M, et al. Mapping of mhc class I and class II regions to different linkage groups in the zebrafish, *Danio rerio*. Immunogenetics 1997;46(2):129–34.

[65] Sato A, Figueroa F, Murray BW, Malaga-Trillo E, Zaleska-Rutczynska Z, Sultmann H, Toyosawa S, Wedekind C, Steck N, Klein J. Nonlinkage of major histocompatibility complex class I and class II loci in bony fishes. Immunogenetics 2000;51(2):108–16.

[66] Stet RJM, Kruiswijk CP, Dixon B. Major histocompatibility lineages and immune gene function in teleost fishes: the road not taken. Crit Rev Immunol 2003;23(5–6):441–71.

[67] Langefors A, Lohm J, Grahn M, Andersen O, von Schantz T. Association between major histocompatibility complex class IIB alleles and resistance to *Aeromonas salmonicida* in Atlantic salmon. Proc R Soc Lond B Biol Sci 2001; 268(1466):479–85.

[68] Grimholt U, Drablos F, Jorgensen SM, Hoyheim B, Stet RJM. The major histocompatibility class I locus in Atlantic salmon (*Salmo salar* L.): polymorphism, linkage analysis and protein modelling. Immunogenetics 2002;54(8): 570–81.

[69] Wegner KM, Reusch TBH, Kalbe M. Multiple parasites are driving major histocompatibility complex polymorphism in the wild. J Evol Biol 2003;16(2):224–32.

[70] Wegner KM, Kalbe M, Kurtz J, Reusch TBH, Milinski M. Parasite selection for immunogenetic optimality. Science 2003;301(5638):1343.

[71] Dickerson H, Clark T. *Ichthyophthirius multifiliis*: a model of cutaneous infection and immunity in fishes. Immunol Rev 1998;166:377–84.

Aim and outline
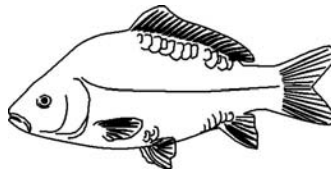
The hypothesis pertinent to this thesis is that homologous (naturally occurring) infection models are fundamental to a proper extrapolation of experimental data towards a practical implementation of prophylactic strategies such as immunomodulation and vaccination. Protection against infection relies on the integrated activity of innate and adaptive parts of the immune system and requires three fundamental components: 1) a molecular recognition system to identify the presence of the infectious organism, 2) an eliminating system to destroy the invaders at both molecular and cellular levels and 3) a communication system to coordinate these activities, that consists of soluble and cell-bound molecules.

All living organisms can be hosts and therefore can house parasites. The only limit is size: the smaller an organism, the more limited the list of parasites it can house. It may be most correct to differentiate between microparasites (viruses, bacteria, fungi and protists) and macroparasites (helminths, arthropods and other metazoans). In this thesis, we study three fundamentally different homologous infection models of common carp, including microparasitic infections with spring viraemia of carp virus (SVCV) and the protist *Trypanoplasma borreli* as well as macroparasitic infections with the ectoparasite *Argulus japonicus* (arthropod). The **first aim** of the research described in this thesis is to develop both molecular and cellular tools to be implemented in the characterization of the innate and adaptive immune response of carp to infections. The **second aim** of this thesis is to integrate molecular and cellular approaches to investigate the immune response of carp to infections, taking into account the nature of the pathogen. In the second part of this thesis, we focus on one model in particular, *i.e.* infections with the extracellular blood parasite *T. borreli* (Parabodonida; Kinetoplastida).

The potential of the *T. borreli* infection model of carp is extensively discussed in **chapter 1** (general introduction). To date, the discipline of comparative immunology is receiving increased attention and is advancing rapidly, especially because of the developments in molecular biology and the progress made with molecular techniques. These developments include wide access to genome information on a number of fish species including pufferfish, stickleback and zebrafish, a close relative of carp. The combination of an increased amount of sequence information and the development of more sensitive and accurate methods to measure gene expression in real-time (**chapter 2**), has pushed forward the discipline of comparative immunology. In this thesis, we use the real-time quantitative PCR technique to describe the kinetics of the immune response to the ectoparasite *Argulus japonicus* (**chapter 3**) and to infection with the spring viraemia of carp virus (SVCV; **chapter 4**). In the latter study, we not only report the cloning of cell surface markers (CD8α and CD8β) for carp cytotoxic T cells (CTL), and the possible involvement of CTL in the immune response against this viral infection, but also point out the importance of interleukin-12, a cytokine with a crucial role in the development of an effective CTL response. In **chapter 5,** we therefore examine and discuss the possibility to co-administer an IL-12 expression plasmid in combination with a plasmid encoding for the G-protein of SVCV with the aim to improve DNA vaccination strategies against this virus. The experimental data obtained with the SVCV infection model provide a valuable example of how a thorough understanding of the immune response could lead to the successful design of an improved prophylactic strategy for vaccination in aquaculture practice.

The second part of this thesis focuses in particular on the *T. borreli* infection model. Experimental

infection of carp with *T. borreli* results in pathological changes also associated with trypanosome infections of warm-blooded vertebrates such as anaemia, splenomegaly and polyclonal lymphocyte activation. Typical of *T. borreli* infections only, is the induction of extremely elevated serum nitrite levels. Previous studies suggested the ability of *T. borreli* to induce elevated nitric oxide (NO) would represent a strategy of the parasite to induce immunosuppression and evade the host immune system. The strong immune reaction would thus be disadvantageous to the host. In this thesis, we challenge this view and hypothesize that a timely production of NO could also be beneficial to the host and that a balance between the host's immune response and immune evasion strategies of the parasite would serve best both, host and parasite.
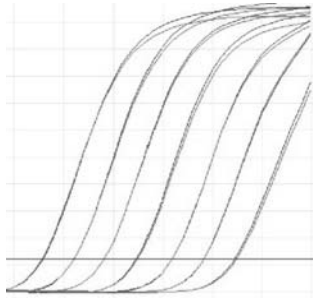
In **chapter 6**, we use an anti-nitrotyrosine antibody in combination with monoclonal antibodies that specifically recognize carp leukocyte sub-populations of macrophages and neutrophilic granulocytes to examine the relative contribution of these two cell types to the nitration process *in vivo*. In the same chapter, we examine, *in vitro,* the effect of reactive nitrogen species on parasite motility and viability, using NO and peroxynitrite donors. We also examine, *in vivo*, the effects of nitrosative stress on the parasite itself using *T. borreli*-specific antibodies for immuno-histochemistry. Given the phylogenetic relationship of *T. borreli* with other mammalian trypanosomes and the similarity observed in the pathology of these parasitic infections in warm-blooded vertebrates and carp, in the same chapter we examine the potential of *T. borreli* to serve as an alternative tool for pharmacological studies on human anti-trypanosome drugs. In **chapter 7**, we hypothesize that during the early phase of infection, when antibody titers and nitrite concentrations are still moderate, the trypanostatic effects of NO could favor rather than hinder the host defense mechanism. In this scenario, reduced parasite motility would hinder the hydrodynamic flow-mediated removal of IgM from the parasite surface. As a result, parasite-bound surface IgM concentrations would remain high, favoring complement activation and parasite lysis, resulting in clearance of the parasite from the bloodstream.

Owing to the use of a monoclonal antibody specific for B-lymphocytes, we could visualize a massive B cell proliferation in the spleen of *T. borreli*-infected fish (chapter 6). The T cell response, however, has not been investigated. In **chapter 8**, we report the cloning of three new sequences, additional to the cell surface markers reported in chapter 4, that are all specific for the T-cell-lineage in carp: CD3ε, Lck and ZAP-70. The identification of conserved epitopes in the newly described sequences allows for the selection of antibodies developed for use in mammalian immunology and specific for the corresponding human proteins. The selected antibodies are used for the identification of T cells in carp and for a preliminary investigation of the T cell response during *T. borreli* infection. In addition, using a different approach, affinity-purified polyclonal antibodies specifically directed against selected peptides in the extracellular domain of carp CD4 and CD8, are also produced. These antibodies are required for a proper identification of T cell subsets in carp during infection.

In the last part of this thesis (**chapter 9**), a comprehensive *in vitro* and *in vivo* analysis of the biological activities of the cytokine tumor necrosis factor-alpha (TNFα) is performed. A bacterial recombinant carp TNFα is produced and receptor-dependent as well as receptor-independent activities of carp TNFα are investigated, *in vitro*. The role of TNFα during *T. borreli* infections, is examined using three fundamentally different but complementary approaches: 1) inhibition of TNFα gene expression,

2) overexpression of TNFα and 3) inhibition of membrane-bound TNFα (mTNFα) shedding. Inhibition of TNFα gene expression *in vivo* allowed us to discriminate between parasite-derived components and TNFα with respect to their contribution to the high nitrite levels associated with *T. borreli* infections. The yet unexploited role in fish of mTNFα and its role in protection against *T. borreli* infection are discussed. The molecular, histological and cellular methodologies used throughout this study are integrated in an attempt to emphasize the value of homologous infection models for the discipline of comparative immunology. **Chapter 10** discusses the progress made in the understanding of the protective immune response of carp to the parasite *T. borreli* as well as future perspective concerning the exploitation and implementation of the zebrafish animal model alongside the carp animal model.

The studies described in this thesis, showed that the identification of more components of the fish innate and adaptive immune system increasingly permits to study functional activities within the protective immune response. Whole animal infection experiments are essential for a true understanding of the immune system and parasite infections in particular, thus deserve a more central role as model systems to help understand basic questions in comparative immunology.

CHAPTER

2

The use of Real-Time quantitative PCR (RT-qPCR) for the analysis of cytokine mRNA levels

Maria Forlenza, Thomas Kaiser, Huub F.J. Savelkoul
and Geert F. Wiegertjes

The use of Real-Time quantitative PCR (RT-qPCR) for the analysis of cytokine mRNA levels

Maria Forlenza[1], Thomas Kaiser[2], Huub F.J. Savelkoul[1] and Geert F. Wiegertjes[1]

[1] Cell Biology and Immunology Group, Wageningen Institute of Animal Sciences, Wageningen University, Wageningen, The Netherlands.

[2] Corbett Life Science, Australia

1. Introduction

Over the last decade, Real Time-quantitative PCR (RT-qPCR) analysis has become the method of choice for quantitative and accurate measurement of mRNA expression levels but also for sensitive detection of rare or mutated DNA species in diagnostic research (**1, 2**). RT-qPCR is based on the standard principles of PCR amplification in addition to the use of specific probes or intercalating dyes. Various probe systems are available among which TaqMan probes, Molecular Beacons, MGB probes, and others increasing specificity and sensitivity of the Real Time assays. RT-qPCR using intercalating dyes that become fluorescent upon binding to double-stranded DNA, has the advantage of running melting curve analysis after each run in order to check specificity. In most cases Sybr-Green I is used, but other dyes are available including Eva-Green, Syto9, etc.

Under optimal conditions, every PCR cycle should result in a doubling of the amplification product. At the end of every cycle the intercalating dye will bind to all double-stranded DNA. Ideally, the increase in amount of template will be directly proportional to the increase in fluorescence. Fluorescence data are collected during each cycle allowing for real-time monitoring of amplification. A typical RT-qPCR profile is shown in Figure 1: it can be divided in the initial, exponential and plateau phase. The exponential phase of the amplification provides the most useful and reproducible data. **There is a quantitative relationship between the amount of starting DNA and the amount of amplification product during the exponential phase**. The number of cycles required for a sample to rise above the background fluorescence

and reach the threshold level is called **Ct-value** (threshold cycle). The threshold is set at a level where the rate of amplification is greatest during the exponential phase, allowing for the most accurate and reproducible results. An advantage of RT-qPCR over conventional PCR is the possibility to assess the **Amplification Efficiency (E)**. Particularly when the expression profile of more genes need to be compared, it is important to take the efficiency into account and adjust for differences between different genes to be compared. In addition, at the end of every run a **Melting Curve Analysis** can be performed to assess amplification specificity. Taken together, this leads to increased sensitivity, specificity and efficiency of the PCR analysis. To obtain meaningful RT-qPCR data, the quality of the starting material (RNA, DNA) and the analysis method of choice are of crucial importance. In this chapter we will focus on the details of **RNA solation** and **cDNA synthesis** methods, the application of RT-qPCR for measurements of **cytokine mRNA levels** using **Sybr-Green I** as detection chemistry and finally, we will discuss the pro and contras of the **Absolute Quantification** versus **Relative Quantification** analysis.

1.1 Absolute Quantification

Absolute quantification analysis ideally determines the absolute copy number of a gene of interest (GOI) in an unknown sample. The unknown sample is compared to a standard curve with known concentrations of template. In most cases recombinant plasmid DNA (recDNA), cDNA, recRNA, sample, pooled samples or PCR products are used for this purpose. Therefore, **the accuracy of the absolute quantification assay**
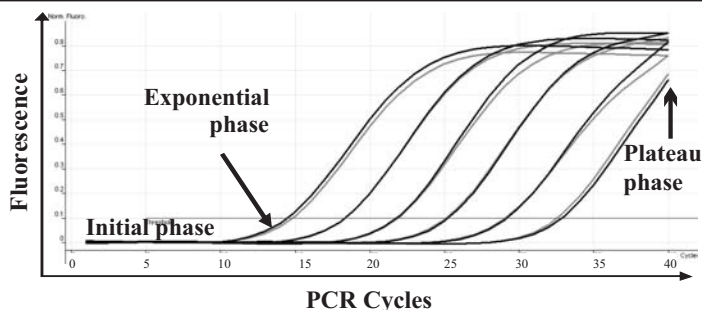
Figure 1. **A typical RT-qPCR profile can be divided in the initial, exponential and plateau phase.**

entirely dependents on the accuracy of the standard (3). No matter how accurate the concentration of the standard material is **the final result is always expressed relatively to a defined unit of interest**: *e.g.* copies per ng of total RNA, copies per cell, copies per gram of tissue, copies per ml blood. When absolute changes in copy numbers are important, the denominator has to be shown to be **absolutely stable** across the comparison. Although the word "absolute" suggests an exact measurement, one has to be aware that absolute quantification is relative to the standards used.

1.2 Relative Quantification

Relative quantification analysis determines the levels of expression of a GOI and expresses it relative to the levels of an internal control or reference gene (RG). Results are given as ratio of GOI versus one or more RGs (**4**). In this type of analysis the function of the RG is to **normalize** the data for differences in RNA (DNA) quantification and template input. Therefore, expression of the RG has to be analysed in the same sample as the GOI and can be co-amplified in the same tube as a multiplex assay (probes), or the same sample

should be used in separate tubes as a simplex assay (Sybr-Green I).

Reference genes are genes that are not affected by the treatment in any way and are constant under the tested conditions. Hence, **the reliability of the relative quantification analysis is strongly dependent on the stability of the RG**. Several tools are available for the determination of the best RG: **TATA Biocenter AB**: http://www.tataa.com/Products/Human-Endogenous-Control-Panel.html; **geNorm** (**5**): http:// medgen.ugent.be/~jvdesomp/genorm/; **BestKeeper** (**6**): http://www.gene- quantification.info. We have extensive experience with the BestKeeper software.

1.3 Real-time PCR Cyclers

Most RT-qPCR cyclers make use of a solid-block (96- or 384-wells) for thermal cycling while others use hot- and cooled-air. Most of the solid-block based real-time instruments are affected by thermal variation across the block and by differences in illumination and optical signals detected from each sample. Both aspects greatly contribute to well-to-well variability. Two air-based cyclers employ a rotary design using capillaries or plastic tubes

and one of them uses a centrifuge, which guarantees optimal thermal and optical uniformity. Samples are continuously rotating in the thermal chamber, guaranteeing minimal temperature variation between tubes in contrast to positional effects such as the recognized "edge effect" observed in block-based designs. In addition, every tube moves past the identical excitation light source and detection pathway, which guarantees optical uniformity. In our laboratory we have extensive experience with the Rotor-Gene 6000™.

2. Material:

2.1 RNA isolation and cDNA synthesis

1. RNA isolation including on column DN*ase* treatment: RNeasy Mini Kit and RNase-free DNase set (QIAgen)

2. cDNA synthesis including DN*ase* treatment: DN*ase* I, Amplification Grade; Superscript™ III First Strand Synthesis Systems for RT-PCR Systems (Invitrogen).

3. Nuclease-free water (Promega)

4. NanoDrop spectrophotometer (Thermo Scientific)

2.2 Plasmid construction and isolation:

1. Luria Bertani (LB) medium (1L)

2. LB plates

3. *E. coli* JM109 High Efficiency Competent Cells (Promega)

4. pGEM-T easy Ligation Kit (Promega)

5. QIA prep Spin Miniprep kit (QIAgen)

6. Gel Extraction Kit (QIAgen)

2.3 RT-qPCR Master mix: ABsolute™ QPCR SYBR® Green Mix (ABgene)

2.4 Thermal cycler: Rotor-Gene 6000™ (Corbett Research)

More details information to any RT-qPCR topic can be found on the following web site: http://www.gene-quantification.info

3. Methods:

3.1 RNA isolation and quantification

Isolation and quantification of good quality RNA (see **Note 1** at the end of the chapter) is of extreme importance to obtain meaningful gene expression data by RT-qPCR. Several commercial kits are available; for RNA isolation from small (30 mg) fresh-frozen or RNA-*later* stored tissue samples and from primary cells or cell lines (10^7 cells) we obtained high-quality results with the RNeasy kit from Qiagen.

1. Isolate RNA according to the manufacture's instructions. Work fast, clean, wear gloves and use RNase-free tubes and tips. To reduce genomic DNA (gDNA) contaminations, include an on-column DNase digestion step. Elute RNA in 30-50 µl RNase-free water.

2. Use 1 to 2 µl of the eluted sample to determine RNA concentration (OD measurement at 260 nm) and RNA quality (OD 260/280 ratio) with the NanoDrop spectrophotometer. An OD 260/280 ratio greater than 1.8 is usually considered an acceptable indicator of good RNA quality. The presence of gDNA in the sample will

lead to an overestimation of the RNA concentration.

3. RNA integrity and the absence of gDNA can be assessed by loading 1-2 µl of RNA sample on a 1% agarose gel. Two major bands corresponding to the 28S and 18S rRNA should be clearly visible. In case of gDNA contaminations, an additional band of higher molecular weight than the two rRNA bands can be observed.

3.2 cDNA synthesis

Several kits are available for cDNA synthesis. We routinely use the SuperScript ^{TM} III First strand cDNA synthesis kit with random primers from Invitrogen.

1. Prior to cDNA synthesis from 1 µg of total RNA (**Note 2**), perform a second DNase digestion step using the DNase I Amplification Grade Kit (Invitrogen).

2. Proceed with the cDNA synthesis protocol according to the manufacturer's instructions. For each sample, always include a control for gDNA contaminations: in this sample the same amount of RNA is used but no Reverse Transcriptase is added to the mix (-RT control).

3. After cDNA synthesis the final volume for each sample is 20 µl. We routinely bring the volume up to 100 µl and consider this our stock sample solution. Depending on the organ or cell type, we further dilute the stock 5 to 10 times. This will allow performing up to 200 reactions for each sample when using 5 µl of template in each PCR reaction.

3.3 Construction of recombinant plasmid DNA (recDNA)

The calibration curves used in absolute quantification can be based on known concentrations of DNA standard molecules, *e.g.* recDNA, gDNA, RT-PCR product, commercially synthesized big oligonucleotide (**Note 3**). In this section we will describe how to construct a recombinant plasmid DNA containing the sequence of any GOI.

1. Design primers to amplify a large (500-1000 bp) fragment of the gene. The region should of course contain the sequence to which the primers designed for RT-qPCR will anneal. Amplify the large product by conventional PCR or Reverse Transcriptase-PCR.

2. Gel-purify the product using the QIAgen Gel Extraction Kit and elute in 30 µl of water.

3. Ligate the product into the vector by combining 3.5 µl of the gel purified product to 5 µl of 2x Ligation buffer, 0.5 µl (25 ng) of pGEM-T easy and 1 µl (3UI) of T4 DNA ligase. Mix by pipetting, and incubate for 1h at room temperature or overnight at 4°C for the maximum number of transformants.

3.4 Amplification and quantification of recDNA

1. Prepare LB agar plates containing ampicillin, X-Gal and IPTG.

2. Centrifuge the ligation reactions briefly. Add 2-5 µl of each ligation reaction to a sterile 10 ml tube on ice.

3. Thaw one vial (200 µl) of JM109 High Efficiency Competent Cells on ice. When just thawed, mix the cells by gently flicking the tube. Carefully transfer 50 µl of cells to the ligation tube from step 2. Gently flick the tube and incubate on ice for 20 min.

4. Heat-shock the cells for 45-50 sec in water bath at exactly 42°C. DO NOT SHAKE. Immediately return the tube to ice for 2 min.

5. Add 950 µl room temperature SOC medium to each reaction tube. Incubate for 1.5h at 37°C with shacking (~150rpm).

6. Transfer the total volume of the transformation reaction to an Eppendorf tube, centrifuge for 10 min at 2000 rpm. Remove 900 µl of medium and resuspend the bacterial pellet in the remaining 100 µl. Spread 90 µl and 10 µl of cell suspension onto two LB agar plates containing ampicillin, X-Gal and IPTG and incubate overnight at 37°C.

7. With a sterile pipette tip, tick-pick 5-8 white colonies and transfer each of them in 4 ml LB medium containing ampicillin (50µg/ml). Grow overnight with shacking at 300 rpm.

8. Isolate plasmid from 3 ml of the overnight culture using the QIAgen QIA prep Spin Miniprep kit. Elute plasmid in 50 µl of water.

9. Make glycerol stocks by combining the remaining 1 ml overnight culture to 200 µl 100% glycerol.

10. Load 1-2 µl of isolated plasmid on a 1% agarose gel. Three bands of high molecular weight corresponding to the linear, circular and supercoiled form of the plasmid should be visible.

11. Linearize the plasmid by combining 30 µl of purified plasmid to 3 µl of restriction enzyme of choice, 5 µl of the appropriate 10x reaction buffer and water up to a final volume of 50 µl.

12. Gel purify the linearized plasmid using the QIAgen Gel Extraction Kit and elute in 30 µl of water.

13. Determine plasmid concentration using the NanoDrop. Take an average out of at least five measurements (better ten) and perform the measurement at multiple template dilutions. **The concentration of the plasmid has to be calculated very accurately because this measurement will determine the outcome of the absolute quantification analysis**. For use in RT-qPCR, prepare the plasmid as described below.

3.5 Calculation of plasmid copy number and preparation of the standard curve

Once the size of the plasmid containing the GOI is known, it is possible to calculate the number of grams/molecule, also known as copy number, as in the following example:

Weight in Daltons (g/mol) =

(bp size of plasmid+insert)(330 Da x 2 nucleotide/bp)

Ex. g/mol=(5950 bp)(330 Da x 2 nucleotide/bp)= 3927000 g/mol

Hence: (g/mol)/Avogadro's number $6.02214199 \times 10^{23}$= g/molecule = copy number

Ex. 3927000g/mol/ $6.02214199 \times 10^{23} = 6.52 \times 10^{-18}$ g/molecule.

The precise number of molecules can be determined as follows:

Concentration of plasmid (g/μl)/copy number

Ex. $(3 \times 10^{-7}$ g/μl) / $(6.52 \times 10^{-18}$ grams/molecules) = 4.6×10^{10} molecules/μl.

Once the number of molecules in 1 μl of linearized plasmid solution is calculated, prepare standard dilutions to obtain an X plasmid copy number in 5 μl of water. Accurate pipetting is essential because the standards must be diluted over several orders of magnitude. It is recommended to divide standards into small aliquots, store at –80°C, and thaw only once before use.

3.6 Primer design

The design of specific primers that work at a good efficiency is of crucial importance in RT-qPCR. Use the Primer3 program (http://frodo.wi.mit.edu/cgi-bin/primer3/ primer3_www.cgi) to design primers of a length of 18-22 bp, with an annealing temperature of 60°C and a minimum self and 3' complimentarily. To accomplish rapid quantification, short PCR cycling (45-75 sec) and efficient PCR conditions, optimal length of the PCR product is 100-200 bp. Use the OligoAnalyzer program (http:// eu.idtdna.com/analyzer/Applications/OligoAna

lyzer/Default.aspx?c=EU) to verify that the primers have low self- and hetero-complementarity. To increase the annealing temperature of primers, to improve the specificity of allele-specific primers or for Single Nucleotide Polymorphism (SNP) analysis, the incorporation of Locked Nucleic Acids (LNA) modifications can be of great advantage (**7, 8**). A software program to estimate melt behaviours of a template is: POLAND MELTSIM (http://www.bio informatics.org/meltsim/wiki/)

3.7 PCR Profile and Melting Curve Analysis

A typical PCR profile includes an initial denaturation step of 10-15 min at 95°C, depending on the Taq-Polymersase (**Note 4**), followed by 35-40 cycles including: 95°C for 5-15 sec (denaturation), 60°C for 15-30 sec (annealing), 72°C for 15-30 sec (elongation). This profile is a general suggestion and the annealing temperature has to be verified. At the end of the run, a melting step needs to be performed to assess amplification specificity (**Note 5**; Figure 2). Each PCR product will have a specific melting temperature, resulting in a single melting peak with no additional peaks at lower temperatures. Additional peaks can be primer dimers or unspecific products due to excessive amount of primers in the reaction, low annealing temperature, too high $MgCl_2$-concentration, or too long hold times. Primer dimers formation can be reduced or eliminated by accurate design of the primers and optimization of primer concentration.
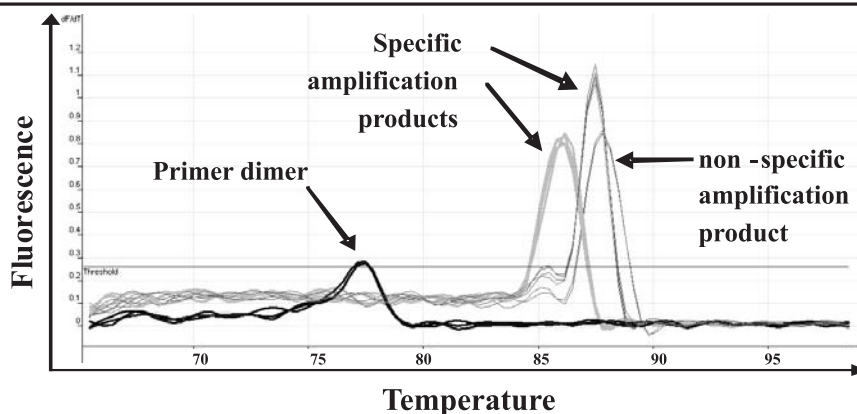
Figure 2. **Melting Curve profile of PCR products amplified with three different primer sets.** Light grey: four PCR products each showing the same specific melting peak. Dark grey: four PCR products of which three showing a specific melting peak and a fourth one being a non-specific amplification product with a different melting temperature. In black: amplification with the third set of primers resulted only in primer dimer formation.

When using a primer set for the first time, despite the presence of only one amplification peak, it is advised to sequence at least once the amplification product to confirm sequence specificity.

3.8 Optimization of Primer Concentration

Select a cDNA template or recDNA containing the sequence of the GOI. Prepare a master mix containing 7 µl of 2x Sybr-Green I Mix and 5 µl of DNA. Aliquot 12 µl of the master mix into reaction tubes and add 1 µl of each primer to give final concentrations as outlined in the table below.

Reverse Primer	Forward Primer		
	100	**300**	**500**
100	100/100	300/100	500/100
300	100/300	300/300	500/300
500	100/500	300/500	500/500

The final reaction volume is 14 µl (**Note 6**). The primer stock concentrations are **1.4**, **4.2**, **7 µM** and give final concentrations of **100**, **300**, **500 nM** respectively. We usually find 300 nM the optimal concentration for both, forward and reverse primer. As a general guideline, choose the primer combination which gives the lowest Ct value for the same amount of template and does not lead to primer dimer formation. In every run, **always include a Non-Template control (NTC)** where the template is replaced by the same amount of water, in order to test for primer specificity and contaminations.

3.9 Determination of Primer Amplification Efficiency

Depending on the subsequent method of analysis there are several ways to determine primer amplification efficiencies. The most commonly used is the standard curve method: a dilution series of a reference template or pooled samples of unknown concentration is generated. The reference sample can be cDNA or recDNA (of unknown concentration) that contains the target gene. The units used to describe the concentration of the dilution series are relative, as long as they reflect the dilution factor of the standard curve (Figure 3).

Set the threshold just above the take-off point of the reactions (if the result for more genes over

different experiments need to be compared, set the threshold at the same level for all genes, for example 0.1). Record the Ct values and plot them against the log template concentration. Use the slope of the regression line to calculate the amplification efficiency for each primer according to the following formula: $E = 10^{(-1/slope)}$. The optimal amplification efficiency of a reaction is 2 but we consider **E** values between 1.7 and 2 as acceptable, as long as the reproducibility over several runs as well as the replicates is good. Usually all RT-qPCR software provide this type of calculations (see example in Table 2 and Figure 4). In general, it is important that **the amplification efficiency of the reference template reflects the amplification efficiency of the unknown sample**.

3.10 Relative Quantification Analysis

Relative Quantification is the method of choice for RT-qPCR analysis when investigating physiological changes in gene expression levels. It does not require standard curves with known concentration of templates and results are given as the ratio (**R**) of GOI versus one or more RGs. To date several mathematical models have been developed and can be generally divided into two major categories: **without** and **with** primer
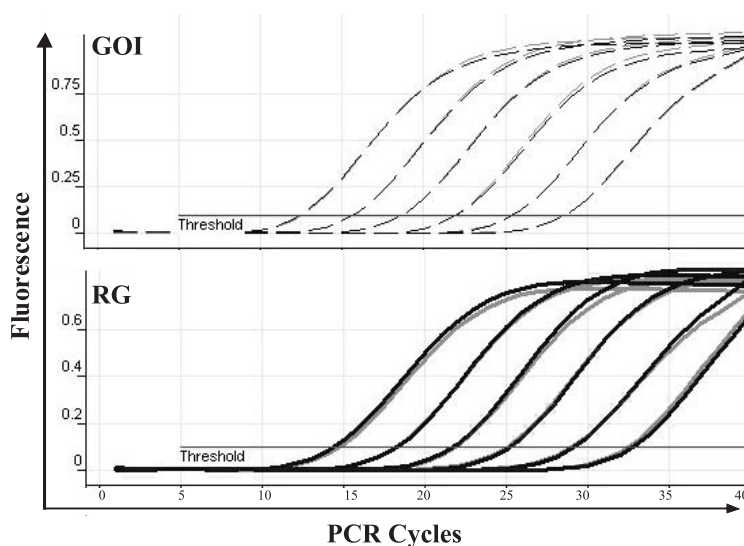

Figure 3. Standard curve of a 10-fold dilution series of a reference cDNA sample used to calculate the amplification efficiency of the primer sets for the RG and GOI.

Table 2 Results obtained from the RG standard curve described in figure 3. By plotting the averaged Ct values from duplicate samples against the log of the given concentration, the corresponding standard curve will be obtained

Name	Type	Ct	Given Conc (Copies)	log (conc)	Averaged Ct
RG 1	Standard	14.86	10,000,000,000	10	14.70
RG 2	Standard	18.38	1,000,000,000	9	18.38
RG 3	Standard	21.91	100,000,000	8	21.88
RG 4	Standard	25.17	10,000,000	7	25.25
RG 5	Standard	29.14	1,000,000	6	29.20
RG 6	Standard	32.62	100,000	5	32.77
RG 1	Standard	14.54	10,000,000,000		
RG 2	Standard	18.38	1,000,000,000		(-1/-3.604)
RG 3	Standard	21.84	100,000,000		E = 10
RG 4	Standard	25.32	10,000,000		
RG 5	Standard	29.26	1,000,000		E = 1.89
RG 6	Standard	32.91	100,000		
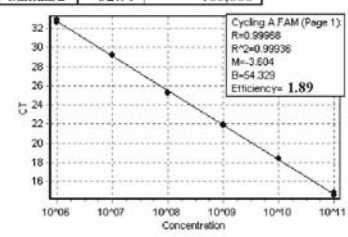
efficiency correction. In this section we will provide examples on how to analyse an experiment applying both of those methods. For example, we want to determine the fold change in interleukin-10 (IL-10) mRNA expression at various time points after treatment. The 40S ribosomal protein S11 will be used as RG.

Set up the first run of the day by amplifying a standard curve for each target gene using a template cDNA or recDNA of unknown concentration (Figure 4; it might not be necessary to run a standard curve every time depending on the chosen method of analysis). Set up a second run where in separate tubes, the 40S and IL-10 genes are amplified for each of the samples under investigation. Include a triplicate sample of one dilution point of the same standard from the first run. Analyse the results according to one of the methods outlined below.

3.10.1 Relative quantification __without__ efficiency correction: **ΔΔCt method**

The ΔΔCt method (**9**) is based on the assumption that the primers of the GOI will have the same amplification efficiency as the primers for the RG. This assumption needs to be validated at least once before proceeding with the analysis of the experiment. See **Note 8** for instructions on the **validation experiment**. In case of positive results from the validation experiment proceed as follows:

- Set the threshold to 0.1 for all genes.
- Export the Ct values to Excel
- Select the sample at time point 0 (zero) as the **calibrator** (the calibrator is usually an untreated, unhandled sample).
- Apply the following formula:

$$R_{IL-10} = 2^{\left(\dfrac{Ct_{40S \text{ (calibrator)}} - Ct_{IL-10 \text{ (calibrator)}}}{Ct_{40S \text{ (sample 1-7)}} - Ct_{IL-10 \text{ (sample 1-7)}}}\right)}$$

This method has the advantage that standard curves are required only once for the validation experiment and allows for normalization relative to an internal reference gene (RG). However, the assumption that different primer sets will perform with the same amplification efficiency over different runs and over different templates might not always be valid. Therefore, the efficiency of all RG and GOI should be checked regularly, as changes in reagents, concentrations, calibrator etc could influence the efficiency of one or various genes differently.

3.10.2 Relative quantification _with efficiency correction_: **The Pfaffl method**

This method does not require the amplification efficiency of different primer sets to be similar; it rather takes into account the possibility that the efficiencies can be different and offers a way to correct for such differences (**4, 10**). Optimally, a standard curve for each of the target genes is amplified in the same run together with the unknown samples. However, when a large number of samples and numerous genes need to be analyzed, standard curves for several genes can be amplified in the first run of the day or even on a different day (Figure 4).

- Set the same threshold for all genes to be analyzed (_i.e._ 0.1) and record the amplification efficiency (E) for each primer set as described in the previous paragraph.
- In the experimental run it is possible to either import the standard curve from the previous run and ask the software to adjust it to the standard in the current run (Run 2 in figure 4) or the threshold can be directly set manually to 0.1.
- Export the Ct values to Excel.
- Select the sample at time point 0 (zero) as calibrator and apply the following formula.
-

$$R_{\text{IL-10}} = \frac{E_{\text{(IL-10)}}^{(\text{Ct}_{\text{IL-10 (calibrator)}} - \text{Ct}_{\text{IL-10 (sample 1-7)}})}}{E_{\text{(40S)}}^{(\text{Ct}_{\text{40S (calibrator)}} - \text{Ct}_{\text{40S (sample 1-7)}})}}$$

The Pfaffl method is a modification of the ΔΔCt method with the obvious advantage that it does take into account differences in amplification efficiencies between primer sets.

In order to obtain direct and valuable statistical information it is possible to import the above mentioned data in the gene quantification software called REST (Relative Expression Software Tool, freely available at http://rest.gene-quantification.info.This software uses the Pfaffl formula and generates statistical data including the standard error and the confidence interval by using randomisation tests via hypothesis testing P(H1) = difference between sample and control is due only to chance.

3.10.3 Relative quantification _with efficiency correction_: **"sigmoidal" or "logistic" curve fitting models**

To date, several methods have been developed to calculate the amplification efficiency of each primer set in each single sample (**11-13**). The great advantage of all these methods is that they do not require the preparation of standard curves or validation experiments and no assumption has to be made regarding the amplification efficiency of each primer set over different runs, templates or master mixes.

The method developed by Corbett Research has been incorporated in the Rotor-Gene 6000 software under the 'Comparative Quantitation' analysis option and we routinely use it for our relative quantification of gene expression. We directly apply the set up of Run 2 in figure 4 (without the need of the standard samples). The Ct values and the amplification efficiency for each sample are directly obtained from the software and exported to Excel.

- The average amplification efficiency (E_A) for each primer in each run is calculated and the relative fold change for each GOI is calculated according to the Pfaffl formula as above.
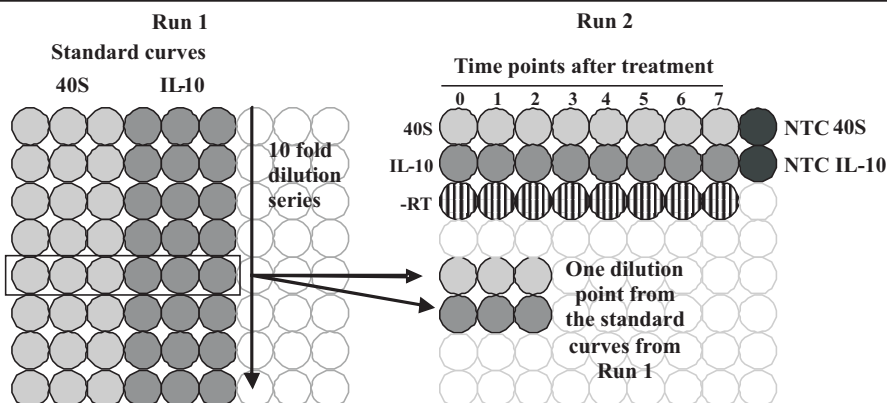
Figure 4. Possible RT-qPCR set up for relative quantification of IL-10 mRNA expression levels. A first run where a standard curve for each of the analysed genes is amplified has to be performed when analysing the data using **ΔΔCt** and **Pfaffl** method (see text). Particularly for the validation experiment required for the ΔΔCt method it is important the template to be the same for each gene which needs to be compared. In a second run (the experimental run) amplify the RG (40S) and the GOI (IL-10) in each of the samples under investigation. Always include a Non-Template Control (NTC) where water substitutes the template, and a control for genomic contamination (-RT). When a standard curve should be imported from a previous run, include a triplicate sample of one dilution point of the same standard curve in the current run (**Note 7**).

- It often happens that the analysis of one large experiment cannot be completed within one run. In that case we calculate the E_A of each primer set over the whole experiment (two, three or more runs). To reduce variation between runs, we usually prepare one master mix for each primer set which is enough for all runs of the day and not one master mix for each run. By doing so we observe only a ± 0.02 variation in E_A for each primer set between two, three or more runs on a single day.

Before using a new primer set for the first time we perform a dilution series of a cDNA sample containing the target gene. This provides us with an estimation of the amplification efficiency and the Melting curve analysis provides us the specificity of the assay.

3.11 Absolute Quantification Analysis: external standard curve model

Absolute quantification refers to an analysis where unknown samples are compared to a standard curve of cDNA, recDNA or recRNA where the absolute concentration is known. Especially for Absolute Quantification Analysis, the standard curve for the target gene should be amplified in the same run together with the unknown samples. However, when a large number of samples and numerous genes need to be analyzed, it is possible to import a standard curve from a previous run.

- Standard curves for several GOI can be amplified in the first run of the day and in every subsequent run, together with the unknown samples. A triplicate of one dilution point of the standard curve should be included.

- At the end of the run, ask the software to import the standard curve for the GOI from a

previous run and adjust it to the standard in the current run (**Note 7**). Read the absolute copy number given by the software.

- Alternatively it is possible to export data to excel and perform the quantification analysis by plotting the Ct values of the unknown sample against the standard line obtained by plotting the Ct values and the log concentration of the recDNA as described before.

- Express data as GOI (copy number)/ x ng total RNA

- To normalize data and correct for variations in template input, a normalizer (RG) is used. In this way, the absolute copy number of a RG and GOI in an unknown sample is determined from the standard curve. The absolute value obtained for the GOI is divided by the absolute value obtained for the RG in the same sample. Obtained are the normalized data of the GOI in the unknown sample. **The quality of the gene quantification data cannot be better than the quality of the denominator. Any variation in the denominator will obscure real changes, produce artificial changes and wrong quantification results**.

When optimised, standard curves are highly reproducible and allow the generation of highly specific, sensitive and reproducible data. However, the external standard curve model has to be thoroughly validated as the accuracy of absolute quantification in real-time RT-PCR depends entirely on the accuracy of the standards. Standard design, production, determination of the exact standard concentration and stability over long storage time is not straightforward and can be problematic.

3.12 Technical or biological replicates?

Depending on the applications, the use of technical and biological replicates, or both, has to be considered. A technical replicate refers to a sample, for example a piece of tissue, from which the RNA isolation and cDNA synthesis has been performed more than one time under the same identical conditions. This type of replicate will tell us something about the variation in the chemistry we are using. Often the same cDNA sample is analyzed in triplicate in one RT-qPCR run. This type of technical replicate only tells something about the pipetting skills of the operator and the accuracy of the PCR instrument (see also paragraph 1.3), but should absolutely NOT be considered for statistical analysis. Biological replicates refer to the application of the same treatment to two or more samples. From each of the samples the RNA isolation and cDNA synthesis is performed independently but under identical conditions. Each of the obtained cDNA samples can be analyzed once by RT-qPCR.

Both type of replicates (technical or biological) provide information about the experimental variation and allow statistics to be applied to identify differences in expression levels between samples. Being a beginner it is a good practice to include technical replicates to test for pipetting skills. When testing the amplification efficiency of a new primer set it is advisable to include at least a triplicate of each dilution point. When investigating the effects of a treatment the use of biological replicates we think is of greater value (**14**).

For example: in an *in vitro* experiment cells are incubated in the presence or absence of a stimulus. The treatment is repeated in at least three replicate wells. Each of the three wells is a

biological replicate; however, the cells are derived from a single individual. More relevant would be to repeat the same *in vitro* experiment on cells isolated from three different individuals, each of them being a biological replicate.

Notes:

1. The extraction and purification procedure of total RNA must fulfill the following criteria: free of protein (absorbance 260 nm/280 nm); free of genomic DNA; should be non degraded (28S:18S ratio should be roughly between 1.8 and 2.0, with low amount of short fragments); free of enzymatic inhibitors for RT and PCR reaction, which is strongly dependent on the purification and clean-up methods; free of any substances which complex essential reaction co-factors, like Mg^{2+} or Mn^{2+}; free of nucleases for extended storage (**15**).

2. From 0.1 ng up to 5 µg total RNA can be transcribed into cDNA using this kit. Optimally, 1 µg of total RNA is used. In general, it is important to use the same amount of starting RNA material for each sample within the same experiment. This will greatly reduce the sample-to-sample variation due to differences in cDNA synthesis efficiency and will simplify the subsequent analysis, particularly when absolute quantification is used. In some cases not all samples (within the same experiment) would yield RNA amounts sufficient to use 1 µg of RNA/sample, it is possible to lower the amounts down to 0.1 µg, but again this amount should be used for all samples within the same experiment.

3. Cloned recDNA and gDNA are very stable and generate highly reproducible standard curves even after a long storage time. Furthermore, the longer templates derived from recDNA and gDNA mimic the average native mRNA length of about 2 kb better than shorter templates derived from RT-PCR product or oligonucleotides. A problem with DNA-based calibration curves is that they are subject to the PCR step only, unlike the unknown mRNA samples that must first be reverse transcribed. This increases the potential for variability of the RT-PCR results and the amplification results may not be strictly comparable with the results from the unknown samples (**3**).

4. The initial denaturation time depends on the type of *Taq* Polymerase present in the master mix. We strongly advise Hot-Start Taq Polymerases that require 2 to 15 min at 95°C, depending on the *Taq*-Polymerase. This allows performing the preparation and aliquoting of the master mix on the bench at room temperature.

5. At the end of a run, after the last annealing step, all amplification products will be present as double-stranded (ds) DNA and Sybr Green I will be bound to it. During the Melting step the decrease in fluorescence is measured due to melting of dsDNA products and consequent release of the fluorescent dye. Each product will melt at a specific temperature. Primer dimers usually have a lower melting temperature than PCR products ranging between the 80 and 200 bp.

6. Usually companies advise a final volume of 50 µl but the reaction can easily be scaled down to save costs. We always try to add at

least 5 µl of template. Lower volumes might increase the chance of pipetting errors.

7. The slope of the calibration curve is more reproducible than the intercept, and the slope directly correlates with PCR efficiency. Hence only a single standard point will be required to "re-register" a previously performed calibration curve level for the new unknown samples. However, this assumes that the efficiency in a given run is the same as in a previous run.

8. Amplify a standard curve as described in the paragraph "Determination of Primer Amplification Efficiency". In this case the reference template **has to be the same** for

9. both primer sets, and preferably one of the cDNA samples which is going to be used for the subsequent experiment.

- After having set the threshold (0.1) export the Ct values to EXCEL and average the Ct of replicate samples.

- Calculate the LOG_{10} of the given arbitrary concentration (LOGconc).

- Obtain the **ΔCt**: for each dilution point calculate the difference between the $Ct_{(RG)}$ and $Ct_{(GOI)}$. Plot the LOGconc vs ΔCt and obtain the equation of the curve.

If the efficiencies of the two primer sets are approximately equal, the obtained curve should be a nearly horizontal line with a slope $< \pm 0.1$. If this is the case the experiment can be analysed with the **ΔΔCt** method.

References

1. Nolan, T., Hands, R. E., and Bustin, S. A. (2006) Quantification of mRNA using real-time RT-PCR. *Nat. Protocols 1*, 1559-1582.
2. Bustin, S. A., Benes, V., Nolan, T., and Pfaffl, M. W. (2005) Quantitative real-time RT-PCR - a perspective. *J Mol Endocrinol 34*, 597-601.
3. Pfaffl, M. W., and Hageleit, M. (2001) Validities of mRNA quantification using recombinant RNA and recombinant DNA external calibration curves in real-time RT-PCR. *Biotechnology Letters 23*, 275-282.
4. Pfaffl, M. W. (2001) A new mathematical model for relative quantification in real-time RT-PCR. *Nucleic Acids Res 29*, e45.
5. Vandesompele, J., De Preter, K., Pattyn, F., Poppe, B., Van Roy, N., De Paepe, A., and Speleman, F. (2002) Accurate normalization of real-time quantitative RT-PCR data by geometric averaging of multiple internal control genes. *Genome Biol 3*, RESEARCH0034.
6. Pfaffl, M. W., Tichopad, A., Prgomet, C., and Neuvians, T. P. (2004) Determination of stable housekeeping genes, differentially regulated target genes and sample integrity: BestKeeper--Excel-based tool using pair-wise correlations. *Biotechnol Lett 26*, 509-15.
7. Latorra, D., Arar, K., and Hurley, J. M. (2003) Design considerations and effects of LNA in PCR primers. *Mol Cell Probes 17*, 253-9.
8. Latorra, D., Campbell, K., Wolter, A., and Hurley, J. M. (2003) Enhanced allele-specific PCR discrimination in SNP genotyping using 3' locked nucleic acid (LNA) primers. *Hum Mutat 22*, 79-85.
9. Livak, K. J., and Schmittgen, T. D. (2001) Analysis of Relative Gene Expression Data Using Real-Time Quantitative PCR and the 2-[Delta][Delta]CT Method. *Methods 25*, 402-408.
10. Pfaffl, M. W., Horgan, G. W., and Dempfle, L. (2002) Relative expression software tool (REST) for group-wise comparison and statistical analysis of relative expression results in real-time PCR. *Nucleic Acids Res 30*, e36.
11. Liu, W., and Saint, D. A. (2002) A new quantitative method of real time reverse transcription polymerase chain reaction assay based on simulation of polymerase chain reaction kinetics. *Anal Biochem 302*, 52-9.
12. Ramakers, C., Ruijter, J. M., Deprez, R. H., and Moorman, A. F. (2003) Assumption-free analysis of quantitative real-time polymerase chain reaction (PCR) data. *Neurosci Lett 339*, 62-6.
13. Tichopad, A., Dilger, M., Schwarz, G., and Pfaffl, M. W. (2003) Standardized determination of real-time PCR efficiency from a single reaction set-up. *Nucleic Acids Res 31*, e122.
14. Forlenza, M., de Carvalho Dias, J. D., Vesely, T., Pokorova, D., Savelkoul, H. F., and Wiegertjes, G. F. (2008) Transcription of signal-3 cytokines, IL-12 and IFN alpha beta, coincides with the timing of CD8

alpha beta up-regulation during viral infection of common carp (Cyprinus carpio L). *Mol Immunol* **45**, 1531-47.

15. Fleige, S., and Pfaffl, M. W. (2006) RNA integrity and the effect on the real-time qRT-PCR performance. *Molecular Aspects of Medicine* **27**, 126-139.
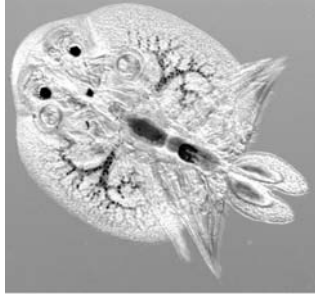
CHAPTER

3

Transcriptional analysis of the common carp (*Cyprinus carpio* L.) immune response to the fish louse *Argulus japonicus* Thiele (Crustacea:Branchiura)

Maria Forlenza*, Peter D. Walker*, Beitske J. de Vries, Sjoerd E. Wendelaar Bonga and Geert F. Wiegertjes
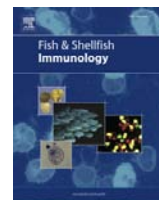
* Both authors contributed equally to the work.

Transcriptional analysis of the common carp (*Cyprinus carpio* L.) immune response to the fish louse *Argulus japonicus* Thiele (Crustacea: Branchiura)

Maria Forlenza [a,1], Peter D. Walker [b,1], Beitske J. de Vries [a], Sjoerd E. Wendelaar Bonga [b], Geert F. Wiegertjes [a,*]

[a] *Cell Biology and Immunology Group, Wageningen Institute of Animal Sciences, Wageningen University, PO Box 338, 6700 AH Wageningen, The Netherlands*
[b] *Department of Animal Ecology and Ecophysiology, Faculty of Science, Radboud University of Nijmegen, Toernooiveld 1, 6525 ED Nijmegen, The Netherlands*

Abstract   In the present study we investigated changes in transcription levels of a panel of selected immune relevant genes in peripheral blood leucocytes (PBL) and skin samples collected from carp exposed to larval *Argulus japonicus*. We show that in skin up-regulation of gene transcription of the chemokine CXCa, and to a lesser extent the chemokine receptor CXCR1 and the cytokine TNFα, are good indicators of parasite-induced skin damage at 2 days post-parasite exposure. Up-regulation of gene transcription corresponded well with an increase in leucocytes, probably neutrophilic granulocyte numbers in skin samples collected at the sites of infection. We show that time-point controls are essential when studying gene expression, especially in peripheral blood leucocytes (PBL). In addition, we demonstrate that non-infected control samples isolated from the skin of infected fish are suitable autologous controls, at least until after larval *A. japonicus* have undergone their first moult and begun to demonstrate increased mobility over their host's integument. The observed results are indicative of *A. japonicus* affecting the skin as a whole organ, particularly after the parasites' first moult, a phenomenon which has a great impact on correct skin sampling for RNA isolation.
© 2008 Elsevier Ltd. All rights reserved.

Introduction

Parasite-induced damage and disease in fish is currently receiving more intensive research focus from the scientific community. Fish lice have been shown to be a threat to

* Corresponding author. Tel.: +31 317 482732; fax: +31 317 483955.
   E-mail address: geert.wiegertjes@wur.nl (G.F. Wiegertjes).
[1] Both the authors contributed equally to the work.

farmed fish over countless decades and, more recently, to wild fish stocks. Sea lice, particularly those from the genus *Caligus* and *Lepeophtheirus*, have undergone intensive study as organisms in their own right [1,2] and over the last few decades the interactions between these animals and their hosts have also been the subject of several scientific investigations [2–5]. However, certain groups of parasites, whilst economically important, have not been intensively studied with regard to the effects they have on their fish hosts.

Argulus spp. are typically regarded as generalist parasites and have been recorded from practically every species of fish occurring in the same habitat ([7] and references therein). Occupying a similar niche to sea lice, the generalist freshwater lice from the genus *Argulus* have received a considerable amount of attention concerning their life cycle, morphology and ecology. However, the effects they have on their hosts are still poorly understood. Some of the most recent work has examined physiological and ultrastructural changes associated with stress induced by this parasitic organism [4,6]. However, despite the economic importance of this group of pathogens (in terms of their deleterious effects on fish stocks, [7]) few studies have addressed the immune response of fish to an infestation with these parasites. To combat these pathogens successfully it is vital to gain a comprehensive understanding of the natural defense mechanisms employed by fish [7], for example by gene transcription studies in tissue samples of infected fish.

Skin is an essential protective barrier for fish and functions as a first line of defense against infectious microbes from the aqueous environment. The cell composition of the epidermis is well known and in common carp (*Cyprinus carpio* L.) the epidermis consists mainly of filament cells, mucous cells, club cells and an upper layer of pavement cells. The dermis contains chromatophores and melanophores [8]. In the epidermis and dermis of healthy fish small numbers of lymphocytes and macrophages can be found [8]. Nevertheless, limited information is available for this organ with regard to immune response mechanisms and associated gene transcription. A few recent studies have shown regulation of immune gene transcription in fish skin following infection with ectoparasites [9–13]. Further, blood is essential for mounting a rapid immune response for example by transportation of the relevant leucocytes, often neutrophilic granulocytes, to the site of inflammation.

In the present study we investigated changes in gene transcription in peripheral blood leucocytes (PBL) and in the skin of common carp (*C. carpio*) infected with larval stages of the ectoparasite *Argulus japonicus*. Larval stages were chosen over adult stages not only due to the fact that larger numbers were obtainable resulting in a potentially higher number of attached parasites per fish but also because larval lice appear to migrate over the surface of their host to a much lesser degree than their adult counterparts (unpublished observation). This will increase the probability of a synchronized timing of the immune response resulting in reduced variation measured between samples. We collected time-point control samples from non-infected fish for the gene transcription studies and, in addition, for the studies on the host skin, we included autologous

time-point control samples corresponding to non-infected spots isolated from infected fish. We performed a histological examination of the sites of infection to examine the putative contribution of migrating leucocytes to changes in gene transcription.

Materials and methods

Animals

European common carp (*Cyprinus carpio carpio* L.) were bred in the central fish facility of Wageningen University, The Netherlands, raised in recirculating UV-treated water at 23 °C (±1 °C) with a 12:12 light:dark photoperiod in the central fish facility of Nijmegen University, The Netherlands and fed pelleted dry food (Trouvit, Nutreco) daily. R3R8 carp which are the offspring of a cross between fish of Hungarian origin (R8 strain) and of Polish origin (R3 strain) were used [14]. Fish were divided into eight aquaria, each containing 10 fish. All studies were performed with the approval of the animal experimental committee of Radboud University of Nijmegen.

Parasites

A population of *A. japonicus* was maintained on 'stock' carp (approximately 1000 g fish). Infestation intensities typically varied from 10 to 30 lice per fish. Eggs were deposited on the glass sides and bottom of the aquaria. Host fish were monitored regularly and parasite eggs were removed to control parasite numbers when infestation intensities appeared to be too heavy as indicated by the host condition and host-behavioral changes e.g. lethargy and loss of appetite.

Parasite collection

Adult *A. japonicus* were collected from stock carp that had been anaesthetised in a 2-phenoxyethanol (Sigma–Aldrich, St Louis, MO, USA) solution (dilution = 1:1000). Parasites were subsequently removed from all fish using a set of blunt forceps and then held in beakers containing tap water (non-chlorinated) at 23 °C for 48 h. During this time any eggs deposited by lice were collected and incubated in tap water at 23 °C with daily refreshment of the water. Upon hatching larval lice were held in groups of 150 individuals/beaker under identical conditions as for the eggs/ adult lice for 24 h prior to the start of the experiment. This increased the likelihood that stored food reserves were fully diminished prior to the start of the experiment [15], increasing the likelihood that parasites would immediately seek out and attach to a fish.

Infection of carp with *A. japonicus*

To infect the carp, the beakers of water containing larval lice were emptied into five (randomly selected) of the eight experimental aquaria. An identical amount of tap water was also poured into each of the 'control', non-infected tanks. This marked the time zero (T0) time point. One fish was then

removed from each of the tanks at T0, 10 h, 24 h (1 day), 48 h (2 days), 72 h (3 days) and 6 days post infection. Upon removal, the fish were irreversibly anaesthetised in 2-phenoxyethanol (dilution = 1:500) and subsequently weighed, measured (standard length) and the number of attached parasites recorded.

Peripheral blood leucocytes (PBL) and skin isolation

Blood was collected via puncture of the caudal vessel and diluted 1:1 with cRPMI (RPMI 1640 (Cambrex, Verviers, Belgium) adjusted to 270 mOsmol/kg) containing 50 IU ml^{-1} of heparin (Leo Pharmaceutical Products, Weesp, The Netherlands). After centrifugation at 600 g for 10 min, the buffy-coat containing leucocytes was collected and layered on 5 ml of Ficoll-Paque™ Plus (Amersham Biosciences, Uppsala, Sweden). Following subsequent centrifugation at 800 g for 25 min, the PBL at the interface were collected and washed three times with cRPMI. Cell pellets were collected, immediately snap frozen in liquid nitrogen and stored at $-80\,°C$ until used for RNA isolation.

Several 5×5 mm samples of skin were carefully removed from the ventral region of the flanks of uninfected (control) and infected fish. For infected fish, the samples were taken from sites of parasite attachment/feeding (infected spots) and also from sites distant to the sites of infection (autologous controls). The number of infected spots differed between individual fish. Skin samples were then immediately snap frozen in liquid nitrogen and stored at $-80\,°C$ until use or immersed in Bouin's fixative for subsequent processing and histological analysis.

Histological analysis

Skin samples for histological analyses were fixed for a minimum of 24 h in Bouin's fixative. Samples were subsequently dehydrated through a graded series of ethanol and embedded in paraffin. Five μm sections were mounted on gelatinized glass slides and dried overnight in an oven at 40 °C. Slides were then stained with hematoxylin and eosin and examined microscopically for evidence of parasite-induced damage and host inflammatory responses (i.e. infiltration of leucocytes).

RNA isolation and quantification

For real-time quantitative polymerase chain reaction (RT-qPCR) analysis total RNA was isolated from PBL and skin using the RNAeasy Mini Kit (Qiagen, Leusden, The Netherlands) according to the manufacturer's instructions. On-column DN*ase* treatment with the RN*ase*-free DN*ase* set (Qiagen) was also included.

RNA was isolated, separately from three skin pieces from each of the three non-infected controls or from five pieces (autologous controls) and one to four pieces (infected spots) from each of the five infected fish. The RNA isolated from more pieces from the same individual was never pooled and each piece was handled and analyzed separately.

The concentration of RNA was measured spectrophotometrically (GeneQuant, Pharmacia Biotech) at OD$_{260\,nm}$ and the purity determined as the OD$_{260\,nm}$/OD$_{280\,nm}$ ratio with expected values between 1.8 and 2.0. The integrity of RNA was determined by electrophoresis on 1% agarose gel containing 0.5 μg ml^{-1} ethidium bromide at 100 V. Total RNA was stored at $-80\,°C$ until further use.

cDNA synthesis

Prior to cDNA synthesis, a second DN*ase* treatment was performed using DN*ase* I, amplification grade (Invitrogen, Breda, The Netherlands). Briefly, 1 μg of RNA from each sample was combined with 1 μl 10× DN*ase* reaction buffer and 1 U DN*ase* I up to a final volume of 10 μl, mixed and incubated at RT for 15 min, followed by the inactivation of DN*ase* I by adding 1 μl of 25 mM EDTA. Synthesis of cDNA was performed with Invitrogen's Superscript™ III First Strand Synthesis Systems for RT-PCR, according to the manufacturer's instructions. Briefly, DN*ase* I-treated RNA samples (11 μl) were mixed with 5× first strand buffer, 300 ng random primers, 10 mM dNTPs, 0.1 M DTT, 10 U RN*ase* inhibitor, and 200 U Superscript III Reverse Transcriptase (Invitrogen) up to a final volume of 20 μl. The mixture was incubated at 37 °C for 60 min followed by an inactivation step at 70 °C for 15 min. A non-reverse transcriptase control was included for each sample. Before use as template in RT-qPCR experiments, the cDNA was further diluted 25 times in nuclease-free water.

Real-time quantitative polymerase chain reaction (RT-qPCR)

RT-qPCR using SYBR Green I technology was performed using Rotor-Gene™ 2000 (Corbett Research, Mortlake, Sydney, Australia) with the Brilliant® SYBR® Green QPCR (Stratagene, La Jolla, CA, USA) as detection chemistry. The primers used for RT-qPCR are listed in Table 1. PCR conditions were optimized by analyzing the melting curves of the products and product specificity was assessed by analysis on a 1% agarose gel. Master-mix for each PCR run was prepared as follows: 0.32 μl of water, 0.84 μl of each primer (5 μM), 7 μl Master SYBR Green I mix. Finally, 5 μl of diluted cDNA was added to 9 μl of master-mix and transferred to a 0.1 ml tube. The following amplification program was used: after 15 min of denaturation at 95 °C, 40 cycles of RT-qPCR with three-step amplification were performed—15 s at 95 °C for denaturation, 30 s at 60 °C for annealing and 30 s at 72 °C for elongation followed by a final holding step of 1 min at 60 °C. A melting step was then performed with continuous fluorescence acquisition starting at 60 °C with a rate of 1 °C/5 s up to 99 °C to determine the amplification specificity. In all cases, the amplifications were specific and no amplification was observed in the negative controls (non-template control and non-reverse transcriptase control). Fluorescence data from RT-qPCR experiments were analyzed using Rotor-Gene version 6.0.21 software and exported to Microsoft Excel. The cycle threshold C_t for each sample and the reaction efficiencies (E) for each primer set were obtained upon comparative quantitation analysis from the Rotor-Gene version 6.0.21 software. Briefly, the E for each primer set was recorded per sample and an average E (E_A) was then calculated for

Table 1 Primers used in RT-qPCR gene expression analysis

Primer	Sequence $5' \rightarrow 3'$	Product (bp)	Acc no
qIL-1β.FW	ACGCCACCAAGAGCCTTTTA		
qIL-1β.RV	GCAGCCCATATTTGGTCAGA	69	AJ245635
qTNFα.FW	GCTGTCTGCTTCACGCTCAA		
qTNFα.RV	CCTTGGAAGTGACATTTGCTTTT	106	AJ311800
qCXCa.FW	CTGGGATTCCTGACCATTGGT		
qCXCa.RV	GTTGGCTCTCTGTTTCAATGCA	88	AJ421443
qCXCRI.FW	GCAAATTGGTTAGCCTGGTGA		
qCXCRI.RV	AGGCGACTCCACTGCACAA	144	AB010468
qIL-10.FW	CGCCAGCATAAAGAACTCGT		
qIL-10.RV	TGCCAAATACTGCTCGATGT	103	AB110780
q40S.FW	CCGTGGGTGACATCGTTACA		
q40S.RV	TCAGGACATTGAACCTCACTGTCT	69	AB012087

each primer set. The relative expression ratio (R) of a target gene was calculated based on the E_A and the C_t deviation of sample versus control, and expressed in comparison to a reference gene [16,17]. Gene expression analysis in skin tissue was performed for each sample separately, even for those isolated from the same individual. The R in each treated sample (autologous control and infected spot) was calculated relative to a total of nine non-infected pieces collected from three time-point controls. For analysis in PBL, controls at time-point zero ($n = 5$) were used for the relative expression analysis. Only at the end the mean R of each sample in each time point was calculated and used for statistical analysis. The 40S ribosomal protein S11 was used as an internal reference gene.

Statistics

Relative expression ratios (R) were calculated as described above. Transformed values ($\ln(R)$) were used for statistical analysis in SPSS software (version 15.0). Homogeneity of variance was analyzed using the Levene's test. Significant differences ($P < 0.05$) were determined by a two-way AN-OVA followed by a Sidak test. In case of unequal variances between groups, the two-way ANOVA was followed by a Games—Howell test.

Results

General observations

Larval parasites were found attached to fish just 2 h post infection. Infection was confirmed for all carp exposed to the parasites. However, the number of attached lice/fish was low and varied between individual fish (mean $= 3.8 \pm 3.1$ S.D.) in all tanks. Infection intensities did not exhibit a time related change in parasite numbers. No significant behavioral changes in the host fish were observed at any time during the course of the experiment. The first gross pathological signs of infection were visible as red spots/lesions on the surface of infected fish and appeared between 24 and 48 h post infection. These lesions varied in size up to a maximum diameter of 6 mm. Parasites were only

observed as larval stages until approximately day 5 post infection, at which time the vast majority of observed parasites had undergone their first moult becoming juveniles.

Gene expression analysis in PBL

We investigated the kinetics of expression of several immune relevant genes in PBL of non-infected fish and fish infected with the ectoparasite *A. japonicus*. On day 1—2 post infection (p.i.) a significant ($P < 0.05$) up-regulation of IL-1β (6-fold), TNFα (3.2-fold) and of the chemokine receptor CXCR1 (3.5-fold) but not CXCa was observed when compared to the control at time-point zero (T0, Fig. 1). However, no significant differences were observed when the gene expression levels were compared with the respective time-point controls. In fact, the same genes were up-regulated in PBL samples from individual time-point controls, possibly owing to unknown environmental stimuli. On day 6 p.i. both IL-1β and IL-10 transcript levels were significantly up-regulated when compared to the control at time-point zero (Fig. 1) but, again, not when compared to the time-point controls.

Gene expression analysis in skin

To investigate not only the local immune response at the site of infection but also a more generalized response which might affect the skin as a whole organ, we analyzed the kinetics of expression of several immune relevant genes in samples collected from both, infected spots and non-infected spots (autologous controls) of infected fish. The kinetics of expression were compared to those observed in samples collected from non-infected fish at each individual time point. For clarity, since infected spots were not visible until 24 h, the 10 h time point was excluded from the analysis. Two days post infection CXCa showed a significant up-regulation when compared to the autologous controls and also when compared to the non-infected time-point control (Fig. 2). TNFα and CXCR1 transcription levels were also elevated at 2 days p.i. but this difference was significant only when compared to the non-infected autologous control. At day 6 p.i., TNFα, CXCa and IL-10 transcription levels were significantly up-regulated in skin samples collected from infected spots when compared to the non-infected
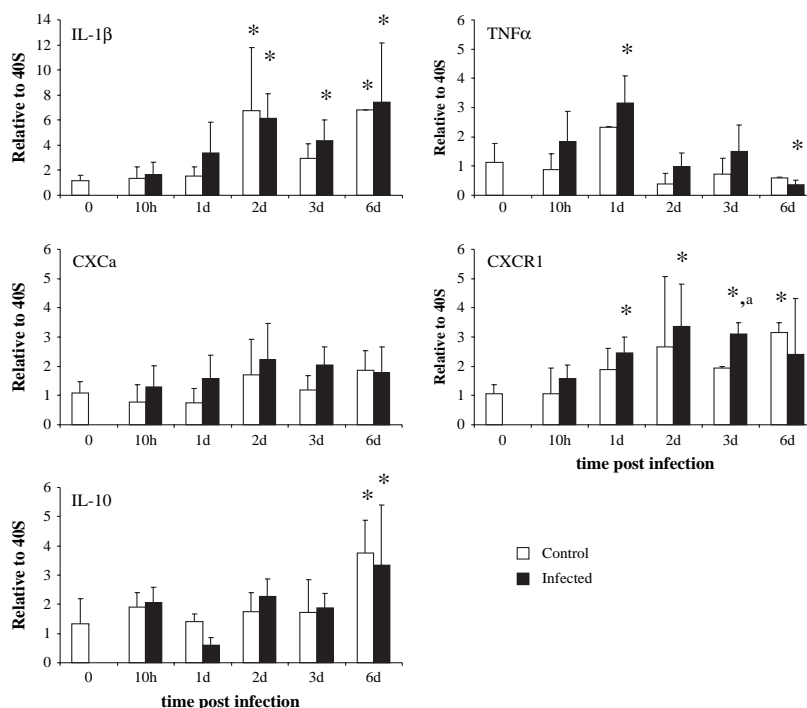
Figure 1   Kinetics of gene expression in PBL after *Argulus japonicus* infection of common carp (*Cyprinus carpio* L.). Fish were exposed to 150 larval parasites/tank by bath challenge. PBL from non-infected and infected fish were collected at different time points post infection. Expression was determined by real-time quantitative PCR and expressed relative to S11 protein of the 40S subunit. Data represent mean values of $n = 5$ time-zero controls, $n = 5$ infected fish and $n = 3$ time-point controls ($\pm$SD). Symbol '*' represents a significant difference as compared to non-infected controls at time-point zero. 'a' indicates a significant difference as compared to the non-infected time-point control.

time-point control. At the same time point, only for TNFα and CXCa, significantly elevated transcription levels were observed in the autologous control samples when compared to the respective non-infected time-point control.

Histological analysis

To investigate whether chemokine (CXCa) up-regulation of gene transcription could be related to increased transcription activity in leucocytes already present in the skin or to an increased number of leucocytes in the skin following infection we performed a histological analysis of the skin samples. Fig. 3B shows a massive infiltration of leucocytes at the site of infection. A large amount of inflammatory infiltrate can be observed not only in both the mildly hyperplastic epidermal and dermal tissues but also throughout the whole subcutaneous fatty layer. A very low number of leucocytes could be observed in the control skin samples (Fig. 3A).

Discussion

We investigated the immune response of common carp to freshwater lice from the genus *Argulus*. The most pronounced up-regulation of gene transcription was observed for the chemokine CXCa in the skin at 1—2 days post infection with larval *A. japonicus*. At the same time a massive infiltration of leucocytes, most likely neutrophilic granulocytes, at the site of infection could be observed in histological sections of the skin. At day 6 post infection immune gene transcription was up-regulated not only in the infected skin but also, although to a lesser extent, in autologous skin sample controls collected from non-infected spots of infected fish. This suggests that the response to *A. japonicus* larval stages is initially restricted to the site of infection but is extended to a generalized response throughout the skin as a whole organ at a later stage of the infection. In PBL, transcription levels of the investigated genes varied greatly in control fish, emphasizing the importance of time-point control samples for gene transcription studies.

During our experiment, the first visible red, inflamed spots were not observed until approximately 2 days post infection, despite the attachment of several larval lice to the skin of exposed fish as early as 2 h post infection. In other experiments, the first notable response to argulid infestations, observed as small red areas (up to several mm in diameter), has been noted even within a few hours post infection [7]. Although we could confirm infection
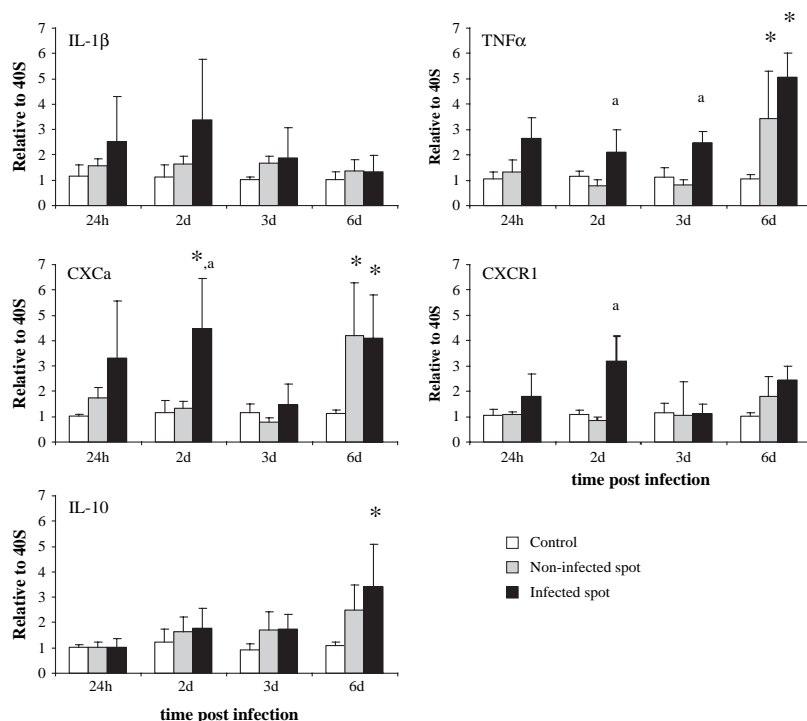
CHAPTER 3

Figure 2 Kinetics of gene expression in skin after *Argulus japonicus* infection of common carp (*Cyprinus carpio* L.). Fish were exposed to 150 larval parasites/tank by bath challenge. Skin samples were collected at different time points post infection from non-infected fish, non-infected spots of infected fish (autologous control) and infected spots of infected fish. Expression was determined by real-time quantitative PCR and expressed relative to S11 protein of the 40S subunit. Data represent mean values of $n = 5$ infected fish and $n = 3$ time-point controls ($\pm$SD). Symbol '*' represents a significant difference as compared to the non-infected time-point control. 'a' indicates a significant difference as compared to the autologous control.

for each individual fish, the infection pressure in our experiment was relatively mild as shown by a mean infection intensity of 3.8 attached parasites per fish. Further, we chose to investigate the immune response to larval rather than juvenile or adult lice. Adult argulids are quite mobile being able to glide over the surface of their hosts with relative ease using their maxillary suckers [18]. This can result in multiple sites of infection on the same host being caused by one parasite at different times. However, larval stages tend to be less mobile and remain relatively stationary, anchoring themselves to their hosts integument via the use of their hook-like second antennae [7]. *Argulus* spp. cause direct damage to the fish skin through their attachment and feeding mechanisms although, typically, the craters do not penetrate much deeper than the epidermis [19]. Skin damage is the result of mechanical actions of the maxillary suckers in adult lice and hooks or spines in larval and juvenile stages and the sharp mandibles. In addition, damage results from various toxins or digestive enzymes secreted via the pre-oral stylet and labial spines [20].

Two days post infection, levels of CXCa transcripts were up-regulated in skin samples collected at the sites of infection (infected spots), and were significantly different from the levels measured in skin isolated not only from non-infected control fish but also from autologous skin samples collected from non-infected spots of infected fish. At the same time point, TNFα and CXC receptor-1 (CXCR1) transcription were found to be up-regulated with respect to the autologous control. In comparison to the response observed 1–2 days post infection, at 6 days post infection a clear up-regulation of CXCa, TNFα and, to a lesser extent, that IL-10 transcripts was observed in skin samples collected from both infected and non-infected spots of the infected fish. These results indicate that whilst the immune response to *A. japonicus* larval stages (2 days post infection) is restricted to the site of infection, the response to juvenile stages (6 days post infection) is extended throughout the skin as a whole organ. For *A. japonicus*, in fact, a succession of moults takes place approximately every 5 days, depending on the ambient temperature [21]. It is likely, also during our experiment, after 5 days *A. japonicus* larval stages started to moult and migrate over the skin of the fish host. This would explain why the change in gene expression profile was comparable, although smaller, between autologous skin sample controls and infected samples.
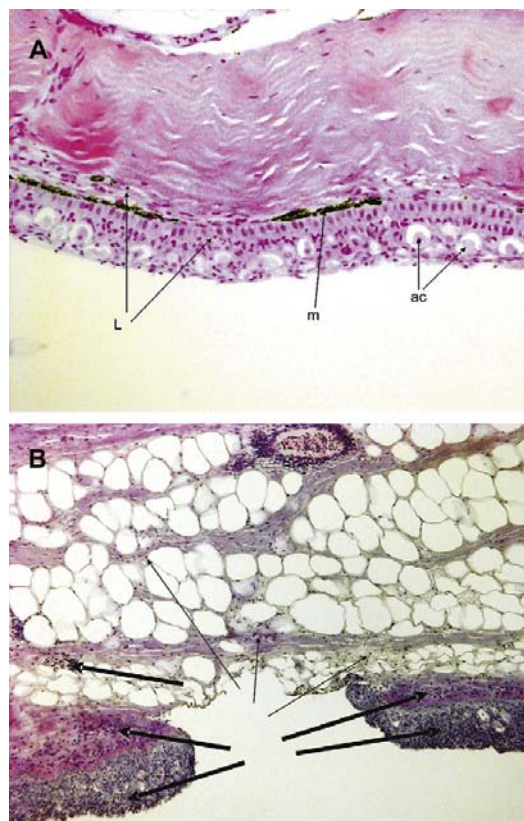
Figure 3 Histological analysis of carp skin. (A) Skin sample from a control, non-infected fish. Note that there are only a few scattered leucocytes and no inflammation of the tissues (magnification = 1000×), L = leucocytes, m = melanophores and ac = club cells. (B) Skin sample from *Argulus japonicus* infected fish. Infected spot collected 2 days p.i. at the site of parasite feeding. A crater can be observed in the epidermis and apical part of the dermis. A high degree of leucocyte infiltration can be observed in both the mildly hyperplastic epidermal and dermal tissues (thick arrows) and a large number of leucocytes can also be seen dispersed throughout the subcutaneous fatty layer (thin arrows). Note the leucocytes dispersing from the blood vessel at the top of the image (magnification = 300×).

The observed results are suggestive of migrating *A. japonicus* affecting the skin as a whole organ.

In contrast to the results obtained after the analysis of the skin samples, changes in gene expression in samples collected from PBL were found to be significantly different only when compared to the controls at time zero, indicating the vital importance of time-point controls when employing RT-qPCR analyses of gene expression, at least in PBL. The same PBL samples were used for a flow cytometric analysis (unpublished data) using antibodies directed against carp macrophages [22] and granulocytes [23]. In this flow cytometer experiment we found a very high fish-to-fish variation not only between infected but also between non-infected individuals, confirming the importance of proper time-point controls, especially when analyzing PBL.

In the present study we show an up-regulation of the chemokine CXCa in the skin of common carp exposed to larval *A. japonicus* at 1—2 days post infection. Although at the same time-point transcription of the chemokine receptor CXCR1 and the cytokines IL-1β and TNFα seemed to be up-regulated, these changes were not significantly different from the non-infected controls. Although not significant owing to the large individual variation, these changes might reflect a biologically relevant phenomenon. The same immune genes (CXCa, CXCR1, IL-1β), in fact, were up-regulated in carp skin 1.5—2 days after infection with the ectoparasite *Ichthyophthirius multifiliis* [13]. The chemokine CXCa and the chemokine receptor, CXCR1, have been implicated as factors stimulating the migration of neutrophilic granulocytes towards sites of infection [24]. We noticed an increase in the number of infiltrating leucocytes, most likely neutrophilic granulocytes, at sites of skin damage in histological sections of carp skin infected by *A. japonicus*. This would suggest a correlation between up-regulation of CXCa (CXR1) and the migration of neutrophilic granulocytes. Recently, a study in carp skin on the changes in gene transcription induced purely by mechanical injury reported an up-regulation of the same set of genes: CXCa, CXCR1, IL-1β and to a lesser extent TNFα 2—3 h after injury [25]. In the latter study also migrating neutrophils were observed in histological sections of the damaged skin. In general, the results of tissue damage are recognized at the cell level via receptor-mediated detection of intracellular proteins (alarmins) released by dead cells. Not only endogenous alarmins but also exogenous pathogen-associated molecular patterns (PAMPs) convey similar (immune) responses and can be considered subgroups of a larger set, the damage-associated molecular patterns (DAMPs) [26]. The CXCa, CXCR1 and IL-1β genes especially seem to be part of a set of immune genes in fish that are commonly induced by DAMPs.

We aimed to design an optimal animal experiment by using a mild pathogen load mimicking a natural situation where both the host and parasite are anticipated to co-exist and survive. We used time-point controls for both the skin and PBL samples. These time-point controls were shown to be essential since differences in transcription levels noted especially in the PBL samples were significant only when compared to the controls at time-point zero. In addition, we used autologous skin samples as controls for infected spots from the same fish whose approach was shown to be highly informative, especially at later time points. In conclusion, we demonstrate that in the skin of carp exposed to larval/juvenile *A. japonicus* up-regulation of gene transcription for the chemokine CXCa and to a lesser extent the chemokine receptor CXCR1 and the cytokines IL-1β and TNFα are good indicators of parasite-induced skin damage. Up-regulation of gene transcription corresponded well with an increase in leucocyte numbers, possibly neutrophilic granulocytes, in skin samples collected at the sites of infection.

CHAPTER 3

Acknowledgements

References

[1] Boxshall GA, Defaye D. Pathogens of wild and farmed fish – sea lice. Francis: Chichester, UK; 1993.

[2] Johnson SC, Albright LJ. The developmental stages of *Lepeophtheirus salmonis* (Krøyer, 1837) (Copepoda: Caligidae). Can J Zool 1991;69:929–50.

[3] Krkošek M, Lewis MA, Volpe JP. Transmission dynamics of parasitic sea lice from farm to wild salmon. Proc R Soc Lond Ser B Biol Sci 2004;272:689–96.

[4] Nolan DT, van der Salm AL, Wendelaar Bonga SE. The host–parasite relationship between the rainbow trout (*Oncorhynchus mykiss*) and the ectoparasite *Argulus foliaceus* (Crustacea: Branchiura): epithelial mucous cell response, cortisol and factors which may influence parasite establishment. Contrib Zool 2000;69:57–63.

[5] Wells A, Grierson CE, MacKenzie M, Russon IJ, Reinardy H, Middlemiss C, et al. Physiological effects of simultaneous, abrupt seawater entry and sea lice (*Lepeophtheirus salmonis*) infestation of wild, sea-run brown trout (*Salmo trutta*) smolts. Can J Fish Aquat Sci 2006;63:2809–21.

[6] Van der Salm AL, Nolan DT, Spannings FAT, Wendelaar Bonga SE. Effects of infection with the ectoparasite *Argulus japonicus* (Thiele) and administration of cortisol on cellular proliferation and apoptosis in the epidermis of common carp *Cyprinus carpio* (L.) skin. J Fish Dis 2000;23:173–84.

[7] Walker PD, Flik G, Wendelaar Bonga SE. The biology of parasites from the genus *Argulus* and a review of the interactions with its host. In: Wiegertjes GF, Flik G, editors. Host–parasite interactions. Abingdon, UK: Garland/BIOS Scientific Publishers; 2004. p. 107–29.

[8] Iger Y, Lock RA, van der Meij JC, Wendelaar Bonga SE. Effects of water-borne cadmium on the skin of the common carp (*Cyprinus carpio*). Arch Environ Contam Toxicol 1994;26: 342–50.

[9] Lindenstrøm T, Buchmann K, Secombes CJ. *Gyrodactylus derjavini* infection elicits IL-1beta expression in rainbow trout skin. Fish Shellfish Immunol 2003;15:107–15.

[10] Lindenstrøm T, Secombes CJ, Buchmann K. Expression of immune response genes in rainbow trout skin induced by *Gyrodactylus derjavini* infections. Vet Immunol Immunopathol 2004;97:137–48.

[11] Sigh J, Lindenstrøm T, Buchmann K. The parasitic ciliate *Ichthyophthirius multifiliis* induces expression of immune relevant genes in rainbow trout, *Oncorhynchus mykiss* (Walbaum). J Fish Dis 2004;27:409–17.

[12] Sigh J, Lindenstrøm T, Buchmann K. Expression of pro-inflammatory cytokines in rainbow trout (*Oncorhynchus mykiss*) during an infection with *Ichthyophthirius multifiliis*. Fish Shellfish Immunol 2004;17:75–86.

[13] Gonzalez SF, Buchmann K, Nielsen ME. Real-time gene expression analysis in carp (*Cyprinus carpio* L.) skin: inflammatory responses caused by the ectoparasite *Ichthyophthirius multifiliis*. Fish Shellfish Immunol 2007;22:641–50.

[14] Irnazarow I. Genetic variability of Polish and Hungarian carp lines. Aquacult Res 1995;129:215–9.

[15] Tam Q, Avenant-Oldewage A. The digestive system of larval *Argulus japonicus* (Branchiura). J Crustacean Biol 2006;26: 447–54.

[16] Pfaffl MW. A new mathematical model for relative quantification in real-time RT-PCR. Nucleic Acids Res 2001;29:e45.

[17] Tichopad A, Dilger M, Schwarz G, Pfaffl MW. Standardized determination of real-time PCR efficiency from a single reaction set-up. Nucleic Acids Res 2003;31:122.

[18] Kearn GC. Leeches, lice and lampreys: a natural history of skin and gill parasites of fishes. Dordrecht: Springer; 2004.

[19] Lester RJG, Roubal F. Phylum Arthropoda. In: Woo PTK, editor. Fish diseases and disorders. Wallingford, UK: CAB International; 1995. p. 475–598.

[20] Shimura S, Inoue K. Toxic effects of extract from the mouthparts of *Argulus coregoni* Thorell (Crustacea: Branchiura). Bull Jpn Soc Sci Fish 1984;50:729.

[21] Fryer G. The parasitic Copepoda and Branchiura of British freshwater fishes: a handbook and key. Freshwater Biological Association, Scientific Publications; 1982.

[22] Weyts FAA, Rombout JHWM, Flik G, Verburg-Van Kemenade BML. A common carp (*Cyprinus carpio* L.) leucocyte cell line shares morphological and functional characteristics with macrophages. Fish Shellfish Immunol 1997;7: 123–33.

[23] Nakayasu C, Omori M, Hasegawa S, Kurata O, Okamoto N. Production of a monoclonal antibody for carp (*Cyprinus carpio* L.) phagocytic cells and separation of the cells. Fish Shellfish Immunol 1998;8:91–100.

[24] Huising MO, Stolte E, Flik G, Savelkoul HF, Verburg-van Kemenade BML. CXC chemokines and leukocyte chemotaxis in common carp (*Cyprinus carpio* L.). Dev Comp Immunol 2003;27:875–88.

[25] Gonzalez SF, Huising MO, Stakauskas R, Forlenza M, Verburg-van Kemenade BML, Buchmann K, et al. Real-time gene expression analysis in carp (*Cyprinus carpio* L.) skin: inflammatory responses to injury mimicking infection with ectoparasites. Dev Comp Immunol 2007;31:244–54.

[26] Bianchi ME. DAMPs, PAMPs and alarmins: all we need to know about danger. J Leukoc Biol 2007;81:1–5.

CHAPTER

4

SVCV

Transcription of signal-3 cytokines,
IL-12 and IFNαβ, coincides with the timing
of CD8αβ up-regulation during viral
infection of common carp (*Cyprinus carpio*)

Maria Forlenza, João D.A. de Cavalho Dias, Tomas Veselý,
Dagmar Pokorová, Huub F.J. Savelkoul and Geert F. Wiegertjes

ERRATUM: please refer to the figure below for Figure 1 in this manuscript.

```
                      Leader                        IgSf domain   CDR1
carp1       --------MKQICIGFFVI--------------LSLFNGNFANTIYQEGQAVPVNCDTKQPG--VITFWFKIN-TSGAK- 54
carp2       --------.Y.......M.--------------.....G.G..DNVFE...E.T.D..P....-....Q..-R..P.- 54
goldfish1-1 MSALRIEN.N......C.--------------....S.....IA.KN..E.L.D..P..A.--.....Q.K-...P.- 62
goldfish2-1 --------.Y....V...-------------....D.G..DNV.K..EE.T...........-......Q..-K.SL.- 54
zebrafish   --------.Y.......C.-------------....Y.-CSANFH..NST.A...NP.TS.--T...M.Q..-ST..N- 53
rb.trout    ---MKMVQKWMQTLVLLFF-------------CQETLQLSSL.EKTD.ER.EIT.APVSKTKSNMVI..RVQDNA.ME- 62
salmon      ---MKMVRKWMETLVLLFF-------------CQETLQLSSL.EKTD.ER.EIT.APVSKTKSNMVI..RVQDNA.ME- 62
human       ---MALPVTALLLPLALLL--------HAARPSQ--.RVSPLDRTWNL.ET.ELK.QVLLSNPTSGCS.LFQ-PRGA.AS 66
mouse       ---MASPLTRFLSLNLLLLGESIILGSSGEAKPQAPELRIFPKKMDAEL..K.DLV.EVLGS-VSQGCS.LFQ.SS.KLPQ 76

              CDR2                    IgSf V domain              CDR3
carp1       --YLFTVKGTDVKVNAD-----VAKYK--VNKSGKVSLAIQSFNKKTDSGFYTCA-AMNNNKLIFGELTEINGEPDPTIS 124
carp2       --.......S...RA.V.-----WT...--..TN..........Q......L..-.....R.....VK..K.K..LVTP 124
goldfish1-1 --.......A...S.T.-----KQ..I--.KTG........N...E.........-....S.Q.M...M...I.Q....T. 132
goldfish2-1 --.......S.EI.A..-----PK...--.QNA..........E.N.........A.GV......F..K.Q...VSQ 124
zebrafish   --C.LIA.Q.E..H..N-----SK..SGHIDSN.NLNVK.K..A.R....L.V..-T......F...V.K.Q.V...VTQ 125
rb.trout    --FIASFSTK.GMKKT-----DFNNEVFSEEQIN.NI.ILKA.K.AR...V.S..-SI.G.A.V...V.RLA.PAPM.TT 134
salmon      --FIASFSTK.GTKKT-----DFNNEVFSEEQIN.NI.ILKA.K.AR...V.S..-SI.G.A.V...V.RLA.PAPT.TT 134
human       PTF.LYLS--QN.PK.AEGLDTQR-FSGKR-LGDTFV.TLSD.RRENE-.Y.F.S-.LS.SIMY.SHFVPVFLPAK..TT 130
mouse       PTFVVYMASSHN.ITW.EKLNSSKLFSAMRDTNN.YV.TLNK.S.ENE-.Y.F.S-VIS.SVMY.SSVVPVLQKVNS.TT 154

                  Hinge region        TM                    CY
carp1       ----PPKIAP-LPSTTT-MATTKSQCKCPK-----QGKPSINCEIWILSSLASGCVLLLILLIITILYCNRLRTRFCPH-H 193
carp2       ----...KD.ER.K.A.PVI...PP...Q.Q----DP......T......VA..GV......F.............. 196
goldfish1-1 ----S.T...-.......-T...P...I...-----KV.S..................................... 200
goldfish2-1 ----...EETAP.T..SPVI.....N.K.P----DP..I...T.......A..GV......F..H............ 196
zebrafish   ----G..MIQTTLKPVVKTTMI.-..V.D.K----GA..MFK..T..FT..VG..G.F.V...A..V.......... 196
rb.trout    ----TTTTTPMTTTIELTSS..AKS..------VGKVD.TAS..LIVWAP.TA..GF.FL.....VCH...I..K.... 204
salmon      ----TTTTTPMTTAIELTSS..AKS..-------VGKVD.TAS.DLIVWAP..A..GF..L..L..VCH....I..K.... 204
human       -PAPR.PTPA-PTIASQPLSLRPEA.RPAAGGAVHTRGLDFA.D.Y.WAP..GT..GV..LS.V..LYCNH.N.R.V..KCP 218
mouse       KPVLRTPSPVHPTG.SQPQ--RPED.RPR--GSVKGTGLDFA.D.Y.WAP..GI..A..LS....LICYH.S.K.V..KCP 230

carp1       YKRQPR--PAGHAKLPNNHF-- 211
carp2       N.....--............-- 214
goldfish1-1 ......--............-- 218
goldfish2-1 ......--.......T..PL-- 214
zebrafish   ......GP......M..S..-- 216
rb.trout    ......MAAP.QQHPIA.NRLF 226
salmon      ......MAAP.QQHPIA.NRLF 226
human       ---R.VVKSGDKPS.SARYV-- 235
mouse       ---R.LVRQE.KPRPSEKIV-- 247
```
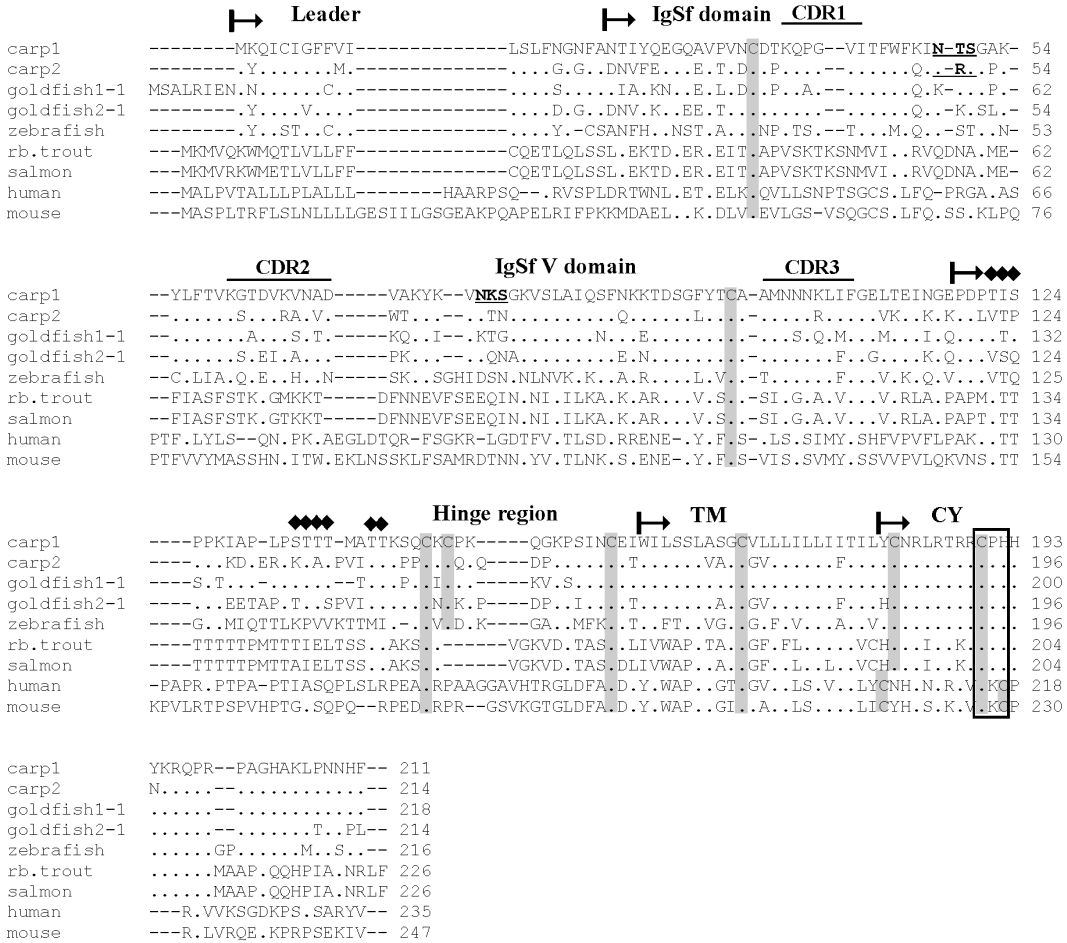
Fig. 1. Clustal W alignment of amino acids from CD8α chain precursors. Regions corresponding to the putative leader, IgSf V domain, hinge, transmembrane (TM), and cytoplasmatic (CY) region in the European common carp (Cyprinus carpio carpio) sequences are shown in bold above the sequence. Each region border is indicated by right arrows. Dots indicate identities to the carp CD8α1 (carp1) sequence and dashes denote gaps used to maximize the alignment. The Complementary Determining Regions (CDRs), designated based on the human sequence, are indicated by overlining the carp sequence. Predicted N-glycosilation sites are underlined and bold in the carp sequence. Conserved cystein residues are shaded in grey; (♦) possible O-linked glycosilation sites (S or T) for carp. The boxed region represents a conserved cytoplasmic domain in teleosts which corresponds to the region comprising the lck binding motif found in mammals. GenBank Accession nos.: goldfish (Carassius auratus, AB186395; AB186397); zebrafish (Danio rerio, AB186400); rainbow (rb) trout (Oncorhynchus mykiss, AF178053); Atlantic salmon (Salmo salar, AY693393); human (Homo sapiens, NP001759); mouse (Mus musculus, XP132621).

ELSEVIER

Transcription of signal-3 cytokines, IL-12 and IFNαβ, coincides with the timing of CD8αβ up-regulation during viral infection of common carp (*Cyprinus carpio* L.)

Maria Forlenza [a], João D.A. de Carvalho Dias [a], Tomas Veselý [b], Dagmar Pokorová [b], Huub F.J. Savelkoul [a], Geert F. Wiegertjes [a,*]

[a] *Department of Animal Sciences, Cell Biology and Immunology Group, Wageningen Institute of Animal Sciences, Wageningen University, P.O. Box 338, 6700 AH, Wageningen, The Netherlands*
[b] *Veterinary Research Institute, Hudcova 70, 621 32 Brno, Czech Republic*

Abstract

Mammalian naïve CD8^{+} T cells are activated by antigen (signal 1) and CD28 costimulation (signal 2) to undergo several rounds of cell division, but programming for survival, effector function and memory requires a third signal that can be provided by IL-12 and/or type I interferons. Functional studies indicate that the route of antigen presentation and costimulation are conserved from fish to mammals. However, the potential of IL-12 and IFNαβ to act as signal-3 cytokines in infections inducing a CTL response has not been examined in fish. We report the cloning of CD8α and CD8β homologues, each present in duplicate copies and of two TCR-Cα isoforms in European common carp. The identification of (cytotoxic) T cell marker sequences and the availability of sequences coding for the signal-3 cytokines in the same fish species, allowed us to investigate by RT-qPCR their kinetics of gene expression during viral and parasitic infection. Our results show that transcription of signal-3 cytokines occurred concomitantly with CD8αβ up-regulation exclusively at 4 days post-primary viral infection. No regulation of IL-12 and IFNαβ was observed after parasitic infection. Our data provide evidences for an evolutionary conservation of function for IL-12 and IFNαβ to act as third signal during CTL activation. In addition, we suggest that a CD8α2/β1 and a p35p40b association could be the preferred combinations for the formation of a functional CD8 co-receptor and an IL-12p70 heterodimer during viral infection. The relevance of our findings to future vaccination strategies in fish is discussed.
© 2007 Elsevier Ltd. All rights reserved.

Keywords: CD8; IL-12; Type I interferon; Cytotoxic T cells; Fish; Virus

1. Introduction

Mammalian naïve CD8^{+} T cells are activated by antigen (Ag, signal 1) and CD28 costimulation (signal 2) to undergo several rounds of cell division. However, programming for survival (i.e. clonal expansion), effector function and memory requires a third signal delivered by cytokines. These three signals together form the basis for CD8^{+} T cell-mediated immunity. The third signal is provided by interleukin (IL)-12 and/or type I interferons (IFNs), reviewed in (Mescher et al., 2006).

In fish, cytotoxic cells are allospecific (Fischer et al., 1998; Hasegawa et al., 1998; Boudinot et al., 2001) and their cytotoxic functions are restricted to MHC class I-matched target cells (Utke et al., 2007). The presence of fish homologues to TCR, CD3, CD8, CD28 and MHC-I, among others, suggests that the route of antigen presentation (signal 1), costimulation (signal 2) and thus, the mechanisms at the base of cell-mediated cytotoxicity are conserved from fish to mammals (Bernard et al., 2006a,b; Fischer et al., 2006). At present, CD8 gene expression is the best tool available to monitor cytotoxic T lymphocyte (CTL) activity in fish. For example, in trout, CD8α expression directly correlates with an increased antiviral cytotoxic activity against MHC class I-matched cells and with the induction of alloreactive cytotoxic cells, both *in vitro* and *in vivo*, after sensitisation with the allotarget (Fischer et al., 2003; Utke et al., 2007). In Ginbuna crucian carp TCRβ and CD8α kinetics of gene expression correspond well with second scale allografting (Somamoto et al., 2005) and with virus-specific cell-mediated

* Corresponding author.
E-mail address: geert.wiegertjes@wur.nl (G.F. Wiegertjes).

cytotoxic activity (Somamoto et al., 2006). However, despite the increase in information on T cell-mediated immune responses, coordinated studies on the signal-3 requirements for T cell-mediated immunity have not been performed in fish.

In mammals, signal-3 is provided by IL-12 and/or type I IFNs (Mescher et al., 2006) and acts as a switch that determines whether exposure to Ag results in tolerance or in full activation and development of memory (Hernandez et al., 2002; Curtsinger et al., 2003b). Effects of IL-12 and type I IFNs result from their direct action on CD8$^+$ T cells rather than on an indirect influence on levels of antigen or costimulatory molecules (B7-1 ligand) on antigen presenting cells (Curtsinger et al., 2003a, 2005). Recent *in vivo* studies suggest that the relative importance of IL-12 and/or IFNs to act as signal-3 cytokine is dependent on the type of response under examination. For example, in lymphocytic choriomeningitis virus infection, type I IFNs are the predominant third signal required to support the CD8$^+$ T cell response (Kolumam et al., 2005). In contrast, in acute vaccinia virus infection it is likely that both IL-12 and type I IFNs contribute to the CD8$^+$ T cell response (van Den Broek et al., 2000), while IL-12 alone provides the necessary third signal during allospecific CD8$^+$ T cell responses to transplants (Filatenkov et al., 2005).

In fish, the potential of IL-12 and IFNαβ to act as signal-3 cytokines in infections inducing a CTL response has not been examined. The involvement of type I IFN and IFN-induced genes (e.g. GTP*ase* Mx protein) has been shown in immune responses induced by dsRNA, CpGs or during *in vivo* viral infections, (Robertsen, 2006), but never in correlation with CD8 gene expression. The sequence for the European common carp (*Cyprinus carpio carpio* L.) type I interferon (designated as carp IFNαβ) has been described only very recently (Gonzalez et al., 2007). Sequences homologous to the mammalian IL-12p35 and IL-12p40 genes have been described for a number of fish species (Yoshiura et al., 2003; Huising et al., 2006; Nascimento et al., 2007) but only few studies on the function of fish IL-12 have been performed. *In vitro*, IL-12 regulation is seen in macrophages after stimulation with, e.g. poly(I:C), LPS, Con A and PMA (Yoshiura et al., 2003; Huising et al., 2006). In carp, three highly distinct IL-12p40 genes (named IL-12p40a, IL-12p40b and IL-12p40c) were described and their *in vitro* expression profiles differed profoundly (Huising et al., 2006). In sea bass, up-regulation of IL-12p40 expression, but not IL-12p35, was observed *in vivo* after injection of UV-killed but not live bacteria. In the latter case a more prominent up-regulation of IL-1β was observed (Nascimento et al., 2007).

In the present study, we report the cloning of four cDNA sequences coding for two CD8α and two CD8β genes in the European common carp. The CD8β sequences are the first reported so far in a cyprinid species. Two sequences coding for the constant domain of the TCRα chain are also cloned. The identification of sequences coding for the signal-3 cytokines, IL-12 and type I IFN, as well as for (cytotoxic) T cell markers in the same fish species, allowed us to investigate their kinetics of gene expression during primary and secondary infection of carp with spring viraemia of carp virus (SVCV) (Ahne et al., 2002). To further investigate whether signal-3 cytokines would play a role in infections other than viral, where a CTL response is not

required, we analysed IL-12 and IFNαβ gene expression during primary infection with the extracellular parasite *Trypanoplasma borreli*. Taken together, our results strongly suggest that both, IL-12 and IFNαβ signal-3 cytokines might be required exclusively during primary viral, but not parasitic infection, when also up-regulation of CD8 transcription is observed. The implications of our findings for future vaccination strategies are discussed.

2. Materials and methods

2.1. Animals

European (*C. carpio carpio*) and East-Asian (*C. carpio haematopterus*) common carp diverged more than 500,000 years ago (Kohlmann et al., 2003; Zhou et al., 2003; Thai et al., 2004) and both subspecies are commonly studied in fish research. In the present study, European common carp of the R3 × R8 strain which are the offspring of a cross between fish of Hungarian origin (R8 strain) and of Polish origin (R3 strain) were used (Irnazarow, 1995). In this study, we refer to the European common carp subspecies as carp, unless stated otherwise. Carp were bred in the central fish facility of Wageningen University, The Netherlands, and raised either in this facility or at the Veterinary Research Institute (VRI), Brno, Czech Republic, in recirculating UV-treated water and fed pelleted dry food (Trouvit, Nutreco) daily. Al studies were performed with the approval of the animal experimental committee of Wageningen University.

2.2. Identification of carp CD8α and CD8β cDNAs

Degenerate primers (Table 1) were designed on conserved regions of known fish CD8α and CD8β sequences (GenBank Accession nos. CD8α: AAF32266; AAW33878; BAD89371–BAD89374; 001015040; CD8β: AY563420; AY693392; AY701524). (Anchored) PCR was performed on a λgt10 cDNA library of carp thymus. The library was constructed using mRNA isolated from ten 5-month-old individuals of a second generation gynogenetic European common carp line (van Erp et al., 1996). Aliquots (300 ng) of the library were combined in Taq buffer with 1 U Taq polymerase (Goldstar, Eurogentec S.A., Seraing, Belgium), MgCl$_2$ (1.5 mM), dNTPs (200 μM) and primers (400 nM each) in a total volume of 50 μl. The PCR was performed using a GeneAmp PCR system 9700 (PE Applied Biosystems, Foster City, CA, USA) under the following conditions: 4 min at 94 °C, followed by 35 cycles of 30 s at 94 °C, 30 s at 55 °C and 2 min at 72 °C, finally an extension step of 7 min at 72 °C was performed. Degenerate primers, CD8α.FW4 and CD8α.RV5, were used in combination to amplify a product with 82–91% of identity with other known cyprinid CD8α1 sequences. The specific primer cycaCD8α.FW3 was used in combination with λgt10.RV specific primer for the amplification of CD8α 3′UTR. Similarly, cycaCD8α.RV3 in combination with λgt10.FW primer was used for the amplification of the 5′ UTR. The second reaction led to the amplification of a second CD8α sequence.

A similar strategy was used to amplify the CD8β gene. Degenerate primers CD8β.FW1, CD8β.FW2 were used as

Table 1
Primers used in (anchored) PCR and RACE PCR

Primer	Sequence 5′ → 3′	Position[a]
λgt10.FW	TTGAGCAAGTTCAGCCTGGTTAAG	
λgt10.RV	GGCTTATGAGTATTTCTTCCAGGG	
T7	TAATACGACTCACTATAGGG	
SP6	TTCTATAGTGTCACCTAAAT	
CD8α.FW4	AATTMWWGGASWACCAGATCCA	420[b]
CD8α.RV5	GTGRGGACATCGTCTTGTTCTT	611[b]
cycaCD8α.FW3	AATGGCTACGACAAAATCAC	484
cycaCD8α.RV3	GAGGAGAAGAACACAACCAG	553
cycaCD8α1.RV1	GCCATTGTTGTTGTCGATGGTA	448
cycaCD8α1.RV8 (nested)	TTTGTTCACTTTGTATTTTGCAAC	264
cycaCD8α2.RV1	CGTAATCACTGGTGTTGCAGTT	458
cycaCD8α2.RV8 (nested)	TGTGTTCACTTTGTATTTTGTCCA	274
cycaCD8α1/2.FW1	TGCGCAGCCATGAACAACAATA	373
cycaCD8α1.FW8 (nested)	GATGTAAAGGTTAATGCTGATGTTG	268
cycaCD8α2.FW8 (nested)	GATGTAAGGGCTAATGTTGATTGGA	278
CD8β.FW1	YGRCWCAGARRKYSTSAMCTGTGA	200[b]
CD8β.FW2 (nested)	ACRACWMCRSYTTYCAGTTCC	292[b]
CD8β.RV1	ATGCGCAGKKTGWARGMCACCTT	394[b]
CD8β.RV2 (nested)	TCCTGYATGYTYCARARCCARAAA	454[b]
cycaCD8β.FW4	ACCCTCTCTTGCATGTGCTT	57
cycaCD8β1.RV6	GGGTTTGCAATTACAGGTCTTCTTG	484
cycaCD8β1.RV5 (nested)	CGCTCTCTGCCAGCGCTGTTACA	245
cycaCD8β2.RV6	GGGTTTGCAATTACAGATCTTCACA	497
cycaCD8β2.RV5 (nested)	TTCTCTGCCAGCACTGTTGAC	258
cycaCD8β1.FW6	CAACAGTTAAGACCAAGACACCCAA	487
cycaCD8β1.FW7 (nested)	CACACTCTTCATGTCAAACAAATCTG	701
cycaCD8β2.FW6	TAACTGTCAAGACCAAGAAACCTGT	500
cycaCD8β2.FW7 (nested)	CACGCTTCATGTTGAAACAAATGCA	715
cycaTCRα1.FW1	TAGAACCACCAGCCTTTTAC	20
cycaTCRα2.FW2	GATGCTGTAAAATTCCAAAAC	21

[a] 3′ position of the primer on the corresponding European common carp sequence.
[b] 3′ position based on the complete European common carp CD8α1 or CD8β1 sequence.

external and nested primers in two successive rounds of anchored-PCR in combination with λgt10.RV specific primer for the amplification of putative CD8β 3′UTR. Similarly CD8β.RV1 and CD8β.RV2 were used as external and nested primer for the amplification of 5′UTR. The second reaction led to the amplification of a second CD8β sequence. The specific primer cycaCD8β.FW4 was used in combination with λgt10.RV to confirm the presence of both isoforms. Based on the obtained partial sequences new specific primers were designed and used to obtain the full length mRNA sequences of carp CD8α and CD8β (Table 1).

2.3. Identification of carp TCR-Cα1 and TCR-Cα2 cDNA

Based on previously described sequences coding for the constant region (Cα) of the TCR gene in East-Asian common carp (GenBank Accession nos.: AB120613 [Cα1], AB120620 [Cα2a], AB120621 [Cα2b]), primers were designed to amplify the corresponding cDNA regions in the European common carp (Table 1). CycaTCRα1.FW1 and cycaTCRα2.FW2 were used in combination with λgt10.RV primer in order to amplify the constant regions of the respective genes. PCR conditions were as described for the identification of carp CD8 genes.

2.4. Rapid amplification of cDNA ends (RACE)

Full length carp CD8α and CD8β mRNA sequences were obtained by RACE (GeneRacer™, Invitrogen, Breda, The Netherlands) according to the manufacturer's instructions. Total RNA (1 μg) isolated from the thymus of a single 9-month-old individual of the R3 × R8 strain was used as template and reverse transcribed using the SuperScript™ III RT and the GeneRacer Oligo dT primer. For the 5′ or 3′ RACE-PCR 2 μl of the obtained cDNA was combined with Taq buffer, 1.75 U Expand High Fidelity Taq polymerase (La Roche, Germany), MgCl$_2$ (1.5 mM), dNTPs (200 μM) and primers (400 nM each) in a total volume of 50 μl. The PCR was performed using a GeneAmp PCR system 9700 under the following conditions: 2 min at 94 °C, followed by 6 cycles of 30 s at 94 °C, 2 min at 72 °C, 6 cycles of 30 s at 94 °C, 2 min at 70 °C, 26 cycles of 30 s at 94 °C, 30 s at 55 °C or 58 °C and 2 min at 72 °C, finally an extension step of 10 min at 72 °C was performed. Primers used for the RACE-PCR are listed in Table 1. Specific primers cycaCD8α1.RV1, cycaCD8α1.RV8 or cycaCD8α2.RV1, cycaCD8α2.RV8 were used as external and nested primers in two successive rounds of anchored-PCR and led to the amplification of the complete 5′ UTRs of both CD8α

isoforms. Similarly, cycaCD8α1/2.FW1, cycaCD8α1.FW8 or cycaCD8α1/2.FW1, cycaCD8α2.FW8 specific primers were used for the amplification of the complete 3′ UTRs. A similar strategy was used to amplify the complete CD8β gene. Specific primers cycaCD8β1.RV6, cycaCD8β1.RV5 or cycaCD8β2.RV6, cycaCD8β2.RV5 were used as external and nested primers in two successive rounds of anchored-PCR and led to the amplification of the complete 5′ UTRs of both CD8β isoforms. Similarly cycaCD8β1.FW6, cycaCD8β1.FW7 and cycaCD8β2.FW6, cycaCD8β2.FW7 specific primers were used for the amplification of the complete 3′ UTRs.

2.5. Cloning, sequencing and protein analysis

Products amplified by PCR were ligated and cloned in JM109 cells using the pGEM-T easy kit (Promega, Leiden, The Netherlands) according to the standard protocol. Positive clones were selected by blue-white screening on agar plates containing 100 μg/ml Ampicillin. At least eight clones for each PCR product were selected for subsequent colony-PCR using T7 and SP6 plasmid-specific primers. A standard PCR program was performed as described for the identification of carp CD8 genes. From each PCR product both strands were sequenced using the ABI Prism Big Dye Terminator Cycle Sequencing Ready Reaction kit and analysed using a 3730 DNA analyser. Nucleotide sequences were translated using the ExPASy translate tool (http://us.expasy.org/tools/dna.html) and aligned with Clustal W and BLAST software (http://www.ebi.ac.uk/clustalw and http://www.ncbi.nlm.nih.gov/BLAST). The signal peptide cleavage site and the transmembrane region were predicted by using the SignalP 3.0 (http://www.cbs.dtu.dk/services/SignalP/) and the TMHMM 2.0 (http://www.cbs.dtu.dk/services/TMHMM-2.0/) servers. Post-translational modifications were predicted using the NetOGlyc 3.1 (http://www.cbs.dtu.dk/services/NetOGlyc/) and the NetNGlyc 1.0 (http://www.cbs.dtu.dk/services/NetNGlyc/) servers.

2.6. Viral infection of carp

Spring viraemia of carp virus (SVCV) strain CAPM V 539 (Koutna et al., 2003) was propagated in EPC (Epithelioma Papulosum Cyprini, (Fijan et al., 1983)) cells at 15 °C. Cells were grown in Eagle′s Minimal Essential Medium (MEM) containing 2% fetal bovine serum (FBS) and standard concentration of antibiotics. The virus titers, given as tissue culture infective dose (TCID$_{50}$/ml), were calculated by the method of Reed and Muench (1938).

Ten-month-old carp were raised at 15 °C to an average weight of 30–40 g. This temperature is optimal for SVCV infectivity (Ahne et al., 2002). Fish ($n = 110$) were exposed, by immersion, to SVCV-infected tissue culture (10^3 TCID$_{50}$/ml) for 2 h. Control fish ($n = 62$) were treated similarly and exposed to control cultures only. Infected fish were divided over two replicate tanks for subsequent blood and tissue sampling. At 0, 6 h, 1 day, 2 days, 4 days, 7 days, 2 weeks, 3 weeks and 4 weeks post-infection (p.i.), six fish were killed to collect blood and tissue samples. Eight weeks after the first infection, survivors ($n = 74$)

were reinfected using the same conditions as for the primary infection and divided over two replicate tanks. Samples were taken at the same time points and from the same number of fish as after the primary infection. Control fish were exposed to control cultures only. Infection of carp with SVCV was performed at the central fish facility of the Veterinary Research Institute (VRI), Brno, Czech Republic.

2.7. Parasitic infection of carp

T. borreli was cloned and characterized before (Steinhagen et al., 1989) and maintained by syringe passage through carp. Parasites were monitored in blood (10× diluted in RPMI 1640 (Cambrex, Verviers, Belgium) adjusted to 270 mOsmol kg^{-1}, cRPMI) using a Bürker counting chamber. The minimum detection limit of this method was 10^5 parasites/ml of blood.

Six-month-old carp were raised at 23 °C to an average weight of approximately 160 g, and acclimatized for 2 weeks to 20 °C. This temperature is optimal for parasite growth (unpublished data). Fish ($n = 90$) were anaesthetised in 0.3 g/l Tricaine Methane Sulfonate (TMS, Crescent Research Chemicals, Phoenix, USA) and intra-peritoneally (i.p.) injected with a dose of 10^4 parasites/fish, PBS-injected individuals served as unchallenged control group. Infected and non-infected fish were equally divided over 6 tanks. Infected fish were distinguished from the controls by a tattooed number. At 0, 1, 3, 10 days, 3, 4, and 6 weeks, $n = 5$ infected and $n = 3$ control fish were killed to collect blood and tissue samples. Infection of carp with T. borreli was performed at the central fish facility of the Wageningen University, The Netherlands.

2.8. Organ and peripheral blood leukocytes (PBL) isolation

Fish were killed by an overdose of TMS. Fish were bled by puncture of the caudal blood vessel. After viral infection, organs were collected and immediately transferred to RNAlater (Ambion, Inc., Austin, USA). Following an overnight incubation at 4 °C the samples were stored at −20 °C until use. Alternatively, after parasitic infection organs were snap frozen in liquid nitrogen and stored at −80 °C until use.

For blood collection, carp were anaesthetised in 0.3 g/l TMS. Blood was collected by puncture of the caudal blood vessel and diluted 1:1 with cRPMI medium containing 50 IU/ml of heparin (Leo Pharmaceutical products, Weesp, The Netherlands). After centrifugation at $600 \times g$ for 10 min, the buffy-coat containing the leukocytes was collected and layered on 5 ml of Ficoll-Paque^{TM} Plus (Amersham Biosciences, Uppsala, Sweden). Following subsequent centrifugation at $800 \times g$ for 25 min, the leukocyte layer at the interface was collected and washed three times with cRPMI. Cell pellets were collected and either stored in RNAlater, directly lysed prior to RNA isolation or immediately used for magnetic activated cell sorting.

2.9. Magnetic activated cell sorting (MACS)

After Ficoll separation, PBL were collected and washed twice in cRPMI. The primary antibody (WCI-12) was added

in a 1:50 dilution and incubated for 30 min on ice. WCI-12 is a mouse monoclonal antibody directed against the heavy chain of carp IgM and was used to separate IgM bearing cells (Koumans-van Diepen et al., 1995). Next, the cells were washed twice with MACS-buffer (0.5% BSA in cRPMI). The secondary antibody (phycoerythrin (PE)-conjugated goat anti-mouse, DAKO, Glostrup, Denmark) was then added in a 1:50 dilution and incubated for 30 min on ice. After extensive washing, total cell number was determined with a Bürker chamber, and 10 μl of magnetic beads (anti-PE Microbeads, Miltenyi Biotec, GmbH, Germany) was added per 1×10^8 cells. After incubation for 15 min at 4 °C, cells were washed and finally resuspended in MACS buffer. The magnetic separation was performed on LS-MidiMACS Columns according to the manufacturer's instructions. The purity of the WCI-12$^+$ and WCI-12$^-$ fractions was assessed by flow cytometric analysis using a FACScan® flow cytometer (Becton Dickinson, Mountain View, CA, USA). Cell pellets were collected and directly lysed prior to RNA isolation.

2.10. RNA isolation and quantification

For real-time quantitative polymerase chain reaction (RT-qPCR) analysis total RNA was isolated from thymus, head kidney, mid kidney, PBL, spleen, liver, gills and gut using the RNAeasy Mini Kit (Qiagen, Leusden, The Netherlands) according to the manufacturer's instructions. On-column DN*ase* treatment with the RN*ase*-free DN*ase* set (Qiagen) was also included. Prior to RNA isolation from liver a Proteinase K treatment was also included. The concentration of RNA was measured on a spectrophotometer (GeneQuant, Pharmacia Biotech) at OD$_{260 nm}$. The purity of the extracted RNA was determined as the OD$_{260 nm}$/OD$_{280 nm}$ ratio with expected values between 1.8 and 2.0. The integrity of RNA was determined by electrophoresis on 1% agarose gel containing 0.5 μg/ml ethidium bromide at 100 V. Total RNA was stored at −80 °C until use.

2.11. cDNA synthesis

Prior to cDNA synthesis, a second DN*ase* treatment was performed using DN*ase* I, Amplification Grade (Invitrogen, Breda, The Netherlands). Briefly, 1 μg of RNA from each sample was combined with 10X DN*ase* reaction buffer and 1 U DN*ase* I, mixed and incubated at RT for 15 min, followed by inactivation of DN*ase* I by adding 1 μl of 25 mM EDTA. Synthesis of cDNA was performed with Invitrogen's SuperScript™ III First Strand Synthesis Systems for RT-PCR Systems, according to the manufacturer's instructions. Briefly, DN*ase* I-treated RNA samples were mixed with 5× first strand buffer, 300 ng random primers, 10 mM dNTPs, 0.1 M DTT, 10 U RN*ase* inhibitor, and 200 U SuperScript III Reverse Transcriptase (Invitrogen) up to a final volume of 20 μl. The mixture was incubated at 37 °C for 60 min followed by an inactivation step at 70 °C for 15 min. A non-reverse transcriptase control was included for each sample. cDNA samples were further diluted 50 times (25 times for PBL samples) in nuclease-free water before use as template in real-time PCR experiments.

2.12. Detection of SVCV

To confirm that all fish used in our experiment were infected by the SVC virus, virus-specific primers were used in a single-tube reverse transcription (RT)-PCR and nested PCR reaction (Koutna et al., 2003).

For RT-PCR the SuperScript One-Step RT-PCR system (Invitrogen) was used. Briefly, 0.5 μg of total RNA isolated from head kidney of infected or control fish was combined with 25 μl 2X rection buffer, 20 pmol of the external primers (extFW: 5′-GCCTAAATGTGTTGATGGAACG-3′; extRV: 5′-GGATAATATCGGCTTGGAAAGC-3′), 40 U RN*ase* inhibitor, 100 U SuperScript II RT/*Taq* and diethyl pyrocarbonate (DEPC)-treated water up to a final volume of 25 μl. RT-PCR was carried out under the following conditions: cDNA synthesis for 30 min at 50 °C, one cycle of 2 min 30 s at 94 °C, followed by 35 cycles of 30 s at 94 °C, 1 min at 50 °C, and 1 min at 68 °C, with final extension step for 7 min at 72 °C. Nested PCR reactions were performed by combining 2 μl of the amplification product obtained by RT-PCR with Taq buffer (10×), 1 U Taq polymerase, MgCl$_2$ (1.5 mM), 20 pmol of each of the internal primers (intFW: 5′-CAAGAGAAGCTGACATCAGTGG-3′; intRV: 5′-GACAATAGGTCCCTCTACTTCG-3′), 200 μM dNTPs, and DEPC water up to a final volume of 50 μl. PCR conditions included one cycle of 4 min at 94 °C, followed by 25 cycles of 30 s at 94 °C, 30 s at 55 °C and 30 s at 72 °C followed by a final extension step for 7 min at 72 °C. RT-PCR and nested PCR were run using a GeneAmp PCR system 9700.

2.13. Real-time quantitative polymerase chain reaction (RT-qPCR)

RT-qPCR using SYBR Green I technology was performed using a Rotor-Gene™ 2000 (Corbett Research, Mortlake, Sydney, Australia) with the Brilliant® SYBR® Green QPCR (Stratagene, La Jolla, CA, USA) as detection chemistry. The primers used for RT-qPCR are listed in Table 2. PCR conditions were optimized by analyzing the melting curves of the products (Ririe et al., 1997) and product specificity was assessed by analysis on a 1% agarose gel. Master-mix for each PCR run was prepared as follows: 0.32 μl of water, 0.84 μl of each primer (5 μM), 7 μl Master SYBR Green I mix. Finally, 5 μl of diluted cDNA was added to 9 μl of master mix and transferred to a 0.1 ml tube. The following amplification program was used: after 15 min of denaturation at 95 °C, 40 cycles of RT-qPCR with three-step amplification were performed: 15 s at 95 °C for denaturation, 30 s at 60 °C for annealing and 30 s at 72 °C for elongation followed by a final holding step of 1 min at 60 °C. A melting step was then performed with continuous fluorescence acquisition starting at 60 °C with a rate of 1 °C/5 s up to 99 °C to determine the amplification specificity. In all cases, the amplifications were specific and no amplification was observed in negative controls (non-template control and non-reverse transcriptase control). Fluorescence data from RT-qPCR experiments were analysed using Rotor-Gene version 6.0.21 software and exported to Microsoft Excel. The cycle threshold C_t for each sample and the reaction efficiencies (E) for each

Table 2
Primers used in RT-qPCR gene expression analysis + indicates LNA (locked nucleic acid) substitutions

Primer	Sequence $5' \rightarrow 3'$	Product (bp)	Acc no
qCD8α1/2.FW1	TGCGCAGCCATGAACAACAATA		
qCD8α1.RV1	GCCATTGTTGTTGTCGATGGTA	119	EU025118
qCD8α2.RV1	CGTAATCACTGGTGTTGCAGTT	129	EU025119
qCD8β1.FW3	AATCAA+CGGCT+CGGAAACTATC		
qCD8β1.RV3	CGCTCTCTGCCAGCGCTGTTACA	132	EU025120
qCD8β2.FW3	AAT+CAATGGCT+CGGAAGTTCTG		
qCD8β2.RV3	CCAGCA+CTGTTGA+CATACACTAA	123	EU025121
qTCRα1.FW2	TTCACA+CAA+CATAATG+CTGTAAATGA		
qTCRα1.RV2	TTGA+CTGGATGATCCTGACATGC	144	EU025122
qTCRα2.FW2	CAGTG+CGATATGCAGAACGAAGT		
qTCRα2.RV2	TTGACTGGATGAT+CCTTGCTGA	95	EU025123
qp35.FW1	TGCTTCTCTGTCTCTGTGATGGA		
qp35.RV1	CACAGCTGCAGTCGTTCTTGA	86	AJ580354
qp40a.FW1	GAGCGCATCAACCTGACCAT		
qp40a.RV1	AGGATCGTGGATATGTGACCTCTAC	151	AJ621425
qp40b.FW2	TCTTGCACCGCAAGAAACTATG		
qp40b.RV2	TGCAGTTGATGAGACTAGAGTTTCG	121	AJ628699
qp40c.FW1	TGGTTGATAAGGTTCACCCTTCTC		
qp40c.RV1	TATCTGTTCTACAGGTCAGGGTAACG	127	AJ628700
qIFNαβ.FW1	GGCAGATATG+GGACGGTGAG		
qIFNαβ.RV1	GTCCTCCA+CCTCAGCTTTGTC	132	EC393381
qβAct.FW2	GCTATGTGGCTCTTGACTTCGA		
qβAct.RV2	CCGTCAGGCAGCTCATAGCT	89	M24113
q40S.FW1	CCGTGGGTGACATCGTTACA		
q40S.RV1	TCAGGACATTGAACCTCACTGTCT	69	AB012087

primer set were obtained upon Comparative Quantitation Analysis from the Rotor-Gene version 6.0.21 software. Briefly, the E for each primer set was recorded per sample and an average E (E_A) was then calculated for each primer set. The relative expression ratio (R) of a target gene was calculated based on the E_A and the C_t deviation of sample versus control, and expressed in comparison to a reference gene (Pfaffl, 2001; Tichopad et al., 2003). Basal expression of immune-related genes was calculated as a ratio of reference gene versus target gene in different organs. Three different house keeping genes, the 40S ribosomal protein S11, 18S and β-actin, were tested for their suitability as reference genes in RT-qPCR analysis. The 18S was highly expressed and required high dilution of the template, furthermore both ribosomal genes were found to be highly regulated during viral but not during parasitic infection. Therefore, β-actin was used as reference gene for the analysis of SVCV infected samples while the 40S ribosomal protein S11 was used as reference gene to calculate the basal expression of a target gene in different organs and in MACS sorted cell fractions, as well as in samples from *T. borreli*-infected fish.

2.14. Statistics

Relative expression ratios (R) were calculated as described above. Transformed (LN(R)) values were used for statistical analysis in SPSS Software (15.0). Significant differences ($P < 0.05$) were determined by a one-way ANOVA followed by a Dunnett t-test for the viral infection study and by a two-way ANOVA followed by a Sidak's test for the parasite infection study.

3. Results

3.1. Carp has two CD8α genes

Using a homology cloning approach we obtained the full-length mRNA sequence coding for carp CD8α. Two isoforms were identified and were designated as CD8α1 and CD8α2 (GenBank Accession nos.: EU025118; EU025119). cDNA sequences of 949 and 948 bp were identified for carp CD8α1 and CD8α2, respectively. The translated peptides are 211 aa for the CD8α1 and 214 aa for the CD8α2 and share 73% of overall identity. Carp CD8α has a comparable size to other known fish sequences, which have an average length of about 197 aa but is smaller than the mammalian CD8α molecules which have an average length of about 217 aa. Analysis of the protein sequences revealed the presence of a putative 20 aa leader peptide which upon cleavage would release proteins of about 21.1 kDa. Alignment of the translated sequences (Fig. 1) showed 54–80% of overall identity with cyprinid, 26% with salmonid and 16% with mammalian sequences.

The variable domain, characteristic of the immunoglobulin superfamily (IgSf V), which is also typical of all described CD8α molecules, was highly similar between the two carp
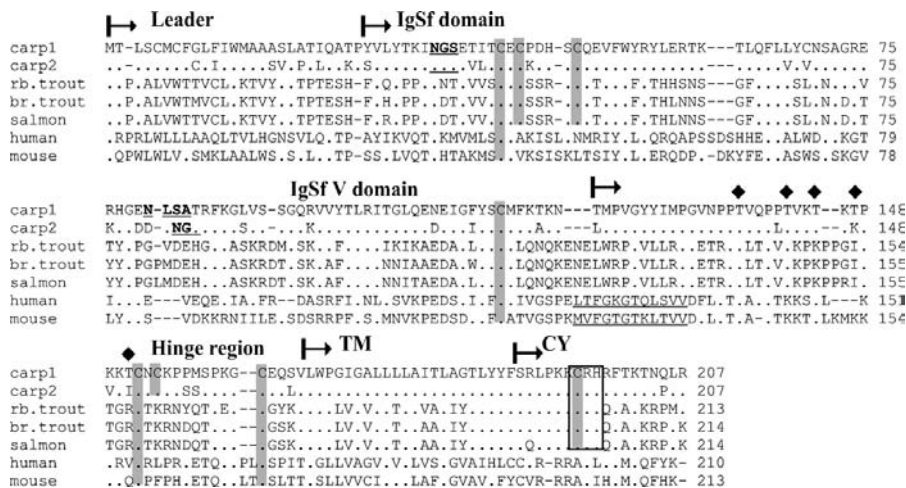
Fig. 1. Clustal W alignment of amino acids from CD8α chain precursors. Regions corresponding to the putative leader, IgSf V domain, hinge, transmembrane (TM), and cytoplasmatic (CY) region in the European common carp (*Cyprinus carpio carpio*) sequences are shown in bold above the sequence. Each region border is indicated by right arrows. Dots indicate identities to the carp CD8α1 (carp1) sequence and dashes denote gaps used to maximize the alignment. The Complementary Determining Regions (CDRs), designated based on the human sequence, are indicated by overlining the carp sequence. Predicted *N*-glycosilation sites are underlined and bold in the carp sequence. Conserved cystein residues are shaded in grey; (♦) possible O-linked glycosilation sites (S or T) for carp. The boxed region represents a conserved cytoplasmic domain in teleosts which corresponds to the region comprising the *lck* binding motif found in mammals. GenBank Accession nos.: goldfish (*Carassius auratus*, AB186395; AB186397); zebrafish (*Danio rerio*, AB186400); rainbow (rb) trout (*Oncorhynchus mykiss*, AF178053); Atlantic salmon (*Salmo salar*, AY693393); human (*Homo sapiens*, NP001759); mouse (*Mus musculus*, XP132621).

CD8α proteins (Fig. 1). Also in the carp sequence, the cysteins required for the intrachain disulphide bond as well as the invariant tryptophan were found appropriately located (Fig. 1; Cys-14/Trp-25/Cys-79 of the mature peptide corresponding to human Cys-22/Trp-35/Cys-94). The additional cysteine (Cys-33) found in mammalian CD8α sequences is missing in all teleost sequences including carp. Interestingly, the distance between the two cysteins in the carp CD8α Ig domain is 8 aa shorter than the corresponding region in the human sequence and 11 aa shorter than the mouse CD8α sequence. Within the Ig domain, two potential *N*-glycosylation sites were identified for carp CD8α1 and one for carp CD8α2 (Figs. 1 and 11) and their position was conserved when compared to the other teleost but not mammalian species.

The hinge region, in mammals, is characterised by the presence of multiple potential O-linked glycosylation sites. The hinge region of the carp CD8α1 is approximately 3 aa shorter than the corresponding region in the carp CD8α2 and displays a higher number (8 versus 5) of potential O-linked glycosylation sites (Figs. 1 and 11) which possibly contribute to a more rigid structure. In mammals, CD8α is capable of forming homo (αα)- and heterodimers (αβ with the CD8β chain) upon disulphide bond formation between two conserved cysteins within the extracellular hinge region. In carp, the cysteins corresponding to the human Cys-143/160 are highly conserved suggesting that also carp CD8α is capable of dimerization. Notably, in the known cyprinid CD8α sequences, but not in the salmonid and mammalian sequences, a third cystein residue is found within the hinge region (Figs. 1 and 11). Noteworthy, a third cystein

residue is also found in the hinge region of carp CD8β but not in the corresponding region in the salmonid CD8β sequences (Figs. 2 and 11).

Analysis of the hydrophobicity plot (data not shown) revealed a strongly hydrophobic region followed by a hydrophilic sequence in the area proximal to the COOH terminus. These regions corresponded to the transmembrane (TM; residues 138–160 for CD8α1; 142–165 for CD8α2) and cytoplasmatic regions (CY; residues 161–191 and 166–194) present in mammals and in other teleosts.

Both isoforms of carp CD8α did not contain the typical binding motif (CXC) for the tyrosine protein kinase *lck*, which is consistent with the results obtained for other fish species. However, high similarity at the amino acid level is observed in the corresponding region in all described teleost CD8α sequences, identified by the motive RTR/KRCPH, where the underlined CXH motif was suggested to be an alternative binding site for the *lck* protein (Hansen and Strassburger, 2000).

3.2. Carp has two CD8β genes

Using a similar strategy applied for the identification of the carp CD8α cDNAs we cloned the full-length mRNA sequence coding for carp CD8β. Also for the carp CD8β two isoforms were identified and designated as CD8β1 and CD8β2 (GenBank Accession nos.: EU025120; EU025121). cDNA sequences of 1137 and 1153 bp were isolated for carp CD8β1 and CD8β2, respectively. The translated peptides are both 207 aa long and they share 84% of overall identity. Protein analysis revealed
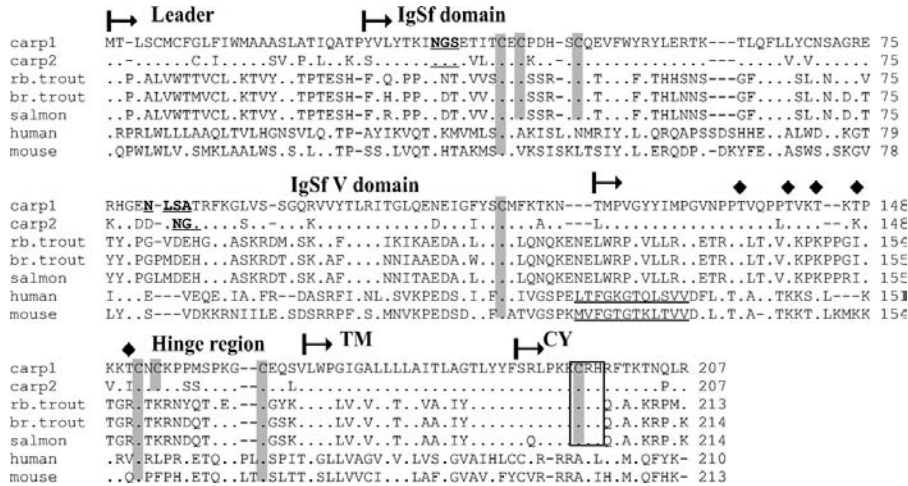
```
              ⊢ Leader                      ⊢ IgSf domain
carp1    MT-LSCMCFGLFIWMAAASLATIQATPYVLYTKINGSETITCECPDH-SCQEVFWYRYLERTK---TLQFLLYCNSAGRE 75
carp2    ..-......C.I.....SV.P.L..K.S........VL....K..-.................---.....V.V...... 75
rb.trout ..P.ALVWTTVCL.KTVY..TPTESH-F.Q.PP...NT.VVS....SSR-..T...F.THHSNS---GF....SL.N...V 75
br.trout ..P.ALVWTTVCL.KTVY..TPTESH-F.H.PP..DT.VV....SSR-..T...F.THLNNS---GF....SL.N.D.T 75
salmon   ..P.ALVWTTVCL.KTVY..TPTESH-F.R.PP..DT.VV....SSR-..T...F.THLNNS---GF....SL.N.D.T 75
human    .RPRLWLLLAAQLTVLHGNSVLQ.TP-AYIKVQT.KMVMLS...AKISL.NMRIY.L.QRQAPSSDSHHE..ALWD..KGT 79
mouse    .QPWLWLV.SMKLAALWS.S.L..TP-SS.LVQT.HTAKMS..VKSISKLTSIY.L.ERQDP.-DKYFE..ASWS.SKGV 78

              IgSf V domain                                     ⊢                   ◆  ◆  ◆
carp1    RHGEN-LSATRFKGLVS-SGQRVVYTLRITGLQENEIGFYSCMFKTKN---TMPVGYYIMPGVNPPTVQPPTVKT--KTP 148
carp2    K..DD-.NG....S..-..K.........D...I.....A..---L.................L.....--.K. 148
rb.trout TY.PG-VDEHG..ASKRDM.SK..F....IKIKAEDA.L...LQNQKENELWRP.VLLR..ETR..LT.V.KPKPPGI. 156
br.trout YY.PGPMDEH...ASKRDT.SK.AF....NNIAAEDA.W...LQNQKENELWRP.VLLR..ETR..LT.V.KPKPPGI. 155
salmon   YY.PGLMDEH...ASKRDT.SK.AF....NNITAEDA.L...LQNQKENELWRP.VLLR..ETR..LT.V.KPKPPRI. 155
human    I...E---VEQE.IA.FR--DASRFI.NL.SVKPEDS.I.F..IVGSPELTFGKGTQLSVVDFL.T.A..TKKS.L---K 151
mouse    LY..S---VDKKRNIILE.SDSRRPF.S.MNVKPEDSD..F.ATVGSPKMVFGTGTKLTVVD.L.T.A-.TKKT.LKMKK 156

          ◆ Hinge region        ⊢ TM             ⊢CY
carp1    KKTCNCKPPMSPKG--CEQSVLWPGIGALLLLAITLAGTLYYFSRLPKKCRHRFTKTNQLR 207
carp2    V.I....SS....-...L..........................P.. 207
rb.trout TGR.TKRNYQT.E.--.GYK....LV.V..T..AA.IY............Q.A.KRPM. 213
br.trout TGR.TKRNDQT...--.GSK....LV.V..T..VA.IY............Q.A.KRP.K 214
salmon   TGR.TKRNDQT.....--.GSK....LV.V..T..AA.IY.....Q....Q.A.KRP.K 214
human    .RV.RLPR.ETQ..PL.SPIT.GLLVAGV.V.LVS.GVAIHLCC.R-RRA.L..M.QFYK- 210
mouse    ..Q.PFPH.ETQ..LT.SLTT.SLLVVCI...LAF.GVAV.FYCVR-RRA.IH.M.QFHK- 213
```

Fig. 2. Clustal W alignment of amino acids from CD8β chain precursors. Regions corresponding to the putative leader, IgSf V domain, hinge, transmembrane (TM), and cytoplasmatic (CY) region in the European common carp (*Cyprinus carpio carpio*) sequences are shown in bold above the sequence. Each region border is indicated by right arrows. Dots indicate identities to the carp CD8β1 (carp1) sequence and dashes indicate gaps used to maximize the alignment. Predicted *N*-glycosilation sites are underlined and bold in the carp sequence. Conserved cystein residues are shaded in grey; (◆) possible O-linked glycosilation sites (S or T) for carp. The J-like domain following the IgSf domain is found only in the mammalian CD8β and is underlined in the human and mouse sequences. The boxed region represents a conserved cytoplasmic domain in teleosts that is also found in the cytoplasmic tail of fish CD8α, which corresponds to the region comprising the *lck* binding motif found in mammals. GenBank Accession nos.: rainbow (rb) trout (*Oncorhynchus mykiss*, AAT68458), brown (br) trout (*Salmo trutta*, AAW23970), Atlantic salmon (*Salmo salar*, AAW33877), human (*Homo sapiens*, Y00805), mouse (*Mus musculus*, P10300).

that the mature peptides have a predicted molecular weight of 20.8 and 20.6 kDa for the CD8β1 and CD8β2, respectively, with a leader peptide of 21 residues. Alignment of the translated sequences (Fig. 2) showed 38–40% of overall identity with the salmonid sequences and 18–20% with the mammalian sequences.

The IgSf V domain was found highly conserved in both carp CD8β proteins (Fig. 2). Also in the carp sequences, the cysteins required for the intrachain disulphide bond as well as the invariant tryptophan were found appropriately located (Fig. 2; Cys-17/Trp-29/Cys-91 of the mature peptide corresponding to human Cys-20/Trp-33/Cys-95). Interestingly, in all teleost species, in the region between the first cystein and the proximal tryptophan, two additional cysteins were found (at position 19 and 24 in carp). Whether one or both residues can form a disulphide bond with the more distal cystein requires further investigation. Within the Ig domain two potential *N*-glycosylation sites were identified for carp CD8β1 and CD8β2 (Figs. 2 and 11), their position was conserved when compared to other teleost but not mammalian sequences (Fig. 2). Notably, no teleost CD8β have a J-like region following the IgSf V-like domain. This suggests that the insertion (in mammals, (Sakano et al., 1979; Nakauchi et al., 1987)) or loss (in fish) of a J-like region must have occurred after the split between fish and tetrapods.

Five *O*-glycosylation sites were predicted within the hinge region of the CD8β1 isoform, while only one was predicted for the CD8β2 (Figs. 2 and 11). In carp, the cysteins corresponding to the human Cys-134/147 are highly conserved suggesting

that also carp CD8β is capable of dimerization. As previously mentioned, within the hinge region of both carp CD8α1/2 and CD8β1/2 an additional cystein was found, suggesting that a third disulphide bond could be involved in the heterodimerization between the carp CD8α and CD8β.

Analysis of the hydrophobicity plot (data not shown) revealed a strongly hydrophobic region followed by a hydrophilic sequence in the area proximal to the COOH terminus. These regions corresponded to the transmembrane (TM; residues 143–165) and cytoplasmatic (CY; residues 166–183) present in mammals and in other teleosts. In common with the carp CD8α chain, the β chain also contains the alternative CXH *lck*-binding motif in the cytoplasmic domain, suggesting that in fish CD8β might have signalling functions. In carp no spliced variants could be detected while in humans, the presence of alternatively spliced variants and a genome duplication event contribute to the generation of CD8β isoform diversity (DiSanto et al., 1993).

3.3. Carp has two TCR-Cα genes

Primers based on East-Asian carp TCRα sequences identified two isoforms coding for the constant region of the TCRα gene in European common carp, designated as TCR-Cα1 and TCR-Cα2 (sequences not shown; GenBank Accession nos.: EU025122; EU025123). Two isoforms were described for the region coding the constant domain of the East-Asian common carp TCRα antigen, Cα1 and Cα2. The second isoform was present in two allelic variants named Cα2a and Cα2b. European common carp
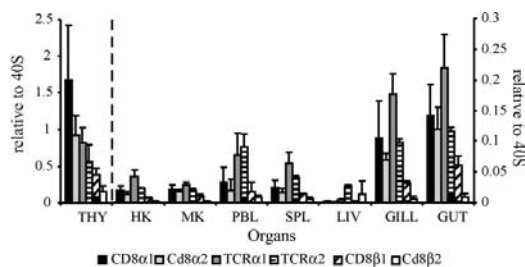
Fig. 3. Real-time quantitative PCR analysis of constitutive gene expression of T cell markers in thymus (THY), head kidney (HK), mid kidney (MK), PBL, spleen (SPL), liver (LIV), gills (GILL) and gut from $n = 3$ healthy carp. mRNA levels are expressed relative to the house keeping gene 40S. For clarity, the left Y-axis shows the relative gene expression in thymus, while the right Y-axis shows the relative gene expression in the other organs.

TCR-Cα1 shared 97% of identity with the previously described Cα1 gene and TCR-Cα2 shared 96% and 73% of identity with the previously described East-Asian carp Cα2a and Cα2b allelic variants, respectively. For clarity, in the text, we will refer to the European carp TCR-Cα1 and TCR-Cα2 sequences as TCRα1 and TCRα2.

3.4. Differential expression of T cell markers

Clearly, the highest mRNA expression of all investigated T cell markers was observed in the thymus (Fig. 3, notice the different Y-axis), confirming the role of the thymus as primary T cell organ in fish. For all investigated genes, a high constitutive expression was observed also in gut, gills and PBL. Differences were noted between isoforms. CD8α1 consistently showed a higher expression than the CD8α2 gene. CD8β mRNAs were the lowest expressed among the investigated T cell markers with the β1 isoform generally being higher expressed then the β2. The TCRα2 isoform was generally lower expressed than the TCRα1.

3.5. T cell marker genes are expressed only in IgM$^-$ PBL

PBL isolated from healthy control carp were separated in WCI12$^+$ (IgM$^+$) lymphocytes and WCI12$^-$ (IgM$^-$) leukocytes by magnetic sorting using an anti-carp-IgM monoclonal antibody (WCI12). The purity of the IgM$^-$ fraction was assessed by flow cytometry and only fractions with purity higher than 95% were used. Total RNA was isolated from each fraction and transcription of T cell marker genes was assessed by RT-qPCR. Fig. 4 represents a typical gene expression profile of the investigated genes clearly indicating the marked difference in transcripts expression between the IgM$^+$ and IgM$^-$ fraction.

3.6. Primary viral infection of carp induces an early up-regulation of CD8α and CD8β but not of TCRα genes

The head kidney is considered both a primary (bone marrow equivalent) and a secondary (lymph node equivalent) lymphoid organ in carp. To confirm infection by spring viraemia of carp
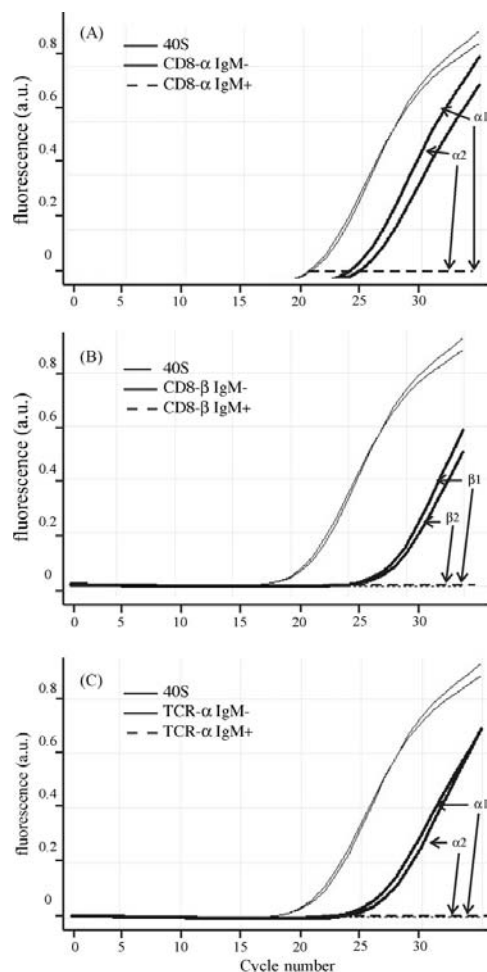
Fig. 4. T cell marker gene expression in IgM$^+$ and IgM$^-$ populations isolated from unstimulated PBL. Representative real-time quantitative PCR profiles that display the expression of 40S, CD8α1 and CD8α2 (A), CD8β1 and CD8β2 (B), TCRα1 and TCRα2 (C) illustrate the marked difference in constitutive expression between IgM$^+$ and IgM$^-$ populations. Data are from one out of two experiments with comparable results.

virus (SVCV), prior to RT-qPCR analysis, RNA samples from all head kidney isolates were tested positive for the presence of viral RNA (data not shown). We monitored changes in gene expression in head kidney from virus-infected carp over a period of 4 weeks post-infection (p.i.) but for clarity show the results until 14 days post-primary infection. Excluded time points did not show significant changes from non-infected fish, unless stated otherwise.

After primary infection, for CD8α effects were different for the two isoforms. CD8α1 mRNA expression did not change significantly post-primary infection. CD8α2 mRNA, in contrast,
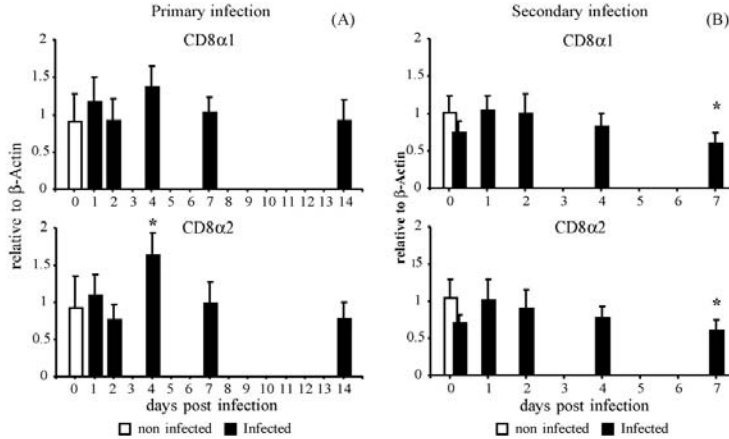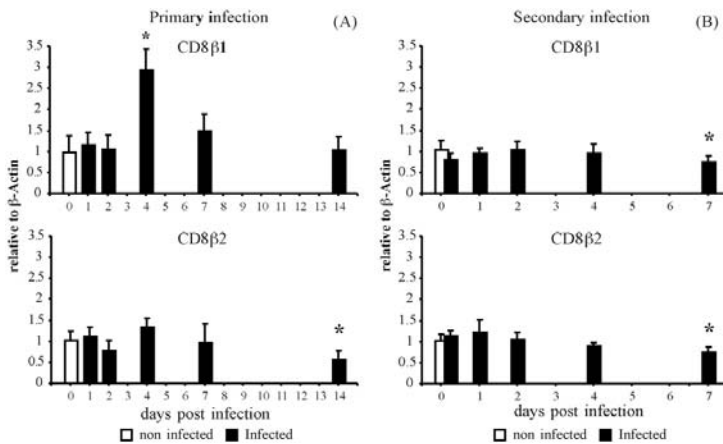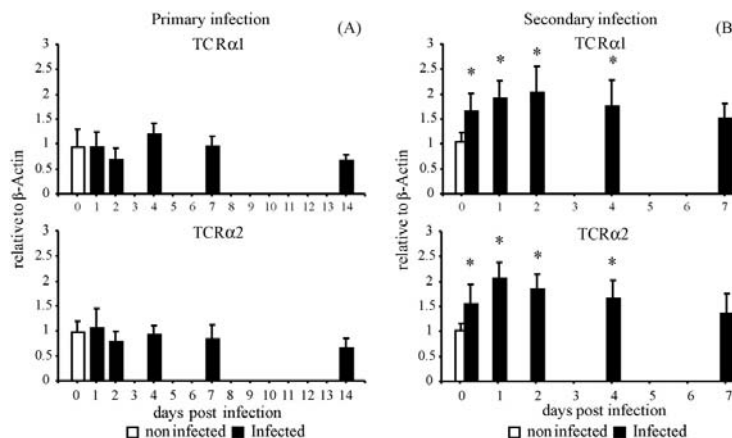
Fig. 5. Kinetics of CD8α1 and CD8α2 gene expression after primary (A) and secondary (B) spring viraemia of carp virus (SVCV) infection of European common carp (*Cyprinus carpio carpio*). Fish were exposed to SVCV (10^3 TCID$_{50}$/ml) by bath challenge for 2 h. Eight weeks after the first infection fish were exposed to the same viral dose. Head kidney from non-infected and infected fish were collected at different time points post-infection. Expression was determined by quantitative real-time PCR and expressed relative to β-actin. Data represent mean values of $n = 6$ fish (±S.D.). Symbol '*' represents a significant difference as compared to non-infected carp.

showed a moderate but significant up-regulation at day 4 p.i. with SVCV when compared to non-infected fish (Fig. 5A). For the CD8β genes, effects were also different for the two iso-forms. CD8β1 mRNA levels, again at 4 days p.i., showed a moderate but significant up-regulation in head kidney from primary infected fish (Fig. 6A). CD8β2 mRNA levels were not significantly different at 4 d.p.i. although at 14 d.p.i. a moderate down-regulation was observed. For neither of the TCRα genes a significant change in gene expression was observed after primary infection (Fig. 7A).

3.7. Secondary viral infection of carp induces an early up-regulation of TCRα but not of CD8α and CD8β genes

All samples from the secondary challenge (re-infection) were tested positive for the presence of viral RNA prior to RT-qPCR analysis of gene expression (data not shown). We monitored changes in gene expression in head kidney from virus-infected carp over a period of 4 weeks post-infection (p.i.) but for clarity show the results from 6 h until 7 days post-secondary infection.

Fig. 6. Kinetics of CD8β1 and CD8β2 gene expression after primary (A) and secondary (B) spring viraemia of carp virus (SVCV) infection of European common carp (*Cyprinus carpio carpio*). Fish were exposed to SVCV (10^3 TCID$_{50}$/ml) by bath challenge for 2 h. Eight weeks after the first infection fish were exposed to the same viral dose. Head kidney from non-infected and infected fish were collected at different time points post-infection. Expression was determined by quantitative real-time PCR and expressed relative to β-actin. Data represent mean values of $n = 6$ fish (±S.D.). Symbol '*' represents a significant difference as compared to non-infected carp.

Fig. 7. Kinetics of TCRα1 and TCRα2 gene expression after primary (A) and secondary (B) spring viraemia of carp virus (SVCV) infection of European common carp (*Cyprinus carpio carpio*). Fish were exposed to SVCV (10^3 TCID$_{50}$/ml) by bath challenge for 2 h. Eight weeks after the first infection fish were exposed to the same viral dose. Head kidney from non-infected and infected fish were collected at different time points post-infection. Expression was determined by quantitative real-time PCR and expressed relative to β-actin. Data represent mean values of $n = 6$ fish (±S.D.). Symbol '*' represents a significant difference as compared to non-infected carp.

Differently from what observed after primary viral infection, no significant up-regulation of any of the cytotoxic T cell markers was observed during secondary infection of carp with SVCV (Figs. 5 and 6B). We rather observed a moderate but significant down-regulation of both isoforms of CD8α and CD8β at 7 days post-secondary infection. At time points later than 7 days mRNA levels returned to control levels (not shown).

Interestingly, the picture for the TCRα genes was completely different. mRNA levels of both TCRα1 and TCRα2 were up-regulated already 6 h post-secondary infection and remained high until 7 days (Fig. 7B). mRNA levels returned to control levels after this period (not shown).

3.8. Primary, but not secondary, viral infection of carp induces an up-regulation of signal-3 cytokines, IL-12 and IFNαβ

We investigated the kinetics of both IL-12 and IFNαβ gene expression during an *in vivo* viral infection of carp. Fig. 8A shows that 4 days post-primary infection greatly elevated mRNA levels were observed for IL-12p35. The regulation of the three IL-12p40 isoforms differed profoundly. IL-12p40b transcripts, again at 4 days p.i., were significantly elevated. In contrast, no significant changes were observed for the IL-12p40a and IL-12p40c isoforms in head kidney from virus infected carp after primary infection. Fig. 9A shows that at 4 days p.i. significantly elevated mRNA levels were observed for IFNαβ. Notably, the highest mRNA expression for carp CD8α2, CD8β1, IL-12p35, IL-12p40b and finally for IFNαβ occurred simultaneously at 4 days post-primary infection.

During secondary infection no changes in mRNA levels were observed for the IL-12p40a and IL-12p40c genes. A moderate but significant up-regulation was observed 6 h p.i. for

the IL-12p40b gene and at 1 day p.i. for the IFNαβ gene (Figs. 8 and 9B). Up-regulation of carp IL-12p40b and IFNαβ genes coincided with the modest increase in mRNA levels observed for TCRα1 and TCRα2 genes around the same time point.

3.9. Parasitic infection of carp does not induce an up-regulation of the signal-3 cytokines, IL-12 and IFNαβ

In order to investigate whether IL-12 or IFNαβ could play a role during infections other than viral, we measured the expression of carp IL-12p35 and IL-12p40, along with IFNαβ genes during infection of carp with the extracellular blood parasite *T. borreli*. Carp infected with 10^4 parasites/fish were followed over a period of 6 weeks. The peak of parasitaemia was observed at week 3 p.i. (10^8 parasites/ml) and by week 6 the parasite number was reduced to 10^5 parasites/ml. No significant changes were observed in mRNA levels of IL-12 and IFNαβ genes over the whole infection period (Fig. 10). These results indicate that neither of the two signal-3 cytokines plays a role in the immune response to *T. borreli* infections in carp.

4. Discussion

In the present study we show that transcription of putative signal-3 cytokines, IL-12 and IFNαβ, coincided with the transcription of CD8α and CD8β during a rhabdoviral infection of carp. These results strongly suggest an evolutionary conservation of function for IL-12 and IFNαβ to act as necessary third signal required for optimal CTL activation, down to teleost fish. Previous studies already established the correlation between T cell markers gene expression and T cell functions (Fischer et al., 2003; Somamoto et al., 2005, 2006; Utke et al., 2007), which
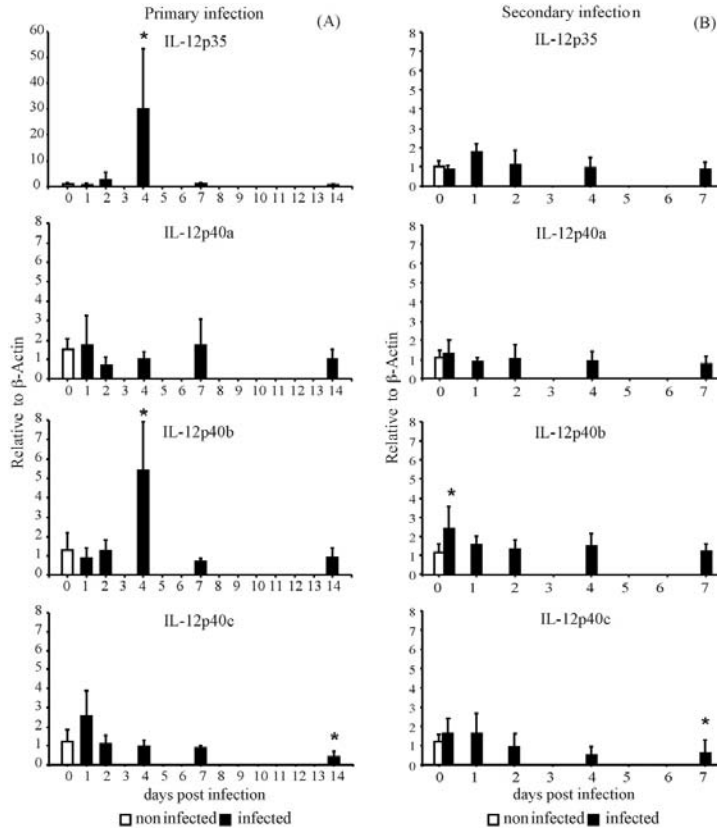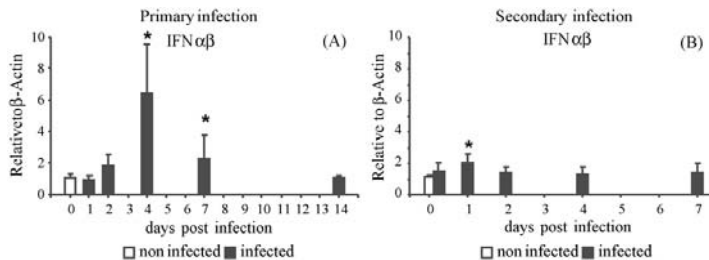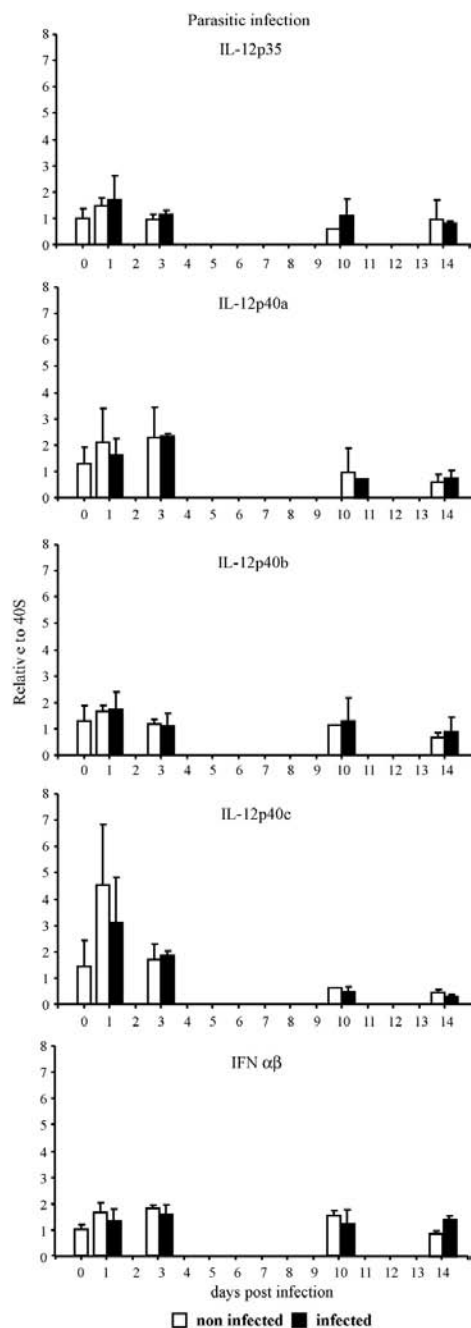
Fig. 8. Kinetics of IL-12p35, IL-12p40a, IL-12p40b and IL-12p40c gene expression after primary (A) and secondary (B) spring viraemia of carp virus (SVCV) infection of European common carp (*Cyprinus carpio carpio*). Fish were exposed to SVCV (10^3 $TCID_{50}$/ml) by bath challenge for 2 h. Eight weeks after the first infection fish were exposed to the same viral dose. Head kidney from non-infected and infected fish were collected at different time points post-infection. Expression was determined by quantitative real-time PCR and expressed relative to β-actin. Data represent mean values of $n = 6$ fish (±S.D.). Symbol '*' represents a significant difference as compared to non-infected carp.

Fig. 9. Kinetics of IFNαβ gene expression after primary (A) and secondary (B) spring viraemia of carp virus (SVCV) infection of European common carp (*Cyprinus carpio carpio*). Fish were exposed to SVCV (10^3 $TCID_{50}$/ml) by bath challenge for 2 h. Eight weeks after the first infection fish were exposed to the same viral dose. Head kidney from non-infected and infected fish were collected at different time points post-infection. Expression was determined by quantitative real-time PCR and expressed relative to β-actin. Data represent mean values of $n = 6$ fish (±S.D.). Symbol '*' represents a significant difference as compared to non-infected carp.

Fig. 10. Kinetics of signal-3 cytokines gene expression after *Trypanoplasma borreli* infection of European common carp (*Cyprinus carpio carpio*). Fish were injected (i.p.) with a dose of 10^4 parasites/fish, PBS-injected individuals served as unchallenged controls. Head kidney from non-infected and infected fish were collected at different time points post-infection. Expression was determined by quantitative real-time PCR and expressed relative to the house keeping gene 40S. Data represent mean values of $n = 5$ infected and $n = 3$ non-infected fish ($\pm$S.D.).

allowed us to use CD8α and CD8β transcription as a marker for CTL activation during the response to a viral infection in carp.

Up to date, sequences homologous to CD8α have been described for several fish species (Hansen and Strassburger, 2000; Moore et al., 2005; Somamoto et al., 2005; Buonocore et al., 2006), but sequences homologous to CD8β have only been reported for salmonid fish and for the tiger puffer fish (Moore et al., 2005; Suetake et al., 2007). In this study, we report the cloning of both CD8α and CD8β genes for the European common carp, each present in duplicate copies. We confirm the presence of two sequences coding for the constant domain of the TCRα chain in the European common carp. Previous studies in East-Asian common carp also reported on two isoforms coding for the constant domain of the TCRα chain (Imai et al., 2005). The evolutionary distance between the two subspecies of more than 500,000 years (Kohlmann et al., 2003; Zhou et al., 2003; Thai et al., 2004) resulted in differences at the nucleotide level between the sequences coding for the orthologous TCR genes. Based on the newly described TCR sequences for European common carp, specific primers for RT-qPCR could be designed.

In mammalian T cells, CD8 glycoproteins are expressed as either αα homodimers or αβ heterodimers, the latter considered a more efficient co-receptor for peptide antigen recognition by the T cell receptor (Renard et al., 1996; Witte et al., 1999). The enhancement of CD8 co-receptor stability by the CD8β molecule is ascribed primarily to the hinge region of CD8β (Wong et al., 2003). The distinct protein structure of CD8β, its smaller physical size and the differential regulation of the sialylation of the O-linked carbohydrates present in the hinge region, are thought to play a decisive role in the enhancement of CD8 co-receptor stability (Casabo et al., 1994; Priatel et al., 2000; Daniels et al., 2001; Moody et al., 2001). For fish, it is not known whether CD8 glycoproteins are expressed as αα homodimers and/or as αβ heterodimers. However, identification of the cDNA sequences for both CD8α and CD8β in the same fish species does allow us to reason on the structural motifs composing a functional CD8 co-receptor in fish.

As schematically depicted in Fig. 11, both isoforms of carp CD8α and CD8β displayed all structural motifs typical of the mammalian CD8 antigens. Both α and β chains have predicted *N*-glycosylation sites in their immunoglobulin domain and the CD8β chain was smaller than the α chain, the shorter cytoplasmic region accounting for the difference in size. A high number of predicted O-linked glycosylation sites was found in the hinge region of both CD8 chains, although differences could be observed between isoforms. The cysteines required for homo- and heterodimerization present in the hinge region of mammalian α and β chains, were also highly conserved. This suggests that carp CD8 could exist as αα homodimer and as αβ
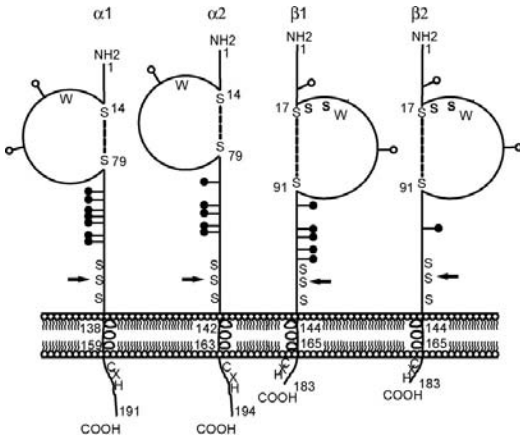
Fig. 11. Schematic representation of carp CD8α and CD8β chains on the cell membrane. All CD8 isoforms have an extracellular IgSf V-like domain (indicated by a circle), a hinge region, a transmembrane domain and a cytoplasmic tail. Conserved cysteins (S) and tryptophans (W) are indicated. S residues present exclusively in fish (and not mammalian) sequences are in bold; those present only in cyprinid fish are indicated by a black arrow. Predicted *N*-glycosylation and *O*-glycosylation sites are indicated by open circle lollipops and by black circle lollipops, respectively. Notice the difference in predicted *O*-glycosylation sites between isoforms. The hinge region of carp CD8α1 is 3 aa shorter than the CD8α2 isoform. The length of the extracellular portion of carp α and β chains is comparable and the cytoplasmic tail accounts for the overall difference in length. Both carp CD8α and CD8β contain an *lck*-like motif (CXH) in their cytoplasmic tail, indicating that in fish both chains might have signalling functions.

heterodimer. Moreover, the smaller physical size and the heterogeneous number of potential O-linked glycosylation sites in the CD8β molecule suggest that also in (cyprinid) fish, CD8β might be responsible for the enhanced co-receptor functions of a heterodimeric CD8. In cyprinid fish, but not in salmonids nor in mammals, an additional cystein, which might be involved in the formation of a third disulphide bond during carp CD8 dimerization, was found in the hinge region of both CD8α and CD8β chains.

To further study, the homo- or heterodimerization of carp CD8α and CD8β a comparative protein modelling approach could be considered. However, given the low percentage of identity between fish and human CD8 sequences, any error introduced by the alignment algorithm will have profound effects on the model, making the interpretation of the results difficult. Instead, the production of specific antibodies directed against the CD8α and CD8β antigens could be more informative to elucidate their structural organization in fish.

In mammalian and avian species, CD8 signalling occurs via the interaction of the tyrosine protein kinase *lck* with a motif (CXCP) present in the long cytoplasmic tail of the CD8α chain (Shaw et al., 1990). The short cytoplasmic tail of the CD8β chain lacks the consensus sequence required for the interaction with *lck* and seems to have no involvement in signalling (Zamoyska, 1994). When we move away from mammalian and avian models and consider fish, neither the CD8α nor the CD8β chain contains the typical *lck* binding motif. However, an alter-

native *lck*-binding site, identified by the CXH motif, is present in all fish CD8α sequences directly following a highly charged proximal consensus motif (RTR/KR) (Hansen and Strassburger, 2000; Somamoto et al., 2005). Notably, the same CXH motif is also found highly conserved in the CD8β cytoplasmic tail. All together, these data suggest that both CD8α and CD8β might have signalling functions in fish and that the same adaptor molecule (*lck*) might be involved. However, these findings should also be seen in the context of a current debate supporting the hypothesis that in higher vertebrates co-receptor signalling might also occur through molecules other than *lck* (Zamoyska, 1994; Groves et al., 1996; Zamoyska et al., 2003). Further studies on the signalling mechanisms of CD8 in lower vertebrates such as fish, might contribute to a better understanding of the CD8 signalling pathways of higher vertebrates. Based on the CD8β structural motifs the possibility of CD8ββ homodimers in fish cannot be excluded. Human, but not mouse, CD8β can be expressed on the cell surface without the need of CD8α coexpression (Devine et al., 2000). However, in contrast to CD8αα, the CD8ββ homodimer is unable to bind to MHC class I. Although the presence of a potential signaling motif in the CD8β cytoplasmic tail supports the idea of a functional CD8ββ co-receptor in carp, this requires further investigation.

Both carp CD8α and CD8β were found as duplicated genes. At present, CD8 is described most often as co-receptor molecule but recent data have expanded the function of CD8 further to that of an adhesion molecule and of an immuno-modulator, reviewed in (Cole and Gao, 2004). In this context, it is tempting to speculate that the multiple functions executed by a single molecule in higher vertebrates, might be specifically assigned to different isoforms in lower vertebrates. In addition, the presence of multiple gene copies for both carp CD8α and CD8β raised the question whether there would be a preference for particular combinations of CD8α and CD8β in the formation of a functional co-receptor. Differences in the induction of carp CD8α and CD8β after viral infection were seen and a simultaneous up-regulation of the CD8α2 and CD8β1 isoforms was noted exclusively at 4 days p.i. (Figs. 5 and 6A). As schematically depicted in Fig. 11, CD8α2 has five predicted O-linked glycosylation sites and a longer (3 aa) hinge region than CD8α1, and CD8β1 was predicted to have a higher number (5 versus 1) of O-linked glycosylation sites than the CD8β2 isoform. The simultaneous mRNA expression in combination with the structural characteristics of carp CD8α2 and CD8β1, both required for optimal co-receptor activities, suggests that a CD8α2/β1 heterodimer could be the preferred CD8 co-receptor in carp during SVCV infection. Whether the same heterodimeric co-receptor would be expressed during infection with other pathogens remains to be investigated.

CD8 co-receptor functions are restricted to the first phase of T cell activation, the antigen recognition phase (signal 1). However, to achieve full CD8^{+} T cell stimulation, clonal expansion, development of effector functions and memory, a CD28-dependent costimulation (signal 2) as well as signal-3 delivered by cytokines are required. These three signals together form the basis for CD8^{+} T cell-mediated immunity. Although the presence of fish homologues to TCR, CD3, CD8, CD28 and

MHC-I, among others, suggests that the presence of signal 1 and signal 2 is conserved from fish to mammals (Bernard et al., 2006a,b; Fischer et al., 2006), in fish, the potential of IL-12 and IFNαβ to act as signal-3 cytokines in infections inducing a CTL response has not been examined. We used a natural viral infection of carp to study the timing of mRNA expression of the CD8 cytotoxic T cell markers and of the putative signal-3 cytokines IL-12 and IFNαβ. Our results show that, both, IL-12 and IFNαβ, are involved during the onset of a CTL response which strongly suggests that also in fish these cytokines might provide the necessary third signal for complete T cell activation. In fact, during primary SVCV infection, up-regulation of carp CD8 gene expression occurred simultaneously with an up-regulation of IL-12 and IFNαβ. In mammals, *in vitro* and *in vivo* studies examining the timing requirements for exposure to Ag, costimulation and signal-3 cytokine showed that optimal overall stimulation and development of function required Ag/B7 to be present for about 36 h, with IL-12 being present as early as 12 h, up to 3 days (van Stipdonk et al., 2001; Curtsinger et al., 2003a). Coordinated timing of expression of carp CD8, IL-12 and IFNαβ was always seen 4 days post-infection, corresponding well to the timing observed in higher vertebrates.

We used a natural parasite infection of carp (Wiegertjes et al., 2005) to assess whether IL-12 and IFNαβ signal-3 cytokines would be upregulated in infections other than viral, where a CTL response is not required. After infection with the extracellular blood flagellate *T. borreli*, no changes in IL-12 or in IFNαβ gene transcription could be observed in head kidney from parasite-infected carp. In contrast, a significant (6.6-fold) up-regulation of TNFα was observed concomitantly with the peak of parasitaemia (unpublished data), while TNFα mRNA expression was only moderately (1.6-fold) increased 4 days post-primary viral infection (data not shown). This suggests that the TNFα cytokine plays a more important role during parasitic than during viral infections of carp. In mammals, in fact, the signal required for optimal CTL stimulation cannot be provided by the cytokines IL-1, IL-2, IL-4, IL-7, IL-15, IL-18, tumor necrosis factor-α (TNF-α) and IFN-γ (Mescher et al., 2006). All together, our results suggest that IL-12 and IFNαβ gene expression are required during viral, but not during parasitic infection.

During secondary infection (re-infection) with SVCV, no up-regulation of the CD8 genes and only a marginal increase in mRNA expression of the signal-3 cytokines IL-12 (IL-1240b) and IFNαβ was observed. The latter finding is not surprising since memory CD8$^+$ T cells do not require a third signal to develop effector functions (Curtsinger et al., 1999; Schmidt and Mescher, 2002) and confirms that also in carp, signal-3 cytokines are not involved during the course of a secondary infection. The absence of a clear up-regulation of any of the CD8 genes might be indicative of the fact that other types of effector mechanisms, such as B cell or non-CTL-mediated T cell responses, might be involved during secondary infection. This is supported by the observation that transcription of both TCR isoforms was clearly elevated during second exposure to the virus. Similar results were observed after primary and secondary ranavirus infection of *Xenopus laevis* (Morales and Robert, 2007). At present, sequences coding for genes homologous to CD3ε or

CD4 are not yet available in carp; their identification could provide a better insight into the role played by CD4$^+$ T cells during the course of a secondary SVCV infection. Acutely cytopathic viruses, such as vaccinia virus, promote CTL responses upon primary infection and humoral responses involving IgM neutralizing antibodies early upon secondary infection. In the latter case, virus-specific CTL are neither necessary nor sufficient to control infection, reviewed in (Hangartner et al., 2006). SVC is a severe infection of cyprinid carp that is widespread throughout Europe, causing high mortalities during spring (Ahne et al., 2002). SVCV belongs to the group of acutely cytopathic viruses and it has been tentatively assigned to the genus Vesiculovirus of the Rhabdoviridae family. Outbreaks of SVCV can result in mortality rates between 40 and 90% and only recently data are becoming available indicating that DNA vaccination of carp can protect against SVCV (Kanellos et al., 2006). It is becoming clear that during primary SVCV infection an early moderate cytotoxic response occurs (Kanellos et al., 2006), followed by a later development of neutralizing antibodies directed against the glycoprotein of the virus (Ahne et al., 2002). Upon infection following DNA vaccination (Kanellos et al., 2006) or after secondary SVCV infection a protective humoral response, rather than a cytotoxic, response is achieved (Ahne et al., 2002; Kanellos et al., 2006).

In vivo peptide immunization studies in mice have shown that administration of IL-12 along with the immunizing peptide had the same effect as adjuvant in preventing tolerance, stimulating a CTL response and establishing a memory development. In carp IL-12p35 was reported as a single copy gene while three highly distinct IL-12p40 genes, with distinct gene expression patterns, were identified (Huising et al., 2006). Coexpression of IL-12p35 and IL-12p40 genes is required in order to yield the functional IL-12p70 heterodimer (Gubler et al., 1991). Thus, for IL-12 to be used as an immunostimulant in carp, the identification of the functional IL-12p70 heterodimer is required. We found neither regulation of IL-12p40a and IL-12p40c expression nor after primary nor after secondary SVCV infection, while we observed simultaneous expression of the IL-12p35 and IL-12p40b genes 4 days post-primary infection, in head kidney from infected fish. Our findings, therefore, suggest that it is the p35p40b association that leads to the formation of a functional carp IL-12p70 heterodimer. Given the potential role of IL-12 as adjuvant, our findings should be taken into consideration for future vaccination strategies against viral infection of fish. Of course, the possibility that other heterodimeric combinations may be formed during the immune response to infections other than the one examined in this study, cannot be excluded. Future studies on the coexpression of IL-12p35 and the different IL-12p40 isoforms are required to confirm the preference for a p35p40b association in carp.

In conclusion, we report the cloning of CD8α and CD8β homologues, each present in duplicate copies, and confirm the presence of two TCR-Cα isoforms in European common carp (*C. carpio carpio*). Based on structural analysis, carp CD8 molecules could exist as αα and αβ dimers although the presence of CD8ββ homodimers cannot be excluded. The presence of potential signalling motifs in the cytoplasmic tail of

both CD8α and CD8β indicates that both chains might have signalling functions in fish. Coordinated kinetics of mRNA transcription suggest that a CD8α2/β1 heterodimer could be the preferred CD8 co-receptor in carp. Similarly, our expression study provides evidences that it is the association between the p35p40b molecules which will lead to the formation of a functional IL-12p70 heterodimer during viral infection of carp. Further, transcription of signal-3 cytokines coincided with the timing of CD8αβ up-regulation during viral infection of carp. This strongly suggests that IL-12 and IFNαβ signal-3 cytokines are particularly required after primary viral infection when also up-regulation of cytotoxic T cell markers is observed.

Acknowledgments

References

Ahne, W., Bjorklund, H.V., Essbauer, S., Fijan, N., Kurath, G., Winton, J.R., 2002. Spring viremia of carp (SVC). Dis. Aquat. Org. 52, 261–272.

Bernard, D., Riteau, B., Hansen, J.D., Phillips, R.B., Michel, F., Boudinot, P., Benmansour, A., 2006a. Costimulatory receptors in a teleost fish: typical CD28, elusive CTLA4. J. Immunol. 176, 4191–4200.

Bernard, D., Six, A., Rigottier-Gois, L., Messiaen, S., Chilmonczyk, S., Quillet, E., Boudinot, P., Benmansour, A., 2006b. Phenotypic and functional similarity of gut intraepithelial and systemic T cells in a teleost fish. J. Immunol. 176, 3942–3949.

Boudinot, P., Boubekeur, S., Benmansour, A., 2001. Rhabdovirus infection induces public and private T cell responses in teleost fish. J. Immunol. 167, 6202–6209.

Buonocore, F., Randelli, E., Bird, S., Secombes, C.J., Costantini, S., Facchiano, A., Mazzini, M., Scapigliati, G., 2006. The CD8alpha from sea bass (*Dicentrarchus labrax* L.): cloning, expression and 3D modelling. Fish Shellfish Immunol. 20, 637–646.

Casabo, L.G., Mamalaki, C., Kioussis, D., Zamoyska, R., 1994. T cell activation results in physical modification of the mouse CD8 beta chain. J. Immunol. 152, 397–404.

Cole, D.K., Gao, G.F., 2004. CD8: adhesion molecule, co-receptor and immunomodulator. Cell. Mol. Immunol. 1, 81–88.

Curtsinger, J.M., Johnson, C.M., Mescher, M.F., 2003a. CD8 T cell clonal expansion and development of effector function require prolonged exposure to antigen, costimulation, and signal 3 cytokine. J. Immunol. 171, 5165–5171.

Curtsinger, J.M., Lins, D.C., Mescher, M.F., 2003b. Signal 3 determines tolerance versus full activation of naive CD8 T cells: dissociating proliferation and development of effector function. J. Exp. Med. 197, 1141–1151.

Curtsinger, J.M., Schmidt, C.S., Mondino, A., Lins, D.C., Kedl, R.M., Jenkins, M.K., Mescher, M.F., 1999. Inflammatory cytokines provide a third signal for activation of naive CD4+ and CD8+ T cells. J. Immunol. 162, 3256–3262.

Curtsinger, J.M., Valenzuela, J.O., Agarwal, P., Lins, D., Mescher, M.F., 2005. Type I IFNs provide a third signal to CD8 T cells to stimulate clonal expansion and differentiation. J. Immunol. 174, 4465–4469.

Daniels, M.A., Devine, L., Miller, J.D., Moser, J.M., Lukacher, A.E., Altman, J.D., Kavathas, P., Hogquist, K.A., Jameson, S.C., 2001. CD8 binding to MHC class I molecules is influenced by T cell maturation and glycosylation. Immunity 15, 1051–1061.

Devine, L., Kieffer, L.J., Aitken, V., Kavathas, P.B., 2000. Human CD8 beta, but not mouse CD8 beta, can be expressed in the absence of CD8 alpha as a beta beta homodimer. J. Immunol. 164, 833–838.

DiSanto, J.P., Smith, D., de Bruin, D., Lacy, E., Flomenberg, N., 1993. Transcriptional diversity at the duplicated human CD8 beta loci. Eur. J. Immunol. 23, 320–326.

Fijan, N., Sulimanovic, D., Bearzotti, M., Muzinic, D., Zwillenberg, L.O., Chilmonczyk, S., Vautherot, J.F., de kinkelin, P., 1983. Some properties of the *Epithelioma papulosum cyprini* (EPC) cell line from carp *Cyprinus carpio*. Ann. Virol. (Institue Pasteur) 134, 207–220.

Filatenkov, A.A., Jacovetty, E.L., Fischer, U.B., Curtsinger, J.M., Mescher, M.F., Ingulli, E., 2005. CD4 T cell-dependent conditioning of dendritic cells to produce IL-12 results in CD8-mediated graft rejection and avoidance of tolerance. J. Immunol. 174, 6909–6917.

Fischer, U., Ototake, M., Nakanishi, T., 1998. *In vitro* cell-mediated cytotoxicity against allogeneic erythrocytes in ginbuna crucian carp and goldfish using a non-radioactive assay. Dev. Comp. Immunol. 22, 195–206.

Fischer, U., Utke, K., Ototake, M., Dijkstra, J.M., Kollner, B., 2003. Adaptive cell-mediated cytotoxicity against allogeneic targets by CD8-positive lymphocytes of rainbow trout (*Oncorhynchus mykiss*). Dev. Comp. Immunol. 27, 323–337.

Fischer, U., Utke, K., Somamoto, T., Kollner, B., Ototake, M., Nakanishi, T., 2006. Cytotoxic activities of fish leucocytes. Fish Shellfish Immunol. 20, 209–226.

Gonzalez, S.F., Chatziandreou, N., Nielsen, M.E., Li, W., Rogers, J., Taylor, R., Santos, Y., Cossins, A., 2007. Cutaneous immune responses in the common carp detected using transcript analysis. Mol. Immunol. 44, 1664–1679.

Groves, T., Smiley, P., Cooke, M.P., Forbush, K., Perlmutter, R.M., Guidos, C.J., 1996. Fyn can partially substitute for Lck in T lymphocyte development. Immunity 5, 417–428.

Gubler, U., Chua, A.O., Schoenhaut, D.S., Dwyer, C.M., McComas, W., Motyka, R., Nabavi, N., Wolitzky, A.G., Quinn, P.M., Familletti, P.C., et al., 1991. Coexpression of two distinct genes is required to generate secreted bioactive cytotoxic lymphocyte maturation factor. Proc. Natl. Acad. Sci. U.S.A. 88, 4143–4147.

Hangartner, L., Zinkernagel, R.M., Hengartner, H., 2006. Antiviral antibody responses: the two extremes of a wide spectrum. Nat. Rev. Immunol. 6, 231–243.

Hansen, J.D., Strassburger, P., 2000. Description of an ectothermic TCR coreceptor, CD8 alpha, in rainbow trout. J. Immunol. 164, 3132–3139.

Hasegawa, S., Nakayasu, C., Yoshitomi, T., Nakanishi, T., Okamoto, N., 1998. Specific cell-mediated cytotoxicity against an allogeneic target cell line in isogeneic ginbuna crucian carp. Fish Shellfish Immunol. 8, 303–313.

Hernandez, J., Aung, S., Marquardt, K., Sherman, L.A., 2002. Uncoupling of proliferative potential and gain of effector function by CD8(+) T cells responding to self-antigens. J. Exp. Med. 196, 323–333.

Huising, M.O., van Schijndel, J.E., Kruiswijk, C.P., Nabuurs, S.B., Savelkoul, H.F.J., Flik, G., Verburg-van Kemenade, B.M.L., 2006. The presence of multiple and differentially regulated interleukin-12p40 genes in bony fishes signifies an expansion of the vertebrate heterodimeric cytokine family. Mol. Immunol. 43, 1519–1533.

Imai, E., Ishikawa, J., Moritomo, T., Tomana, M., 2005. Characterisation of T cell antigen receptor alpha chain isotypes in the common carp. Fish Shellfish Immunol. 19, 205–216.

Irnazarow, I., 1995. Genetic variability of Polish and Hungarian carp lines. Aquacult. Res. 129, 215–219.

Kanellos, T., Sylvester, I.D., D'Mello, F., Howard, C.R., Mackie, A., Dixon, P.F., Chang, K.C., Ramstad, A., Midtlyng, P.J., Russell, P.H., 2006. DNA vaccination can protect *Cyprinus Carpio* against spring viraemia of carp virus. Vaccine 24, 4927–4933.

Kohlmann, K., Gross, R., Murakaeva, A., Kersten, P., 2003. Genetic variability and structure of common carp (*Cyprinus carpio*) populations throughout the distribution range inferred from allozyme, microsatellite and mitochondrial DNA markers. Aquat. Living Res. 16, 421–431.

Kolumam, G.A., Thomas, S., Thompson, L.J., Sprent, J., Murali-Krishna, K., 2005. Type I interferons act directly on CD8 T cells to allow clonal expansion and memory formation in response to viral infection. J. Exp. Med. 202, 637–650.

Koumans-van Diepen, J.E., Egberts, E., Peixoto, B.R., Taverne, N., Rombout, J.H.W.M., 1995. B cell and immunoglobulin heterogeneity in carp (*Cyprinus carpio* L.); An immuno(cyto)chemical study. Dev. Comp. Immunol. 19, 97–108.

Koutna, M., Vesely, T., Psikal, I., Hulova, J., 2003. Identification of spring viraemia of carp virus (SVCV) by combined RT-PCR and nested PCR. Dis. Aquat. Org. 55, 229–235.

Mescher, M.F., Curtsinger, J.M., Agarwal, P., Casey, K.A., Gerner, M., Hammerbeck, C.D., Popescu, F., Xiao, Z., 2006. Signals required for programming effector and memory development by CD8+ T cells. Immunol. Rev. 211, 81–92.

Moody, A.M., Chui, D., Reche, P.A., Priatel, J.J., Marth, J.D., Reinherz, E.L., 2001. Developmentally regulated glycosylation of the CD8alphabeta coreceptor stalk modulates ligand binding. Cell 107, 501–512.

Moore, L.J., Somamoto, T., Lie, K.K., Dijkstra, J.M., Hordvik, I., 2005. Characterisation of salmon and trout CD8alpha and CD8beta. Mol. Immunol. 42, 1225–1234.

Morales, H.D., Robert, J., 2007. Characterization of primary and memory CD8 T-cell responses against ranavirus (FV3) in *Xenopus laevis*. J. Virol. 81, 2240–2248.

Nakauchi, H., Shinkai, Y., Okumura, K., 1987. Molecular cloning of Lyt-3, a membrane glycoprotein marking a subset of mouse T lymphocytes: molecular homology to immunoglobulin and T-cell receptor variable and joining regions. Proc. Natl. Acad. Sci. U.S.A. 84, 4210–4214.

Nascimento, D.S., Vale, A.d., Tomas, A.M., Zou, J., Secombes, C.J., dos Santos, N.M.S., 2007. Cloning, promoter analysis and expression in response to bacterial exposure of sea bass (*Dicentrarchus labrax* L.) interleukin-12 p40 and p35 subunits. Mol. Immunol. 44, 2277–2291.

Pfaffl, M.W., 2001. A new mathematical model for relative quantification in real-time RT-PCR. Nucleic Acids Res. 29, e45.

Priatel, J.J., Chui, D., Hiraoka, N., Simmons, C.J., Richardson, K.B., Page, D.M., Fukuda, M., Varki, N.M., Marth, J.D., 2000. The ST3Gal-I sialyltransferase controls CD8+ T lymphocyte homeostasis by modulating O-glycan biosynthesis. Immunity 12, 273–283.

Reed, R.J., Muench, H., 1938. A simple method of estimating 50% endpoints. Am. J. Hyg. 27, 493–497.

Renard, V., Romero, P., Vivier, E., Malissen, B., Luescher, I.F., 1996. CD8 beta increases CD8 coreceptor function and participation in TCR-ligand binding. J. Exp. Med. 184, 2439–2444.

Ririe, K.M., Rasmussen, R.P., Wittwer, C.T., 1997. Product differentiation by analysis of DNA melting curves during the polymerase chain reaction. Anal. Biochem. 245, 154–160.

Robertsen, B., 2006. The interferon system of teleost fish. Fish Shellfish Immunol. 20, 172–191.

Sakano, H., Huppi, K., Heinrich, G., Tonegawa, S., 1979. Sequences at the somatic recombination sites of immunoglobulin light-chain genes. Nature 280, 288–294.

Schmidt, C.S., Mescher, M.F., 2002. Peptide antigen priming of naive, but not memory, CD8 T cells requires a third signal that can be provided by IL-12. J. Immunol. 168, 5521–5529.

Shaw, A.S., Chalupny, J., Whitney, J.A., Hammond, C., Amrein, K.E., Kavathas, P., Sefton, B.M., Rose, J.K., 1990. Short related sequences in the cytoplasmic domains of CD4 and CD8 mediate binding to the amino-terminal domain of the p56lck tyrosine protein kinase. Mol. Cell. Biol. 10, 1853–1862.

Somamoto, T., Yoshiura, Y., Nakanishi, T., Ototake, M., 2005. Molecular cloning and characterization of two types of CD8alpha from ginbuna crucian carp, *Carassius auratus langsdorfii*. Dev. Comp. Immunol. 29, 693–702.

Somamoto, T., Yoshiura, Y., Sato, A., Nakao, M., Nakanishi, T., Okamoto, N., Ototake, M., 2006. Expression profiles of TCRbeta and CD8alpha mRNA correlate with virus-specific cell-mediated cytotoxic activity in Ginbuna crucian carp. Virology 348, 370–377.

Steinhagen, D., Kruse, P., Körting, W., 1989. The parasitemia of cloned *Trypanoplasma borreli* Laveran and Mesnil, 1901 in laboratory-infected common carp (*Cyprinus carpio* L.). J. Parasitol. 75, 685–689.

Suetake, H., Araki, K., Akatsu, K., Somamoto, T., Dijkstra, J.M., Yoshiura, Y., Kikuchi, K., Suzuki, Y., 2007. Gene organization and expression of CD8α and CD8β genes in fugu *Takifugu rubripes*. Fish Shellfish Immunol. 23, 1107–1118.

Thai, B.T., Burridge, C.P., Pham, T.A., Austin, C.M., 2004. Using mitochondrial nucleotide sequences to investigate diversity and genealogical relationships within common carp (*Cyprinus carpio* L.). Anim. Gen. 36, 23–28.

Tichopad, A., Dilger, M., Schwarz, G., Pfaffl, M.W., 2003. Standardized determination of real-time PCR efficiency from a single reaction set-up. Nucleic Acids Res. 31, e122.

Utke, K., Bergmann, S., Lorenzen, N., Kollner, B., Ototake, M., Fischer, U., 2007. Cell-mediated cytotoxicity in rainbow trout, *Oncorhynchus mykiss*, infected with viral haemorrhagic septicaemia virus. Fish Shellfish Immunol. 22, 182–196.

van Den Broek, M., Bachmann, M.F., Kohler, G., Barner, M., Escher, R., Zinkernagel, R., Kopf, M., 2000. IL-4 and IL-10 antagonize IL-12-mediated protection against acute vaccinia virus infection with a limited role of IFN-gamma and nitric oxide synthetase 2. J. Immunol. 164, 371–378.

van Erp, S.H., Dixon, B., Figueroa, F., Egberts, E., Stet, R.J.M., 1996. Identification and characterization of a new major histocompatibility complex class I gene in carp (*Cyprinus carpio* L.). Immunogenetics 44, 49–61.

van Stipdonk, M.J., Lemmens, E.E., Schoenberger, S.P., 2001. Naïve CTLs require a single brief period of antigenic stimulation for clonal expansion and differentiation. Nat. Immunol. 2, 423–429.

Wiegertjes, G.F., Forlenza, M., Joerink, M., Scharsack, J.P., 2005. Parasite infections revisited. Dev. Comp. Immunol. 29, 749–758.

Witte, T., Spoerl, R., Chang, H.C., 1999. The CD8beta ectodomain contributes to the augmented coreceptor function of CD8alphabeta heterodimers relative to CD8alphaalpha homodimers. Cell Immunol. 191, 90–96.

Wong, J.S., Wang, X., Witte, T., Nie, L., Carvou, N., Kern, P., Chang, H.C., 2003. Stalk region of beta-chain enhances the coreceptor function of CD8. J. Immunol. 171, 867–874.

Yoshiura, Y., Kiryu, I., Fujiwara, A., Suetake, H., Suzuki, Y., Nakanishi, T., Ototake, M., 2003. Identification and characterization of Fugu orthologues of mammalian interleukin-12 subunits. Immunogenetics 55, 296–306.

Zamoyska, R., 1994. The CD8 coreceptor revisited: one chain good, two chains better. Immunity 1, 243–246.

Zamoyska, R., Basson, A., Filby, A., Legname, G., Lovatt, M., Seddon, B., 2003. The influence of the src-family kinases, Lck and Fyn, on T cell differentiation, survival and activation. Immunol. Rev. 191, 107–118.

Zhou, J.F., Wu, Q.J., Ye, Y.Z., Tong, J.G., 2003. Genetic devergence between *Cyprinus carpio carpio* and *Cyprinus carpio haematopterus* as assessed by mitochondrial DNA analysis, with enphasis on origin of European domestic carp. Genetica 119, 93–97.
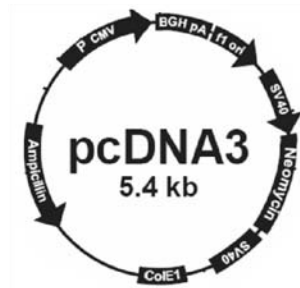
DNA vaccination strategies in common carp (Cyprinus carpio L.) against spring viraemia of carp virus (SVCV)

Maria Forlenza, Tomas Veselý, Dagmar Pokorová, Niels Lorenzen, Katja Einer-Jensen, Anne Kozijn, Huub F.J. Savelkoul and Geert F. Wiegertjes

DNA vaccination strategies in carp (*Cyprinus carpio*) against spring viraemia of carp virus (SVCV)

Maria Forlenza[1], Tomas Veselý[2], Dasa Pokorová[2], Niels Lorenzen[3], Katja Einer-Jensen[3], Anne Kozijn[1], Huub F.J. Savelkoul[1] and Geert Wiegertjes[1]

[1] Department of Animal Sciences, Cell Biology and Immunology Group, Wageningen Institute of Animal Sciences, Wageningen University, P.O. Box 338, 6700 AH, Wageningen, The Netherlands

[2] Veterinary Research Institute, Hudcova 70, 621 32 Brno, Czech Republic

[3] Department of Fish, National Veterinary Institute, Technical University of Denmark, DK-8200 Arhus N, Denmark

Abstract

Spring viraemia of carp virus (SVCV; *Rhabdoviridae*) causes a severe infection of carp with high mortalities especially at reduced water temperatures during spring. DNA vaccination can protect carp against SVC, although the mechanisms of protection have not been elucidated. We report the cloning of a carp myxovirus resistance (Mx1) cDNA and describe the changes in gene expression of a number of additional immune genes after DNA vaccination and after bath challenge with SVCV. Surprisingly, Mx1 up-regulation was observed not only in fish that received the vaccine plasmid, but also in carp that received the empty plasmid only, indicating the induction of an innate immune response, not specifically triggered by the viral G protein. The possibility that CpG motifs contained in the backbone of the pcDNA3 plasmid could induce a species-specific recognition of these pathogen-associated molecular patterns, is discussed. Besides a clear up-regulation of Mx1 gene expression, DNA vaccination itself, but also challenge with SVCV of vaccinated carp did not induce strong changes in the expression of other investigated genes. Challenge of naïve carp, however, showed an up-regulation of several genes including IFNαβ, Mx, IL-12p35, IFNγ2 and IL-10, particularly at 4 days post-challenge. The timing of up-regulation confirms our previous observation that infection of naïve fish with SVCV induces an early, simultaneous up-regulation of putative signal-3 cytokines IFNαβ and IL-12. DNA vaccination resulted in 85% survival after bath challenge, with a relative percent survival (RPS) of 66.7%. DNA vaccination against other rhabdoviruses such as VHS or IHNV, can result in RPS values of 90% or higher. Therefore, despite the promising results observed in this study, the DNA vaccine shows potential for further improvement. In mammals, IL-12 has been shown to serve as a potent immunoadjuvant when administered along with the immunizing antigen, sustaining cell-mediated immunity in particular. In fish, evidence points towards a role for cell-mediated responses in the protection against SVCV. We therefore constructed a plasmid coding for carp IL-12 composed of the p40b subunit fused to the p35 subunit and show that we can detect secreted, and possibly bioactive IL-12 in the supernatant of transfected cells. Administration of the IL-12p40b*L*p35 construct along with the DNA vaccine as a means of improving the efficacy of the SVCV DNA vaccine is discussed.

Introduction

Spring viraemia of carp (SVC) is a severe viral infection of carp that is widespread throughout Europe, causing high mortalities during spring (1). SVCV belongs to the group of acutely cytopathic viruses and it has been tentatively assigned to the genus *Vesiculovirus* of the *Rhabdoviridae* family. Outbreaks of SVCV can result in mortality rates between 40 and 90% and only recently new data indicate that DNA vaccination can protect carp against this viral infection (2). In general, DNA vaccination is particularly effective in fish and notably the first DNA vaccine commercialized for an edible animal species (Apex-IHN) is directed against a fish virus and protects Atlantic salmon from infectious hematopoietic necrosis (IHN) (3). Other successful examples include DNA vaccines against viral haemorrhagic septicaemia virus (VHSV) in trout (4) against hirame rhabdovirus (HIRRV) and VHSV in Japanese flounder (5, 6) and against SVCV in carp (2, 7). The DNA vaccines developed against these fish rhabdoviruses are based on the intramuscular injection of microgram quantities of naked DNA plasmid encoding the viral glycoprotein (G protein). Co-vaccination with DNA plasmids encoding the G protein of VHSV and the G protein of IHNV has been shown to successfully induce specific divalent protection against both viruses (8). In general, DNA vaccines against VHSV and IHNV and similar vaccines against other fish rhabdoviruses induce an early, transient, non-specific anti-viral immunity, followed in time by a protective antibody response (4, 9-15).

A number of studies have provided further insights in the immune response induced by DNA vaccines using microarray and real-time quantitative PCR describing the kinetics of gene expression following DNA vaccination (5, 6, 16-18). Most of these studies have been performed in salmonid fish species or in Japanese flounder but in carp, gene expression following DNA vaccination against SVCV has not been investigated. Despite differences in the fold change or peak of gene expression, often due to differences in the sampling time points, tissue origin and temperature at vaccination, a factor common to all DNA vaccination studies is the early up-regulation of type I interferon (IFN)-induced genes such as Mx (myxovirus resistance gene). The expression of IFN and Mx has been correlated temporally with the non-specific protection conferred during the early phase after vaccination. Sequences for Mx genes have been reported for most fish species, including rainbow trout (19), Atlantic salmon (20, 21), Japanese flounder (22), halibut (23), channel catfish (24), grouper (25), pufferfish (26) crucian carp (27) and zebrafish (28), but not common carp. In the present study we first report the cloning of a carp Mx gene homologous to other Mx1 genes described for teleost fish. Next, following DNA vaccination and challenge with SVCV, we examined the kinetics of carp Mx1 gene expression, together with the expression of other relevant genes such as type I interferon (referred to as IFNαβ in carp), IL-12p35 and IL-12p40, IL-1β1, CxCa, IL-10 and IFNγ2 to provide further

insight in the immune response of carp induced by DNA vaccination.

We recently reported on the cloning of CD8α and CD8β homologues, each present in duplicate copies, and on the kinetics of expression of these genes during primary and secondary infection of carp with SVCV (29). In the same study we noted that the expression of putative signal-3 cytokines such as IL-12 and IFN-αβ was also upregulated, concomitantly with the CD8α and CD8β gene expression, all at 4 days after primary infection. In mammals, signal-3 cytokines are required for optimal programming for survival, effector function and memory of CD8^{+} T cells (30). IL-12 is a heterodimeric protein composed of a p35 and a p40 subunit. In carp three p40 subunits, designated p40a, p40b and p40c have been identified (31) and during primary viral infection, expression of p35 was up-regulated concomitantly with the expression of the p40b subunit only (1). As a preliminary work, in the present study, we report the construction of a DNA vector encoding carp IL-12, obtained by fusing the p35 and p40b subunits with an interspacing linker (p40b*L*p35). We show that recombinant carp IL-12 can be expressed in a carp cell line resulting in a soluble protein of the expected size of 80 kDa. Future applications of the carp IL-12 DNA plasmid as molecular adjuvant to improve DNA vaccination of carp against SVCV will be discussed.

Materials and methods

Animals

European common carp (*Cyprinus carpio carpio*) of the R3 x R8 strain, which are the offspring of a cross between fish of Hungarian origin (R8 strain) and of Polish origin (R3 strain), were used (32). In this study, the European common carp subspecies will be referred to as carp, unless stated otherwise. Carp were produced in the central fish facility of Wageningen University, The Netherlands, then transported to the Veterinary Research Institute (VRI), Brno, Czech Republic, and raised in recirculating UV-treated water and fed pelleted dry food (Trouvit, Nutreco) daily. SVCV-vaccination and challenge experiments were performed in the latter facility. Adult carp (16 months) with an average weight of 30-40 g were used.

DNA vaccination

Carp were raised at 15°C, the optimal temperature for SVCV infectivity (1) and randomly assigned to one of three groups: pcDNA3 (empty plasmid), pcDNA3-SVCV-G and an unhandled group. pcDNA3-SVCV-G was prepared as described previously (9). Plasmid-injected groups were divided over two duplicate tanks (*n*=57 fish/tank). Fish were anesthetized in 100 mg/l ethyl p-amino-benzoate (Benzocaine). Except for the unhandled group, fish in each group were injected with 10 μg plasmid DNA by two intramuscular injections in a total volume of 50 μl. At time points 0, 1 day (d), 2 d, 3 d, 4 d, 5 d, 1 week and 2 weeks post vaccination, *n*=6

fish per group were euthanized to collect tissue samples as outlined in figure 1.

Viral challenge

SVCV strain CAPM V 539 (33) was propagated in EPC (epithelioma papulosum cyprini (34) cells at 15°C. EPC cells were grown in Eagle's minimal essential medium (MEM) containing 2% fetal bovine serum (FBS) and standard concentration of antibiotics. The virus titers, given as tissue culture infective dose ($TCID_{50}$/ml), were calculated by the method of Reed and Muench (35). Twelve weeks post-injection with plasmid, the remaining (*i.e.* fish not euthanized for sampling) vaccinated or non-vaccinated fish (*n*=66/group) were challenged by bath by adding SVCV-containing culture supernatants (10^{-3} $TCID_{50}$/ml) to the water for 2 h. Vaccinated or non-vaccinated fish (*n*=66 each) were divided over three tanks: two tanks with *n*=24 fish each were used for organ collection and one tank with *n*=18 fish was used to record mortality. At time points 0, 6h, 1d, 2d, 3d, 4d,

5d and 1 week post infection (p.i.), *n*=6 fish from the vaccinated or non-vaccinated group were euthanized for organ collection as outlined in figure 1. No samples were collected from moribund fish.

RNA isolation and cDNA synthesis

Total RNA was isolated from mid kidney using the RNAeasy Mini Kit according to the manufacturer's instructions, including on column DNase treatment with the RNase-free DNase set (Qiagen) and stored at -80°C until use. Prior to cDNA synthesis, to 1 μg total RNA, a second DNase treatment was performed using DNase I, Amplification Grade (Invitrogen). Synthesis of cDNA was performed using random primers (300 ng) and Superscript[TM] III (200U) First Strand Synthesis Systems for RT-PCR (Invitrogen). A non-reverse transcriptase control was included for each sample. cDNA samples were further diluted 1:5 in nuclease-free water prior to real-time quantitative PCR analysis.
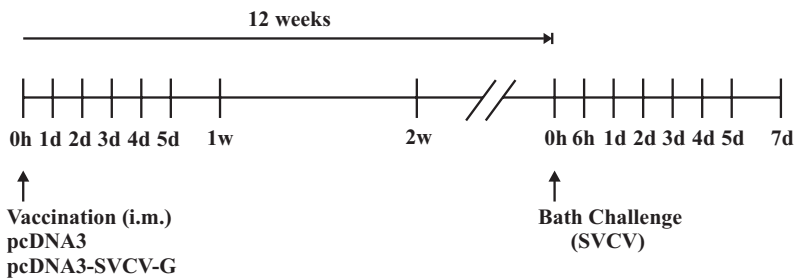
Figure 1. Timeline of DNA vaccination, challenge with SVCV and tissue sampling.

Identification of carp Mx-1 cDNA

Total RNA from head kidney of carp infected with SVCV, 4 days p.i. (29), was isolated as described above and used as a template for RT (reverse transcriptase)-PCR. RT-PCR was performed using the SuperScript™ One-Step RT-PCR with Platinum® Taq kit (Invitrogen). 1 μL (722.1 ng/μL) of total RNA was combined with 15 μL of 2x Reaction Mix with 0.6 μL RT/Platinum® Taq Mix, 0.2 μL (40 U/μL) RNaseOUT™ (Invitrogen) and primers (400 nM each) in a total volume of 30 μL. The PCR was performed with a GeneAmp PCR system 9700 (PE Applied Biosystems) under the following conditions: 30 min at 50°C and 2 min at 95°C, followed by 25-45 cycles of 30 s at 94°C, 30 s at 50-55°C and 1-2 min at 72°C, finally an extension step of 7 min at 72°C was performed. Primers Mx1FW and Mx1RV (Table 1) were designed on known Mx1 sequences of goldfish (*Carrassius auratus*) (Acc. No. AY303813) and zebrafish (*Danio rerio*) (Acc. No. NM_182942) and used in combination to amplify a short fragment of 332 bp for carp Mx1 (Fig. 2). Primer cycaMx1FW1 and Mx1RV3 and subsequently cycaMx1FW3 and Mx1RV5 were used to extend the known sequence to the 3'end. Primers Mx1FW5 and Mx1RV6 were used in combination to extend the sequence to the 5'end. The primer cycaMx1FW5 was used in combination with cycaMx1RV1, in order to obtain nearly the whole sequence cloned thus far. Products amplified by PCR were ligated into pGEM-Teasy vector and cloned in JM109 competent cells using the pGEM-T Easy kit

(Promega) according to standard protocols. Positive clones were selected by blue-white colony screening on agar plates containing 50 μg/mL Ampicillin. At least 5 clones for each PCR product were selected for subsequent colony-PCR using T7 and SP6 plasmid-specific primers. A standard PCR program was performed, using the GoldStar® DNA polymerase (Eurogentec) for small inserts (<1 kb) and the Expand High Fidelity^PLUS PCR System (Roche Diagnostics) for long inserts (> 1 kb). From each PCR product both strands were sequenced using the ABI Prism Big Dye Terminator Cycle Sequencing Ready Reaction kit (Applied Biosystems) and analysed using a 3730 DNA analyser. Nucleotide sequences were translated using the ExPASy translate tool (http://us.expasy.org/tools/dna.html) and aligned with Clustal W (http://www.ebi.ac.uk./clustalw). Potential identity of the proteins encoded was determined by a homology search with the protein-protein BLAST method (http://www.ncbi.nlm.nih.gov/blast).

Table 1 Primers used in RT-PCR

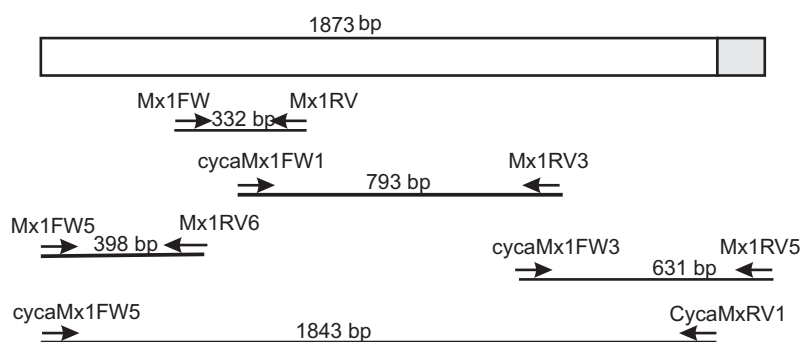| Primer	Sequence 5'→3'
T7	TAATACGACTCACTATAGGG
SP6	TTCTATAGTGTCACCTAAAT
Mx1FW	CTGAGAATATTGGAGATCAGATCAAGAG
Mx1RV	GTCAACATTACATGGCACCACAA
cycaMx1FW1	CAAAGCAAGAAACTATCAACC
Mx1RV3	TTTAACGCAGGTTCCTCCAACAGC
cycaMx1FW3	TTGAAGGGATGGTCAGGGA
Mx1RV5	GTAACCAAGAGGCTGCGTGC
Mx1FW5	ACGTCCTTGCATCGACAC
Mx1RV6	AGGAACATTGGCAGAGGTGAT
cycaMx1FW5	ACGTCCTTGCATCGACAC
cycaMx1RV1	AAGCGAGAGAACTTACTGAGCCGCCAGAACCG

Figure 2. Schematic representation of the cloning strategy for carp Mx. The position of primers for RT-PCR (Table 1) and the length of each amplicon are indicated. In white is the region of carp Mx cDNA which has been confirmed by sequencing the full-length 1843 bp fragment, in grey the cDNA sequence which has been obtained but not yet fully confirmed.

Gene expression analysis

Real time quantitative PCR (RT-qPCR) using SYBR Green I technology was performed with Rotor-Gene™ 6000 (Corbett Research) and the Brilliant® SYBR® Green QPCR (Stratagene) as detection chemistry as described previously (29). Primers used for RT-qPCR are listed in Table 2. Fluorescence data from RT-qPCR experiments were analyzed using Rotor-Gene version 6.0.21 software and exported to Microsoft Excel. The cycle threshold C_t for each sample and the reaction efficiencies (E) for each primer set were obtained upon comparative quantitation analysis from the Rotor-Gene version 6.0.21 software. The relative expression ratio (R) of a target gene was calculated based on the E and Ct deviation of sample versus control (36, 37), and expressed relative to a reference gene. Three different reference genes, the 40S ribosomal protein S11, 18S and β-actin, were tested for their suitability using BESTKeeper-1 XL tool (38). Both ribosomal genes but not β-

actin were found to be highly regulated during viral infection, whereas the 40S ribosomal protein S11 gave the most stable results in samples obtained from fish that were vaccinated but not challenged. Therefore, the 40S ribosomal protein S11 was used as reference gene for the analysis of samples collected after vaccination, wheras β-actin was used as reference gene for the analysis of samples collected after challenge with SVCV.

Construction of the carp p40b and p35 fused heterodimer

A schematic representation of the cloning strategy used to construct a functional IL-12p40b-p35 heterodimer is shown in figure 3. Total RNA (1 μg) isolated from mid kidney from healthy fish was used as template to amplify carp p40b (Acc No **AJ628699)** and total RNA (1 μg) from thymus was used as template to amplify carp p35 (Acc No: **AJ580354)**. Primers p40bFW0 (ttaag**atg**aacaagattgtctttgt) and p40bRV0

Table 2 Primers used in RT-qPCR

Primer	FW primers (5'→3')	RV primers (5'→3')	Acc. no.
β-actin	GCTATGTGGCTCTTGACTTCGA	CCGTCAGGCAGCTCATAGCT	M24113
40S	CCGTGGGTGACATCGTTACA	TCAGGACATTGAACCTCACTGTCT	AB012087
IFNγ2	TCTTGAGGAACCTGAGCAGAA	TGTGCAAGTCTTTCCTTTGTAG	AM168523
IL-10	CGCCAGCATAAAGAACTCGT	TGCCAAATACTGCTCGATGT	AB110780
IL-12p35	TGCTTCTCTGTCTCTGTGATGGA	CACAGCTGCAGTCGTTCTTGA	AJ580354
IL-12p40b	TCTTGCACCGCAAGAAACTATG	TGCAGTTGATGAGACTAGAGTTTCG	AJ628699
Mx1	TGGATAAGGGAACTGAAGAG	AGTGGCTGTCAAAGGTCA	-
IFNαβ	GGCAGATATG+GGACGGTGAG	GTCCTCCA+CCTCAGCTTTGTC	EC393381
CXCa	CTGGGATTCCTGACCATTGGT	GTTGGCTCTCTGTTTCAATGCA	AJ421443
IL-1β1	AAGGAGGCCAGTGGCTCTGT	CCTGAAGAAGAGGAGGCTGTCA	AJ245635
SVCV-N	TGAGGTGAGTGCTGAGGATG	CCATCAGCAAAGTCCGGTAT	NC_002803

'+' indicate LNA (Locked Nucleic Acid) modifications

(gacc**tta**tttttctgaggtgtgcc) or p35FW0 (caaca**atg**ctgtccagggtttgtaa) and p35RV0 (aattgctagtttg**cta**ttttgacaa) were used to amplify a region spanning the full coding sequence of the respective genes. The start and the stop codon are indicated in bold in the primer sequence. RT-PCR conditions were as described above (55°C; 35 cycles). Purified products were subsequently used as template for a PCR using the High Fidelity Taq polymerase PCR Kit (Roche). The forward primer used for p40b amplification (tca*AAGCTT*<u>ACCATGG</u>acaagattgtctttgttattc) included the *Hind*III restriction site (bold and italics), a Kozak sequence (bold and underlined) for optimal expression in eukaryotic cells (39) and the first 21 nucleotides of the leader sequence. The reverse primer (<u>ccacccgacccaccaccgcccgagccaccgcca</u> <u>cc</u>tttttctgaggtgtgccggtgttttc) included the last 26 nucleotides of the p40b coding sequence

immediately preceding the stop codon and a 35-nucleotide linker (underlined). Translation of the p40b final sequence leads to one single aa substitution in position +2 (N→D) immediately following the initial methionine due to insertion of the Kozak sequence. SignalP analysis (www.cbs.dtu.dk/ services/SignalP) confirmed that such a substitution has no effect on the cleavage of the leader sequence. The forward primer used for p35 amplification (<u>ggctcgggcggtggtgggtcg</u> <u>ggtggcggcggaggtccggtcggagcacgt</u>) included a 33-nucleotide linker overlapping for 26 nucleotides with the linker sequence included in the reverse primer used for p40b amplification and the first 18 nucleotides encoding for the mature p35 peptide (the nucleotides encoding for the p35 leader sequence were excluded). The reverse primer (catg*GCGGCCGC*<u>**ta**</u>*atggtgatggtgatgatg*ttttgac aaaatgtagttgaaaaca) included a *Not*III

A

B

IL-12p40b Leader peptide

<u>MDKIVFVILQAVLQLAGS</u>TSLRFIKPNVVALEVSDLSSFEVSLHCGEQYKGEQICW

N

EKDGESISETGNHITVMIDGLRGGNFTCHRPNRDLLNYTLLLVHPVEFPKGGILIQS

SDTEFISCTARNYDGQFHCSWKWHQNRNQRAVVYSTAIRNSSLINCTLDSDISGLT

CIDQDYCPYSEESRSINLTLFVRNLYRLEEHHRTFLIRDIVKPDKVSITKIQDDVFE

WQPPETWSFPCSFFPLSYEVKVVPNNHSCDYKGSRVEKNETNETHYNVKFKKPY

IL-12p35 →

TFCIRAQDPLTKNIWGDWTHFHQRKHRHTSEK<u>GGGGSGGGGSGGGG</u>GPVGARES

linker

PLNLTGKCNELARSLLWNVSAVLEMDHLFSGFDCSQQNAEVHLRRQTVSACTPQ

NSNCAHSAVLNIDENECLQRILEDLHYYRETLRAYSNPELTNSVVWSIDDLLQNC

FSVSVMDISPAKVSVDHQKSFQERLQLCKVLKGFNLRTITINRVFNYILSK<u>HHHHHH</u>

6xHIS tag

Figure 3. Construction of the pcDNA3-p40b*L*p35 recombinant plasmid. A) Schematic representation of the IL-12 cloning strategy. The p40b and p35 cDNA sequences were individually amplified and subsequently fused in frame with an intervening linker sequence by overlap PCR. The final cDNA sequence included the p40b start codon and leader peptide sequence, the p35 sequence without the leader peptide, a 6xHIS tag sequence and the stop codon. B) The deduced amino acid sequence of the fused heterodimeric carp IL-12 protein. The single amino acid substitution (N → D) at position two of the final peptide is shown.

restriction site (bold and italics), the p35 stop codon (underlined), an 18-nucleotide sequence coding for a 6xHistidine tag (6HIS) and the last 25 nucleotides of the p35 coding sequence.

Products were amplified under the following conditions. Five µl of purified RT-PCR products were combined with 1.7 U High Fidelity Enzyme (Roche), dNTPs (200 µM), forward and reverse primers (300 nM each), 5 µl 10X buffer and nuclease-free water up to a final volume of 50 µl. Reaction was performed with the following profile: 94°C for 4 min followed by 30 PCR cycles at 94°C for 15 sec, 50°C for 30 sec and 72°C for 1 min and a final extension step at 72°C for 7 min. Purified products were directly cloned in pGEM-T easy vector (Promega) and transformed in JM109 competent cells (Promega). The recombinant plasmids were isolated using the QIAGEN plasmid purification kit and the sequence was confirmed using the ABI Prism Big Dye Terminator Cycle Sequencing Ready Reaction kit (Applied Biosystems) and analysed using a 3730 DNA analyser. p40b and p35 sequences were re-amplified using high fidelity enzyme and 1 µl of the respective plasmids as templates. Following amplification of the individual subunits, the p40 and p35 products containing the linker sequences were amplified together by overlap PCR using high fidelity enzyme and the forward p40b and reverse p35 primers. The amplification product containing the p40b subunit fused in frame with the p35 subunit was cloned in the *Hind*III and *Not*I sites of the pcDNA3 plasmid (pcDNA3-p40b*L*p35) and its correct sequence was

verified. Plasmids were isolated using the endotoxin-free midi isolation kit (Invitrogen).

Nucleoporation of EPC (epithelioma papulosum cyprini) cells

EPC cells were cultured in RPMI 1640 (Gibco) supplemented with 10% foetal calf serum (FCS; Gibco), 2 mM L-Glutamin, 100 U/ml Penicillin-G and 50 mg/ml Streptomycin sulphate and grown to confluency in 75 cm^2 flasks. Two days before nucleoporation cells were passaged in a 1:3 ratio. On the day of nucleoporation, cells were washed twice in carp PBS (cPBS, 150 mM NaCl, 2 mM KCl, 20 mM Na$_2$HPO$_4$, 2 mM KH$_2$PO$_4$) and trypsinized using a solution of 0. 25% (w/v) trypsin and 0.1% (w/v) EDTA in cPBS. Reaction was stopped by addition of 20% FCS and the single cell suspension was collected and washed twice in cPBS. Cells (1 x 10^6) were resuspended in 100 µl solution V (Amaxa) and nucleoporated with 2.5 µg or 5 µg of pcDNA3-p40b*L*p35 plasmid using the T20 program, according to the manufacturer's instructions (Amaxa). Empty pcDNA3 plasmid (5 µg) was used as negative control and 2.5 µg of pGFPMax (Amaxa) was used as positive control. Transfected cells were immediately transferred to a 6 well plate in 2 ml complete medium supplemented with 7.5% FCS and left undisturbed for 5h. At this time point, medium was replaced with complete medium supplemented with 2.5% FCS.

Carp IL-12 (p40bLp35) protein expression

First, at time point 72h post-transfection, cells treated with pGFPMax plasmid were analyzed by flow cytometry for GFP expression to assess nucleoporation efficiency. Then, two approaches were taken to analyze IL-12 protein expression. In the first approach, supernatants of EPC cells transfected with pcDNA3-p40b*L*p35 or pcDNA3 were collected after 72h, centrifuged for 10 min at 800 x *g* and immediately used for Western blot analysis, or stored at -20˚C. Twenty μl of supernatants from nucleoporated cells were resolved on a 10% SDS-PAGE and proteins were subsequently transferred to a nitrocellulose membrane (Protran®, Schleicher & Schuell, Bioscience). Membranes were incubated with a 1:1500 dilution of mouse anti-6xHIS antibody (Qiagen) in TBS-BSA (10 mM Tris-Cl, pH 7.5, 150 mM NaCl, 3% (w/v) BSA) overnight at 4˚C. After washing twice in TBS and once in TBS-Tween/Triton (TBS, 0.05% (v/v) Tween, 0.2% (v/v) Triton X-100), membranes were incubated in a 1:1000 dilution of horseradish peroxydase conjugated goat-anti-mouse antibody (Dako) in 5% (w/v) non-fat dried milk in TBS for 1h at room temperature. After four washes in TBS-Tween/Triton, proteins were visualized by chemiluminescence detection (Amersham, ECL detection system for Western blot).

In the second approach, IL-12 protein expression was shown by immuno histochemical detection of transfected EPC monolayers, using a mouse anti-TetraHIS antibody (1:10; Qiagen) followed by incubation with an alkaline phosphatase-conjugated rabbit anti-mouse antibody (1:1000) as previously described (40).

Statistical analysis

Relative expression ratios (R) were calculated as described above. Transformed (LN(R)) values were used for statistical analysis in SPSS Software (15.0). Significant differences ($P < 0.05$) were determined by a one-way ANOVA followed by the Games-Howell test for samples from both, the vaccination and challenge experiment.

Results

Cloning of carp Mx1

Using a homology cloning approach we identified a carp Mx sequence of 1843 bp long covering the almost complete full length coding sequence. Sequence analysis revealed high similarity to known Mx1 sequences. The sequence encodes for a protein of 624 amino acids and misses short aa stretches at both ends. Carp Mx1 has all characteristics of the dynamin superfamily (Fig. 4): the N-terminal GTPase domain containing a dynamin family signature at amino acid positions 56-65 and the tripartite GTP-binding domain located at positions 33–50, 139–142, and 208–211; the dynamin central domain, stretching from position 221-516; the C-terminal GTPase effector domain (GED) including a putative leucine zippers motif, situated in a coiled-coil region and represented by a stretch of Leu residues spaced seven amino acid residues apart. Similar to human MxA and other fish Mx1 sequences, carp Mx1 does not contain a nuclear localization signal (NLS), suggesting

```
Carp        ----------------------------------------FSQQYEEKIRPCIDTIDRLRSLGVEKDLALPAIAVIGDQS 40
Zebrafish   ------------------------------MEKLSYTFSQQYEEKIRPCIDTIDNLRSLGVEKDLALPAIAVIGDQS 47
Goldfish    ------------------------------MEKMSYTFSQHYEEKIRPCIDTIDNLRSLGVEKDLALPAIAVIGDQS 47
Pufferfish  ----------------------------------MN-SLNQQYEEKVRPCIDLIDSLRSLGVEKDLALPAIAVIGDQS 43
Trout       -----------------------------------MNNTLNQHYEEKVRPCLDLIDSLRSLGVEKDLALPAIAVIGDQS 44
Human       MVVSEVDIAKADPAAASHPLLLNGDATVAQKNPGSVAENNLCSQYEEKVRPCIDLIDSLRALGVEQDLALPAIAVIGDQS 80
                           : .:****:***** ** **:****:************

                                   N-terminal GTPase Domain
Carp        SGKSSVLEALSGVALPRGSGIITRCPLELKMIRTKDEEKWQGRISYLGKEEDIDDPAEVEKKIREAQDEMAGPGVGISNE 120
Zebrafish   SGKSSVLEALSGVPLPRGSGIVTRCPLELKMIRTKDQDKWHGRISYKTYEEDFDDPAEVEKKIRQAQDEMAGAGVGISEE 127
Goldfish    SGKSSVLEALSGVALPRGSGIVTRCPLELKMIRTKGEGKWHAKISYQDYEEDIDDPAEVEKKIREAQDEMAGAGVGISDD 127
Pufferfish  SGKSSVLEALSGVALPRGSGIVTRCPLELKMKRRKVGEPWYGNISYLEKEEVIEDPADVEKKIKEAQDEMAGVGVGISDD 123
Trout       SGKSSVLEALSGVALPRGSGIVTRCPLELKMKRKKEGEEWHGKISYQDHEEEIEDPSDVEKKIREAQDEMAGVGVGISDD 124
Human       SGKSSVLEALSGVALPRGSGIVTRCPLVLKLKKLVNEDKWRGKVSYQDYEIEISDASEVEKEINKAQNAIAGEGMGISHE 160
            **************.*.******:***** .**  . ..:** :*   :.*.:::***:*.:**: :** **:***.:

                                   N-terminal GTPase Domain
Carp        LISLQITSANVPDLTLIDLPGIARVAVKGQQPENIGDQIKRLIRKFVTKQETINLVVVPCNVDIATTEALQMAQEEDPEGE 200
Zebrafish   LISLQITSANVPDLTLIDLPGIARVAVKGQQPENIGDQIKRLIRKFVTRQETINLVVVPCNVDIATTEALQMAQAEDPDGE 207
Goldfish    LISLQITSANVPDLTLIDLPGIARVAVKGQQPENIGDQIKRLIRKFVTKQETINLVVVPCNVDIATTEALQMAQEEDPEGE 207
Pufferfish  LISLEIASPEVVPDLTLIDLPGIARVAVKGQQPENIGEQIKRLIRKFITKQETISLVVVPCNVDIATTEALKMAQEVDPDGE 203
Trout       LISLEIGSPDVVPDLTLIDLPGIARVAVKGQQPENIGEQIKRLIRKFIMKQETISLVVVPCNVDIATTEALKMAQEVDPDGE 204
Human       LITLEISSRDVPDLTLIDLPGITRVAVGNQPADIGYKIKTLIKKYIQRQETISLVVVPSNVDIATTEALSMAQEVDPEGD 240
            **:*.*:* * .:*************:**** .** :** :** **:*:: :****.*****.**********.*** **:*:

                               ------------------------------------
Carp        RTLGILTKPDLVDKGTEETVVDIVHNEIIHLTKGYMIVRCRGQKEILDQVTLNEATVTEKAFFQDHPHFSKLYEEGFATI 280
Zebrafish   RTLGILTKPDLVDKGTEGTVVDIVHNEVIHLTKGYMIVRCRGQKEIMDQVTLNEATETESAFFKDHPHFSKLYEEGFATI 287
Goldfish    RTLGILTKPDLVDKGTEGTVVDIVHNEVIHLTKGYMIVRCRGQKEIIDHVTLNEATATENAFFQDHPQFSKLYEEGFATI 287
Pufferfish  RTLGILTKPDLVDKGTEETVVDIIHNEVIHLKKGYMIVRCRGQKEIIDKVSLAEATETETAFFRDHAHFQTLYDDGQATI 283
Trout       RTLGILTKPDLVDKGTEETVVDIVHNEIIHLTKGYMIVRCRGQKEIMERVSLTEATEREKAFFKEHAHLSTLYDEGHATI 284
Human       RTIGILTKPDLVDKGTEDKVVDVVRNLVFHLKKGYMIVKCRGQQEIQDQLSLSEALQREKIFFENHPYFRDLLEEGKATV 320
            **:************** .***::*: :.:**.******* *:.**  .   *  .* **.:*.  . *  ::* **:

                                   Dynamin central Domain
                            --------------------------------------
Carp        PKLAEKLTIELVHHIQRSLPRLEEQIETKLAETQKELEKYGNGPPSDPAERLSFFIDKVTAFTQDMFNLTGTGEEVKCASD 360
Zebrafish   PKLAEKLTIELVHHIQKSLPRLEEQIETKLAETQKELEAYGNGPPSEPAARLSFFIDKVTAFTQDMFNLTGEEVKCTTD 367
Goldfish    PKLAEKLTIELVHHIQKSLPRLEEQIETKLAETQKELEAYGNGPPDPVVRLSFLIDKVTAFTHDMFNLTGTGEEVKCSSD 367
Pufferfish  LKLAEKLTLELVNHIEKSLPRLEEQIEEKLAHTRAELERYGTGPPSDPAEKVTFLMDKLTAFTHDAISLTTGEDICCGEN 363
Trout       PKLAEKLTLELVHHIEKSLPRLEEQIEAKLSETHAELERYGTGPPEDSAERLYFLIDKVTAFTQDAINLSTGEEMKSGVR 364
Human       PCLAEKLTSELITHICKSLPLLENQIKETHQRITEELQKYGVDIPEDENEKMFFLIDKVNAFNQDITALMQGEETVGEED 400
             **.**** **: ** :***  **:**.  . : .:  :::**.::.**.:* .  *. **:.*. :  * .:*  :

                                   Dynamin central Domain
                            --------------------------------------
Carp        LLIFPELRDVFAKWNSFLDRLGVSFNKKIEKQVGDYEAKYRGRELPGFINYKTFEGMVREQMKLLEEPALKMLKTVSDVV 440
Zebrafish   LLLFPELRQEFAKWSHILDRSGDSFNKKIEKDVNYEVKYRGRELPGFINYKTFEGLVRDQIKLLEEPALKTLKTVSDVV 447
Goldfish    LLVFPELREEFLKWNGFLERSGHSFNKKIEKEVDNYEAKYRGRELPGFSNYKTLEGLVREQIKLLEEPALKTLKTVSDVV 447
Pufferfish  INIFSTLRQKFGEWIRHLDISGVKFNERLERELVQEYEVNKYRGRELPGFINYKTFEYMVKEQVKQLEEPAVRNLKDIGDDV 443
Trout       LNVFSTLRKEFGKWKLHLERSGEIFNQRIEGEVDDYEKTYRGRELPGFINYKTFEVMVKDQIKQLEGPAVKKLKEISDAV 444
Human       IRLFTRLRHEFHKWSTIIENNFQEGHKILSRKIQKFENQYRGRELPGFVNYRTFETIVKQQIKALEEPAVDMLHTVTDMV 480
             : :*. **. * :*    ::       :: :. :: .* .*:::*. :*:*:*:* ** **:  *: : * *

                                   Dynamin central Domain
                            --------------------------------------
Carp        RKKFIQLAQFSFVGFPNLLKIAKTKIEAIKHDKESQAESMLRTQFKMELIVYSQDGTYSQSLQDVKEMLEDEEDES---S 517
Zebrafish   RKKFIQLAQCSFIGFPNLLKIAKTKIEGIKLNKESLAESMLKTQFKMELIVYSQDGTYSQSLKHAKDKLEEMEKER---P 524
Goldfish    RKKFIQLAQYSFIGFPNLLKIAKTKIEAIKQDKESQAESMLRTQFKMELIVYSQDGTYSQSLQHAKDKLEEIENDKQQLP 527
Pufferfish  RKVFIHLAQTSFAGLPNLIKTAKAKIETIKQRMEKDAEKLLRTQFKMELLVYTQDRTYSSSLDESKK--EEQEDKC----V 518
Trout       RKVFLLLAQSSFTGFPNLLKSAKTKIEAIKQVNESTAESMLRTQFKMELIVYTQDSTYSHSLCERKR--EEDEDQ----P 518
Human       RLAFTDVSIKNFEEFFNLHRTAKSKIEDIRAEQEREGEKLIRLHFQMEQIVYCQDQVYRGALQKVRE--KELEEEK---- 554
             *  *  ::  .*  : **  : **:*** *:   *  .*.::: :*:** :** ** .*  : .*  :  : *.

                                   GTPase effector domain (GED)
Carp        HRKPKKFNFVSVDICTGSRATLREMKLHLESYYKIASKRLADQIPMVIRYLLLQEAALELQRNMLQLLQDKDEVDNLLKE 597
Zebrafish   QPKIKLPLLSSFDLGTDNHATLREMRLHLKSYYTIASKRLADQIPMVIRYMLLQEAALELQRNMLQLLQDKDGVDNLLKE 604
Goldfish    QFNAKKLNFVSVDVSTGTHATLREMRLHLESYYTIASKRLADQIPMVIRYLLLQEAALELQRNMLQLLQDKDGVDILLKE 607
Pufferfish  QTKIVRPPAFRFPFKQDNHATLTELMLHLKSYYRIASQRLSDQIPIMIRYHMLQEFAIQLQREMLQLLQDRENTELFLKE 598
Trout       LTEIRST-----IFSTDNHATLQEMMLHLKSYYWISSQRLADQIPMVIRYLVLQEFASQLQREMLQTLQEKDNIEQLLKE 593
Human       --KKKSWDFGAFQSSSATDSSMEEIFQHLMAYHQEASKRISSHIPLIIQFFMLQTYGQQLQKAMLQLLQDKDTYSWLLKE 632
              :            . :::  *:  ** :*:  :*:*:::.:**:*:: :**  . :*: *** **::  . :***

Carp        DYDIGLKRENLLSRQNRLMKARSLLV---- 623
Zebrafish   DCDIGQKRENLLSRQKRLMKARSLLVTF-- 632
Goldfish    DFDIGQKRESLLSRQKRLMKARSLLVTF-- 635
Pufferfish  DLDVGTKRAALQSRQKRLTQAREYLVKF-- 626
Trout       DIDIGSKRAALQSKLKRLMKARSYLVEF-- 621
Human       RSDTSDKRKFLKERLARLTQARRRLAQFPG 662
            * . ** * .: ** :** *.
```

Figure 4. ClustalW alignment of carp Mx1 with selected fish and human Mx genes. Regions corresponding to highly conserved domains in the dynamin superfamily are marked above the sequence alignment: the N-terminal GTPase domain, containing a conserved tripartite GTP-binding motif (grey shaded) and dynamin family signature (bold and underlined). The dynamin central domain is marked by a dashed line. The GTPase effector domain (GED) is indicated with a box representing a coiled-coil region containing the C-terminal leucine zipper motif. Symbol (*) indicates identities and symbol (:) or (.) denotes similarities. Dashes indicate gaps used to maximize the alignment. NCBI references/Genbank accession nos.: zebrafish (*Danio rerio*, NM_182942.3); goldfish (*Carassius auratus,* AY303813.1); pufferfish (*Takifugu rubripes*, AAO37934) rainbow trout (*Oncorhynchus mykiss*, U30253.1); human (*Homo sapiens*, NM_001144925.1).

that carp Mx1 remains localized within the cytoplasm. K-Nearest Neighbors (k-NN) Prediction, a protein prediction tool for subcellular localization, confirmed this suggestion with a probability of 78.3% (k=23) for cytoplasmic localization, as opposed to probabilities of 17.4% for nuclear and 4.3% for peroxisomal localization.

DNA vaccination confers protection against bath challenge with SVCV

After infection with SVCV, the first mortalities were recorded on day 6 p.i. in the non-vaccinated group (pcDNA3) and on day 8 p.i. in the vaccinated group (pcDNA3-SVCV-G; Fig. 5A). After 30 days p.i., mortality was

48% in the non-vaccinated group but only 15% in the vaccinated group. The relative percent survival of 64.7% indicates that the DNA vaccination against SVCV conferred a good but not complete protection. To confirm successful bath infection by SVCV, mid kidneys of challenged fish were analysed for the expression of the viral N gene by real-time quantitative PCR (Fig. 5B). Non-vaccinated fish showed N gene expression starting at day 2 p.i. and peaking at day 4 p.i., whereas expression of the N gene could not be detected in vaccinated fish, indicating clearance of the virus in the vaccinated group. As expected, N gene expression was not observed in the unchallenged control group.
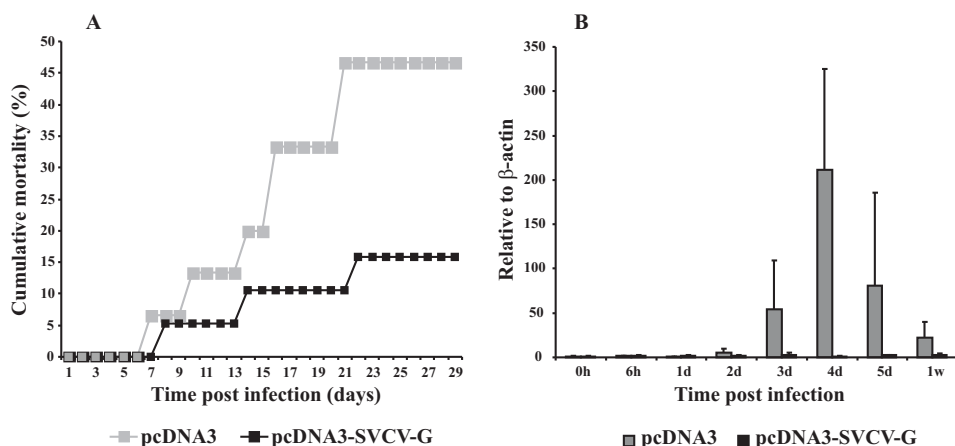
Figure 5. Mortality after bath challenge with spring viraemia of carp virus (SVCV) and detection of the virus by gene expression. SVCV-induced mortality and SVCV-N gene expression in non-vaccinated (pcDNA3 only) and vaccinated (pcDNA3-SVCV-G; 10 µg) carp. Both groups were bath challenged with 10^{-3} TCID50/ml SVCV, twelve weeks post-vaccination. A) Cumulative mortality. B) Gene expression by real-time quantitative PCR at different time points post infection. At each time point fish were sacrificed and the level of N gene expression analysed in mid kidney tissue samples. Data are shown as mean+SD of n=6 fish. Gene expression was normalized relative to β-actin as a reference gene. Abbreviations: h: hour; d: day; w: week.

Mx1, but not IFNαβ gene expression is up-regulated by injection with plasmid DNA

Kinetics of gene expression of IFNαβ and Mx1 were determined in DNA-vaccinated and in non-vaccinated carp for a period of two weeks after plasmid injection (Fig. 6A) and for a period of one week after challenge with SVCV (Fig. 6B). Plasmid injection (Fig. 6A) did not induce up-regulation of IFNαβ expression in neither group. Instead, IFNαβ gene expression was significantly down-regulated at time point > 5 days in both vaccinated and non-vaccinated fish. In contrast, Mx1 gene expression did show a significant up-regulation 3-4 days after plasmid injection. Remarkably, the increase in Mx1 gene expression was significant only in fish injected with pcDNA3 and not in fish injected with the DNA vaccine, owing to high individual variation.

Challenge with SVCV (Fig. 6B) significantly up-regulated IFNαβ gene expression at 4 days p.i. in non-vaccinated fish. Challenge with SVCV also induced a significant up-regulation of Mx1 at time point > 2 days with a peak at 4 days p.i. (Fig. 6B). Mx1 gene expression was induced in both vaccinated and non-vaccinated fish.
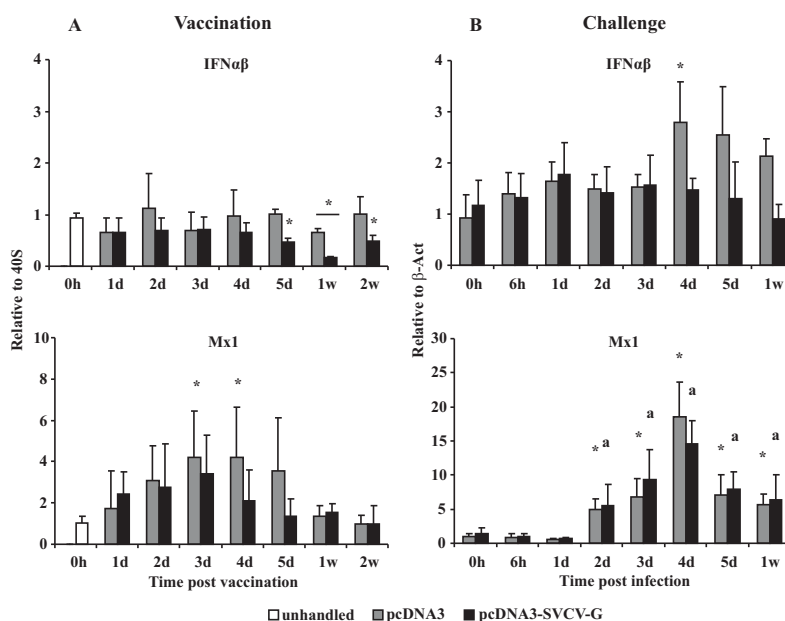
Figure 6. Real-time quantitative PCR analysis of IFNαβ and Mx1. Gene expression was measured in mid kidney of control (unhandled), non-vaccinated (pcDNA3) and vaccinated (pcDNA3-SVCV-G) carp at different time points after vaccination (A) and after SVCV challenge (B). Gene expression in the samples collected after vaccination was normalized relative to the S11 protein of the 40S subunit as a reference gene while in samples collected after infection it was normalized relative to β-actin. Note the difference in Mx1 fold change (y-axis) between the two experiments. Data are shown as mean +SD of n=6 fish. Symbol (*) indicates statistical difference between non-vaccinated and vaccinated fish with respect to the unhandled control (panel A) and statistical difference between non-vaccinated carp and the corresponding 0h control (panel B). Symbol (a) denotes statistical difference between vaccinated carp and the corresponding 0h control (panel B). Abbreviations: h: hour; d: day; w: week.

IL-12p35 gene expression is up-regulated in naïve fish by challenge with SVCV

Kinetics of gene expression of IL-12p35 and IL-12p40b were determined in DNA-vaccinated and in non-vaccinated carp for a period of two weeks after plasmid injection (Fig. 7A) and for a period of one week after challenge with SVCV (Fig. 7B). Plasmid injection (Fig. 7A) did not induce up-regulation of IL-12p35 nor IL-12p40b expression in neither group.

Challenge with SVCV (Fig. 7B), significantly up-regulated IL-12p35 gene expression at 4 days p.i. in non-vaccinated fish. No significant up-regulation of IL-12p40b after viral challenge could be observed in neither group.
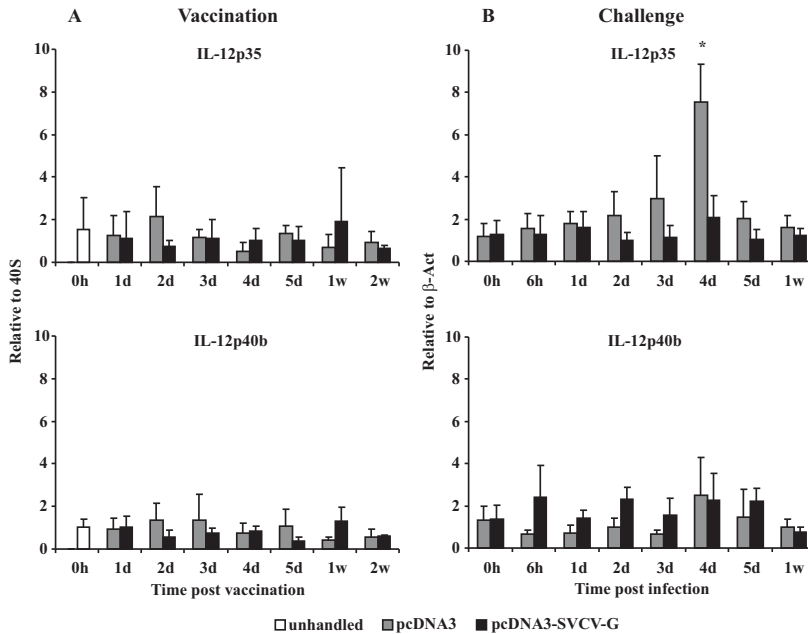
Figure 7. RT-qPCR analysis of IL-12p35 and IL-12p40b. Gene expression was measured in mid kidney of control (unhandled), non-vaccinated (pcDNA3) and vaccinated (pcDNA3-SVCV-G) carp after plasmid injection (A) and after SVCV challenge (B). Data presentation as described in the legend of Fig. 6.

CxCa and IL-1β1 gene expression are up-regulated in naïve fish by challenge with SVCV

Kinetics of gene expression of CXCa and IL-1ß1 were determined in DNA-vaccinated and non-vaccinated carp for a period of two weeks after plasmid injection (Fig. 8A) and for a period of one week after challenge with SVCV (Fig. 8B). Plasmid injection (Fig. 8A) induced a significant down-regulation of CXCa gene expression at 4-7 days (vaccinated group) or at 7 days (non-vaccinated group) and a significant down-regulation of IL-1ß1 gene expression at 7 days in the vaccinated group.

Challenge with SVCV (Fig. 8B) significantly upregulated CXCa gene expression at 1 and 7 days p.i. in non-vaccinated fish. Challenge with SVCV also induced up-regulation of IL-1β1 gene expression at time point > 4 days p.i., although statistically significant only at 7 days p.i., owing to high individual variation. No significant change in gene expression could be observed in the vaccinated group.
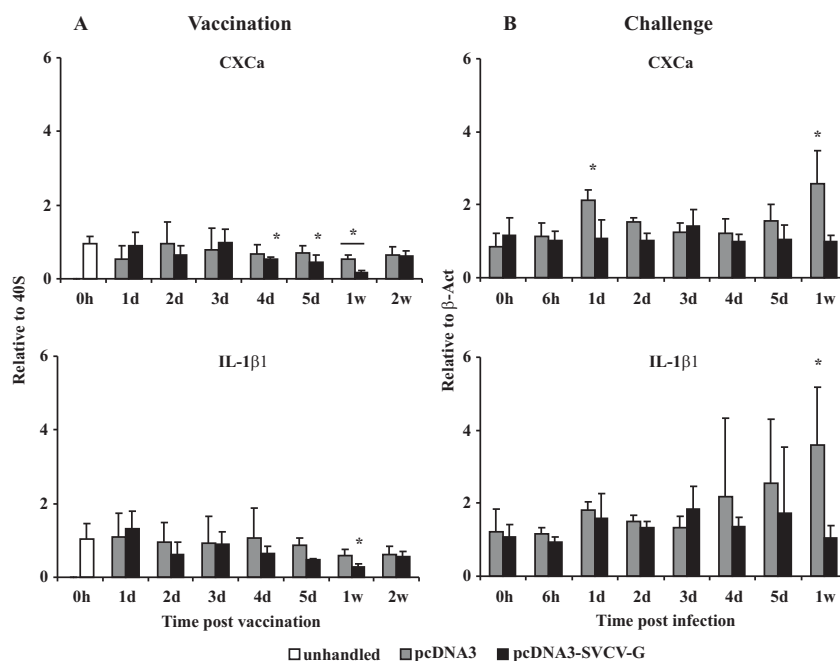
Figure 8. RT-qPCR analysis of CXCa and 1β. Gene expression was measured in mid kidney of control (unhandled), non-vaccinated (pcDNA3) and vaccinated (pcDNA3-SVCV-G) carp after plasmid injection (A) and after SVCV challenge (B). Data presentation as described in the legend of Fig. 6.

IFNγ2 gene expression is up-regulated in naïve fish by challenge with SVCV

Kinetics of gene expression of IFNγ2 and IL-10 were determined in DNA-vaccinated and in non-vaccinated carp for a period of two weeks after plasmid injection (Fig. 9A) and for a period of 1 week after challenge with SVCV (Fig. 9B). Plasmid injection (Fig. 9A) did not induce significant changes in IFNγ2 gene expression in neither group. Plasmid injection induced a significant down-regulation of IL-10 gene expression at 5 days in the vaccinated group. Challenge with SVCV (Fig. 9B), significantly upregulated IFNγ2 gene expression at 4 days p.i. in non-vaccinated fish. In vaccinated fish, up-regulation of IFNγ2 gene expression was earlier (1-2 days p.i.). Challenge with SVCV also induced a significant up-regulation of IL-10 in both vaccinated (2 days p.i.) and non-vaccinated (2 days and 5 days p.i.) fish.
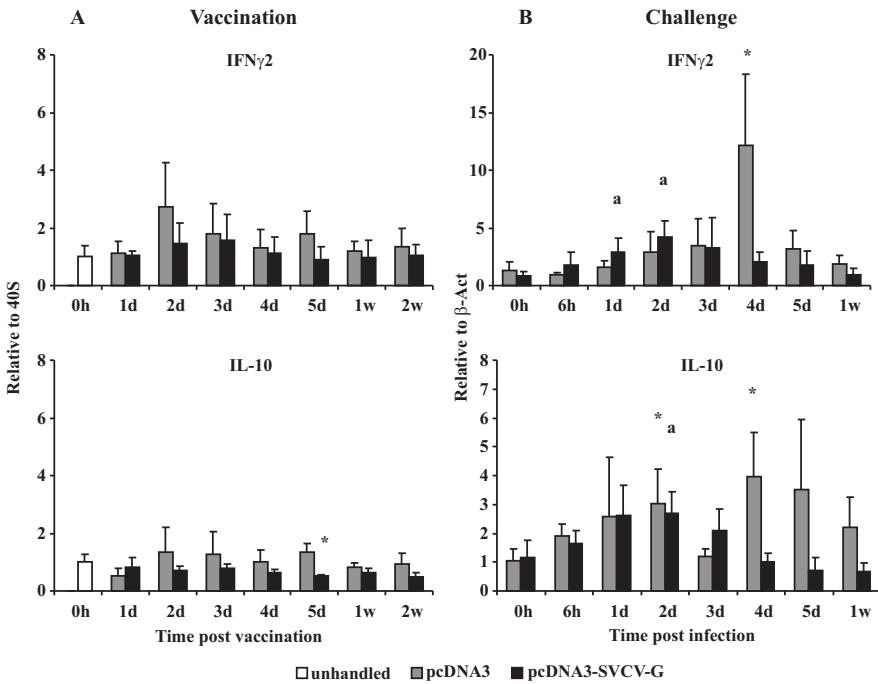
Figure 9. RT-qPCR analysis of IFNγ2 and IL-10. Gene expression was measured in mid kidney of control (unhandled), non-vaccinated (empty plasmid) and vaccinated (pcDNA3-SVCV-G) carp after plasmid injection (A) and after SVCV challenge (B). Data presentation as described in the legend of Fig. 6.

Detection of soluble recombinant carp IL-12p40b*L*p35 fusion protein

In carp, three highly distinct IL-12p40 genes (named IL-12p40a-c) have been described (31). We have previously shown that at 4 days post-infection with SVCV, transcription of only p40b was up-regulated concomitantly with the up-regulation of p35 gene expression (29). In the present study we confirmed the up-regulation of the p35 gene expression, at the same time point of 4 d.p.i. Based on these results, a vector coding for a fused heterodimeric IL-12 protein composed of the p40b and p35 subunit was constructed. Nucleoporation of the EPC carp cell line was used to express the recombinant heterodimeric carp IL-12. We used two approaches to confirm IL-12 protein expression. Western blot analysis using an antibody directed against the 6xHistidine-tag present at the C-terminus of the mature peptide confirmed the presence of a soluble protein of about 80 kDa in the supernatant of EPC cells transfected with the pcDNA3-p40b*L*p35 vector, but not in supernatants of cells transfected with empty plasmid (Fig. 10A). Immunohistochemical detection of HIS-tagged proteins in EPC cells transfected with the pcDNA3-p40b*L*p35 vector, but not in cells transfected with empty plasmid, also confirmed IL-12 expression (Fig. 10B).
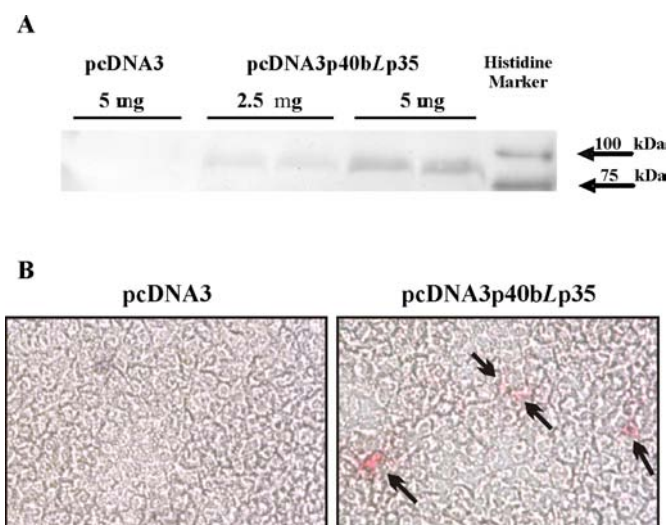
Figure 10. Expression of recombinant carp IL-12 fused heterodimeric protein. EPC cells (1 x 10^6) were nucleoporated with 2.5 or 5 µg of pcDNA3p40b*L*p35 plasmid or with 5 µg of empty plasmid (pcDNA3). Cells were cultured for 72h in RPMI medium supplemented with 2.5% FCS. A) Western blot analysis. Protein expression was analyzed in 20 µl of culture supernatant using a mouse-anti 6xHIS (1:1500) and HRP-conjugated goat-anti-mouse antibody. The results from the supernatants of duplicate wells are shown. B) Immunohistochemical analysis. EPC monolayers were stained with a 1:10 dilution of a mouse-anti Tetra-HIS antibody and AP-conjugated rabbit-anti-mouse secondary antibody. Positive cells (red) are indicated by arrows.

Discussion

In the present study we report the cloning of a carp Mx1 sequence homologous to other known Mx1 sequences together with the gene expression analysis of several other immune relevant genes following DNA vaccination and following challenge of vaccinated carp with spring viraemia of carp virus (SVCV). This is the first report describing changes in gene expression in a cyprinid fish after DNA vaccination and challenge with SVCV.

Only two other studies have reported on the efficacy of a DNA vaccine in (koi) carp against SVCV (2, 7), partly because experimental challenge with SVCV has proven difficult to establish because of low mortality (41). In general, SVC has a seasonal nature and under farming conditions the disease is most severe at temperatures between 11-17 ^{o}C and challenge conditions should respect this temperature range. Of course, the rate of development of a protective immune response following vaccination is temperature dependent in fish. For example, after infection, neutralizing antibodies have been detected after 4 weeks at 20 ^{o}C, after 7 weeks at 15 ^{o}C but not before 10 weeks at 10 ^{o}C (41). In the DNA vaccination study by Kannellos *et al.* (2), carp were vaccinated at 20˚C and after 6 weeks, challenged at 15 ^{o}C by intraperitoneal (i.p.) injection with a heterologous strain of SVCV. Challenge at 15 ^{o}C killed 64% of the control fish, and the strongest protection was observed in carp that received the full-length G-gene expressed by plasmids driven by a CMV-Intron-A rather than the most commonly used CMV promoter, with a relative

percentage survival (RPS) of 48%. In the second study by Emmenegger (7), high value ornamental varieties of carp (koi) received a comparable treatment with DNA vaccination at 20 ^{o}C and SVCV challenge at 10-12 ^{o}C by i.p. injection. Although the RPS values in this study (50-80%) were higher than in the first study (48%) fish were challenged at 4 weeks post-vaccination already, therefore a role for a non-specific (interferon-induced) immune response cannot be excluded. As shown in several studies in salmonids, and tentatively in carp (this study), DNA vaccination induces an early non-specific anti-viral protection mediated by a type I interferon response that can last for several weeks (11).

Ideally, a test challenge method should closely mimic natural exposure to the pathogen and ensure that mucosal immune mechanisms are triggered. Bath and co-habitation challenges best fulfill this requirement, but are more difficult methods to control and standardize than i.p. injection challenge methods. Although Emmenegger *et al.* (7) did develop a bath challenge with SVCV, the dose required to obtain 67% mortality of naïve fish was relatively high ($>10^5$ PFU/ml) and challenge of vaccinated fish was finally performed *via* the i.p. route. We used 10^{-3} TCID$_{50}$ SVCV/ml for our bath challenge which led to 50% mortality of naïve fish. Our DNA vaccination resulted in 85% survival after bath challenge, with a RPS value of 66.7%. Despite these promising results, indeed, our bath challenge has been proven difficult to control and standardize and awaits succesful replication. DNA vaccination of

salmonids against members of the genus *Novirhabdoviridae* (VHS, IHNV and HIRRV) has yielded very strong protection with RPS values of 90% or more, also using bath challenges as the preferred method (11, 15). Although a member of the family *Rhabdoviridaea*, taxonomically, SVCV is classified in the genus *Vesiculoviridae* and not *Novirhabdoviridae* (1). Structural and functional differences between these two genera (1) may help to explain the lower protection generally observed after DNA vaccination against SVCV. In the present study, owing to the lack of suitable antibodies for cytological staining of the SVCV-G protein, expression levels of this protein could not be quantified. However, our construct did confer protection. Possibly, the expression and presentation to the cell surface of the SVCV-G protein might not occur less efficiently than VHS-G protein expression. In the future, the use of a different promoter, such as the CMV-IntronA, or different leader sequences might increase protein expression thereby improving vaccination efficacy.

Extensive gene expression and microarray analysis have been performed in salmonids and Japanese flounder after DNA vaccination against novirhabdoviruses (5, 6, 16-18). As mentioned above, DNA vaccination often induces an early type I interferon and associated Mx response, resulting in non-specific anti-viral protection (11, 15, 42). In these studies, the early Mx up-regulation (4-7 days) was always observed exclusively in fish receiving the DNA vaccine containing the G-protein and not (or to a considerably lower

extent) in control fish treated with an empty plasmid. Surprisingly, in our study, significant Mx1 up-regulation was observed also in carp that received the empty plasmid. Although up-regulation of Mx gene expression in response to empty plasmid DNA contrast with the general findings in salmonids and Japanese flounder, this observation has also been made in DNA vaccination experiments with channel catfish (43). The results in channel catfish and carp indicate the induction of an innate immune response, not triggered by the viral G protein but by plasmid components, in particular fish species. Likely candidates are the several (*n*=25) CpG motifs contained in the backbone of the pcDNA3 plasmid (11). Since the salmonids and Japanese flounder have been found unresponsive to the same CpG motifs in pcDNA3, this would indicate a species-specific recognition of these pathogen-associated molecular patterns by, for example, TOLL-like receptor 9 (44). Interestingly, a recent study using a different plasmid (pAE6) for DNA vaccination of rainbow trout showed increased TLR9 gene expression at the injection site, also after injection of plasmid DNA only (45). Preliminary studies in our laboratory have suggested that unmethylated CpG oligodeoxy- nucleotides (CpG-ODNs), previously shown to induce type I interferon expression and cell proliferation in leukocytes from Atlantic salmon (46), apparently fail to have the same effect in carp (C.M.S. Ribeiro, personal communication). Thus, although salmonids have not been found to respond to the CpG motifs in pcDNA3, it could well be

the case that carp leukocytes are responsive to the CpG-ODN motifs of pcDNA3.

Beside the above-described up-regulation of Mx1 gene expression, none of the other immune relevant genes tested was up-regulated after injection with neither the empty plasmid nor the vaccine plasmid. Nevertheless, carp clearly showed improved protection against bath challenge with SVCV. Although the Mx1 gene expression induced by the empty plasmid suggests the induction of a non-specific immune response, the period of 12 weeks between vaccination and challenge makes it unlikely that the observed protection could be ascribed to an increased non-specific immune response only. As stated, none of the other investigated immune genes was up-regulated in mid kidney after vaccination. On the contrary, a down-regulation of IFNαβ, CXCa, IL-1β1 and IL-10 was observed. Similar results have been obtained in other fish species where, beside a clear Mx gene up-regulation, expression of other immune relevant genes in peripheral organs upon DNA vaccination remained low, especially when compared to the fold changes observed after viral challenge of naïve fish (5, 6, 17, 18). A recent study in trout muscle following DNA vaccination against IHNV, however, clearly shows that local gene expression at the site of injection is much higher (>10 fold) than gene expression in peripheral organs (16). This strongly argues for future studies on gene expression focusing at local sites of plasmid injection in the muscle rather than gene expression studies in peripheral immune organs.

Challenge with SVCV of vaccinated carp did not induce a very strong change in gene expression. Mx1, but also IFNγ2 and IL-10 were upregulated at 1-2 days p.i. with the latter possibly indicating the initiation of a rapid adaptive immune response in vaccinated fish. This is in line with the fact that expression of the SVCV-N gene could not be detected in any of the vaccinated fish after challenge, indicating an immediate clearance of the virus by a protective immune response. Challenge with SVCV of non-vaccinated carp, however, showed an up-regulation of several genes including IFNαβ, Mx, p35, IFNγ2 and IL-10, particularly at 4 days p.i. This confirms our previous observation that infection of naïve fish with SVCV induces a simultaneous up-regulation of IFNαβ, p35 and p40b all at 4 days p.i. (29). In the present study we were unable to confirm the up-regulation of p40b, possibly because of the generally low fold changes in gene expression observed in this study. Analysis of the level of SVCV-N gene expression in challenged naïve carp confirmed that the viral load during the present study was at least 100 times lower than during the previous study (data not shown), although performed under the same conditions. A lower viral load might account for the smaller fold change in gene expression and consequently, for the undetectable change in p40b expression. The clear up-regulation of the p35 subunit, however, again confirms a role for IL-12 during SVCV infection.

In mammals, IL-12 has been shown to serve as a potent immunoadjuvant when administered along with the immunizing

antigen. IL-12 was able to mimic the same phenotype, clonal expansion, effector function, and establishment of memory in CD8^{+} T cells induced by conventional adjuvants. In the present study we constructed a plasmid coding for a carp IL-12 composed of the p40b subunit fused to the p35 subunit through an interspacing linker. A similar strategy has been previously adopted to produce bioactive IL-12 fusion protein in mice, humans and dogs (47, 48). We could detect secreted, and possibly bio-active IL-12 in the supernatant of EPC cells transfected with the pcDNA3-p40b*L*p35 vector. In carp the type of immune response (antibody- or cell-mediated) responsible for protection has not been fully elucidated. Whereas in salmonids, DNA vaccination against IHNV and VHS induces high levels of neutralizing antibodies, in carp several observations point out a major role for cell-mediated immunity in protection against SVCV. In our previous study (29) we observed an up-regulation of cytotoxic T cell (CTL)

markers (CD8αβ) after infection with SVCV. In the study by Kannellos *et al*. (2) the same DNA vaccine which conferred the highest protection in carp after SVCV challenge, consistently induced lymphocyte proliferation rather than neutralizing antibodies in goldfish. In addition, despite the absence of detectable neutralizing antibodies protection against SVCV has been observed after vaccination with inactivated viruses (41). Given the ability of IL-12 to sustain cell-mediated immunity especially, we strongly suggest that administration of the IL-12p40b*L*p35 construct along with the DNA vaccine, will most likely lead to a more robust cell-mediated immune response thereby improving the efficacy of the SVCV DNA vaccine.

Acknowledgements

References

1. Ahne, W., H. V. Bjorklund, S. Essbauer, N. Fijan, G. Kurath, and J. R. Winton. 2002. Spring viremia of carp (SVC). *DAO* 52:261-272.
2. Kanellos, T., I. D. Sylvester, F. D'Mello, C. R. Howard, A. Mackie, P. F. Dixon, K. C. Chang, A. Ramstad, P. J. Midtlyng, and P. H. Russell. 2006. DNA vaccination can protect *Cyprinus carpio* against spring viraemia of carp virus. *Vaccine* 24:4927-4933.
3. Simard, N., C. Lyngoy, V. Funk, G. Traxler, S. LaPatra, and K. Salonius. 2006. Research to market: meeting safety and efficacy requirements for a DNA vaccine used in Atlantic salmon. In *International Veterinary Vaccine and Diagnostics Conference*. I. Olsen, and T. Gjøen, eds. Represntralen, University of Oslo, Oslo, Norway, Oslo, Norway. 46.
4. Lorenzen, N., and S. E. LaPatra. 2005. DNA vaccines for aquacultured fish. *Rev Sci Tech* 24:201-213.
5. Byon, J. Y., T. Ohira, I. Hirono, and T. Aoki. 2006. Comparative immune responses in Japanese flounder, *Paralichthys olivaceus* after vaccination with viral hemorrhagic septicemia virus (VHSV) recombinant glycoprotein and DNA vaccine using a microarray analysis. *Vaccine* 24:921-930.
6. Takano, T., A. Iwahori, I. Hirono, and T. Aoki. 2004. Development of a DNA vaccine against hirame rhabdovirus and analysis of the expression of immune-related genes after vaccination. *Fish Shellfish Immunol* 17:367-374.

7. Emmenegger, E. J., and G. Kurath. 2008. DNA vaccine protects ornamental koi (*Cyprinus carpio koi*) against North American spring viremia of carp virus. *Vaccine* 26:6415-6421.

8. Einer-Jensen, K., L. Delgado, E. Lorenzen, G. Bovo, Ø. Evensen, S. E. LaPatra, and N. Lorenzen. 2009. Dual DNA vaccination of rainbow trout (*Oncorhynchus mykiss*) against two different rhabdoviruses, VHSV and IHNV, induces specific divalent protection. *Vaccine* 27:1248-1253.

9. Utke, K., H. Kock, H. Schuetze, S. M. Bergmann, N. Lorenzen, K. Einer-Jensen, B. Kollner, R. A. Dalmo, T. Veselý, M. Ototake, and U. Fischer. 2008. Cell-mediated immune responses in rainbow trout after DNA immunization against the viral hemorrhagic septicemia virus. *Dev Comp Immunol* 32:239-252.

10. Boudinot, P., D. Bernard, S. Boubekeur, M. I. Thoulouze, M. Bremont, and A. Benmansour. 2004. The glycoprotein of a fish rhabdovirus profiles the virus-specific T-cell repertoire in rainbow trout. *J Gen Virol* 85:3099-3108.

11. Kim, C. H., M. C. Johnson, J. D. Drennan, B. E. Simon, E. Thomann, and J. A. Leong. 2000. DNA vaccines encoding viral glycoproteins induce nonspecific immunity and Mx protein synthesis in fish. *J Virol* 74:7048-7054.

12. LaPatra, S. E., S. Corbeil, G. R. Jones, W. D. Shewmaker, N. Lorenzen, E. D. Anderson, and G. Kurath. 2001. Protection of rainbow trout against infectious hematopoietic necrosis virus four days after specific or semi-specific DNA vaccination. *Vaccine* 19:4011-4019.

13. Lorenzen, N., E. Lorenzen, K. Einer-Jensen, and S. E. LaPatra. 2002. DNA vaccines as a tool for analysing the protective immune response against rhabdoviruses in rainbow trout. *Fish Shellfish Immunol* 12:439-453.

14. Lorenzen, N., E. Lorenzen, K. Einer-Jensen, and S. E. LaPatra. 2002. Immunity induced shortly after DNA vaccination of rainbow trout against rhabdoviruses protects against heterologous virus but not against bacterial pathogens. *Dev Comp Immunol* 26:173-179.

15. McLauchlan, P. E., B. Collet, E. Ingerslev, C. J. Secombes, N. Lorenzen, and A. E. Ellis. 2003. DNA vaccination against viral haemorrhagic septicaemia (VHS) in rainbow trout: size, dose, route of injection and duration of protection-early protection correlates with Mx expression. *Fish Shellfish Immunol* 15:39-50.

16. Purcell, M. K., K. M. Nichols, J. R. Winton, G. Kurath, G. H. Thorgaard, P. Wheeler, J. D. Hansen, R. P. Herwig, and L. K. Park. 2006. Comprehensive gene expression profiling following DNA vaccination of rainbow trout against infectious hematopoietic necrosis virus. *Mol Immunol* 43:2089-2106.

17. Acosta, F., A. Petrie, K. Lockhart, N. Lorenzen, and A. E. Ellis. 2005. Kinetics of Mx expression in rainbow trout (*Oncorhynchus mykiss*) and Atlantic salmon (*Salmo salar* L.) parr in response to VHS-DNA vaccination. *Fish Shellfish Immunol* 18:81-89.

18. Purcell, M. K., G. Kurath, K. A. Garver, R. P. Herwig, and J. R. Winton. 2004. Quantitative expression profiling of immune response genes in rainbow trout following infectious haematopoietic necrosis virus (IHNV) infection or DNA vaccination. *Fish Shellfish Immunol* 17:447-462.

19. Trobridge, G. D., and J. A. Leong. 1995. Characterization of a rainbow trout Mx gene. *J Interferon Cytokine Res* 15:691-702.

20. Kibenge, M. J., K. Munir, and F. S. Kibenge. 2005. Constitutive expression of Atlantic salmon Mx1 protein in CHSE-214 cells confers resistance to infectious salmon anaemia virus. *Virol J* 2:75.

21. Robertsen, B., G. Trobridge, and J. A. Leong. 1997. Molecular cloning of double-stranded RNA inducible Mx genes from Atlantic salmon (*Salmo salar* L.). *Dev Comp Immunol* 21:397-412.

22. Lee, J.-Y., I. Hirono, and T. Aoki. 2000. Cloning and analysis of expression of Mx cDNA in Japanese flounder, *Paralichthys olivaceus*. *Dev Comp Immunol* 24:407-415.

23. Jensen, V., and B. Robertsen. 2000. Cloning of an Mx cDNA from Atlantic Halibut (*Hippoglossus hippoglossus*) and characterization of Mx mRNA expression in response to double-stranded RNA or infectious pancreatic necrosis virus. *J Interferon Cytokine Res* 20:701-710.

24. Plant, K. P., and R. L. Thune. 2004. Cloning and characterisation of a channel catfish (*Ictalurus punctatus*) Mx gene. *Fish Shellfish Immunol* 16:391-405.

25. Lin, C. H., J. A. Christopher John, C. H. Lin, and C. Y. Chang. 2006. Inhibition of nervous necrosis virus propagation by fish Mx proteins. *Biochem Biophys Res Commun* 351:534-539.

26. Yap, W. H., A. Tay, S. Brenner, and B. Venkatesh. 2003. Molecular cloning of the pufferfish (*Takifugu rubripes*) Mx gene and functional characterization of its promoter. *Immunogenetics* 54:705-713.

CHAPTER 5

27. Zhang, Y. B., Q. Li, and J. F. Gui. 2004. Differential expression of two *Carassius auratus* Mx genes in cultured CAB cells induced by grass carp hemorrhage virus and interferon. *Immunogenetics* 56:68-75.

28. Altmann, S. M., M. T. Mellon, M. C. Johnson, B. H. Paw, N. S. Trede, L. I. Zon, and C. H. Kim. 2004. Cloning and characterization of an Mx gene and its corresponding promoter from the zebrafish, *Danio rerio*. *Dev Comp Immunol* 28:295-306.

29. Forlenza, M., J. D. de Carvalho Dias, T. Veselý, D. Pokorová, H. F. J. Savelkoul, and G. F. Wiegertjes. 2008. Transcription of signal-3 cytokines, IL-12 and IFN alpha beta, coincides with the timing of CD8 alpha beta up-regulation during viral infection of common carp (*Cyprinus carpio* L). *Mol Immunol* 45:1531-1547.

30. Mescher, M. F., J. M. Curtsinger, P. Agarwal, K. A. Casey, M. Gerner, C. D. Hammerbeck, F. Popescu, and Z. Xiao. 2006. Signals required for programming effector and memory development by CD8+ T cells. *Immunol Rev* 211:81-92.

31. Huising, M. O., J. E. van Schijndel, C. P. Kruiswijk, S. B. Nabuurs, H. F. J. Savelkoul, G. Flik, and B. M. L. Verburg-van Kemenade. 2006. The presence of multiple and differentially regulated interleukin-12p40 genes in bony fishes signifies an expansion of the vertebrate heterodimeric cytokine family. *Mol Immunol* 43:1519-1533.

32. Irnazarow, I. 1995. Genetic variability of Polish and Hungarian carp lines. *Aquaculture Res* 129:215-219.

33. Koutna, M., T. Vesely, I. Psikal, and J. Hulova. 2003. Identification of spring viraemia of carp virus (SVCV) by combined RT-PCR and nested PCR. *Dis Aquat Organ* 55:229-235.

34. Fijan, N., D. Sulimanovic, M. Bearzotti, D. Muzinic, L. O. Zwillenberg, S. Chilmonczyk, J. F. Vautherot, and P. de Kinkelin. 1983. Some properties of the *Epithelioma papulosum cyprini* (EPC) cell line from carp *Cyprinus carpio*. *Ann. Virol. (Institue Pasteur)* 134:207-220.

35. Reed, R. J., and H. Müench. 1938. A simple method of estimating fifty percent endpoints. *Am. J. Hyg.* 27:493-497.

36. Pfaffl, M. W. 2001. A new mathematical model for relative quantification in real-time RT-PCR. *Nucleic Acids Res* 29:e45.

37. Tichopad, A., M. Dilger, G. Schwarz, and M. W. Pfaffl. 2003. Standardized determination of real-time PCR efficiency from a single reaction set-up. *Nucleic Acids Res* 31:e122.

38. Pfaffl, M. W., A. Tichopad, C. Prgomet, and T. P. Neuvians. 2004. Determination of stable housekeeping genes, differentially regulated target genes and sample integrity: BestKeeper--Excel-based tool using pair-wise correlations. *Biotechnol Lett* 26:509-515.

39. Kozak, M. 1987. At least six nucleotides preceding the AUG initiator codon enhance translation in mammalian cells. *J Mol Biol* 196:947-950.

40. Heppell, J., N. Lorenzen, N. K. Armstrong, T. Wu, E. Lorenzen, K. Einer-Jensen, J. Schorr, and H. L. Davis. 1998. Development of DNA vaccines for fish: vector design, intramuscular injection and antigen expression using viral haemorrhagic septicaemia virus genes as model. *Fish Shellfish Immunol* 8:271-286.

41. Dixon, P. 1997. Immunization with viral antigens: viral diseases of carp and catfish. *Dev Biol Stand* 90:221-232.

42. Sommerset, I., E. Lorenzen, N. Lorenzen, H. Bleie, and A. H. Nerland. 2003. A DNA vaccine directed against a rainbow trout rhabdovirus induces early protection against a nodavirus challenge in turbot. *Vaccine* 21:4661-4667.

43. Harbottle, H., K. P. Plant, and R. L. Thune. 2005. DNA vaccination against Channel Catfish Virus results in minimal immune response and is not efficacious against challenge. *J. Aquat Anim Health* 17:251-262.

44. Kumagai, Y., O. Takeuchi, and S. Akira. 2008. TLR9 as a key receptor for the recognition of DNA. *Adv Drug Delivery Rev* 60:795-804.

45. Ortega-Villaizan, M., V. Chico, A. Falco, L. Perez, J. M. Coll, and A. Estepa. 2009. The rainbow trout TLR9 gene and its role in the immune responses elicited by a plasmid encoding the glycoprotein G of the viral haemorrhagic septicaemia rhabdovirus (VHSV). *Mol Immunol* 46:1710-1717.

46. Strandskog, G., T. Ellingsen, and J. B. Jorgensen. 2007. Characterization of three distinct CpG oligonucleotide classes which differ in ability to induce IFN alpha/beta activity and cell proliferation in Atlantic salmon (*Salmo salar* L.) leukocytes. *Dev Comp Immunol* 31:39-51.

47.   Lieschke, G. J., P. K. Rao, M. K. Gately, and R. C. Mulligan. 1997. Bioactive murine and human interleukin-12 fusion proteins which retain antitumor activity in vivo. *Nat Biotech* 15:35-40.

48.   Saldarriaga, O. A., L. E. Perez, B. L. Travi, and P. C. Melby. 2006. Selective enhancement of the type 1 cytokine response by expression of a canine interleukin (IL)-12 fused heterodimeric DNA. *Vet Immunol Immunopathol* 110:377-388.
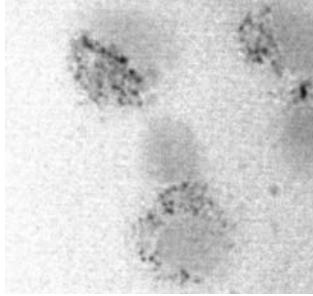
CHAPTER 5

CHAPTER

6

Differential contribution of neutrophilic granulocytes and macrophages to nitrosative stress in a host-parasite infection model

Maria Forlenza, Jörn P. Scharsack, Neli M. Kachamakova,
Anja J. Taverne-Thiele, Jan H.W.M. Rombout and Geert F. Wiegertjes

Chapter 6

MOLECULAR
IMMUNOLOGY
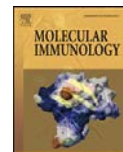
Differential contribution of neutrophilic granulocytes and macrophages to nitrosative stress in a host–parasite animal model

Maria Forlenza[a], Joern P. Scharsack[b], Neli M. Kachamakova[c], Anja J. Taverne-Thiele[a], Jan H.W.M. Rombout[a], Geert F. Wiegertjes[a],[*]

[a] Department of Animal Sciences, Cell Biology and Immunology Group, Wageningen Institute of Animal Sciences, Wageningen University, P.O. Box 338, 6700 AH Wageningen, The Netherlands
[b] University of Münster, Institute for Evolution and Biodiversity, Animal Evolutionary Ecology Group, Huefferstr. 1, D-48149 Münster, Germany
[c] Polish Academy of Sciences, Institute of Ichthyobiology & Aquaculture in Golysz, Zaborze, ul. Kalinowa 2, 43-520 Chybie, Poland

ARTICLE INFO

ABSTRACT

Tyrosine nitration is a hallmark for nitrosative stress caused by the release of reactive oxygen and nitrogen species by activated macrophages and neutrophilic granulocytes at sites of inflammation and infection. In the first part of the study, we used an informative host–parasite animal model to describe the differential contribution of macrophages and neutrophilic granulocytes to *in vivo* tissue nitration. To this purpose common carp (*Cyprinus carpio*) were infected with the extracellular blood parasite *Trypanoplasma borreli* (Kinetoplastida). After infection, serum nitrite levels significantly increased concurrently to the upregulation of inducible nitric oxide synthase (iNOS) gene expression. Tyrosine nitration, as measured by immunohistochemistry using an anti-nitrotyrosine antibody, dramatically increased in tissues from parasite-infected fish, demonstrating that elevated NO production during *T. borreli* infection coincides with nitrosative stress in immunologically active tissues. The combined use of an anti-nitrotyrosine antibody with a panel of monoclonal antibodies specific for several carp leukocytes, revealed that fish neutrophilic granulocytes strongly contribute to *in vivo* tissue nitration most likely through both, a peroxynitrite- and an MPO-mediated mechanism. Conversely, fish macrophages, by restricting the presence of radicals and enzymes to their intraphagosomal compartment, contribute to a much lesser extent to *in vivo* tissue nitration. In the second part of the study, we examined the effects of nitrosative stress on the parasite itself. Peroxynitrite, but not NO donor substances, exerted strong cytotoxicity on the parasite *in vitro*. *In vivo*, however, nitration of *T. borreli* was limited if not absent despite the presence of parasites in highly nitrated tissue areas. Further, we investigated parasite susceptibility to the human anti-trypanosome drug Melarsoprol (Arsobal), which directly interferes with the parasite-specific trypanothione anti-oxidant system. Arsobal treatment strongly decreased *T. borreli* viability both, *in vitro* and *in vivo*. All together, our data suggest an evolutionary conservation in modern bony fish of the function of neutrophilic granulocytes and macrophages in the nitration process and support the common carp as a suitable animal model for investigations on nitrosative stress in host–parasite interactions. The potential of *T. borreli* to serve as an alternative tool for pharmacological studies on human anti-trypanosome drugs is discussed.

1. Introduction

Both activated neutrophilic granulocytes and macrophages have the ability to engulf extracellular pathogens into intracellular phagosomes and, through a series of events that lead to the maturation of the vacuole, destroy the invading agent in the newly 'armed' phagolysosome (Vieira et al., 2002). To the antimicrobial properties of a phagolysosome, greatly contribute the presence of microbicidal peptides, enzymes such as (myelo)peroxidase, elas-

tase and defensins, a very low pH and the production of highly reactive oxygen species (e.g. H_2O_2, $O_2^{\bullet-}$). The production of nitric oxide ($NO^{\bullet}$) by the cytokine-inducible $NO^{\bullet}$-synthase (iNOS) also plays an important part in the microbicidal activity of professional phagocytes (Evans et al., 1996; Xia and Zweier, 1997; Linares et al., 2001). However, the same oxidative agents and enzymes can be released outside the cell, where they not only attack extracellular pathogens but also contribute to nitrosative stress and tissue injury (Ricevuti, 1997; Klebanoff, 2005).

The rapid recruitment of professional phagocytes to infection and inflammatory sites can cause tyrosine nitration, a hallmark of tissue injury (Hurst, 2002). The simultaneous generation of $NO^{\bullet}$ and $O_2^{\bullet-}$ can lead to the formation of peroxynitrite ($ONOO^-$), a

powerful oxidant known to nitrate phenolic compounds, including the tyrosine ring, leading to the formation of nitrotyrosine (Radi et al., 2001). Tyrosine nitration has been associated not only with infectious diseases (e.g. human and murine trypanosomiasis, murine leishmaniasis and bacterial infections) but also with several (neuro)degenerative and inflammatory diseases (Ischiropoulos, 1998; Naviliat et al., 2005). However, significant participation of peroxynitrite in tyrosine nitration has also been questioned (Pfeiffer et al., 2001a,b). Although tyrosine nitration certainly is a specific (bio)marker for nitrosative stress it has often been considered, erroneously, a marker exclusively for peroxynitrite (Hurst, 2002). The most widely discussed alternative mechanism for *in vivo* tyrosine nitration is the myeloperoxidase (MPO)-catalyzed oxidation of nitrite (NO_2^-), a catabolic end-product of $NO^\bullet$ (Eiserich et al., 1998; Hazen et al., 1999; van Dalen et al., 2000; Brennan et al., 2002; Gaut et al., 2002). To date, several pharmacological and genetic studies in various mammalian animal and cellular models of disease (Ischiropoulos, 1998; Radi et al., 2001; Radi, 2004) have been applied to identify the biological mechanisms of nitration and preferential nitration pathway, but the responses have been highly model-dependent. Therefore, additional animal models and strategies are needed to study the balance between protection and pathogenesis caused by nitrosative stress.

Zebrafish (*Danio rerio*) have been found highly valuable for embryologically and genetically tractable diseases (Lieschke and Currie, 2007), and increasingly are also recognized as animal model for immunological studies (van der Sar et al., 2006; Kari et al., 2007; Lin et al., 2007; Meijer et al., 2008). The teleost common carp (*Cyprinus carpio* L.) is genetically very close to the zebrafish but its large body size easily allows for cellular studies. The availability of monoclonal antibodies specifically recognizing various carp leukocytes further supports the use of common carp as animal species suitable for immunological studies. We use the common carp as an animal model to study the balance between protection and pathogenesis caused by nitrosative stress *in vivo* (Saeij et al., 2002, 2003a; Scharsack et al., 2003). To this end, infections with the extracellular blood parasite *Trypanoplasma borreli* (Protozoa, Kinetoplastida) can be highly informative (Wiegertjes et al., 2005). Similar to *Trypanosoma brucei* infections in mice, typical features include the induction of extremely high serum nitrite levels, polyclonal lymphocyte activation, splenomegaly and, in the late stages of infection, anaemia (Saeij et al., 2002, 2003a). Nitrosative agents and enzymes, released outside the cell, can attack these extracellular parasites but also contribute to nitrosative stress and tissue injury. $NO^\bullet$ production was detrimental to the host as suggested by observations where *T. borreli*-infected carp treated with an iNOS inhibitor had higher survival than infected control carp (Saeij et al., 2002). $NO^\bullet$ resulted in apoptosis of carp peripheral blood leukocytes (PBL) and inhibited proliferation of blood, spleen and head kidney (HK) leukocytes (Saeij et al., 2002, 2003b; Scharsack et al., 2003). In two separate studies, effects of $NO^\bullet$ on the parasite itself were also investigated (Saeij et al., 2002; Scharsack et al., 2003), however the results were in apparent contradiction, possibly due to the different read-out systems used by the authors. In conclusion, *T. borreli* infections of common carp are especially suitable to investigate the immuno-modulatory effects of nitrosative stress on both, host and parasite.

The first aim of the present study was to investigate the relative contribution of neutrophilic granulocytes and macrophages to nitrosative stress *in vivo*. To this end, we infected common carp with the parasite *T. borreli* and followed iNOS gene expression over time. We used an anti-nitrotyrosine antibody to investigate the kinetics of nitrotyrosine formation in spleen from infected fish. The anti-nitrotyrosine antibody was also used in combination with a panel of antibodies to probe the pattern and the extent of tyrosine nitra-

tion of neutrophilic granulocytes, macrophages and B cells as well as of the parasites. The most widely discussed alternative for *in vivo* tyrosine nitration by peroxynitrite is MPO-catalyzed oxidation of nitrite. We carefully compared the patterns of tyrosine nitration and a staining specific for MPO enzymatic activity to investigate the contribution of MPO to the nitration process *in vivo*.

The second aim of this study was to examine the immuno-modulatory effects of nitrosative stress on the parasite itself. Studies have demonstrated that different kinetoplastid parasites, among which *Trypanosoma brucei* (Mabbott et al., 1994), *Trypanosoma cruzi* (Denicola et al., 1993) and *Leishmania major* (Assreuy et al., 1994), show different susceptibilities to $NO^\bullet$ and $ONOO^-$. We studied the effects of nitrosative stress on *T. borreli* itself by measuring parasite viability after *in vitro* exposure to $NO^\bullet$ or $ONOO^-$ donors. Further, we investigated parasite susceptibility to the human anti-trypanosome drug Melarsoprol (Arsobal), which directly interferes with the trypanothione anti-oxidant system (Harder et al., 2001). The trypanothione system is exclusive to parasitic protozoa of the order Kinetoplastida, replacing the nearly ubiquitous glutathione/glutathione reductase (GR) couple present in their mammalian hosts (Krauth-Siegel et al., 2003). Melarsoprol is believed to form a stable complex with trypanothione itself thereby inhibiting the activity of the trypanothione reductase (TR) and the ability of the parasite to survive oxidative/nitrosative stress.

Our results support the common carp as a suitable animal model for studies on the relative contribution of neutrophilic granulocytes and macrophages to nitrosative stress. We also provide evidences for an evolutionary conservation in modern bony fish of the function of neutrophilic granulocytes and macrophages in the nitration process. The suitability of the *T. borreli* parasite as an alternative tool for pharmacological studies on human anti-trypanosome drugs is discussed.

2. Materials and methods

2.1. Animals

European common carp (*Cyprinus carpio carpio* L.) were bred and raised in the central fish facility at Wageningen University, The Netherlands, at 23 °C in recirculating UV-treated water and fed pelleted dry food (Trouvit, Nutreco) daily. R3xR8 carp which are the offspring of a cross between fish of Hungarian origin (R8 strain) and of Polish origin (R3 strain) were used (Irnazarow, 1995).

2.2. Parasites and parasitic infection of carp

T. borreli was cloned and characterized by Steinhagen et al. (1989) and maintained by syringe passage through carp following intra-peritoneal (i.p.) injections with 1×10^4 parasites per fish. Parasitaemia was monitored using a Bürker counting chamber after dilution of blood 1:1 in carp RPMI medium (cRPMI, RPMI 1640 [Gibco] adjusted to 280 mOsmol kg^{-1}) containing 50 IU/ml of heparin (Leo Pharmaceutical Products, Weesp, The Netherlands). For parasite isolation, blood was collected from heavily infected carp and after centrifugation *T. borreli* were collected from the buffy coat and purified on a 1 cm × 12 cm ion-exchange column chromatography using diethylaminoethyl cellulose (DE52, Whatman® International Ltd., Maidstone, England) (Overath et al., 1998). After isolation, parasites were harvested by centrifugation and resuspended in fresh complete HML medium (Steinhagen et al., 2000) supplemented with 5% pooled carp serum, L-Glutamine (2 mM), Penicillin-G (100 IU/ml) and streptomycin sulphate (50 mg/l)).

Before infection with *T. borreli*, carp (9-month-old, weighing 160 ± 20 g) were tattooed with individual numbers, acclimatized to

a quarantine unit for 3 weeks and kept at 20 °C. Fish ($n = 52$) were anaesthetised in 0.3 g/l Tricaine Methane Sulfonate (TMS, Crescent Research Chemicals, Phoenix, USA) and i.p. injected with a dose of 1×10^4 T. borreli/fish, PBS-injected individuals served as non-infected control group. Infected and non-infected fish were equally divided over six tanks. At time point 0 d, $n = 5$ control fish were killed and at various time points after infection, $n = 5$ infected and $n = 3$ non-infected fish were killed with an overdose of TMS to collect serum, blood and tissue samples.

2.3. Isolation of organs and peripheral blood leukocytes

Blood was collected by puncture of the caudal vessel and diluted 1:1 with cRPMI medium containing heparin (50 IU/ml). Head kidney, liver and spleen were dissected, immediately frozen in liquid nitrogen and stored at −80 °C until use for RNA isolation and (immuno)histochemistry. For isolation of PBL, heparinised blood was centrifuged at $600 \times g$ for 10 min at 4 °C and the buffy coat containing leukocytes was collected and layered on 5 ml of Ficoll-Paque™ Plus (Amersham Biosciences, Uppsala, Sweden). Following subsequent centrifugation at $800 \times g$ for 25 min at 4 °C, the leukocyte layer at the interface was collected and washed three times with cRPMI. Cell pellets were stored at −80 °C until further use.

2.4. Isolation of total RNA and cDNA synthesis

Total RNA was isolated from head kidney, spleen, liver and PBL using the RNeasy Mini Kit (Qiagen, The Netherlands) according to the manufacturer's instructions, including on column DNase treatment with the RNase-free DNase set (Qiagen). During RNA isolation from liver samples a proteinase-K treatment was included as well. RNA concentration was measured spectrophotometrically (GeneQuant, Pharmacia Biotech, Sweden) at OD_{260nm}. The integrity of RNA was determined by electrophoresis on 1% agarose gel. Total RNA from individual samples was stored at −80 °C until further use.

Prior to cDNA synthesis, a second DNase treatment was performed using DNase I, Amplification Grade (Invitrogen, Carlsbad, CA). Briefly, 1 μg of RNA was combined with 10× DNase reaction buffer and 1 U DNase I, mixed and incubated at room temperature (rT) for 15 min, followed by inactivation of DNase I by addition of 25 mM EDTA. Synthesis of cDNA was adapted from Invitrogen's Superscript™ III First Strand Synthesis Systems for RT-PCR. Briefly, DNase I-treated RNA samples were mixed with 5× first strand buffer, 300 ng random primers, 10 mM dNTPs, 0.1 M DTT, 40 U RNase inhibitor, followed by incubation at rT for 10 min and at 37 °C for 2 min. Superscript III Reverse Transcriptase (200 U) was added and the mixture was incubated at 37 °C for 50 min. The reaction was stopped at 70 °C for 15 min. A non-reverse transcriptase control was included for each sample. cDNA samples were diluted 1:50 (PBL samples diluted 1:25) in nuclease-free water before using as template in real-time quantitative PCR analysis.

2.5. Real-time quantitative polymerase chain reaction (RT-qPCR)

RT-qPCR using SYBR Green I technology was performed with Rotor-Gene™ 2000 (Corbett Research, Mortlake, Sydney, Australia) and the Brilliant® SYBR® Green QPCR (Stratagene) as detection chemistry as described previously (Forlenza et al., 2008). Briefly, master mix for each PCR run was prepared as follows: 0.32 μl of water, 0.84 μl of each primer (5 μM) and 7 μl Master SYBR Green I mix were combined. Finally, 5 μl of diluted cDNA were added to 9 μl of master mix and transferred to a 0.1 ml tube. Specific primers for iNOS and for the S11 protein of the 40S subunit (qiNOSFW aacaggtctgaaagggaatcca; qiNOSRV cattatctctcatgtccagagtctcttct; q40SFW ccgtgggtgacatcgttaca; q40SRV

tcaggacattgaacctcactgtct) were used under the following conditions: 95 °C for 15 min; 40 cycles at 95 °C for 15 s, 60 °C for 30 s and 72 °C for 30 s followed by a final holding step at 60 °C for 1 min. A melting step was then performed with continuous fluorescence acquisition from 60 °C, with a rate of 1 °C/5 s, up to 99 °C to confirm amplification specificity. In all cases, amplification was not observed in negative controls (non-template control and non-reverse transcriptase control). The cycle threshold (C_T) values for each sample and the reaction efficiencies (E) for each primer set were obtained upon Comparative Quantitation analysis from the Rotor-Gene Version 6.0.21 software. The relative expression ratio (R) of a target gene was calculated based on the averaged E and the C_T deviation of sample versus control, and expressed in comparison to a reference gene (Pfaffl, 2001; Tichopad et al., 2003). The 40S ribosomal protein S11 was used as internal reference gene.

2.6. Primary antibodies

The mouse monoclonal antibody WCI-12 binds to the heavy chain of carp IgM and was used to identify B cells (Secombes et al., 1983; Koumans-van Diepen et al., 1995). The TCL-BE8 monoclonal antibody binds to carp neutrophilic granulocytes (strong affinity), monocytes (low affinity) (Nakayasu et al., 1998), and basophilic granulocytes (intermediate affinity; unpublished results). In tissue sections, the monoclonal antibody WCL-15 reacts with the cytoplasm of monocytes and macrophages (Weyts et al., 1997; Romano et al., 1998). A polyclonal rabbit antiserum against T. borreli was used as described elsewhere (Joerink et al., 2007). For the detection of nitrotyrosine, anti-nitrotyrosine rabbit immunoaffinity purified IgG (Bio-connect, Upstate, The Netherlands) was used.

2.7. (Immuno)histochemistry

Cryosections (7 μm) of spleen tissue were mounted on poly-L-lysine-coated glass slides (BDH Laboratory Supplies, Poole, UK), air-dried for 60 min and incubated in a 0.3% H_2O_2 solution in methanol for 20 min to inactivate endogenous peroxidase. Following steps were performed at rT unless stated otherwise. Sections were washed for 5 min with PBS, then with distilled water and incubated in proteinase-K solution (50 μg/ml proteinase-K in distilled water) for 10 min at 37 °C. Samples were fixed in 4% paraformaldehyde in PBS for 5 min at 4 °C followed by washing in 0.1% Triton PBS (PBS-T) for 5 min at 4 °C and subsequently in PBS-T for 7 min at rT. A blocking solution of 5% normal goat serum was then added onto the slides and incubated for 30 min. Anti-nitrotyrosine antibody (1:20) was then added alone or in combination with WCI-12 (1:20) or TCL-BE8 (1:20) or WCL-15 (1:50) in PBS for 1 h. After washing twice for 10 min in PBS-T, sections were incubated for 1 h in a 1:200 dilution in PBS of horseradish peroxidase-conjugated goat-anti-rabbit antibody (HRP-GAR, Dako, Glostrup, Denmark) alone or in combination with the same dilution of alkaline phosphatase-conjugated goat-anti-mouse antibody (AP-GAM, Dako). When only HRP-GAR antibodies were used, after washing twice in PBS-T, sections were incubated for 10 min in 0.05 M sodium acetate buffer, pH 5 and following addition of 0.4 mg/ml 3-amino-9-ethyl-carbazole (AEC; Sigma–Aldrich, St. Louis, USA) in sodium acetate buffer containing 0.03% H_2O_2 incubated again for 25 min. Sections were then rinsed four times in distilled water. Alternatively, when both secondary antibodies were used (double-staining), sections were first incubated in AP-buffer (0.1 M Tris–Cl, 0.1 M NaCl, 0.05 M $MgCl_2$, pH 9.5) for 10 min and then stained using AP-substrate (4.5 μl/ml nitro-blue-tetrazoleum [Roche Applied Science] and 3.5 μl/ml 5′-bromo-4′-chloro-3′-indolyl phosphate [BCIP; Roche Applied Science] in AP-buffer) for 2–5 min followed by four washes in distilled water and subsequent AEC stained as described above. Finally,

sections were rinsed in distilled water and embedded in Kaiser's glycerine gelatin (Merck, Darmstadt, Germany). Sections treated without first antibody showed no staining and pre-incubation for 1 h of anti-nitrotyrosine rabbit immunoglobulins with 10 mM nitrotyrosine solution completely prevented staining. Hematoxylin and eosin staining was performed according to standard procedures.

2.8. Magnetic activated cell sorting (MACS) of antibody-labelled macrophages and neutrophilic granulocytes

Enriched macrophages and granulocyte fractions were obtained as described previously (Verburg-van Kemenade et al., 1994). Briefly, single cell suspensions from head kidney or spleen isolated from healthy carp were obtained by forcing the tissue through a 100 μm nylon mesh. Subsequently, mixed cell suspensions were layered on a discontinuous Percoll density gradient (Amersham Pharmacia Biotech. AB). Cells at the interface between the 1.0838 g/ml and the 1.06 g/ml density gradient were collected and washed twice in cRPMI. The primary antibodies (WCL-15 or TCL-BE8; both used 1:50) were incubated for 30 min on ice. Next, the cells were washed twice with MACS buffer (0.5% BSA in cRPMI). The secondary antibody (phycoerythrin (PE)-conjugated goat-anti-mouse, DAKO) was then added in a 1:75 dilution and incubated for 30 min on ice. After extensive washing, total cell number was determined with a Bürker chamber, and 10 μl of magnetic beads (anti-PE Microbeads, Miltenyi Biotec, GmbH, Germany) was added per 1×10^8 cells. After incubation for 15 min at 4 °C, cells were washed and finally resuspended in MACS buffer. The magnetic separation was performed on LS-MidiMACS Columns according to the manufacturer's instructions. The purity of the fractions was assessed by flow cytometric analysis (Beckman Coulter, Epics XL-MCL, Miami, FL, USA).

2.9. Myeloperoxidase staining

Myeloperoxidase staining of cryosections or cytospin preparations of adult carp spleen was carried out as previously described (Kaplow, 1965). Briefly, samples were mounted on poly-L-lysine-coated glass slides, air-dried and fixed for 60 s in 10% paraformaldehyde solution in ethanol. Slides were washed for 15–30 s in water and subsequently incubated for 30 s in a freshly prepared staining solution containing 30% ethanol with 3 mg/ml benzidine dihydrochloride [B-3383; Sigma], 1.32 mM $ZnSO_4$, 0.123 M sodium acetate, 0.0146 M sodium hydroxide and 0.02% H_2O_2. Then slides were briefly washed in water, air-dried and mounted in Depex (BDH Laboratory Supplies, Poole, England).

2.10. Myeloperoxidase release assay

MACS-sorted carp neutrophilic granulocytes and macrophages were resuspended in cRPMI, supplemented with 1.5% pooled carp serum at a density of 4×10^7 cells ml^{-1}. Total MPO and MPO release activity were measured as described previously (Quade and Roth, 1997). Briefly, cells (1×10^6) were stimulated in 96-well plates with phorbol myristate acetate (PMA, Sigma)/calcium ionophore (CaI, Sigma) in the presence or absence of Cytochalasin B (Cyto B, Sigma) in a final volume of 150 μl. Cells were incubated for 15 min at 27 °C in a humidified atmosphere in the presence of 5% CO_2. Fifty microliters of pre-warmed ready-to-use es(HS)TMB solution (Stereospecific Detection Technologies, GbR, Baesweiler, Germany) was added to each well followed immediately by 50 μl of pre-warmed 5 mM H_2O_2 solution. After 2 min the colour reaction was stopped by adding 50 μl of 4 M sulfuric acid. Plates were centrifuged at $600 \times g$ for 10 min and 200 μl of supernatant

was transferred to flat-bottom 96-well plates. The optical density (OD) in each well was measured spectrophotometrically at 450 nm (with 620 nm as reference) using a microtiter Anthos 2020 spectrophotometer (CleanAir Techniek B.V., Woerden, The Netherlands). Total MPO content was determined in wells containing 0.02% cetyltrimethylammonium bromide (CTAB, Sigma) solution. Total MPO and background values were determined concurrently with cells exposed to stimuli.

2.11. Susceptibility of Trypanoplasma borreli to NO•, peroxynitrite (ONOO⁻) or Melarsoprol (Arsobal) in vitro

Parasites were seeded out in 96-well flat bottom culture plates in triplicate wells at a density of 1×10^5 parasites/well in a final volume of 150 μl of HML medium. All incubation steps were performed at 27 °C in a humidified atmosphere under 5% CO_2. To assess susceptibility of T. borreli to NO•, parasites were left untreated or incubated with different concentrations of two NO• donors, S-nitroso-N-acetyl-D,L-penicillamine (SNAP, Alexis Biochemicals, San Diego, CA, USA) and S-nitroso-glutathion (GSNO, Sigma). As a control, the degradation product of SNAP, N-acetyl-D,L-penicillamine disulphide (AP-SS), the reduced (GSH) or oxidised (GSO) form of gluthatione, were added to parallel cultures.

To assess susceptibility of T. borreli to ONOO⁻, parasites were left untreated or incubated with different concentrations of a peroxynitrite donor, 3-morpholino-sydnonimine hydrochloride (SIN-1, Sigma). In parallel cultures the antioxidant enzyme superoxide dismutase (SOD, Sigma) was used as scavenger of $O_2^{•−}$ radicals released by the decomposition of SIN-1 in aqueous solutions hence, in these cultures, only NO• was present. Solutions of the donors and control substances were prepared in fresh complete HML medium immediately before addition to the cultures. The amount of NO• released by the different donors and respective control substances, was measured as nitrite (Table 1).

To assess susceptibility of T. borreli to a human anti-trypanosome drug, parasites (10^4 parasites/well) were seeded out in 96-well plates in triplicate wells and incubated in the presence or absence of different concentrations of Melarsoprol (Arsobal, kindly provided by Dr. P.N.J. Langendijk from the Academic Medical Centre in Amsterdam, The Netherlands). Parasite motility was monitored at different intervals using an inverted light microscope. Parasite viability was monitored at 24 h and 48 h by flow cytometric analysis as described later.

2.12. Nitrite and nitrate measurement

After in vitro treatment of parasites with the different donors and respective control substances, nitrite concentration in the culture supernatant was measured as described elsewhere (Green

Table 1
NO• release from NO• and ONOO⁻ donors in culture supernatants

NO• donor (mM)	48 h (μM NO₂⁻)	ONOO⁻ donor (mM)	24 h (μM NO₂⁻)
Control	5.0 ± 0.2	Control	5.0 ± 0.2
0.1 SNAP	26.7 ± 0.5	0.01 SIN	13.5 ± 0.9
0.3 SNAP	44.7 ± 2.4	0.03 SIN	41.9 ± 1.4
0.6 SNAP	66.9 ± 8.3	0.06 SIN	81.9 ± 1.8
1.0 SNAP	106.1 ± 5.6	0.1 SIN	116.6 ± 5.8
AP-SS	1.6 ± 1.2	0.06 SIN + 50 U SOD	85.8 ± 1.1
0.1 GSNO	29.5 ± 2.1	0.06 SIN + 100 U SOD	79.7 ± 4.6
0.3 GSNO	99.1 ± 1.4	0.06 SIN + 200 U SOD	71.8 ± 4.7
0.6 GSNO	132.3 ± 3.5	0.06 SIN + 400 U SOD	66.8 ± 6.0
1.0 GSNO	165.6 ± 4.5	200 U SOD	1.4 ± 0.3
GSH	1.2 ± 0.8		
GSO	0.7 ± 0.4		

et al., 1982). Culture supernatant (50 μl) was added to 50 μl of Griess reagent (1% (w/v) sulphanilamide, 0.1% (w/v) N-naphthyl-ethylenediamine in 2.5% (v/v) phosphoric acid) in a 96-well flat bottom plate. After 10 min the optical density was measured spectrophotometrically at 540 nm (with 690 nm as a reference). In serum samples, total nitrite plus nitrate was quantified using the nitrite/nitrate colorimetric method (Roche Diagnostics GmbH, Mannheim, Germany) according to the manufacturer's instruction. In short, in 100 μl aliquots of diluted serum samples (1:5 in distilled water) nitrate was reduced to nitrite with nitrate reductase and nitrite was determined colorimetrically as described above. Nitrite concentration (μM) was calculated by comparison with a sodium nitrite standard curve. All procedures were performed at rT.

2.13. Flow cytometric analysis of Trypanoplasma borreli viability

T. borreli cultures were thoroughly resuspended and transferred to polystyrene tubes. Propidium iodide (2 μg/ml) was added for detection of dead cells and the volume was adjusted to 400 μl with HML medium. For absolute cell count, a suspension of 5×10^5 standard fluorescent beads (Fluoresbrite™ Carboxy YG 10 micron microspheres, Polysciences, Inc., Eppelheim, Germany) was added. Forward scatter (FSC, corresponding to cell size) and side scatter (SSC, corresponding to cell complexity) characteristics of 3000–10,000 events were acquired in linear mode and fluorescence intensities were acquired at log scale using a Beckman Coulter, Epics XL-MCL flow cytometer. Numbers of viable parasites were calculated according to the formula: events(propidium iodide-negative trypanoplasms) × number(standard beads)/events (standard beads).

2.14. Anti-trypanosomes drug administration

Fish (n = 10) were i.p. injected with T. borreli as described above. Three weeks after infection, at parasitaemia levels around 10^6 parasites/fish, fish (n = 5) received two injections each equivalent to 10 mg/kg Melarsoprol (Arsobal, in 100 μl propylene glycol) separated by a 2-day interval. Fish (n = 5) injected with 100 μl of propylene glycol served as infected control. Two days after the second injection again parasitaemia levels were determined.

2.15. Statistics

Relative expression ratios (R) were calculated as described above. Transformed (LN(R)) values were used for statistical analysis in SPSS Software (15.0). For all tests, homogeneity of variance was assessed using the Levene's test. Significant differences (P < 0.05) were determined by a two-way ANOVA followed by a Sidak test. In case of unequal variances between groups, a two-way ANOVA was performed followed by a Games–Howell test.

3. Results

3.1. Parasite model

Pathological changes associated with T. borreli infection were observed in carp infected with parasites. With increasing parasitaemia, infected fish showed clinical signs of anaemia, splenomegaly, and enlarged head kidney (Bunnajirakul et al., 2000; Rudat et al., 2000). At peak levels of parasitaemia some mortality was recorded (14%).
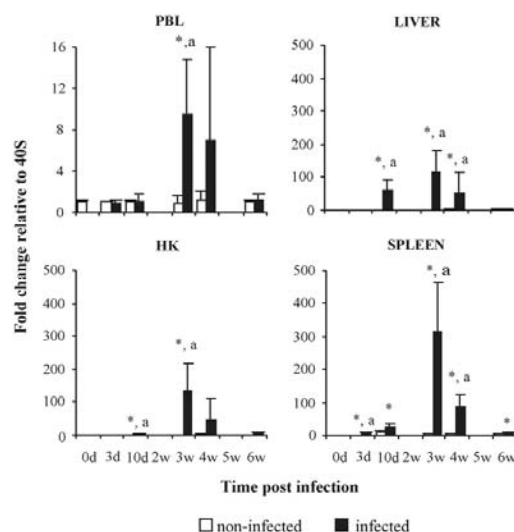
Fig. 1. Real time-quantitative PCR analysis of iNOS gene expression in PBL, liver, HK and spleen isolated from non-infected and T. borreli-infected carp. Gene expression was normalized relative to 40S as reference gene and relative to non-infected fish at time point 0 d. Values are given as mean and S.D. Symbol (*) indicates a significant difference relative to non-infected fish at time point 0 d. Symbol (a) indicates a significant difference relative to non-infected fish at the same time point. Note the difference in fold change (Y-axis) measured in PBL with respect to other organs.

3.2. Infection with Trypanoplasma borreli induces high levels of nitric oxide

The kinetics of in vivo iNOS gene expression in PBL, head kidney, liver and spleen of carp infected with T. borreli was investigated (Fig. 1). In all organs iNOS reached its highest expression at week 3 p.i., and rapidly declined at week 4 p.i. to return to control levels by week 6 p.i. iNOS expression was upregulated more than 100-fold in head kidney, liver and spleen but only 10-fold in PBL. Differences in fold changes could be related to differences in iNOS basal expression in the investigated organs; indeed iNOS transcription was already 10-fold higher in PBL than in head kidney, liver and spleen (data not shown). Interestingly, despite a comparable constitutive mRNA expression in head kidney and spleen, the fold change observed in spleen (313-fold) was notably higher than in head kidney (135-fold; Fig. 1).

In serum samples, total nitrite plus nitrate was quantified in fish infected with T. borreli, and used as a marker for NO• production. Throughout the manuscript, total nitrite plus nitrate will be referred to as nitrite. The kinetics of nitrite production (Fig. 2) corresponded well with the kinetics of iNOS gene expression. Serum nitrite levels in infected fish significantly increased at week 3 p.i. when also the peak of parasitaemia was observed. Serum nitrite levels decreased at week 4 p.i. and returned to control levels by week 6 p.i. The reduction in nitrite levels coincided with the decline of parasitaemia observed between week 4 and 6 p.i.

3.3. Trypanoplasma borreli induces nitration in spleen tissue

Teleost spleen is the major erythropoietic and thrombopoietic organ but also a secondary lymphoid organ. However, the division in red and white pulp is not as defined as in amphibians and homeothermic vertebrates (Fig. 3A).
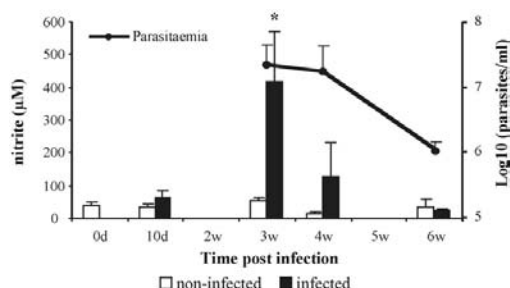
Fig. 2. Parasitaemia and serum nitrite levels during *T. borreli* infection. Carp were infected i.p. with 10^4 *T. borreli*. Parasitaemia and serum nitrite levels are given as mean and S.D. Symbol (*) indicates a significant difference between infected and non-infected fish at the same time point.

The presence of nitrotyrosine in spleen tissue isolated from *T. borreli*-infected carp was used as marker for nitrosative stress. Nitration levels in spleen from infected fish, as indicated by the intensity of the staining and by the extent of the nitrated areas (Fig. 3B–F), were absent or low at day 0 and day 10 p.i., respectively and markedly increased at week 3 and week 4 p.i. Fish which survived the infection recovered from the nitrosative damage as nitration levels declined by week 6 p.i., although they did not completely return to control level. The kinetics of tyrosine nitration corresponded well with the kinetics of iNOS gene expression (Fig. 1) and NO• production (Fig. 2).

3.4. Neutrophilic granulocytes, more than macrophages, contribute to in vivo tissue nitration

Double-staining using an anti-nitrotyrosine antibody (blue) in combination with carp leukocyte-specific monoclonal antibodies (red) was performed to probe the pattern and extent of tyrosine nitration of neutrophilic granulocytes, macrophages and B cells in spleen tissue from non-infected or 4 weeks infected fish (Fig. 4). In tissue from non-infected carp, as indicated by the light blue staining, only a generalised moderate tissue nitration could be observed (A, D and G).

Neutrophilic granulocytes (TCL-BE8+ cells) were present as scattered single cells (Fig. 4A). In tissue from infected carp, neutrophilic granulocytes were present in the centre of highly nitrated areas (B, intense blue staining) and as dispersed single cells in the red pulp (C). Strikingly, nitrotyrosine immunoreactivity was always observed in the area immediately surrounding but never in the cytoplasmic compartment of all neutrophilic granulocytes.

Monocytes/macrophages (WCL-15+ cells) were present as scattered single cells (Fig. 4D). In tissue from infected carp, the intensity and pattern of nitrotyrosine immunoreactivity of macrophages was variable. Nitrotyrosine immunoreactivity was observed in the phagosomes and/or in the area immediately surrounding some, but not all, macrophages (E). Macrophages that did show cytoplasmic tyrosine nitration, displayed a markedly reduced WCL-15 immunoreactivity in contrast to macrophages that did not show cytoplasmic tyrosine nitration, confirming the presence of a heterogeneous splenic macrophage population (F). In addition, comparison of double-staining for WCL-15 with an anti-*T. borreli* antibody or with an anti-nitrotyrosine antibody showed that the presence of nitrotyrosine immunoreactivity in the phagosomes of macrophages could not be ascribed solely to phagocytosis of nitrated parasites (data not shown).

3.5. Enlarged B cell areas in spleen of Trypanoplasma borreli-infected fish show extensive nitration

In spleen from non-infected carp, WCI-12+ (B) cells were present as small aggregates (Fig. 4G, note the different magnification) mainly in association with ellipsoids and small capillaries. Considerably enlarged B cell areas (red staining) were observed in spleen from infected fish (H). Intense WCI-12 immunoreactivity in the lumen of capillaries present in the centre of the B cell area indicates the presence of high levels of circulating antibodies. Strikingly, all
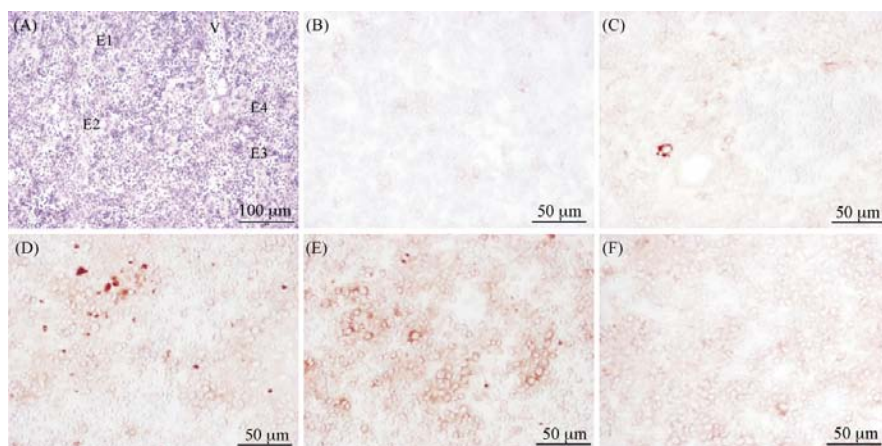
Fig. 3. Extensive tyrosine nitration in carp spleen after *Trypanoplasma borreli* infection. (A) Hematoxylin/eosin staining of spleen from non-infected fish. No clear distinction between white and red pulp is found in carp spleen. Lightly stained areas (red pulp) alternate with numerous ellipsoids (some shown, E1–E4) and with the white pulp (more intensely stained areas) that is mainly located in the proximity of ellipsoids. (B–F) Anti-nitrotyrosine immunoreactivity (red) in carp spleen isolated at 0 d (B), 10 d (C), 3 w (D), 4 w (E) and 6 w (F) after *T. borreli* infection. Incubation of anti-nitrotyrosine antibody with a solution of 10 mM 3-nitrotyrosine, completely abrogated the reaction (not shown).
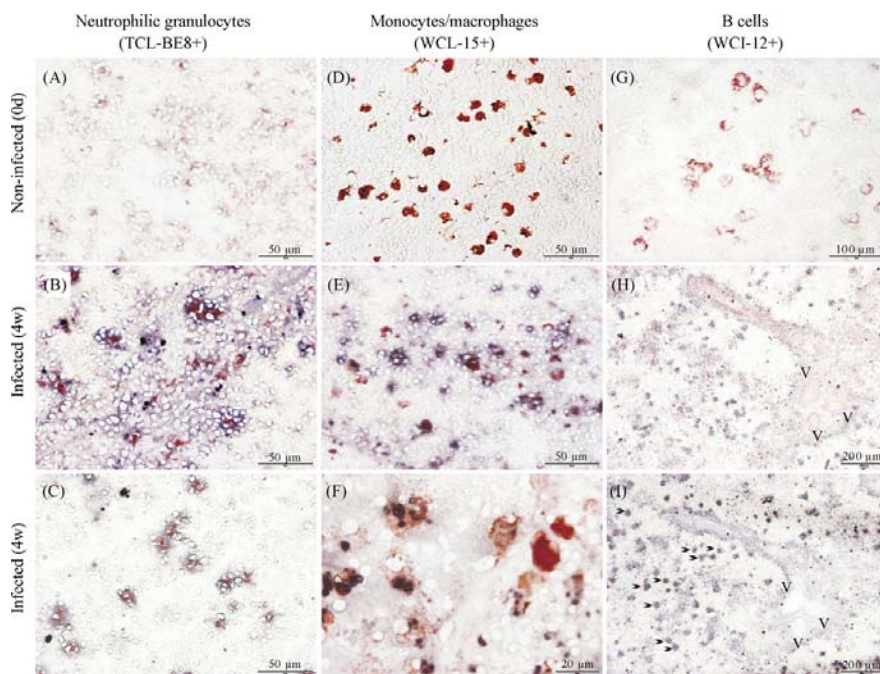
Fig. 4. Differential nitration of carp leukocytes in spleen during *T. borreli* infection. Neutrophilic granulocytes, macrophages and B cells are stained in red. Nitrated areas are stained in blue. (A–C) TCL-BE8 and anti-nitrotyrosine immunoreactivity in control (A) and in 4 weeks infected spleen tissue (B and C). Note the intense nitrotyrosine immunoreactivity in the area immediately surrounding each granulocyte. (D–F) WCL-15 and anti-nitrotyrosine immunoreactivity in control (D) and in 4 weeks infected spleen tissue. Note the difference in WCL-15 immunoreactivity of macrophages present in control and in infected tissue, and also of macrophages in the infected tissue: every macrophage displaying intracellular nitration showed a reduced WCL-15 immunoreactivity. (G and H) WCI-12 and anti-nitrotyrosine immunoreactivity in control (G) and in 4 weeks infected spleen tissue (H). Note the enlargement of the B cell areas in spleen from infected fish. Also note the intense WCI-12 immunoreactivity in the lumen of blood vessels (V) indicating the presence of elevated antibody titers. (I) Consecutive slide stained only with anti-nitrotyrosine antibody showing the extensive nitration associated with every B cell area. Note the presence of numerous discrete intensely nitrated areas dispersed throughout the tissue (arrow heads). Each of these areas was shown to correspond to neutrophilic granulocytes as in (C).

B cell areas were nitrated (blue staining), as shown in a consecutive slide (I), stained only with the anti-nitrotyrosine antibody.

3.6. Neutrophilic granulocytes-derived myeloperoxidase (MPO) contributes to in vivo tissue nitration

The most widely discussed alternative for *in vivo* tyrosine nitration by peroxynitrite is MPO-catalyzed oxidation of nitrite. Staining for MPO of single-cell suspensions of MACS-sorted macrophages (Fig. 5A) and neutrophilic granulocytes (B) revealed MPO activity exclusively in the cytoplasmatic granules of carp neutrophilic granulocytes. High MPO activity, as spectrophotometrically determined, was detected only in neutrophilic granulocytes (C). MPO release assays demonstrated the ability of neutrophilic granulocytes to secrete MPO (D).

To investigate whether the extensive tissue nitration observed after infection could be ascribed to an MPO-mediated mechanism, we stained spleen tissue from (non-)infected fish. In non-infected fish (Fig. 6A) strong MPO activity (blue) could be detected and exclusively localized in the cytoplasmatic granules of single neutrophilic granulocytes. Clearly, in spleen from infected fish (B) the extent and intensity of the MPO staining markedly increased throughout the tissue, especially in areas which also showed a marked nitrotyrosine immunoreactivity (not shown).

3.7. Trypanoplasma borreli is killed by peroxynitrite (ONOO⁻) but not by NO• in vitro

We used two NO• donors, SNAP and GSNO and a peroxynitrite donor, SIN-1 to examine parasite motility and viability after exposure to different concentrations of these chemicals. Parasite motility was monitored using a light microscope while the effect on viability was assessed by flow cytometry. Administration of SIN-1 for 24 h resulted in an NO• release close to the physiological range and to the amounts released by the NO• donors (Table 1).

Administration of the two different NO• donors (SNAP and GSNO) for 48 h resulted in moderately decreased parasite motility only at the highest concentrations (0.6–1.0 mM) (data not shown). Flow cytometric analysis showed clear changes in size and complexity of the parasites noted as decreased forward scatter (size) and increased side scatter (complexity) compared to the respective controls (data not shown). However, no significant differences in the number of viable parasites were measured (Fig. 7A).

Administration of the peroxynitrite donor (SIN-1) for 24 h resulted in strongly decreased parasite motility (data not shown) especially at the highest concentration (0.1 mM). Viability, as monitored by flow cytometry, was strongly reduced (Fig. 7B). To parallel cultures SOD was added as oxygen scavenger to allow for NO• pro-
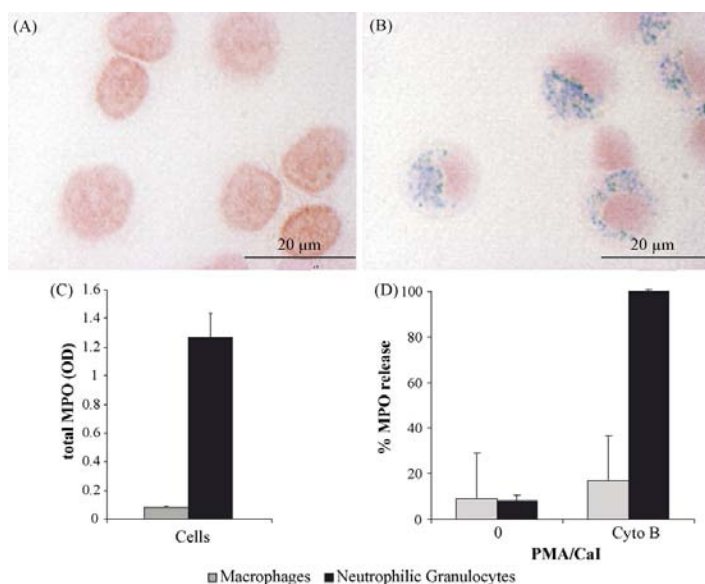
Fig. 5. Myeloperoxidase (MPO) activity in carp leukocytes. MPO activity in sorted WCL-15^{+} carp macrophages (A) and TCL-BE8^{+} carp neutrophilic granulocytes (B). MPO staining is present as blue/azurophil granules, and cells are counterstained with safranin (red). Total MPO activity in carp macrophages and neutrophilic granulocytes (C). MPO release from carp macrophages and neutrophilic granulocytes stimulated with PMA (0.1 μg/ml)/CaI (5 μg/ml) in the presence or absence of Cytochalasin B (Cyto B, 5 μg/ml) (D). Values represent means and S.D. of triplicate wells of one representative experiment out of two independent experiments with similar results.
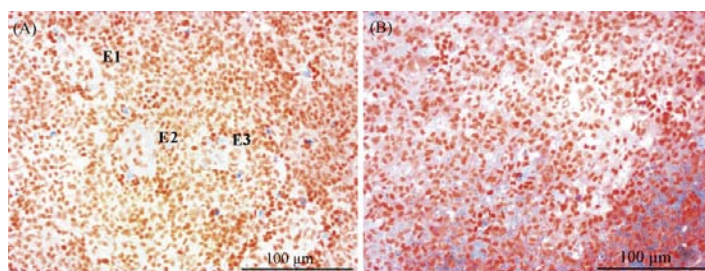
Fig. 6. Myeloperoxidase (MPO) activity *in vivo*. MPO histochemical staining of spleen isolated from non-infected (A) and 4 weeks *T. borreli* infected fish (B). MPO activity is present as blue/azurophil granules, and cells are counterstained with safranin (red). Note the intense MPO activity detected throughout the spleen of infected fish as compared to non-infected tissue. Ellipsoids (E1–4) in non-infected tissue also showed weak MPO activity.

duction but to prevent peroxynitrite formation (Table 1). In cultures where SOD was combined with SIN-1, parasite viability remained unaffected (B).

3.8. Trypanoplasma borreli is not nitrated in vivo

We used a rabbit antibody to detect *T. borreli* in spleen tissue (Fig. 8). *T. borreli* lives primarily in the blood of its fish host but, at the late stages of infection (3–4 weeks), extravasation can lead to extensive parasite infiltration of the spleen (A and B). Double-staining for *T. borreli* and B cells showed an almost exclusive co-localization of the parasites with enlarged B cell areas (C and D), in the proximity of blood vessels and ellipsoids. Double-staining for *T. borreli* and nitrotyrosine showed that the parasites also co-localized with nitrated (B cell) areas (E and F). Remarkably, the cytoplasm

of the parasites present in the tissue never showed nitrotyrosine immunoreactivity.

3.9. Arsobal has cytotoxic effects on Trypanoplasma borreli both, in vitro and in vivo

Many kinetoplastid parasites possess an effective anti-oxidant system and Melarsoprol (Arsobal) directly interferes with such a system. We monitored *T. borreli* motility and viability, *in vitro*, upon exposure to different concentrations of Melarsoprol. Already after 15 min of incubation, motility was strongly reduced at 10 μg/ml and no motile parasites were observed at 50 μg/ml of Arsobal. After 3 h of incubation, motility was also affected at lower concentrations (5 μg/ml Arsobal). No significant differences in viability were observed at these short incubation periods (data not shown).
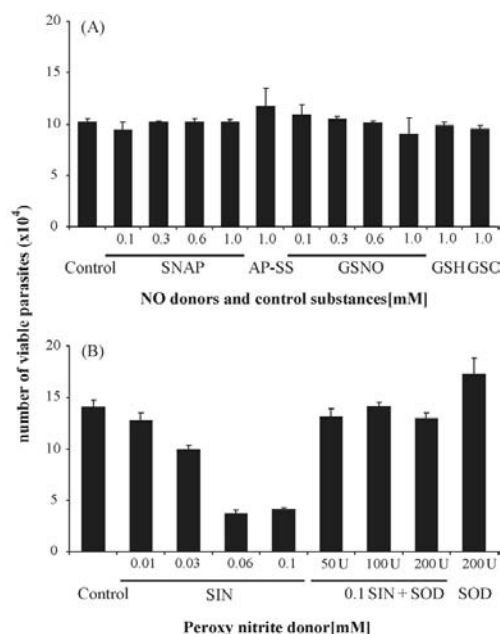
Fig. 7. Effects of NO• and peroxynitrite donors on *Trypanoplasma borreli* viability *in vitro*. Freshly isolated parasites were seeded out at a density of 1×10^5 cells/well. (A) Parasites were incubated in the presence of different concentrations of NO donors, SNAP or GSNO, or with 1 mM of the respective control substances AP-SS or GSH and GSO. After 48 h, parasite viability was measured by flowcytometer. (B) Parasites were incubated with different concentrations of a peroxynitrite donor (SIN-1) and with 0.1 mM SIN-1 in combination with different concentrations of SOD or SOD alone. After 24 h, parasite viability was measured by flowcytometer. Data are expressed as absolute number of parasites per well. Values represent means and S.D. of triplicate wells of one representative experiment out of three independent experiments with similar results.

However, after 48 h, motility was affected at all concentrations with the exception of 1 μg/ml Arsobal (not shown) while viability was reduced to 30% at the highest concentration (Fig. 9A).

The effects of Arsobal on parasite viability were also investigated *in vivo* (B). At parasitaemia in the order of 10^6 parasites/ml blood (2–3 weeks post infection), fish were treated twice with Arsobal. Two days after the second injection, parasitaemia further increased in the infected control group while parasitaemia decreased in the infected Arsobal-treated group.

4. Discussion

In the present study we demonstrate a differential contribution of carp neutrophilic granulocytes and macrophages to nitrosative stress *in vivo*. Neutrophilic granulocytes greatly contribute to tissue nitration likely via both a peroxynitrite- and an MPO-mediated mechanism. Macrophages, by restricting the presence of nitrating agents to their phagosomal compartments, become nitrated themselves but do not contribute to extracellular nitration and tissue injury. In addition, we show the potential of experimental infection of carp with the extracellular blood parasite *T. borreli* to serve as useful tool for pharmacological studies on human anti-trypanosome drugs.

During *T. borreli* infection of carp, the kinetics of iNOS gene expression strongly correlated with increased serum nitrite levels and extensive tyrosine nitration in spleen. In a tissue, nitration is preferentially localized around the areas in which peroxynitrite-producing cells or NO-derived oxidants are more abundant and indeed, strong nitrotyrosine immunoreactivity in inflammatory processes is principally observed in macrophage or neutrophil-rich areas (Kooy et al., 1995; Brito et al., 1999; Radi et al., 2001). In light of these observations, the anti-nitrotyrosine antibody was used in combination with monoclonal antibodies directed against carp macrophages and neutrophilic granulocytes to investigate the relative contribution of these cells to *in vivo* tissue nitration.

Nitration was observed in the area directly surrounding each neutrophilic granulocyte, a pattern which is in accordance with the concept that peroxynitrite has a short half-life but can cross biological membranes and diffuse one or two cell diameters (Denicola et al., 1998). However, the possibility of an MPO-mediated mecha-
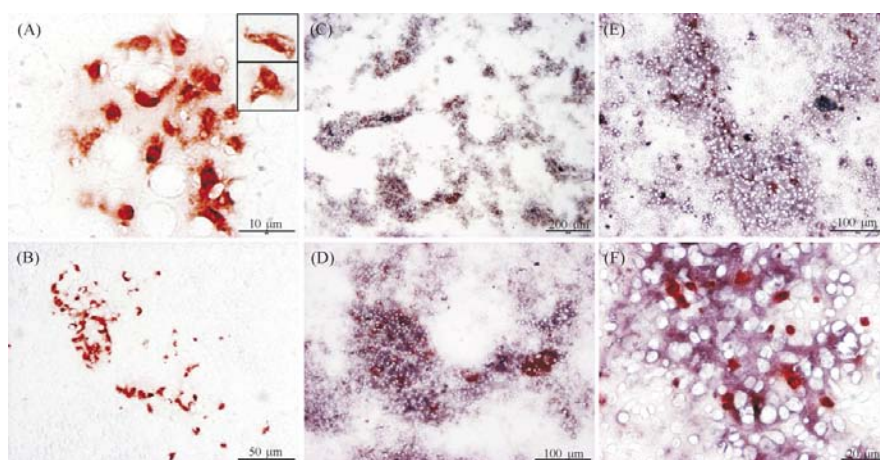
Fig. 8. *T. borreli* localization and nitration in spleen from 4 weeks infected fish. Parasites are stained in red (A–F) and in blue are enlarged B cell areas (WCI-12+ C and D) or nitrated areas (E and F). Details of the parasites are shown in the inset. Notice the almost exclusive co-localization of parasite with B cell and nitrated areas.
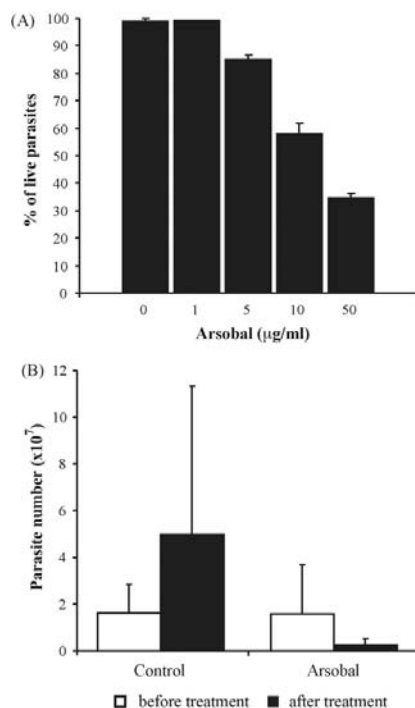
Fig. 9. *T. borreli* susceptibility to Melarsoprol (Arsobal) *in vitro* and *in vivo*. (A) Freshly isolated parasites were plated at a density of 1×10^4 cells/well and incubated in the presence of different concentrations of Arsobal. After 48 h, parasite viability was measured by flowcytometer. Values represent mean and S.D. of six replicate wells. (B) Carp were infected i.p. with 10^4 *T. borreli*. After 3 weeks, fish received two injections each equivalent to 10 mg/kg Arsobal separated by a 2-day interval. Two days after the second injection, parasitaemia levels in blood were monitored again. Values represent mean parasite numbers and S.D. of $n = 5$ fish per group.

nism of tyrosine nitration was also considered. MPO activity was detected exclusively in the granules of carp neutrophilic granulocytes and the same cells showed the ability to release MPO upon *in vitro* stimulation. The obtained results are in line with studies in zebrafish, showing that MPO activity is present mainly in neutrophilic granulocytes and not macrophages (Lieschke et al., 2001). *In vivo*, markedly increased MPO activity was observed throughout the spleen of *T. borreli*-infected fish and MPO activity was not limited to the area immediately surrounding each neutrophilic granulocyte. The latter finding suggests that the intense nitration detected specifically in the area immediately surrounding each carp neutrophilic granulocyte is more likely due to the formation of $ONOO^-$ than to an MPO-mediated mechanism. Despite the presence of MPO in the granules of carp neutrophilic granulocytes, protein nitration was never observed in the cytoplasmic compartments of these cells. The latter observation is in line with studies in mice showing that intraphagosomal nitration in neutrophils is negligible, while extracellular tyrosine nitration by secreted MPO occurs already at physiological concentration levels of NO_2^- (Jiang and Hurst, 1997). In the present study, the presence of secreted MPO dramatically increased particularly in the proximity of B cell areas. B cells, in fact, were found preferentially associated with blood vessels where NO_2^- (MPO substrate) is most abundant. Careful comparison between the pattern of tyrosine nitration and the

MPO specific staining suggests that, in fish, MPO greatly contributes to the generalized tissue nitration.

Carp macrophages showed a nitration pattern completely different from that observed for neutrophilic granulocytes. Nitrotyrosine formation was restricted exclusively to the intraphagosomal compartment but not all macrophages were nitrated. Carp macrophages lack specific MPO activity. Human activated macrophages, however, have the ability to phagocytose extracellular MPO via interaction with the mannose receptor (Schmekel et al., 1990; Shepherd and Hoidal, 1990) leading to enhanced macrophage microbicidal activities. In the present study, the uptake of MPO, together with the simultaneous increase in intracellular radical production might play a role in the process of auto-nitration observed in carp macrophages. Although the formation of peroxynitrite cannot be excluded, we suggest that the contribution of peroxynitrite is less important for auto-nitration due to its rapid diffusion across biological membranes that would result in a more generalized nitration pattern around macrophages.

All together, our data demonstrate a differential contribution of fish neutrophilic granulocytes and macrophages to *in vivo* tissue nitration. Possibly, carp macrophages limit potential damage by restricting the presence of radicals and hydrolytic enzymes to their phagosomal compartments. Conversely, carp neutrophilic granulocytes more easily secrete their toxic compounds to their surroundings thereby contributing more heavily to nitrosative stress and tissue injury *in vivo*. Our study does not provide a definite answer as to which nitration pathway is responsible for the majority of nitrotyrosine generated during infection with *T. borreli*. However, MPO- and peroxynitrite-mediated nitration pathways are not mutually exclusive and may rather operate synergistically.

Other interesting aspects emerged from our histological analysis. In infected fish, not all macrophages were nitrated and individual macrophages that did display intracellular nitration, also showed decreased WCL-15 immunoreactivity. The monoclonal antibody WCL-15 reacts with an intracellular epitope present in the cytoplasm and phagosomes of carp macrophages. The heterogeneous WCL-15 immunoreactivity might be indicative of differential activation states of splenic macrophages. The possibility that this might reflect a different maturation state (i.e. monocyte vs. macrophage) can be excluded, as such a difference would have been visible also in non-infected fish. Recently, we reported the ability of carp macrophages to show plasticity and functional polarization upon stimulation *in vitro* (Joerink et al., 2006). Whether the differential activation state observed *in vivo* reflects the presence of innate and alternatively activated macrophages will be further investigated.

In the present study, the pattern and extent of tyrosine nitration of carp B lymphocytes was also investigated. Large B cell areas were generally found in proximity of small blood vessels and in infected spleen tissue all B cell areas were highly nitrated. Carp PBL (comprising 30–40% B lymphocytes, Koumans-van Diepen et al., 1995), are characterized by low thiol levels and are highly susceptible to the immunosuppressive effects of $NO^\bullet$ (Saeij et al., 2003b). In contrast, carp phagocytes, especially neutrophilic granulocytes, typically show much higher thiol levels and a higher resistance to $NO^\bullet$. Given the high susceptibility of (B) lymphocytes to oxygen and nitrogen radicals, in *T. borreli*-infected tissue, B lymphocytes may suffer from acute nitrosative stress. Greatly enlarged B cell areas in spleen but also intense WCI-12 (IgM) immunoreactivity in the lumen of splenic capillaries of infected fish were observed. This suggests activation and proliferation of a large pool of B cells, leading to the production of high levels of circulating antibodies despite the intense nitration present during *T. borreli* infection. Previous experiments showed a significant increase in antibody levels directed against *T. borreli*-specific but also *T. borreli*-unrelated anti-

gens, most likely due to a non-specific polyclonal B cell activation (Saeij et al., 2003a). Our *in vivo* histological analysis, clearly showed an almost exclusive co-localization of numerous parasites in the centre of enlarged B cell areas, strongly indicating that *in vivo*, a direct B cell activation by *T. borreli* might occur in secondary organs.

The high production of NO• associated with *T. borreli* infections provides a host–parasite animal model to investigate the *in vivo* effects of nitrosative stress on the parasite itself. In a previous study, using light microscopy, Saeij et al. (2000) observed reduced parasite motility when *T. borreli* was co-cultured with activated carp phagocytes; when NO• production by phagocytes was inhibited by the addition of an iNOS inhibitor, the motility of the parasites was equivalent to that of control cultures. Scharsack et al. (2003), however, using flow cytometry, could not detect an effect of the NO-donor GSNO on parasite viability. In the present study, *T. borreli* motility and viability was measured after *in vitro* exposure to nitric oxide donors and we conclusively showed that NO• does have cytostatic (reduced motility, changed scatter profile) but not cytotoxic (unchanged viability) effects on *T. borreli*. Conversely, cytotoxic effects were detected when *T. borreli* was cultured in the presence of a peroxynitrite donor, SIN-1, resulting in high parasite mortality. Addition of superoxide-dismutase (SOD) as $O_2^{•-}$ scavenger to prevent $ONOO^-$ formation, completely protected the parasites from the cytotoxic effects of peroxynitrite. This again confirmed that NO• alone has no cytotoxic effect on *T. borreli*. The intracellular parasite *L. major* can be killed or controlled by NO• (Liew et al., 1990, 1991; Assreuy et al., 1994) while *Trypanosoma cruzi* is more susceptible to peroxynitrite (Denicola et al., 1993). Extracellular bloodstream parasites such as *Trypanosoma brucei* are not susceptible to NO•-mediated killing *in vivo* (Mabbott et al., 1994). Likely, the bloodstream environment of the extracellular parasite *T. borreli* protects the parasite from the toxic effects of NO• and its derived oxidants by a dilution effect and by the scavenger activity of hemoglobin (Pietraforte et al., 2004; Kim-Shapiro et al., 2006).

Remarkably, the histological analysis did not reveal nitrosative damage to the parasite. Numerous parasite infiltrates were detected in spleen from infected fish, primarily located in the centre of B cell areas in the vicinity of blood vessels. Given the close proximity to radical producing cells, such as neutrophilic granulocytes and macrophages, and the massive increase in extracellular MPO activity, parasites should experience large quantities of nitrating compounds. However, the fact that *T. borreli* was not nitrated suggests that the NO-inducing ability of *T. borreli* may be an adaptation strategy of the parasite adopted to survive and evade the immune response of its fish host.

Trypanosomatids such as *Trypanosoma cruzi*, *Trypanosoma brucei*, *L. major* rely on a redox system formed by the thiol polyamine conjugate trypanothione [N^1,N^8-bis(glutathionyl) spermidine] (Fairlamb et al., 1985; Fairlamb and Cerami, 1985) and the NADPH-dependent flavoenzyme TR. In these parasites, the trypanothione–thiol system replaces the nearly ubiquitous glutathione/GR system of other eukaryotes. Using a homology cloning approach we attempted to identify sequences coding for homologues of trypanothione reductase, tryparedoxin and trypanothione peroxidase in *T. borreli* but were not successful, probably due to the phylogenetic distance between *T. borreli* (Kinetoplastida, Parabodonida) and other kinetoplastids (Kinetoplastida, Trypanosomatida). Instead, to investigate the hypothesis that *T. borreli*, similar to other kinetoplastid protozoan parasites, uses the trypanothione antioxidant system, a human anti-trypanosome drug was administered. Melarsoprol (Arsobal) directly inhibits the activity of the trypanothione reductase by forming a stable complex with trypanothione, the substrate of the enzyme (Nok, 2003). The results clearly show susceptibility of *T. borreli* to Melarsoprol

both *in vitro* and *in vivo* suggesting that also *T. borreli* uses the trypanothione–thiol system to prevent oxidative damage during the exacerbated host immune response.

In conclusion, our results clearly demonstrate a conservation of the basic mechanisms underlying nitrosative stress from fish to mammals and strongly support the carp as suitable animal model to investigate the mechanisms of nitrosative stress both, *in vitro* and *in vivo*. In addition, we show that infections with the extracellular blood parasite *T. borreli* can be highly informative in studies on nitrosative stress and can be considered an alternative tool for pharmacological studies on human anti-trypanosome drugs.

Acknowledgements

References

Assreuy, J., Cunha, F.Q., Epperlein, M., Noronha-Dutra, A., O'Donnell, C.A., Liew, F.Y., Moncada, S., 1994. Production of nitric oxide and superoxide by activated macrophages and killing of *Leishmania major*. Eur. J. Immunol. 24, 672–676.

Brennan, M.L., Wu, W., Fu, X., Shen, Z., Song, W., Frost, H., Vadseth, C., Narine, L., Lenkiewicz, E., Borchers, M.T., Lusis, A.J., Lee, J.J., Lee, N.A., Abu-Soud, H.M., Ischiropoulos, H., Hazen, S.L., 2002. A tale of two controversies: defining both the role of peroxidases in nitrotyrosine formation in vivo using eosinophil peroxidase and myeloperoxidase-deficient mice, and the nature of peroxidase-generated reactive nitrogen species. J. Biol. Chem. 277, 17415–17427.

Brito, C., Naviliat, M., Tiscornia, A.C., Vuillier, F., Gualco, G., Dighiero, G., Radi, R., Cayota, A.M., 1999. Peroxynitrite inhibits T lymphocyte activation and proliferation by promoting impairment of tyrosine phosphorylation and peroxynitrite-driven apoptotic death. J. Immunol. 162, 3356–3366.

Bunnajirakul, S., Steinhagen, D., Hetzel, U., Körting, W., Drommer, W., 2000. A study of sequential histopathology of *Trypanoplasma borreli* (Protozoa: Kinetoplastida) in susceptible common carp *Cyprinus carpio*. Dis. Aquat. Org. 39, 221–229.

Denicola, A., Rubbo, H., Rodriguez, D., Radi, R., 1993. Peroxynitrite-mediated cytotoxicity to *Trypanosoma cruzi*. Arch. Biochem. Biophys. 304, 279–286.

Denicola, A., Souza, J.M., Radi, R., 1998. Diffusion of peroxynitrite across erythrocyte membranes. Proc. Natl. Acad. Sci. 95, 3566–3571.

Eiserich, J.P., Hristova, M., Cross, C.E., Jones, A.D., Freeman, B.A., Halliwell, B., van der Vliet, A., 1998. Formation of nitric oxide-derived inflammatory oxidants by myeloperoxidase in neutrophils. Nature 391, 393–397.

Evans, T.J., Buttery, L.D.K., Carpenter, A., Springall, D.R., Polak, J.M., Cohen, J., 1996. Cytokine-treated human neutrophils contain inducible nitric oxide synthase that produces nitration of ingested bacteria. Proc. Natl. Acad. Sci. 93, 9553–9558.

Fairlamb, A.H., Blackburn, P., Ulrich, P., Chait, B.T., Cerami, A., 1985. Trypanothione: a novel bis(glutathionyl)spermidine cofactor for glutathione reductase in trypanosomatids. Science 227, 1485–1487.

Fairlamb, A.H., Cerami, A., 1985. Identification of a novel, thiol-containing co-factor essential for glutathione reductase enzyme activity in trypanosomatids. Mol. Biochem. Parasitol. 14, 187–198.

Forlenza, M., Dias de Carvalho, J.D.A., Veselý, T., Pokorová, D., Savelkoul, H.F.J., Wiegertjes, G.F., 2008. Transcription of signal-3 cytokines, IL-12 and IFNalpha-beta, coincides with the timing of CD8alphabeta up-regulation during viral infection of common carp (*Cyprinus carpio* L). Mol. Immunol. 45, 1531–1547.

Gaut, J.P., Byun, J., Tran, H.D., Lauber, W.M., Carroll, J.A., Hotchkiss, R.S., Belaaouaj, A., Heinecke, J.W., 2002. Myeloperoxidase produces nitrating oxidants in vivo. J. Clin. Invest. 109, 1311–1319.

Green, L.C., Wagner, D.A., Glogowski, J., Skipper, P.L., Wishnok, J.S., Tannenbaum, S.R., 1982. Analysis of nitrate, nitrite, and [^{15}N]nitrate in biological fluids. Anal. Biochem. 126, 131–138.

Harder, A., Greif, G., Haberkorn, A., 2001. Chemotherapeutic approaches to protozoa: kinetoplastida—current level of knowledge and outlook. Parasitol. Res. 87, 778–780.

Hazen, S.L., Zhang, R., Shen, Z., Wu, W., Podrez, E.A., MacPherson, J.C., Schmitt, D., Mitra, S.N., Mukhopadhyay, C., Chen, Y., Cohen, P.A., Hoff, H.F., Abu-Soud, H.M., 1999. Formation of nitric oxide-derived oxidants by myeloperoxidase in monocytes: pathways for monocyte-mediated protein nitration and lipid peroxidation in vivo. Circ. Res. 85, 950–958.

Hurst, J.K., 2002. Whence nitrotyrosine? J. Clin. Invest. 109, 1287–1289.

Irnazarow, I., 1995. Genetic variability of Polish and Hungarian carp lines. Aquaculture 129, 215–219.

Ischiropoulos, H., 1998. Biological tyrosine nitration: a pathophysiological function of nitric oxide and reactive oxygen species. Arch. Biochem. Biophys. 356, 1–11.

Jiang, Q., Hurst, J.K., 1997. Relative chlorinating, nitrating, and oxidizing capabilities of neutrophils determined with phagocytosable probes. J. Biol. Chem. 272, 32767–32772.

Joerink, M., Groeneveld, A., Ducro, B., Savelkoul, H.F.J., Wiegertjes, G.F., 2007. Mixed infection with Trypanoplasma borreli and Trypanosoma carassii induces protection: involvement of cross-reactive antibodies. Dev. Comp. Immunol. 31, 903–915.

Joerink, M., Ribeiro, C.M., Stet, R.J.M., Hermsen, T., Savelkoul, H.F.J., Wiegertjes, G.F., 2006. Head kidney-derived macrophages of common carp (Cyprinus carpio L.) show plasticity and functional polarization upon differential stimulation. J. Immunol. 177, 61–69.

Kaplow, L.S., 1965. Simplified myeloperoxidase stain using benzidine dihydrochloride. Blood 26, 215–219.

Kari, G., Rodeck, U., Dicker, A.P., 2007. Zebrafish: an emerging model system for human disease and drug discovery. Clin. Pharmacol. Ther. 82, 70–80.

Kim-Shapiro, D.B., Schechter, A.N., Gladwin, M.T., 2006. Unraveling the reactions of nitric oxide, nitrite, and hemoglobin in physiology and therapeutics. Arterioscler. Thromb. Vasc. Biol. 26, 697–705.

Klebanoff, S.J., 2005. Myeloperoxidase: friend and foe. J. Leukoc. Biol. 77, 598–625.

Kooy, N.W., Royall, J.A., Ye, Y.Z., Kelly, D.R., Beckman, J.S., 1995. Evidence for in vivo peroxynitrite production in human acute lung injury. Am. J. Respir. Crit. Care Med. 151, 1250–1254.

Koumans-van Diepen, J.E., Egberts, E., Peixoto, B.R., Taverne, N., Rombout, J.H.W.M., 1995. B cell and immunoglobulin heterogeneity in carp (Cyprinus carpio L); an immuno(cyto)chemical study. Dev. Comp. Immunol. 19, 97–108.

Krauth-Siegel, R.L., Meiering, S.K., Schmidt, H., 2003. The parasite-specific trypanothione metabolism of trypanosoma and leishmania. Biol. Chem. 384, 539–549.

Lieschke, G.J., Currie, P.D., 2007. Animal models of human disease: zebrafish swim into view. Nat. Rev. Genet. 8, 353–367.

Lieschke, G.J., Oates, A.C., Crowhurst, M.O., Ward, A.C., Layton, J.E., 2001. Morphologic and functional characterization of granulocytes and macrophages in embryonic and adult zebrafish. Blood 98, 3087–3096.

Liew, F.Y., Li, Y., Moss, D., Parkinson, C., Rogers, M.V., Moncada, S., 1991. Resistance to Leishmania major infection correlates with the induction of nitric oxide synthase in murine macrophages. Eur. J. Immunol. 21, 3009–3014.

Liew, F.Y., Millott, S., Parkinson, C., Palmer, R.M., Moncada, S., 1990. Macrophage killing of Leishmania parasite in vivo is mediated by nitric oxide from L-arginine. J. Immunol. 144, 4794–4797.

Lin, B., Chen, S., Cao, Z., Lin, Y., Mo, D., Zhang, H., Gu, J., Dong, M., Liu, Z., Xu, A., 2007. Acute phase response in zebrafish upon Aeromonas salmonicida and Staphylococcus aureus infection: striking similarities and obvious differences with mammals. Mol. Immunol. 44, 295–301.

Linares, E., Giorgio, S., Mortara, R.A., Santos, C.X.C., Yamada, A.T., Augusto, O., 2001. Role of peroxynitrite in macrophage microbicidal mechanisms in vivo revealed by protein nitration and hydroxylation. Free Radic. Biol. Med. 30, 1234–1242.

Mabbott, N.A., Sutherland, I.A., Sternberg, J.M., 1994. Trypanosoma brucei is protected from the cytostatic effects of nitric oxide under in vivo conditions. Parasitol. Res. 80, 687–690.

Meijer, A.H., van der Sar, A.M., Cunha, C., Lamers, G.E., Laplante, M.A., Kikuta, H., Bitter, W., Becker, T.S., Spaink, H.P., 2008. Identification and real-time imaging of a mycexpressing neutrophil population involved in inflammation and mycobacterial granuloma formation in zebrafish. Dev. Comp. Immunol. 32, 36–49.

Nakayasu, C., Omori, M., Hasegawa, S., Kurata, O., Okamoto, N., 1998. Production of a monoclonal antibody for carp (Cyprinus carpio L.) phagocytic cells and separation of the cells. Fish Shellfish Immunol. 8, 91–100.

Naviliat, M., Gualco, G., Cayota, A., Radi, R., 2005. Protein 3-nitrotyrosine formation during Trypanosoma cruzi infection in mice. Braz. J. Med. Biol. Res. 38, 1825–1834.

Nok, A.J., 2003. Arsenicals (melarsoprol), pentamidine and suramin in the treatment of human African trypanosomiasis. Parasitol. Res. 90, 71–79.

Overath, P., Ruoff, J., Stierhof, Y.-D., Haag, J., Tichy, H., Dyková, I., Lom, J., 1998. Cultivation of bloodstream forms of Trypanosoma carassii, a common parasite of freshwater fish. Parasitol. Res. 84, 343–347.

Pfaffl, M.W., 2001. A new mathematical model for relative quantification in real-time RT-PCR. Nucleic Acids Res. 29, e45.

Pfeiffer, S., Lass, A., Schmidt, K., Mayer, B., 2001a. Protein tyrosine nitration in cytokine-activated murine macrophages. Involvement of a peroxidase/nitrite pathway rather than peroxynitrite. J. Biol. Chem. 276, 34051–34058.

Pfeiffer, S., Lass, A., Schmidt, K., Mayer, B., 2001b. Protein tyrosine nitration in mouse peritoneal macrophages activated in vitro and in vivo: evidence against an essential role of peroxynitrite. FASEB J. 15, 2355–2364.

Pietraforte, D., Salzano, A.M., Scorza, G., Minetti, M., 2004. Scavenging of reactive nitrogen species by oxygenated hemoglobin: globin radicals and nitrotyrosines distinguish nitrite from nitric oxide reaction. Free Radic. Biol. Med. 37, 1244–1255.

Quade, M.J., Roth, J.A., 1997. A rapid, direct assay to measure degranulation of bovine neutrophil primary granules. Vet. Immunol. Immunopathol. 58, 239–248.

Radi, R., 2004. Nitric oxide, oxidants, and protein tyrosine nitration. Proc. Natl. Acad. Sci. 101, 4003–4008.

Radi, R., Peluffo, G., Alvarez, M.N., Naviliat, M., Cayota, A., 2001. Unraveling peroxynitrite formation in biological systems. Free Radic. Biol. Med. 30, 463–488.

Ricevuti, G., 1997. Host tissue damage by phagocytes. Ann. NY Acad. Sci. 832, 426–448.

Romano, N., Picchietti, S., Taverne-Thiele, J.J., Taverne, N., Abelli, L., Mastrolia, L., Verburg-van Kemenade, B.M.L., Rombout, J.H.W.M., 1998. Distribution of macrophages during fish development: an immunohistochemical study in carp (Cyprinus carpio L.). Anat. Embryol. (Berl.) 198, 31–41.

Rudat, S., Steinhagen, D., Hetzel, U., Drommer, W., Körting, W., 2000. Cytopathological observations on renal tubule epithelium cells in common carp Cyprinus carpio under Trypanoplasma borreli (Protozoa: Kinetoplastida) infection. Dis. Aquat. Org. 40, 203–209.

Saeij, J.P., Stet, R.J.M., Groeneveld, A., Verburg-van Kemenade, B.M.L., van Muiswinkel, W.B., Wiegertjes, G.F., 2000. Molecular and functional characterization of a fish inducible-type nitric oxide synthase. Immunogenetics 51, 339–346.

Saeij, J.P., Van Muiswinkel, W.B., Groeneveld, A., Wiegertjes, G.F., 2002. Immune modulation by fish kinetoplastid parasites: a role for nitric oxide. Parasitology 124, 77–86.

Saeij, J.P.J., de Vries, B.J., Wiegertjes, G.F., 2003a. The immune response of carp to Trypanoplasma borreli: kinetics of immune gene expression and polyclonal lymphocyte activation. Dev. Comp. Immunol. 27, 859–874.

Saeij, J.P.J., van Muiswinkel, W.B., van de Meent, M., Amaral, C., Wiegertjes, G.F., 2003b. Different capacities of carp leukocytes to encounter nitric oxide-mediated stress: a role for the intracellular reduced glutathione pool. Dev. Comp. Immunol. 27, 555–568.

Scharsack, J.P., Steinhagen, D., Kleczka, C., Schmidt, J.O., Körting, W., Michael, R.D., Leibold, W., Schuberth, H.J., 2003. The haemoflagellate Trypanoplasma borreli induces the production of nitric oxide, which is associated with modulation of carp (Cyprinus carpio L.) leukocyte functions. Fish Shellfish Immunol. 14, 207–222.

Schmekel, B., Hornblad, Y., Linden, M., Sundstrom, C., Venge, P., 1990. Myeloperoxidase in human lung lavage. II. Internalization of myeloperoxidase by alveolar macrophages. Inflammation 14, 455–461.

Secombes, C.J., van Groningen, J.J., Egberts, E., 1983. Separation of lymphocyte subpopulations in carp Cyprinus carpio L. by monoclonal antibodies: immunohistochemical studies. Immunology 48, 165–175.

Shepherd, V.L., Hoidal, J.R., 1990. Clearance of neutrophil-derived myeloperoxidase by the macrophage mannose receptor. Am. J. Respir. Cell Mol. Biol. 2, 335–340.

Steinhagen, D., Hedderich, W., Skouras, A., Scharsack, J.P., Schuberth, J., Leibold, W., Körting, W., 2000. In vitro cultivation of Trypanoplasma borreli (protozoa: kinetoplastida), a parasite from the blood of common carp Cyprinus carpio. Dis. Aquat. Org. 41, 195–201.

Steinhagen, D., Kruse, P., Körting, W., 1989. The parasitemia of cloned Trypanoplasma borreli Laveran and Mesnil, 1901, in laboratory-infected common carp (Cyprinus carpio L.). J. Parasitol. 75, 685–689.

Tichopad, A., Dilger, M., Schwarz, G., Pfaffl, M.W., 2003. Standardized determination of real-time PCR efficiency from a single reaction set-up. Nucleic Acids Res. 31, e122.

van Dalen, C.J., Winterbourn, C.C., Senthilmohan, R., Kettle, A.J., 2000. Nitrite as a substrate and inhibitor of myeloperoxidase. Implications for nitration and hypochlorus acid production at sites of inflammation. J. Biol. Chem. 275, 11638–11644.

van der Sar, A.M., Stockhammer, O.W., van der Laan, C., Spaink, H.P., Bitter, W., Meijer, A.H., 2006. MyD88 innate immune function in a zebrafish embryo infection model. Infect. Immun. 74, 2436–2441.

Verburg-van Kemenade, B.M.L., Groeneveld, A., van Rens, B.T.T.M., Rombout, J.H.W.M., 1994. Characterization of macrophages and neutrophilic granulocytes from the pronephros of carp (Cyprinus carpio). J. Exp. Biol. 187, 143–158.

Vieira, O.V., Botelho, R.J., Grinstein, S., 2002. Phagosome maturation: aging gracefully. Biochem. J. 366, 689–704.

Weyts, F.A.A., Rombout, J.H.W.M., Flik, G., Verburg-Van Kemenade, B.M.L., 1997. A common carp (Cyprinus carpio L.) leucocyte cell line shares morphological and functional characteristics with macrophages. Fish Shellfish Immunol. 7, 123–133.

Wiegertjes, G.F., Forlenza, M., Joerink, M., Scharsack, J.P., 2005. Parasite infections revisited. Dev. Comp. Immunol. 29, 749–758.

Xia, Y., Zweier, J.L., 1997. Superoxide and peroxynitrite generation from inducible nitric oxide synthase in macrophages. Proc. Natl. Acad. Sci. 94, 6954–6958.
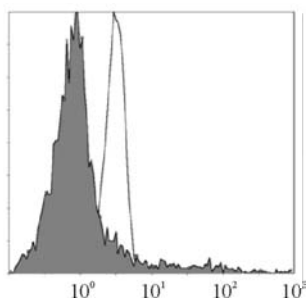
CHAPTER

7

Nitric oxide hinders antibody clearance from the surface of *Trypanoplasma borreli* and increases susceptibility to complement-mediated lysis

Maria Forlenza, Miki Nakao, Indra Wibowo, Maaike Joerink, Joop A.J. Arts, Huub F.J. Savelkoul and Geert F. Wiegertjes

CHAPTER 7

Nitric oxide hinders antibody clearance from the surface of *Trypanoplasma borreli* and increases susceptibility to complement-mediated lysis

Maria Forlenza [a], Miki Nakao [b], Indra Wibowo [a], Maaike Joerink [c], Joop A.J. Arts [a], Huub F.J. Savelkoul [a], Geert F. Wiegertjes [a,*]

[a] *Department of Animal Sciences, Cell Biology and Immunology Group, Wageningen Institute of Animal Sciences, Wageningen University, P.O. Box 338, 6700 AH Wageningen, The Netherlands*
[b] *Department of Bioscience and Biotechnology, Kyushu University, Hakozaki, Fukuoka 812-8581, Japan*
[c] *Department of Medicine Clinical Allergy Research Unit, Karolinska University, Hospital Solna L2:04, SE-171 76 Stockholm, Sweden*

ABSTRACT

Trypanoplasma borreli is an extracellular blood parasite of carp belonging to the same Order (Kinetoplastida) as African trypanosomes. These mammalian parasites have developed different strategies to evade the host immune system including antigenic variation, immunosuppression and clearance of surface-bound antibodies. The latter mechanism allows trypanosomes to use their swimming movement to cause surface-bound antibodies to 'sail' and accumulate at the posterior end of the parasite, to be internalized *via* the flagellar pocket and be degraded. There is no evidence that *T. borreli* shows antigenic variation, but during the late phases of infection NO-mediated immunosuppression is observed. High levels of nitric oxide (NO) lead to extensive tissue nitration whereas the parasite itself is not affected. Therefore, the induction of NO has thus far been considered a parasite-driven response with immunosuppressive effects. In the present study, we show that the induction of NO, particularly during the early phase of *T. borreli* infections, should be re-considered an effective part of the host immune response. We show that *T. borreli* rapidly removes surface-bound IgM. In addition, moderate concentrations of NO, by hindering surface antibody clearance, maintain high the concentrations of membrane-bound IgM, thereby favoring antibody-dependent complement-mediated parasite lysis. We performed a comprehensive quantitative gene expression analysis of in total seven different complement factors involved in all three activation pathways, differentiating between 1 and 4 isoforms for each complement gene. Our gene expression analysis supports an important role for antibody-dependent complement-mediated lysis of *T. borreli in vivo*. To our knowledge, NO-dependent inhibition of antibody clearance from the surface of kinetoplastid parasites has not been investigated. Our data support a role for NO as an important player in host–parasite interactions, not only as immune suppressor (late response) but also as immune effector (early response) in infections with bloodstream parasites such as *T. borreli*.

© 2009 Elsevier Ltd. All rights reserved.

1. Introduction

Immune evasion is an essential mechanism by which a pathogen interferes, disrupts or manipulates the immune response to ensure its survival and replication in the host (Schmid-Hempel, 2008). Some of the best studied paradigms of evasion are those described for African trypanosomes (e.g. *Trypanosoma brucei*), protozoan flagellates of the order Kinetoplastida (Donelson et al., 1998; Simpson et al., 2006). For African trypanosomes at least three strategies of immune evasion have been described: (1) antigenic variation of the variant surface glycoprotein (VSG) present on the parasite surface (Antia et al., 1996; Cross, 1996), facilitating escape from

the host humoral immune response; (2) immunosuppression of the host immune response, particularly of the T cell compartment (Donelson et al., 1998; Stijlemans et al., 2007); (3) rapid removal of antibodies from the parasite cell surface (Dean and Matthews, 2007). Although the biological process by which trypanosomes remove antibodies from their surface was proposed already in 1993 (McLintock et al., 1993), the mechanism of antibody clearance was only recently ascribed to hydrodynamic sorting (Dean and Matthews, 2007; Engstler et al., 2007). This mechanism allows trypanosomes (*T. brucei*) to use their swimming movement to create a current that causes surface-bound antibodies to 'sail' and accumulate at the posterior end of the parasite, to be internalized *via* the flagellar pocket and be degraded. Of the three evasion strategies, antigenic variation and immunosuppression ensure the long-term persistence of an infecting population. Antibody clearance seems to be effective mainly at low antibody concentrations and supports

survival of individual parasites, especially during the initial phase of a specific humoral response. In addition, it has been observed that the presence of parasite-specific IgM or IgG initiates a cycle of aggregation–disaggregation of bloodstream forms of *T. brucei* (O'Beirne et al., 1998) and the ability of the parasite to disaggregate will ensure longer survival. Adaptation and evasion strategies allowed the Kinetoplastida to persist in almost all vertebrate groups (Simpson et al., 2006) and infections with these protozoan parasites are widespread not only among warm-blooded but also among cold-blooded vertebrates. The Kinetoplastida is a group of flagellate protozoa that can be subdivided into two major suborders Trypanosomatida and Parabodonida that diverged some 200–300 million years ago (Stevens et al., 2001). The Trypanosomatida include a number of important mammalian pathogens, such as *T. brucei*, that are transmitted by insect vectors. The Parabodonida includes the fish pathogens *Trypanoplasma borreli* (Wiegertjes et al., 2005) an extracellular parasite that is transmitted by a leech vector and is naturally found in the blood of cyprinid common carp (*Cyprinus carpio* L.). Infections with this parasite show most of the typical pathological features also observed during African trypanosomisis in warm-blooded vertebrates such as splenomegaly, anemia and polyclonal B cell activation.

Parasite-specific antibodies (IgM) are produced during *T. borreli* infection (Wiegertjes et al., 1995; Saeij et al., 2003a) and *in vitro*, proof of antibody-dependent complement-mediated parasite lysis suggests that the concerted action of IgM and complement could be responsible for parasite clearance (Saeij et al., 2003a). However, the importance of antibody-dependent complement-mediated lysis has not yet conclusively been shown *in vivo*.

In teleost fish, and particularly in tetraploid species such as common carp, complement components are often encoded by multiple genes (Nakao et al., 1998, 2000, 2001, 2002, 2003a,b, 2006; Nagai et al., 2000; Kato et al., 2003; Mutsuro et al., 2005). It is important that *in vivo* studies take into account the presence of different complement isoforms. In the present study, we performed a comprehensive *in vivo* quantitative gene expression analysis, during infection with *T. borreli*, of in total seven different complement factors involved in all three activation pathways, differentiating between 1 and 4 isoforms for each complement gene. Most clearly, a significant up-regulation of factors involved in the classical, but not lectin, complement activation pathway was observed at 3–4 weeks post-infection, concomitantly with the onset of the specific antibody response. We believe that our gene expression analysis further supports an important role for antibody-dependent complement-mediated lysis of *T. borreli in vivo*.

With regard to the immune evasion strategies, thus far there is no evidence that *T. borreli* makes use of antigenic variation (1). Immunosuppression (2), however, is associated with *T. borreli* infections and is observed as inhibition of lymphocyte proliferation, most probably through a nitric oxide (NO)-dependent mechanism (Saeij et al., 2002, 2003c). Surface antibody clearance has not been examined for *T. borreli*, but there is no reason why hydrodynamic sorting of surface antibodies as an immune evasion strategy (3) should exist only in *T. brucei*. *T. borreli* is a flagellated parasite with typical high motility in the bloodstream, and it is therefore likely that also for this parasite, surface antibody clearance must also occur.

During *T. borreli* infections, the elevated nitrite levels lead to inflammation and nitrosative stress as demonstrated by the extensive tissue nitration observed in organs from infected fish, but the parasite is not affected (Forlenza et al., 2008a). *In vitro*, high concentrations of NO do not affect viability but do inhibit parasite motility (Saeij et al., 2000; Scharsack et al., 2003; Forlenza et al., 2008a). Thus far, we considered the induction of high concentration of NO an immune evasion mechanism induced by *T.*

borreli. However, the induction of high NO levels and the associated reduction of parasite motility could also be considered a host defense mechanism. Reduced motility would hinder the hydrodynamic flow-mediated removal of IgM from the parasite surface. As a result, surface IgM concentrations would remain high, favoring complement activation and parasite lysis, resulting in rapid clearance of the parasite from the bloodstream. To our knowledge, the relation between NO-dependent inhibition of antibody clearance from the parasite surface and the efficacy of the host immune response has not been investigated, not in mammals or in fish.

2. Materials and methods

2.1. Animals

European common carp (*C. carpio carpio* L.) were bred and raised in the central fish facility at Wageningen University, The Netherlands, at 23 °C in recirculating UV-treated tap water and fed pelleted dry food (Trouvit, Nutreco) daily. R3xR8 carp, which are the offspring of a cross between fish of Hungarian origin (R8 strain) and of Polish origin (R3 strain), were used (Irnazarow, 1995).

2.2. Parasites and infection of carp with parasites

T. borreli was cloned and characterized by Steinhagen et al. (1989) and maintained by syringe passage through carp following i.p. injection with 10^4 parasites/fish. Parasitemia was monitored in plasma using a Bürker counting chamber after dilution of blood in RPMI medium adjusted to 280 mOsmol kg^{-1} containing 50 IU/ml of heparin (Leo Pharmaceutical products). For parasite purification, blood was collected from heavily infected carp and after centrifugation, *T. borreli* were collected from the buffy coat and purified on a 1 cm × 12 cm ion-exchange column chromatography using diethylaminoethyl cellulose (DE-52, Whatman® International. Ltd; Overath et al., 1998). After purification, parasites were resuspended in fresh growth medium (Steinhagen et al., 2000) supplemented with 5% pooled carp serum, L-Glutamin (2 mM), Penicillin-G (100 IU/ml) and Streptomycin sulphate (50 mg/l).

Before infection with *T. borreli*, carp (6-months-old, weighing 160 ± 20 g) were tattooed with individual numbers, acclimatized to a quarantine unit for 3 weeks and kept at 20 °C. For gene expression studies, fish ($n = 52$) were anaesthetised in 0.3 g/l Tricaine Methane Sulfonate (TMS, Crescent Research Chemicals) and injected i.p. with 10^4 parasites/fish, PBS-injected individuals served as non-infected control group. Infected and non-infected fish were equally divided over 6 tanks. At time point 0 h, $n = 5$ control fish and at various time points after infection, $n = 5$ infected and $n = 3$ non-infected fish were killed by an overdose of TMS. Fish were bled by vena puncture of the caudal vessel to collect serum or plasma (blood diluted 1:1 in heparinized medium). Tissue samples were collected and immediately snap frozen in liquid nitrogen. Samples were stored at −80 °C until use.

2.3. Quantification of nitrite and T. borreli-specific antibody levels in serum

Total nitrite plus nitrate was quantified in serum samples as described previously (Saeij et al., 2002) with a nitrite/nitrate colorimetric method according to the manufacturer's (Roche Diagnostics) instructions.

T. borreli-specific carp IgM was detected in serum samples by ELISA as previously described (Wiegertjes et al., 1994). Briefly, 96-well ELISA plates were coated overnight at 37 °C with parasite lysate equivalent to 3×10^4 parasites per well in coating buffer

(bi-carbonate buffer, pH 9.6) in a humid chamber. If not stated otherwise all following steps were performed for 1 h at 37 °C. Blocking was performed in 1% BSA in TBS-T (10 mM TrisCl, pH 7.5, 150 mM NaCl, 0.1% Tween-20). Plates were then incubated with carp serum diluted 1:100 in carp PBS (cPBS, 150 mM NaCl, 2 mM KCl, 20 mM Na_2HPO_4, 2 mM KH_2PO_4) and subsequently with mouse anti-carp IgM (WCI-12). Finally, goat anti-mouse horseradish peroxidase conjugate (1:1000, GAM-HRP, Biorad) was used as detecting antibody. Incubation with ABTS peroxidase substrate (Roche) was allowed to proceed at room temperature until sufficient color had developed and optical density was measured spectrophotometrically at 405 nm (with 492 nm as reference) using a microtiter Anthos 2020 spectrophotometer (CleanAir Techniek B.V.). Antibody titers are expressed as arbitrary units calculated relative to serial dilutions of standard immune serum.

2.4. RNA isolation and cDNA synthesis

Total RNA was isolated from carp hepatopancreas using the RNAeasy Mini Kit according to the manufacturer's instructions, including Proteinase K (Qiagen) and on column DNase treatment with the RNase-free DNase set (Qiagen) and stored at −80 °C until use. Prior to cDNA synthesis, 1 μg of RNA from each sample was combined with 10× DNase reaction buffer and 1 U/μl DNase Amplification Grade (Invitrogen), mixed and incubated at RT for 15 min, followed by inactivation of DNase by addition of 25 mM EDTA. Synthesis of cDNA was performed using Superscript^{TM} III First Strand Synthesis Systems for RT-PCR (Invitrogen). A non-reverse transcriptase control was included for each sample. cDNA samples were further diluted 1:10 in nuclease-free water prior to real-time quantitative PCR analysis.

2.5. Gene expression analysis

Based on previously described East-Asian common carp (*C. carpio haematopterus*) sequences coding for the investigated complement factors (GeneBank accession numbers are listed in Table 1) primers were designed in order to amplify the corresponding cDNA regions in the European common carp. Products were sequenced and specific primers were designed to amplify European common carp genes (Table 1). RT-qPCR using SYBR Green I technology was performed with Rotor-Gene^{TM} 6000 (Corbett Research) and the Brilliant® SYBR® Green QPCR (Stratagene) as detection chemistry as described previously (Forlenza et al., 2008b). Primers used for RT-qPCR are listed in Table 1. Fluorescence data from RT-qPCR experiments were analyzed using Rotor-Gene version 6.0.21 software and exported to Microsoft Excel. The cycle threshold Ct for each sample and the reaction efficiencies (E) for each primer set were obtained upon Comparative Quantitation Analysis from the Rotor-Gene version 6.0.21 software. The relative expression ratio (R) of a target gene was calculated based on the E and Ct deviation of sample versus control (Pfaffl, 2001; Tichopad et al., 2003), and normalized relative to the mRNA levels of the S11 protein of the 40S subunit as reference gene. R of *T. borreli*-infected and non-infected fish at the same time points were calculated relative to the 0 h control (n = 5) according to the Pfaffl formula as indicated in Eq. (1) and used for statistical analysis

$$R = \frac{(E_{A\,target\,gene})^{\Delta Ct\,target(0\,h_{(1-5)}-sample)}}{(E_{A\,reference\,gene})^{\Delta Ct\,ref(0\,h_{(1-5)}-sample)}} \tag{1}$$

For clarity, in the results section, R of *T. borreli*-infected fish calculated relative to the non-infected fish at the same time point are presented. Basal expression was calculated as a ratio of reference

Table 1
Primers used for real-time quantitative PCR gene expression analysis.

Name	Sequence	E_A	Ct value	Acc. No
qC1rs-A FW	CAAGCCCATCTTGGCTCCTGG	1.72	20.0 ± 0.8	AB042609
qC1rs-A RV	GTCCAGATCAAGCGGGGACGT			
qC1rs-B FW	CAAGCCCATCTTGGCTCCACA	1.74	16.9 ± 1.4	AB042610
qC1rs-B RV	GGCATATCTGTGAACATGGTGCG			
qB-C2A1FW	ACGTCTGATATGGAAACTGACC	1.78	18.7 ± 0.8	AB007004
qB-C2A1RV	CCTTTGCAGGCAACATCATCTGTTT			
qB-C1A2FW	GCAGTGGTGGTATTGAACCAAAA	1.76	17.6 ± 0.7	AB021177
qB-C2A2RV	ACCAACCTGAATCACTCGACCTT			
qB-C2A3FW	CGGTCATGGGAAAAAGCATTGAGA	1.78	26.6 ± 0.6	AB047361
qB-C2A3RV	GATATCTTTAGCATTTGTCGCAG			
qB-C2Bfw	GCACCGCATCTCTGTCAGAAGTGA	1.78	21.3 ± 1.5	AB007005
qB-C2BRV	CCACTTGGAAATAGCGCATCCTCTT			
qC4-1FW	AGATGATACTGCGCTTATCTTGTGA	1.79	20.2 ± 0.7	AB037278
qC4-1 RV	AGCACATACCTGAAATGTTGTCC			
qC4-2FW	GGGTGTTTGCCAAGAGAAAGCACTG	1.73	19.7 ± 0.9	AB037279
qC4-2 RV	CAACAGGTACTGCATGTTTCC			
qC5-1 Fw2	AGCAGAGAAGAGTCACTGGTGG	1.83	19.3 ± 0.5	AB084635
qC5-1 Rv2	AACCCAAATCACTTCGCTCA			
qC5-2 Fw2	TAAACGTGGACATATCAGTTCGCA	1.79	21.8 ± 0.7	AB084636
qC5-2 Rv2	CTGTATCTACGGCAGAAAAAG			
qfIA-FW2	ACGCCTCTGGTTTGTCGTATC	1.80	23.5 ± 0.5	AB072912
qfIA-RV2	CCAAGATGATTGGTTTCGCTG			
qfIB-FW2	CCGCTGGTGTGCACAGATGCG	1.79	19.9 ± 0.7	AB072913
qfIB RV2	GTTCGCCACATTTATCACCCC			
qC3H1FW	TGCATGGAAAGACAGGCCG	1.81	15.7 ± 0.6	AB016210
qC3H1RV	TCCTCTATAGCAGCAAAGTCAT			
qC3S FW2	GGTTATCAAGGGGAGTTGAGCTAT	1.84	15.7 ± 0.7	AB016215
qC3S RV2	TGCTGCTTTGGGTGGATGGGT			
qMASP2 FW	CAAGCTGTCCAAGGTGATTG	1.77	21.0 ± 0.6	AB234294
qMASP2 RV	AGCAGTGAGGACCCAGTTGT			
q40S FW	CCGTGGGTGACATCGTTACA	1.8	19.1 ± 0.5	AB012087
q40S RV	TCAGGACATTGAACCTCACTGTCT			

Ct value = Averaged threshold values in hepatopancreas of control fish (n = 5).
E_A = averaged efficiency for each primer set. This value will be used for the calculation of relative expression ratios (R) according to the Pfaffl formula (Pfaffl, 2001) as indicated in Eq. (1).
According to this method, E = 2 = 100%, therefore E_A = 1.8 = 80%.

genes vs. target gene according to the following equation

$$R = \frac{(E_{A\,\text{reference gene}})^{Ct\,\text{reference}}}{(E_{A\,\text{target gene}})^{Ct\,\text{target}}} \qquad (2)$$

2.6. Motility score and antibody-dependent complement-mediated lysis

As source of complement, non-immune serum (NIS) from healthy carp was isolated within 1 h after blood collection and used undiluted immediately or aliquoted and stored at $-80\,^{\circ}C$. As source of antibody, heat-inactivated immune serum (IS) obtained from carp 7 weeks post-infection (wpi) was used at a dilution of 1:30, corresponding to 1400 units. As source of nitric oxide, the NO donor S-nitroso-glutathione (GSNO, 1 mM, Sigma) was used. This concentration was previously found to release nitrite concentrations in a physiological range (50–100 μM) common to the early stages of *T. borreli* infection. A semiquantitative motility score was assigned to describe differences in parasite motility under the tested conditions according to a previously described method (Waghabi et al., 2002), with some modifications. Briefly, 5 = very fast; 4 = fast; 3 = motile; 2 = slow; 1 = very slow; 0 = immotile.

For the antibody-dependent complement-mediated lysis assay, freshly isolated parasites were grown overnight in complete HML medium. The next day, parasites were washed twice in incomplete medium and resuspended at a concentration of 2×10^6 parasites/ml. Parasites were seeded in 96-well flat bottom culture plates in triplicate wells at a concentration of 2×10^5 parasites/well and combined with 50% (v/v) NIS as a source of complement and with the NO donor GSNO in a final volume of 100 μl. The reduced form of glutathione (GSH, 1 mM, Sigma) was used as negative control. Parasites were incubated for 12 h at 27 $^{\circ}C$ in a humidified atmosphere containing 5% CO_2. At this time point, parasite motility was only partially affected (motility index reduced from 5 to 3) and no effects on parasite viability were observed. To 50 μl of parasite culture, 50 μl of fresh NIS and 50 μl of IS were added. As negative control for the addition of IS, in parallel cultures, 50 μl of heat-inactivated normal carp serum (NCS) was added. Parasites were incubated at 27 $^{\circ}C$ in a humidified atmosphere. Quantification of parasite lysis, measured as the number of non-motile parasites with a round morphology, was performed using a Bürker counting chamber. Light microscopy pictures were acquired using an inverted light microscope equipped with a Nikon microphot-FXA camera.

2.7. Detection of surface IgM by flow cytometry

Parasites were grown for 12 h in the presence of 50% (v/v) NIS and NO donor as described above. At this time point parasites were collected and washed twice in ice-cold carp PBS/BSA (cPBS, 1% BSA). Unless stated otherwise, all subsequent procedures were performed on ice using ice-cold buffers. Parasites were adjusted to a concentration of 4×10^6 parasites/ml and subsequently incubated for 30 min with IS as source of *T. borreli*-specific carp IgM. The dilution of IS (1:30) was chosen to obtain 100% cell surface staining with low mean fluorescence intensity. An aliquot of parasite suspension was then resuspended in a large volume of cPBS/BSA and immediately fixed in suspension with 4% PFA for 10 min. The remaining parasite suspension was transferred to 350 μl of pre-warmed (27 $^{\circ}C$) medium (4×10^6 parasites/ml) supplemented with 50% heat-inactivated FCS. Immediately (time 0) or after 1, 2, 3, 4 and 5 min, 50 μl of parasite suspension were transferred to cPBS/BSA, washed twice and fixed with 4% PFA for 10 min. Fixed parasites were washed twice with cPBS/glycine (100 mM) and once with cPBS/BSA. Surface-bound carp IgM was detected using biotinylated WCI-12 antibody (mouse anti-carp IgM, 1:40) (Secombes et al., 1983; Koumans-van Diepen et al., 1995) followed by incubation

with FITC-labelled Streptavidin (1:50; Dako). After extensive wash, forward scatter and side scatter characteristics of 5000 events were acquired in linear mode and fluorescence intensities were acquired at log scale using a Beckman Coulter Epics XL-MCL flow cytometer.

2.8. Immunofluorescence detection of parasite-bound carp IgM

Blood smears were prepared on poly-L-lysine coated glass slides, air-dried for 15 min and fixed in ice-cold acetone for 7 min. Slides were washed twice for 5 min in cPBS/BSA and subsequently incubated with 1:20 dilution of biotinylated WCI-12 antibody for 30 min at room temperature in a humidified chamber. After two washes in cPBS/BSA, slides were incubated with a 1:50 dilution of FITC-labelled Streptavidin. As a reference for parasite morphology, slides were stained with a 1:500 dilution of rabbit anti-*T. borreli* antibody (Joerink et al., 2007) and subsequently with a 1:20 dilution of FITC-labelled swine-anti rabbit antibody (Dako). All slides were air-dried for 10 min in the dark, embedded in Vectashield with or without propidium iodide (Vector Laboratories) to counterstain the nucleus and the kinetoplast and immediately examined with a Zeiss LSM-510 laser scanning microscope.

2.9. Statistics

For gene expression analysis, relative expression ratios (R) were calculated as described. Transformed (LN(R)) values were used for statistical analysis in SPSS Software (15.0). Significant differences ($P < 0.05$) were determined by a two-way ANOVA followed by a Sidak's test. A one-way ANOVA was used for the complement lysis, nitrite and ELISA experiments.

3. Results

3.1. Serum nitrite and serum antibody levels during T. borreli infection in vivo

Very high serum nitrite levels (400 μM) were observed at 3 weeks post-infection (wpi) concomitantly with the peak of parasitemia (Fig. 1). By week 6 post-infection, parasite numbers and serum nitrite levels decreased concomitantly with a progressive increase of *T. borreli*-specific antibodies (Fig. 2).
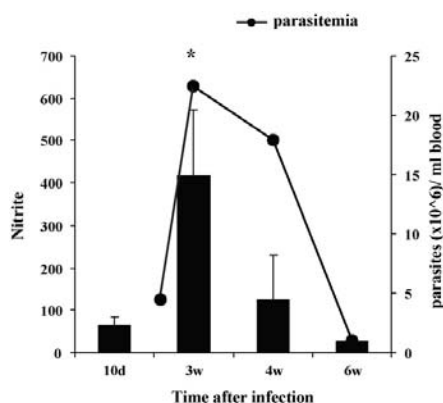
Fig. 1. Serum nitrite levels in relation to parasitemia during *T. borreli* infection *in vivo*. Fish were infected with 10^4 parasites and at the indicated time points samples were collected to measure serum nitrite level and parasitemia (plasma). Values are given as mean (+SD) of $n = 5$ fish. Symbol (*) indicates a significant difference as compared to non-infected fish at the same time point.
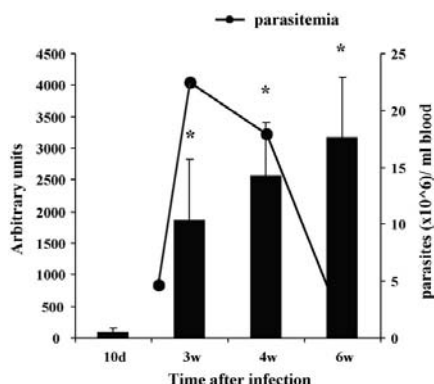
Fig. 2. Specific antibody (IgM) levels in relation to parasitemia during *T. borreli* infection *in vivo*. Fish were infected with 10^4 parasites and at the indicated time points samples were collected to measure *T. borreli*-specific IgM level (serum) and parasitemia (plasma). Values are given as mean (+SD) of *n* = 5 fish. Symbol (*) indicates a significant difference as compared to non-infected fish at the same time point.

3.2. Gene expression of complement factors during T. borreli infection in vivo

All investigated complement genes were first described in East-Asian common carp (*C. carpio haematopterus*). European (*C. carpio carpio*) and East-Asian common carp diverged approximately more than 500,000 years ago (Zhou et al., 2003) and differences at the nucleotide level between sequences coding for orthologous genes are often found. By homology cloning complement genes corresponding to those previously described in East-Asian common carp were amplified. Analysis of the nucleotide sequences confirmed a high percentage of identity (>95%) with the corresponding East-Asian complement genes for all investigated factors with the exception of factor C3-S which showed 85% of identity with the orthologous East-Asian C3-S gene (data not shown). Based on the newly described sequences, specific primers for real-time quantitative PCR could be designed.

In general, changes in gene expression were most clear in the period corresponding to the peak of parasitemia, i.e. 3–4 wpi. C1rs is one of the components of the initiation complex of the classical pathway. Regarding the different isoforms of carp C1rs, although C1rs-A was more expressed than C1rs-B, both isoforms were moderately but significantly up-regulated at 3 wpi (Fig. 3, 1st panel). MASP2, another serine protease sharing the same domain organization as C1r and C1s, is involved in the initiation complex of the lectin pathway. MASP2 was expressed at low levels in hepatopancreas from control fish and was not regulated during infection (Fig. 3, 1st panel). C3 is the central component of the complement system and is involved in all three activation pathways. We studied two C3 isoforms (C3-H1 and C3-S) both displaying a very high basal expression, compared to the other complement factors. During infection, significantly up-regulated gene expression levels of C3-S, but not C3-H1, were observed at 3 wpi (Fig. 3, 2nd panel). C4 is the second acting component of the classical and lectin pathways. The two carp C4 isoforms, C4-1 and C4-2, displayed a differential basal expression and were both significantly up-regulated at 3 wpi, with a greatest effect on C4-2 (Fig. 3, 3rd panel). Factor B and C2 act as the catalytic subunits of the C3/C5-convertases in the alternative and classical pathways, respectively. All sequences isolated from cartilaginous and bony fish to date show nearly equal similarities with mammalian factors B and C2 and are therefore named B/C2-like (Nakao et al., 1998, 2002). We examined 4 isoforms of carp

complement factor B/C2 each showing a differential basal expression in hepatopancreas from control carp. Isoforms B/C2-A1 and B/C2-A2 had a comparable up-regulation, B/C2-B was only moderately up-regulated whereas B/C2-A3, despite the very low basal expression, could be up-regulated up to 30-times (Fig. 3, 4th panel). Complement factor C5 acts downstream of all activating pathways and is the initial component of the lytic pathway leading to the formation of the membrane-attack complex. Carp C5 can be grouped into C5-type I and C5-type II. C5-type I contains multiple genes, one of which is represented by the C5-1 cDNA clone. C5-II is represented by the cDNA clone C5-2. In carp, the two isoforms of C5 (C5-1 and C5-2) were expressed at a very low level and did not show regulation of gene expression during infection (Fig. 3, 5th panel). Factor I is a serine protease that regulates complement activation. Both isoforms of complement factor I (fI-A and fI-B) had a low basal expression and both showed a moderate, but significant, up-regulation at 3 and 4 wpi (Fig. 3, 6th panel). The general up-regulation of complement factors, particularly of those involved in the classical pathway confirms the involvement of the complement system during *T. borreli* infection *in vivo*.

3.3. NO favors parasite aggregation and hinders parasite motility

In vitro, aggregation of *T. borreli* was observed, already at 3 h, in cultures incubated with immune serum (IS) but not in cultures incubated with non-immune serum (NIS) (Fig. 4A). Parasite aggregation was particularly evident in cultures incubated with GSNO where groups of 5–10 parasite aggregates were observed. In control cultures (GSH), groups of only 2–5 parasite aggregates were present.

Examination of parasite motility (Fig. 4B) indicated that in control (GSH) cultures at time point 3 h, the presence of parasite aggregates had no clear effect on parasite motility. In contrast, in cultures incubated with GSNO, motility was strongly reduced (Fig. 4B, 3 h, compare column 2 and 4). At time point 7 h, parasite motility was further reduced but only in cultures incubated with IS. Particularly in the presence of GSNO only very slow-moving parasites (motility index = 1) were observed. Thus, the reduction in parasite motility, owing to the presence of NO prevents parasite disaggregation.

3.4. NO favors antibody-dependent complement-mediated parasite lysis

We now examined if reduced motility owing to the presence of NO would affect antibody-dependent complement-mediated lysis of *T. borreli*. In cultures incubated with IS in the presence of GSH, 100% parasite lysis (non-motile parasites with round morphology) was observed only after 24 h (Fig. 5). In cultures incubated with IS in the presence of GSNO, 88% of the parasites were lysed already after 7 h (Fig. 5). Parasite lysis was not observed in any culture incubated with NIS. These results indicate that in the presence of complement and IgM, NO increases susceptibility of *T. borreli* to complement-mediated lysis.

3.5. NO reduces antibody clearance from the parasite surface

To investigate whether the increased susceptibility of *T. borreli* to complement-mediated lysis was due to an impaired ability of the parasite to rapidly remove surface-bound antibodies, the rate of antibody clearance was investigated by flow cytometric analysis. Parasites were incubated with GSNO, or with GSH, for 12 h and subsequently labelled with parasite-specific IgM using IS. After incubation with IS, a small aliquot of parasite suspension was resuspended in a large volume of ice-cold buffer and immediately fixed. Cell surface labelling confirmed that 100% of the parasites were
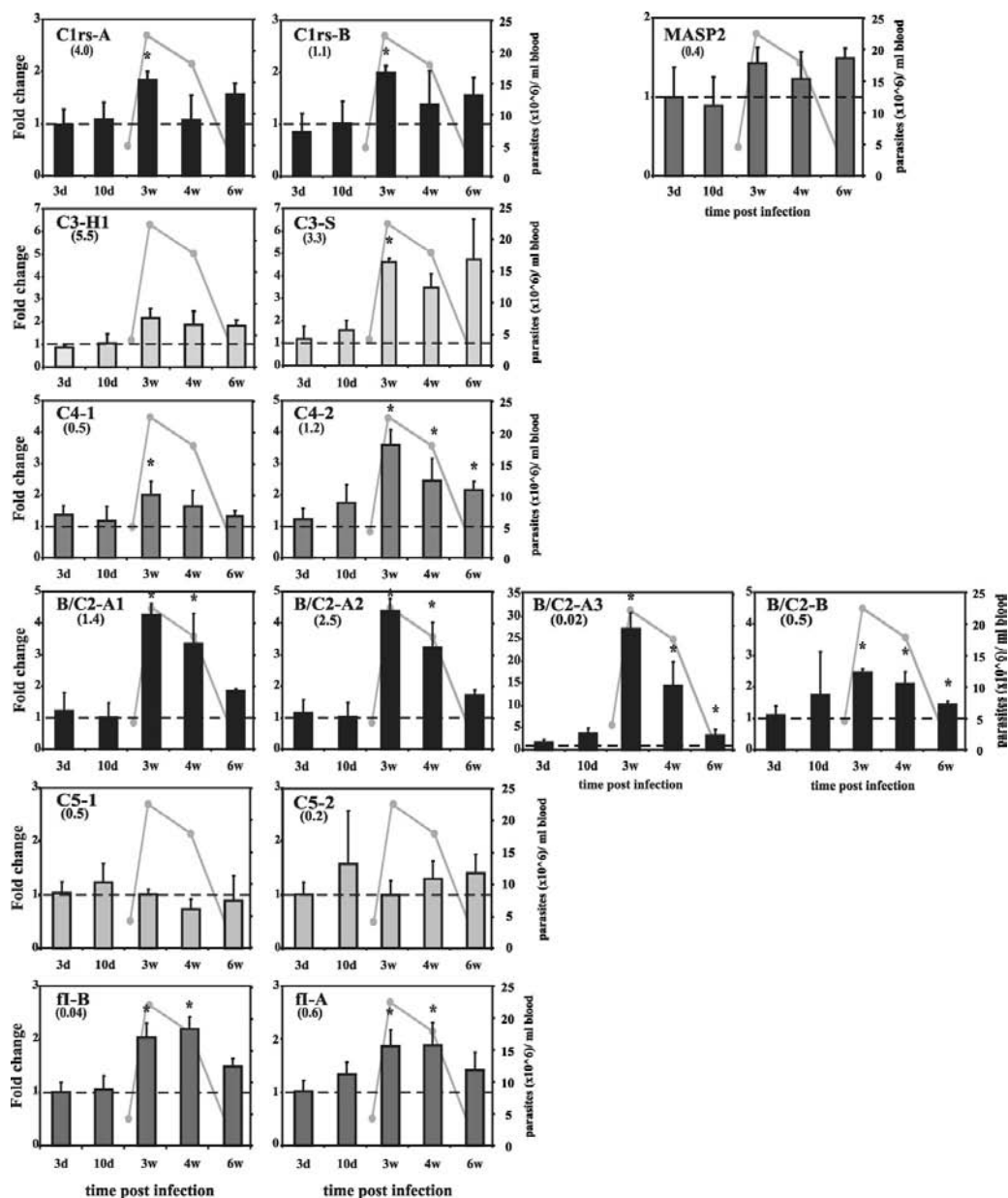
Fig. 3. Complement gene expression in hepatopancreas in relation to parasitemia during *T. borreli* infection *in vivo*. Fish were infected with 10^4 parasites and at the indicated time points parasite numbers were measured in plasma samples and hepatopancreas was collected for subsequent real-time quantitative PCR gene expression analysis. Basal gene expression for different genes and isoforms was measured in hepatopancreas from healthy fish and is given as a number on the upper left corner of each plot. Gene expression was normalized relative to the mRNA of the S11 protein of the 40S subunit (40S) as reference gene. Values are expressed relative to non-infected fish at the same time point. Horizontal line indicates the value of the control time point. Bars indicate *T. borreli*-infected fish. Values are given as mean (+SD). Symbol (*) indicates a significant difference relative to non-infected fish at the same time point.

(A)

(B)

		NIS		IS	
	0h	**3h**	**7h**	**3h**	**7h**
GSH	5	4	4	4	2
GSNO	3	3	3	2	1
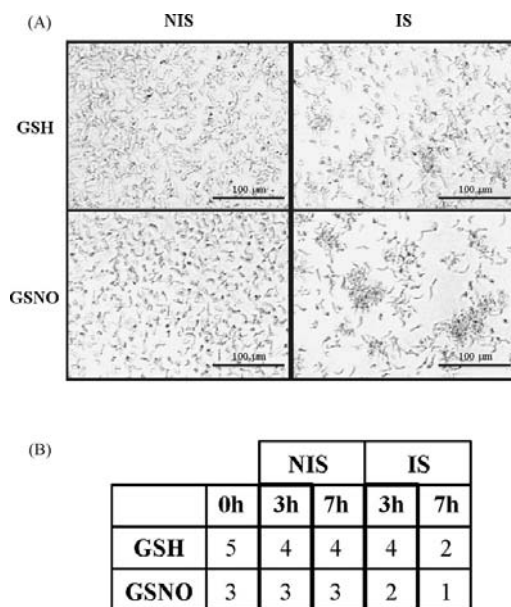
Fig. 4. (A) Nitric oxide favors aggregation of *T. borreli in vitro*. Parasites (2×10^5/well, final volume 100 µl) were cultured for 12 h in the presence of 50% non-immune serum (NIS) as a source of complement and GSNO (1 mM) as a source of nitric oxide. GSH (1 mM) served as negative control. After 12 h, 50 µl of fresh NIS and 50 µl of immune serum (IS; as a source of specific antibodies) were added to 50 µl of the parasite culture. As negative control, heat-inactivated normal carp serum (NCS) was used instead of IS. Again GSNO or GSH were supplied and aggregation was monitored by light microscopy (20× magnification) at time point 3 h. Note the formation of parasite aggregates in cultures incubated with IS (right panels) and note the extent of parasite aggregation in cultures incubated with GSNO. Aggregation was not observed in cultures incubated with NIS (left panels). (B) Nitric oxide lowers motility of *T. borreli in vitro*. Parasite motility was quantified as described in the material and methods section (motility index). After 12 h of incubation with GSNO (referred to as 0 h) only a moderate reduction in motility was observed when compared to GSH cultures. In cultures with GSH, parasite motility was reduced after 7 h only in the presence of IS. In cultures with GSNO parasite motility was reduced already after 3 h in the presence of IS and after 7 h almost all parasites were immotile.

Fig. 5. Nitric oxide favors antibody-dependent complement-mediated lysis of *T. borreli in vitro*. Parasites were first cultured for 12 h in the presence of GSNO or GSH and NIS (complement source) and subsequently IS was added, as described in the legend of Fig. 4. Lysis, measured as the number of non-motile parasites with a round morphology, was monitored over time by light microscopy. Shown are mean (+SD) of triplicate wells of one representative experiment out of four performed independently. Symbol (*) indicates a significant difference compared to the respective sample incubated with NIS.

coated with carp IgM (Fig. 6, open histograms). Cell surface fluorescence could not be detected on parasites incubated with GSH, not even at time point 0 (Fig. 6A, top panels, dark-grey histograms). These parasites were first resuspended in pre-warmed medium and then immediately transferred to ice-cold buffer (referred to as 0 min). Although the whole procedure was performed at 0 °C, parasite motility in GSH cultures could not be stopped completely (not shown), indicating that *T. borreli*, even at low temperature, can be motile and maintain a high rate of endocytosis. In contrast, cell surface fluorescence could still be detected at time 0 on parasites that were cultured with GSNO (Fig. 6B, lower panels, light-grey histograms). Fluorescence intensity decreased over time on parasites incubated with GSNO, and it required 5 min before IgM could no longer be detected on the parasite surface. These results confirm that in the presence of NO, the rate of surface antibody clearance is greatly reduced.

3.6. Antibody clearance during *T. borreli* infection in vivo

In vivo, the presence of carp IgM on the parasite surface was first detected at 3 wpi, exclusively in the area corresponding to the flagellar pocket (Fig. 6B). This indicated that antibody clearance might occur, also *in vivo*, especially during the initial phase of the antibody response when *T. borreli* can still sort and internalize antibody complexes in an effective manner. At 4 and 6 wpi carp anti-*T. borreli* antibodies were detected covering the entire surface of the parasite, indicating that at high antibody levels antibody sorting is less effective.

4. Discussion

In vitro, the concerted action of IgM and complement showed that *T. borreli* can be effectively killed by antibody-dependent complement-mediated parasite lysis. The requirement for IgM but also the fact that clearance of *T. borreli* from the bloodstream of carp coincides with the onset of a specific antibody response *in vivo*, suggests a main role for the classical route of complement activation during the later stage of infection (4–6 wpi). We showed a general up-regulation of most complement factors, confirming the involvement of the complement system during *T. borreli* infection *in vivo*. Blood-dwelling parasites, such as *T. borreli*, by definition are not usually lysed by the lectin or alternative route of complement activation and our *in vitro* experiments showed that complement alone is not sufficient to cause parasite lysis. In addition, the relatively late timing (3–6 wpi) of up-regulation of complement gene expression supports a main role for the classical route of complement activation during *T. borreli* infection.

The classical, lectin and alternative pathways in bony fish, as three distinct but partly overlapping routes leading to complement activation, are considered analogous to those in mammals (Nakao
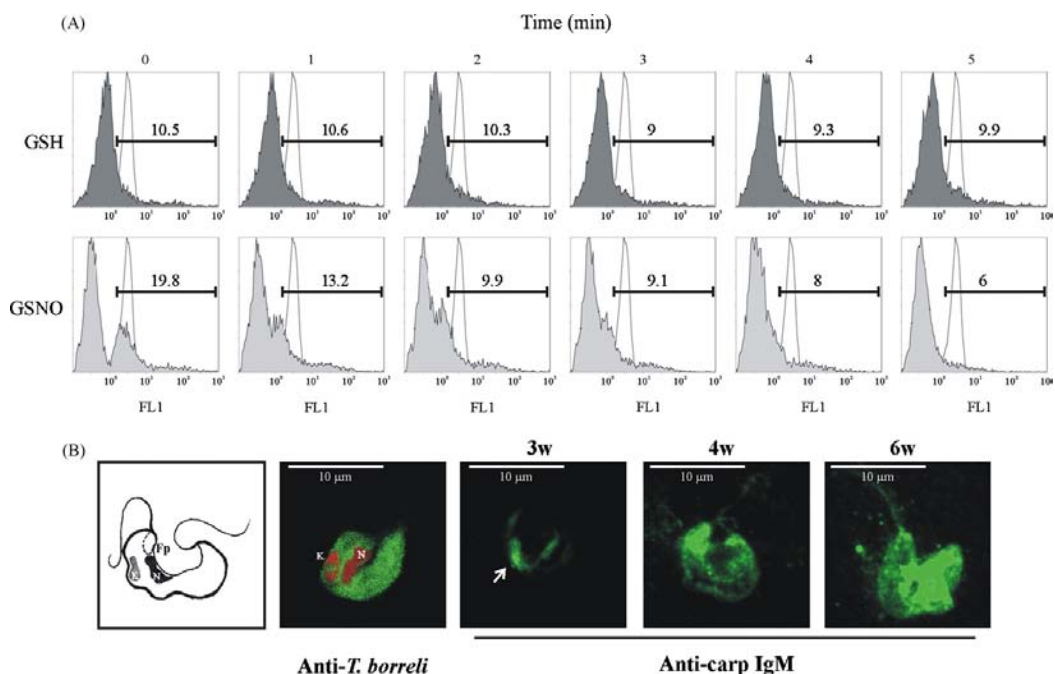
Fig. 6. Antibody clearance from the surface of *T. borreli*. Influence of nitric oxide on antibody clearance *in vitro*. Parasites were first cultured for 12 h in the presence of GSH or GSNO and NIS (complement source) as described in the legend of Fig. 4. After 12 h, parasites were cooled on ice and incubated for 30 min with IS, in the presence of GSH or GSNO. An aliquot of this parasite suspension was collected, resuspended in a large volume of washing buffer and immediately fixed in solution with 4% PFA. Surface-bound IgM staining of this population is shown by the open histograms in each plot. The remaining parasites were transferred to pre-warmed (27 °C) medium containing 50% heat-inactivated FCS and GSH or GSNO. Aliquots were collected immediately (time 0) or at the indicated time points (1–5 min) and transferred to ice-cold medium, washed and fixed. Note the decrease in mean fluorescence intensity (given as numbers in each plot) in cultures previously incubated with GSNO but not in control (GSH) cultures. (B) Clearance of surface IgM *in vivo*. As a reference for parasite morphology, blood smears were stained with rabbit anti-*T. borreli* antibody (green) and counterstained with PI (red) to visualize the position of the nucleus (N) and of the kinetoplast (K). A schematic representation also indicating the position of the flagellar pocket (FP) is given in the left panel. Cell surface staining (green) against parasite-bound carp IgM was performed on blood smears collected at 3w, 4w and 6w post-infection. White arrow indicates the position of the flagellar pocket. (For interpretation of the references to color in this figure legend, the reader is referred to the web version of the article.)

et al., 2003b; Boshra et al., 2006). Molecular studies, however, have revealed a striking feature of the complement factors that is unique to bony fish, i.e. most if not all complement factors are encoded by multiple genes and thus exist in several isoforms (Boshra et al., 2006). For some of these isoforms functional differences have been shown (Sunyer et al., 1996, 1997; Nakao et al., 2000, 2002, 2004), a feature that allows the complement system of fish to recognize a wider variety of foreign surfaces when compared to the mammalian system (Sunyer et al., 1996).

The complement system of common carp is well characterized. We took advantage of the molecular knowledge to study the role of the different complement factors and their respective isoforms during infection with *T. borreli*. In the classical pathway, C1 recognizes antigen-bound antibodies and activates C4 and C2 in this order. We studied two isoforms of carp C1rs and two isoforms of C4. Despite differences in basal gene expression, transcription was up-regulated in a comparable manner for both complement factors, and both their respective isoforms, with the highest gene regulation observed at 3 wpi. The up-regulation of C1rs further supports a role for the classical pathway of complement activation in the immune response to *T. borreli*. The alternative pathway is composed of C3 and factors B and D and can be spontaneously activated by, for example, bacterial lipopolysaccharide and β-glucans. Fish molecules showing nearly equal similarities to both mammalian factors B and C2 have been identified and are therefore named

B/C2-like genes. We examined four isoforms of carp B/C2, each with differences in basal expression in hepatopancreas from healthy carp. We found a very high up-regulation of B/C2-A3 in hepatopancreas of carp infected with *T. borreli*. This isoform was previously found to be expressed and up-regulated at extra-hepatic sites only (Nakao et al., 2002). The results in the present study confirm the very low gene expression of B/C2-A3 in hepatopancreas but also show that upon stimulation with specific stimuli such as *T. borreli*, gene expression of the B/C2-A3 isoform can be up-regulated considerably, also in hepatopancreas. Although this provides additional evidence for a functional differentiation of B/C2 isoforms, conclusions on difference in function require confirmation by studies on the corresponding proteins. For the central complement factor C3, we studied two isoforms (C3-H1 and C3-S) both with a very high basal gene expression in hepatopancreas when compared to the other complement factors. During infection, significantly up-regulated gene expression levels of isoform C3-S, but not C3-H1, were observed at 3 wpi. The differential up-regulation of C3-H1 and C3-S observed in our study is in line with a recent study indicating that the non-His type C3-S is the dominant isoforms reacting to a wider range of targets, such as foreign erythrocytes, yeast and bacteria (Ichiki and Nakao, unpublished data). Previous reports in trout, carp and seabream also showed that different C3 isoforms have different binding efficiencies to several complement activating surfaces (Sunyer et al., 1996, 1997; Nakao et al., 2004) suggesting that

C3 isoforms in teleost fish may have different substrate specificities of the thioester.

In mammals the main mechanism that is believed to mediate control of trypanosome infections is the antibody-mediated phagocytosis of opsonized parasites by liver macrophages, including Kupffer cells (Shi et al., 2004; Magez et al., 2006; Baral et al., 2007). In contrast, the presence of macrophages is not crucial for the clearance of infections with *T. borreli*. Carp infected with *T. borreli* but depleted of macrophages by intraperitoneal injection of clodronate-liposomes showed only a minor increase in parasitaemia (Saeij et al., 2003b). We believe that in *T. borreli* infections, at least during the late phase of infection (>3 wpi), antibody-dependent complement-mediated lysis plays an important role in parasite clearance.

T. borreli infections of carp are characterized by anemia, splenomegaly and polyclonal B cell activation, all features in common with African trypanosome infections of mammals. The ability to induce extremely elevated serum nitrite levels, however, appears a typical feature of *T. borreli* infections. Elevated nitrite levels result in tissue nitration and inflammation (Forlenza et al., 2008a) whereas administration, *in vivo*, of an iNOS inhibitor was beneficial to the host owing to lower parasitemia levels and higher survival (Saeij et al., 2002). *In vitro*, high concentrations of NO were found to inhibit lymphocyte proliferation and to affect parasite motility only, and never viability (Saeij et al., 2002, 2003c; Forlenza et al., 2008a). Hence, all evidence so far suggested that the high NO-inducing ability of *T. borreli* would be a strategy of the parasite to immunosuppress and thus evade the host immune system.

In the present study we examined in more detail the effects of NO on parasite motility, re-considering the high induction of NO during infections with *T. borreli* also as a host defense mechanism. We recreated, *in vitro*, a physiological situation corresponding to the early stages of infection when serum complement factors are not limiting, serum nitrite concentrations are still moderate and the host is initiating a specific antibody response. Our results clearly indicate that while incubation of *T. borreli* in the presence of specific antibodies and complement leads to parasite lysis within a period of 24 h, incubation under the same conditions but in the presence of NO leads to complete parasite lysis within 7 h. In mammals, a crucial role for NO in parasite control has been described during *T. congolense* infections where NO in combination with IFN-γ and IgG2a/3 is a determining factor for the resolution of the infection (Magez et al., 2006, 2007). However, a direct effect of NO on the parasite itself has not been reported. It would therefore be interesting to investigate whether the NO-mediated parasite killing mechanism observed during *T. congolense* infection can be explained by the ability of NO to affect parasite motility and consequently the removal of surface-bound IgG complexes.

All African trypanosomes have developed immune evasion strategies that rely on antigenic variation, immunosuppression, and on the rapid removal of surface-bound antibodies by hydrodynamic sorting (McLintock et al., 1993; Donelson et al., 1998; Engstler et al., 2007). While scrutinizing the effects of NO on parasite motility we measured an increased susceptibility of *T. borreli* to antibody-dependent complement-mediated lysis in the presence of NO, leading us to investigate whether NO would indirectly affect the ability of *T. borreli* to remove surface-bound antibody complexes. Flow cytometric analysis confirmed that NO, by hindering motility, affects the ability of *T. borreli* to remove IgM from its surface. Incubation with NO increased the rate of antibody clearance from a half-time of seconds to a half-time of minutes, suggesting that host-derived NO can interfere with the immune evasion strategy of the parasite. We could also confirm that, during the early stages of infection, surface-bound antibodies are located almost exclusively at the level of the flagellar pocket of these parasites, indicating that antibody sorting might occur on the surface of *T.*

borreli also *in vivo*. Antibody removal must be continuous, and clearance of trypanosomes can only occur when the host is producing immunoglobulins faster than the trypanosomes can degrade them. Carp IgM, once taken up in the flagellar pocket is likely transported to the endosome and digested at low pH by a cysteine proteinase of *T. borreli* with cathepsin L-like activity (Ruszczyk et al., 2008a,b). Later during *T. borreli* infection (>3 wpi), surface-bound IgM was detected on the entire cell surface of the parasite indicating that IgM removal and degradation is less effective when antibody titers increased.

We have shown that antibody clearance occurs also in *T. borreli*, but whether the mechanisms can be ascribed to hydrodynamic flow-mediated sorting still needs to be confirmed. The flagellum of *T. brucei* is attached and runs along the body, propelling the parasite in the direction away from the flagellar pocket, causing a movement of immune complexes by hydrodynamic drag forces in the direction of the flagellar pocket. Owing to the basic mechanism described for hydrodynamic sorting, i.e. directional drag forces, it has also been proven that trypanosomes can more effectively remove IgM-VSG rather than IgG-VSG complexes, simply due to the larger ligand size (Engstler et al., 2007). This endocytic process occurs most effectively at 37 °C and is completely abolished at temperatures lower than 24 °C. Carp do not produce IgG and are ectothermic animals that generally live at temperatures between 4 °C and 25 °C. We noticed, *in vitro*, that even at 0 °C antibody clearance from the surface of *T. borreli* could not be halted, suggesting this parasite has adapted to lower temperatures. Also taking into account that *T. borreli* (Bodonida) has two instead of one flagellum, comparison in a more quantitative manner of cellular motility and rate of endocytosis in representatives of the Bodonida and Trypanosomatida should provide insight into the evolution of immune evasion strategies developed by Kinetoplastida.

All together, our data demonstrate that host-derived NO interferes with clearance of surface IgM as a parasite immune evasion strategy. Particularly during the early phase of an immune response to *T. borreli* this allows the host to gain enough time to mount a specific antibody response, required to develop effective antibody-dependent complement-mediated lysis of *T. borreli* during the late phase of infection. On the other hand, it is essential that the host restricts the production of NO to limit suppressive effects on lymphocyte proliferation. The homologus host–parasite infection model of carp with *T. borreli* provides a clear example of how a balance between parasite virulence and effectiveness of the immune response is required for long-term persistence of an infective parasite population as well as survival of the host.

Acknowledgements

References

Antia, R., Nowak, M.A., Anderson, R.M., 1996. Antigenic variation and the within-host dynamics of parasites. Proc. Natl. Acad. Sci. U.S.A. 93, 985–989.

Baral, T.N., De Baetselier, P., Brombacher, F., Magez, S., 2007. Control of *Trypanosoma evansi* infection is IgM mediated and does not require a type I inflammatory response. J. Infect. Dis. 195, 1513–1520.

Boshra, H., Li, J., Sunyer, J.O., 2006. Recent advances on the complement system of teleost fish. Fish Shellfish Immunol. 20, 239–262.

Cross, G.A., 1996. Antigenic variation in trypanosomes: secrets surface slowly. Bioessays 18, 283–291.

Dean, S.D., Matthews, K.R., 2007. Restless gossamers: antibody clearance by hydrodynamic flow forces generated at the surface of motile trypanosome parasites. Cell Host Microbe 2, 279–281.

Donelson, J.E., Hill, K.L., El-Sayed, N.M., 1998. Multiple mechanisms of immune evasion by African trypanosomes. Mol. Biochem. Parasitol. 91, 51–66.

Engstler, M., Pfohl, T., Herminghaus, S., Boshart, M., Wiegertjes, G., Heddergott, N., Overath, P., 2007. Hydrodynamic flow-mediated protein sorting on the cell surface of trypanosomes. Cell 131, 505–515.

Forlenza, M., Scharsack, J.P., Kachamakova, N.M., Taverne-Thiele, A.J., Rombout, J.H., Wiegertjes, G.F., 2008a. Differential contribution of neutrophilic granulocytes and macrophages to nitrosative stress in a host–parasite animal model. Mol. Immunol. 45, 3178–3189.

Forlenza, M., Walker, P.D., de Vries, B.J., Wendelaar Bonga, S.E., Wiegertjes, G.F., 2008b. Transcriptional analysis of the common carp (Cyprinus carpio L.) immune response to the fish louse Argulus japonicus Thiele (Crustacea: Branchiura). Fish Shellfish Immunol. 25, 76–83.

Irnazarow, I., 1995. Genetic variability of Polish and Hungarian carp lines. Aquac. Res. 129, 215–219.

Joerink, M., Groeneveld, A., Ducro, B., Savelkoul, H.F., Wiegertjes, G.F., 2007. Mixed infection with Trypanoplasma borreli and Trypanosoma carassii induces protection: involvement of cross-reactive antibodies. Dev. Comp. Immunol. 31, 903–915.

Kato, Y., Nakao, M., Mutsuro, J., Zarkadis, I.K., Yano, T., 2003. The complement component C5 of the common carp (Cyprinus carpio): cDNA cloning of two distinct isotypes that differ in a functional site. Immunogenetics 54, 807–815.

Koumans-van Diepen, J.C., Egberts, E., Peixoto, B.R., Taverne, N., Rombout, J.H., 1995. B cell and immunoglobulin heterogeneity in carp (Cyprinus carpio L.); an immuno(cyto)chemical study. Dev. Comp. Immunol. 19, 97–108.

Magez, S., Radwanska, M., Drennan, M., Fick, L., Baral, T.N., Allie, N., Jacobs, M., Nedospasov, S., Brombacher, F., Ryffel, B., De Baetselier, P., 2007. Tumor necrosis factor (TNF) receptor-1 (TNFp55) signal transduction and macrophage-derived soluble TNF are crucial for nitric oxide-mediated Trypanosoma congolense parasite killing. J. Infect. Dis. 196, 954–962.

Magez, S., Radwanska, M., Drennan, M., Fick, L., Baral, T.N., Brombacher, F., Baetselier, P.D., 2006. Interferon-γ and nitric oxide in combination with antibodies are key protective host immune factors during Trypanosoma congolense Tc13 Infections. J. Infect. Dis. 193, 1575–1583.

McLintock, L.M., Turner, C.M., Vickerman, K., 1993. Comparison of the effects of immune killing mechanisms on Trypanosoma brucei parasites of slender and stumpy morphology. Parasite Immunol. 15, 475–480.

Mutsuro, J., Tanaka, N., Kato, Y., Dodds, A.W., Yano, T., Nakao, M., 2005. Two divergent isotypes of the fourth complement component from a bony fish, the common carp (Cyprinus carpio). J. Immunol. 175, 4508–4517.

Nagai, T., Mutsuro, J., Kimura, M., Kato, Y., Fujiki, K., Yano, T., Nakao, M., 2000. A novel truncated isoform of the mannose-binding lectin-associated serine protease (MASP) from the common carp (Cyprinus carpio). Immunogenetics 51, 193–200.

Nakao, M., Fushitani, Y., Fujiki, K., Nonaka, M., Yano, T., 1998. Two diverged complement factor B/C2-like cDNA sequences from a teleost, the common carp (Cyprinus carpio). J. Immunol. 161, 4811–4818.

Nakao, M., Hisamatsu, S., Nakahara, M., Kato, Y., Smith, S.L., Yano, T., 2003a. Molecular cloning of the complement regulatory factor I isotypes from the common carp (Cyprinus carpio). Immunogenetics 54, 801–806.

Nakao, M., Kajita, N., Sato, Y., Somamoto, T., Kato-Unoki, Y., Matsushita, M., Nakata, M., Fujita, T., Yano, T., 2006. Lectin pathway of bony fish complement: identification of two homologs of the mannose-binding lectin associated with MASP2 in the common carp (Cyprinus carpio). J. Immunol. 177, 5471–5479.

Nakao, M., Matsumoto, M., Nakazawa, M., Fujiki, K., Yano, T., 2002. Diversity of complement factor B/C2 in the common carp (Cyprinus carpio): three isotypes of B/C2-A expressed in different tissues. Dev. Comp. Immunol. 26, 533–541.

Nakao, M., Miura, C., Itoh, S., Nakahara, M., Okumura, K., Mutsuro, J., Yano, T., 2004. A complement C3 fragment equivalent to mammalian C3d from the common carp (Cyprinus carpio): generation in serum after activation of the alternative pathway and detection of its receptor on the lymphocyte surface. Fish Shellfish Immunol. 16, 139–149.

Nakao, M., Mutsuro, J., Nakahara, M., Kato, Y., Yano, T., 2003b. Expansion of genes encoding complement components in bony fish: biological implications of the complement diversity. Dev. Comp. Immunol. 27, 749–762.

Nakao, M., Mutsuro, J., Obo, R., Fujiki, K., Nonaka, M., Yano, T., 2000. Molecular cloning and protein analysis of divergent forms of the complement component C3 from a bony fish, the common carp (Cyprinus carpio): presence of variants lacking the catalytic histidine. Eur. J. Immunol. 30, 858–866.

Nakao, M., Osaka, K., Kato, Y., Fujiki, K., Yano, T., 2001. Molecular cloning of the complement C1r/C1s/MASP2-like serine proteases from the common carp (Cyprinus carpio). Immunogenetics 52, 255–263.

O'Beirne, C., Lowry, C.M., Voorheis, H.P., 1998. Both IgM and IgG anti-VSG antibodies initiate a cycle of aggregation–disaggregation of bloodstream forms of Trypanosoma brucei without damage to the parasite. Mol. Biochem. Parasitol. 91, 165–193.

Overath, P., Ruoff, J., Stierhof, Y.-D., Haag, J., Tichy, H., Dyková, I., Lom, J., 1998. Cultivation of bloodstream forms of Trypanosoma carassii, a common parasite of freshwater fish. Parasitol. Res. 84, 343–347.

Pfaffl, M.W., 2001. A new mathematical model for relative quantification in real-time RT-PCR. Nucleic Acids Res. 29, e45.

Ruszczyk, A., Forlenza, M., Joerink, M., Ribeiro, C.M., Jurecka, P., Wiegertjes, G.F., 2008a. Trypanoplasma borreli cysteine proteinase activities support a conservation of function with respect to digestion of host proteins in common carp. Dev. Comp. Immunol. 32, 1348–1361.

Ruszczyk, A., Forlenza, M., Savelkoul, H.F., Wiegertjes, G.F., 2008b. Molecular cloning and functional characterisation of a cathepsin L-like proteinase from the fish kinetoplastid parasite Trypanosoma carassii. Fish Shellfish Immunol. 24, 205–214.

Saeij, J.P., de Vries, B.J., Wiegertjes, G.F., 2003a. The immune response of carp to Trypanoplasma borreli: kinetics of immune gene expression and polyclonal lymphocyte activation. Dev. Comp. Immunol. 27, 859–874.

Saeij, J.P., Groeneveld, A., Van Rooijen, N., Haenen, O.L., Wiegertjes, G.F., 2003b. Minor effect of depletion of resident macrophages from peritoneal cavity on resistance of common carp Cyprinus carpio to blood flagellates. Dis. Aquat. Organ. 57, 67–75.

Saeij, J.P., Stet, R.J., Groeneveld, A., Verburg-van Kemenade, L.B., van Muiswinkel, W.B., Wiegertjes, G.F., 2000. Molecular and functional characterization of a fish inducible-type nitric oxide synthase. Immunogenetics 51, 339–346.

Saeij, J.P., Van Muiswinkel, W.B., Groeneveld, A., Wiegertjes, G.F., 2002. Immune modulation by fish kinetoplastid parasites: a role for nitric oxide. Parasitology 124, 77–86.

Saeij, J.P., van Muiswinkel, W.B., van de Meent, M., Amaral, C., Wiegertjes, G.F., 2003c. Different capacities of carp leukocytes to encounter nitric oxide-mediated stress: a role for the intracellular reduced glutathione pool. Dev. Comp. Immunol. 27, 555–568.

Scharsack, J.P., Steinhagen, D., Kleczka, C., Schmidt, J.O., Korting, W., Michael, R.D., Leibold, W., Schuberth, H.J., 2003. The haemoflagellate Trypanoplasma borreli induces the production of nitric oxide, which is associated with modulation of carp (Cyprinus carpio L.) leucocyte functions. Fish Shellfish Immunol. 14, 207–222.

Schmid-Hempel, P., 2008. Parasite immune evasion: a momentous molecular war. Trends Ecol. Evol. 23, 318–326.

Secombes, C.J., van Groningen, J.J., Egberts, E., 1983. Separation of lymphocyte subpopulations in carp Cyprinus carpio L. by monoclonal antibodies: immuno-histochemical studies. Immunology 48, 165–175.

Shi, M., Wei, G., Pan, W., Tabel, H., 2004. Trypanosoma congolense infections: antibody-mediated phagocytosis by Kupffer cells. J. Leukoc. Biol. 76, 399–405.

Simpson, A.G.B., Stevens, J.R., Lukes, J., 2006. The evolution and diversity of kinetoplastid flagellates. Trends Parasitol. 22, 168–174.

Steinhagen, D., Hedderich, W., Skouras, A., Scharsack, J.P., Schuberth, J., Leibold, W., Körting, W., 2000. In vitro cultivation of Trypanoplasma borreli (protozoa: kinetoplastida), a parasite from the blood of common carp Cyprinus carpio. Dis. Aquat. Org. 41, 195–201.

Steinhagen, D., Kruse, P., Körting, W., 1989. The parasitemia of cloned Trypanoplasma borreli Laveran and Mesnil, 1901, in laboratory-infected common carp (Cyprinus carpio L.). J. Parasitol. 75, 685–689.

Stevens, J.R., Noyes, H.A., Schofield, C.J., Gibson, W., 2001. The molecular evolution of Trypanosomatidae. Adv. Parasitol. 48, 1–56.

Stijlemans, B., Guilliams, M., Raes, G., Beschin, A., Magez, S., De Baetselier, P., 2007. African trypanosomosis: from immune escape and immunopathology to immune intervention. Vet. Parasitol. 148, 3–13.

Sunyer, J.O., Tort, L., Lambris, J.D., 1997. Diversity of the third form of complement, C3, in fish: functional characterization of five forms of C3 in the diploid fish Sparus aurata. Biochem. J. 326 (Pt 3), 877–881.

Sunyer, J.O., Zarkadis, I.K., Sahu, A., Lambris, J.D., 1996. Multiple forms of complement C3 in trout that differ in binding to complement activators. Proc. Natl. Acad. Sci. U.S.A. 93, 8546–8551.

Tichopad, A., Dilger, M., Schwarz, G., Pfaffl, M.W., 2003. Standardized determination of real-time PCR efficiency from a single reaction set-up. Nucleic Acids Res. 31, e122.

Waghabi, M.C., Coutinho, C.M., Soeiro, M.N., Pereira, M.C., Feige, J.J., Keramidas, M., Cosson, A., Minoprio, P., Van Leuven, F., Araujo-Jorge, T.C., 2002. Increased Trypanosoma cruzi invasion and heart fibrosis associated with high transforming growth factor beta levels in mice deficient in alpha(2)-macroglobulin. Infect. Immun. 70, 5115–5123.

Wiegertjes, G.F., Forlenza, M., Joerink, M., Scharsack, J.P., 2005. Parasite infections revisited. Dev. Comp. Immunol. 29, 749–758.

Wiegertjes, G.F., Groeneveld, A., van Muiswinkel, W.B., 1995. Genetic variation in susceptibility to Trypanoplasma borreli infection in common carp (Cyprinus carpio L.). Vet. Immunol. Immunopathol. 47, 153–161.

Wiegertjes, G.F., Stet, R.J., Van Muiswinkel, W.B., 1994. Divergent selection for antibody production in common carp (Cyprinus carpio L.) using gynogenesis. Anim. Genet. 25, 251–257.

Zhou, J.F., Wu, Q.J., Ye, Y.Z., Tong, J.G., 2003. Genetic devergence between Cyprinus carpio carpio and Cyprinus carpio haematopterus as assessed by mitochondrial DNA analysis, with enphasis on origin of European domestic carp. Genetica 119, 93–97.
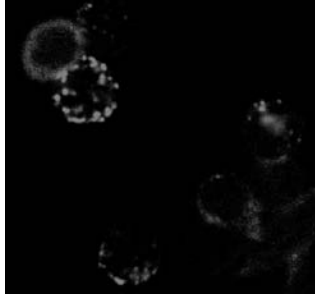
CHAPTER

8

"Fishing" for antibodies to identify T cells in carp

Maria Forlenza, Jan H.W.M. Rombout, Anja J. Taverne-Thiele,
Huub F.J. Savelkoul and Geert F. Wiegertjes

"Fishing" for antibodies to identify T cells in carp

Maria Forlenza[1], Jan H.W.M. Rombout[1], Anja J. Taverne-Thiele[1], Huub F.J. Savelkoul[1] and Geert F. Wiegertjes[1]

[1] Cell Biology and Immunology Group, Wageningen Institute of Animal Sciences, Wageningen University, Wageningen, The Netherlands.

Abstract

The TCR complex consists of a single TCRαβ heterodimer associated with at least three CD3 dimers including γε, δε and ξξ and includes the CD4 or CD8 co-receptors. The protein tyrosine kinases Lck and ZAP-70 provide essential signals in a cascade of events which will finally lead to T cell signalling and activation. In the present study we report the cloning of a full-length mRNA sequence for carp CD3ε and partial mRNA sequences for carp Lck and ZAP-70. Gene expression of the newly described sequences was detected only in thymocytes and not in sorted B cells, granulocytes and macrophages confirming their suitability as T-cell-lineage specific marker. Despite the genetic information available for almost all components of the TCR complex, the number of antibodies available for the identification of T cells in carp is very limited. Commercially available antibodies directed against a highly conserved prolin-rich region in the cytoplasmic tail of hCD3ε, the N-terminal region of ZAP-70 and the C-terminal region of Lck were tested for their ability to specifically recognize carp T cells. The anti-hZAP-70 antibody in particular, recognized carp T cells in both immunohistochemistry and flow cytometry and a 70 kDa protein by Western blot analysis. Two antibodies directed against selected antigenic epitopes of carp CD4 and CD8α were raised in rabbits. Immunohistochemical analysis, using the anti-hCD3ε, anti-hZAP-70, anti-cCD4 and anti-cCD8α antibodies revealed a conserved picture of the structure of carp thymus. The high cell density and intense staining observed in the thymic cortex indicates the presence of double-positive CD4+/CD8+ immature T cells (CD3ε+/ZAP-70+) in the cortical region, similar to what is observed in mammals and other fish. Despite the suitability for immunohistochemistry, both anti-cCD4 and anti-cCD8 they did not show immunoreactivity to live T cells in flow cytometry. Future strategies for an improved production of monoclonal antibodies specifically recognizing carp CD4+ and CD8+ T cells, based on very recent successful attempts in other fish species, are discussed. The anti-hCD3ε and anti-hZAP-70 were used to study T cell distribution in the spleen of *Trypanoplasma borreli*-infected carp. We could show the presence of both enlarged B cell and T cell areas and their co-localization in the spleen tissue. Double staining revealed that B and T cells lie intermingled to each other, with no clear distinction between a B or T cell zone, especially during infection.

Introduction

Comparative genomics has shown that the basic mechanisms responsible for genetic diversification of immunoglobulin (Ig) and T cell receptors, including rag-1 and rag-2 homologues, are present in all jawed vertebrates, including fish (1). The genomic information crucial to an understanding of the immune system of fish, therefore, is well developed. However, where the technological development in mammalian immunology has generated an array of resources in the form of cell lines and monoclonal antibodies, comparative immunologists still have a considerable number of technical hurdles to take. Especially the proper phenotypic classification of the different leukocyte cell types has remained a technical challenge (2-4). Where the development of monoclonal antibodies against the major Ig type in fish has allowed for the recognition of IgM-bearing B cells, the identification of the major T cell subtypes *i.e.* cytotoxic T cells (CTL) and T helper/regulatory T cells (Th), remains problematic in fish. Maybe the oldest (1995) and best characterized T cell-specific monoclonal antibody (DLT15) produced against sea bass (*Dicentrarchus labrax*) peripheral T cells (5), was only recently characterized as a putative marker for CD8+ T cells (6). In carp (*Cyprinus carpio*), the monoclonal antibodies WCL9 and WCL38 have been shown to recognize immature cortical thymocytes and putative mucosal T cells, respectively, (7, 8). Although these antibodies have been proven useful for specific research questions regarding ontogeny of the immune system (9) and mucosal immunity, the identification of mature, peripheral T cells in carp that would allow for studies into the role of cell-mediated immunity in infectious diseases, remains problematic.

To date, homology cloning has led to the identification of all sequences coding for T-cell-lineage specific surface markers (Fig. 1), including TCR(αβγδ), CD3(εγδξ), CD4 and CD8(αβ) in several fish species. This has allowed for studies on T cell and thymic development in fish and several *in situ* hybridization studies confirmed a general similarity between cold- and warm-blooded vertebrates in the development and functional anatomy of the thymus (10-15). Also in fish, immature T cells (rag+) localise to the thymic cortex, whereas mature T cells (rag-) localize in the medulla of the adult thymus (11, 15, 16). Although it is important to respect age-dependent difference as well as differences in T cell development or thymus organisation between fish species (17), T cell development in teleost fish appears to be similar to that of warm-blooded vertebrates.

Comparative sequence analyses clearly indicate that the extracellular domains of recognition molecules such as the B and T cell receptors are poorly conserved across species. However, the signalling domains (cytoplasmic regions) and even more so, the signalling molecules (transcription factors, adaptor molecules and kinases) involved in the initiation and progression of the signalling cascade, generally do show a high   percentage
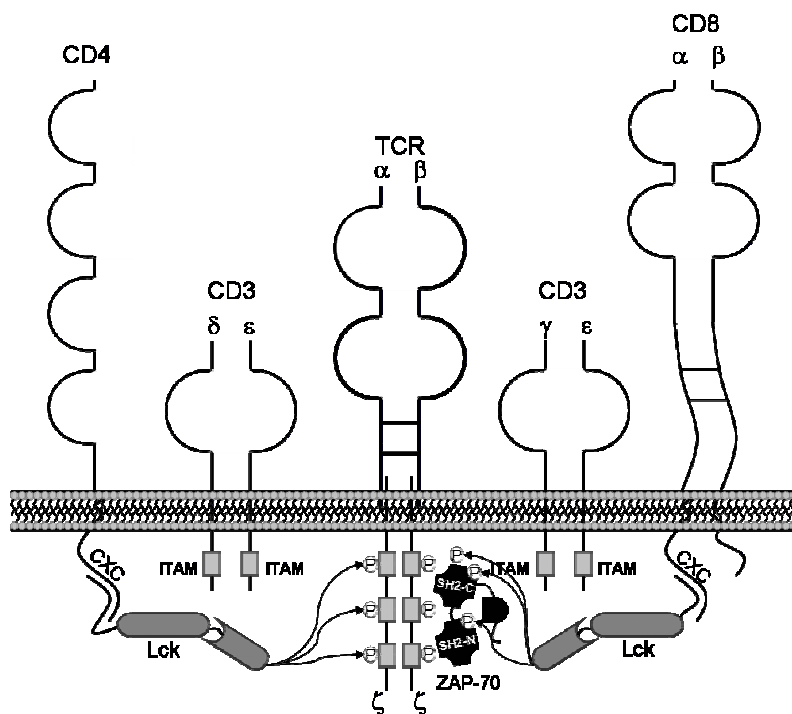
Figure 1. **Schematic representation of the T cell receptor (TCRαβ) complex**.
Both Lck (lymphocyte-specific protein tyrosine kinase) and ZAP-70 (ξ-associated protein) are involved in the very early signalling events occurring soon after antigen recognition by the TCR complex. The TCR complex consists of a single TCRαβ heterodimer associated with at least three CD3 dimers including γε, δε and ξξ. Lck is bound to a specific (CXC) motif present in the cytoplasmic tail of CD4 and CD8α. The conformational change induced upon antigen recognitions by the TCR, and MHC recognition by the CD4 or CD8 co-receptor, brings Lck in the vicinity of the ITAM (immunoreceptor tyrosine-based activation motifs) present in the cytoplasmic tails of the CD3 molecules. Lck can then phosphorylate the cytoplasmic tails of CD3ξ which leads to the recruitment of ZAP-70. ZAP-70 activation, by either autophosphorylation or by phosphorylation by Lck, will initiate a cascade of events which will finally lead to T cell signalling and activation.

of sequence similarity across species (personal observation). In fact, recognition molecules are often associated with conserved signalling cascades throughout phylogeny (18). We made use of the general conservation of intracellular domains and signalling molecules, first by cloning the coding sequences for carp CD3ε, ZAP-70 and Lck and subsequently by identifying commercially available antibodies that would likely recognize conserved epitopes in the corresponding sequences of carp CD3ε, Lck or ZAP-70 proteins.

Antibodies directed against a highly conserved prolin-rich region in the cytoplasmic tail of human CD3ε (hCD3ε), the N-terminal region of ZAP-70 (hZAP-70) and the C-terminal region of Lck (hLck) were tested for their ability to specifically recognize lymphocytes belonging to the T cell lineage of carp. The antibody against hCD3ε has been previously shown to react with blood leukocytes in snapper (*Pagrus auratus*) (19), Japanese flounder (*Paralichthys olivaceus*) (20), Atlantic salmon (*Salmo salar*) (21) and with T cells of the amphibian *Xenopus laevis* (22). For the production of antibodies recognizing carp CD4 (cCD4) (23) and cCD8α (24), a different approach was used. Antigenic peptides selected from the extracellular region of the molecules were used for immunization of rabbits and subsequent affinity purification of rabbit IgG. Among the several components of the TCR complex, CD3ε is specifically expressed on (αβ+ or γδ+) T cells and is therefore considered a useful pan-T cell marker. Lck and ZAP-70 are expressed in T but also in NK cells and are thus considered T-cell-

lineage-specific markers, CD8α is expressed on CTL, γδ+ T cells and on some NK cell types, whereas CD4 is expressed on T cells (Th) but can also be expressed on monocytes (at least in humans and rats but not in mice) (25, 26). In addition, abnormal ZAP-70 expression is regarded as a marker for B cell chronic lymphocytic leukaemia (27). Therefore, the use of only one single marker is not sufficient for an unequivocal identification of T cell-subtypes which requires a combination of pan-T cell and T cell-subtype-specific antibodies.

We have previously shown that upon infection with the extracellular parasite *Trypanoplasma borreli*, extremely enlarged B cell areas can be observed in the spleen of heavily infected fish (28). Owing to the lack of specific antibodies, the relative distribution and involvement of T cells during this parasitic infection was not investigated. Among the panel of antibodies investigated in the present study, the anti-hCD3ε and anti-hZAP-70 antibodies were selected for further use and applied in combination with a monoclonal antibody specifically recognizing IgM-bearing B cells (WCI12) for an immunohistochemical examination of spleen from *T. borreli*-infected carp. This study confirmed the presence of not only proliferating B cells but also T cells in the spleen of infected fish. The evident T cell proliferation could be indicative of polyclonal activation similar to the polyclonal activation observed for B cells during *T. borreli* infections. In the immuno-histochemical analysis, the enlarged T and B cell areas almost completely overlapped and double staining confirmed that B and T cells lie intermingled in

the spleen, particularly in infected spleen tissue.

In this study, the cloning of new markers for the carp T-cell-lineage, as well as the characterization of a number of antibodies with potential use for future comparative studies, is reported. The overall high conservation of the N-terminal region of ZAP-70 makes the anti-hZAP-70 antibody highly suitable for use as a pan T cell marker in carp. This antibody was found highly suitable for the identification of cells from the carp T cell lineage not only in immunohistochemical and Western blot, but also in flow cytometric applications. Future strategies for an improved production of monoclonal antibodies specifically recognizing carp CD4+ and CD8+ T cells and development of additional methods to detect activated T cells in fish will be discussed.

Material and Methods
Animals

European common carp (*Cyprinus carpio carpio* L.) were bred and raised to the age of nine months in the central fish facility at Wageningen University, The Netherlands, at 23°C in recirculating UV-treated tap water and fed pelleted dry food (Trouvit, Nutreco) daily. In this study, the European common carp subspecies will be referred to as carp, unless stated otherwise. R3xR8 carp, which are the offspring of a cross between fish of Hungarian origin (R8 strain) and of Polish origin (R3 strain), were used (29).

Nine-month-old carp were infected with the parasite *Trypanoplasma borreli* (30) as previously described (28). Fish were killed by an overdose of anaesthetic 4 weeks post-infection at parasitemia of 1 x 10^7 parasites/ml. Spleen was collected, immediately snap-frozen in liquid nitrogen and stored at -80°C for histological analysis.

Identification of carp T cell-related cDNA sequences: CD3ε, ZAP-70 and Lck

To identify carp CD3ε, first a degenerate reverse primer (CD3εRV4; see Table 1) was designed in the conserved region spanning the transmembrane and cytoplasmic region of known fish (*Paralichthys olivaceus*: AB044572, AB044573; *Takifugu rubripes*: AB166798, AB166799; *Acipenser ruthenus*: AJ242941) CD3ε sequences. To obtain the carp CD3ε 5'-end, an anchored-PCR using CD3εRV4 in combination with λgt10FW was performed on cDNA from a λgt10 library of carp thymus from 5-month-old individuals (31). The library (300 ng) was combined with 1 IU *Taq* polymerase (Goldstar, Eurogentec), $MgCl_2$ (1.5 mM), dNTPs (200 μM), primers (400 nM each), 5 μl 10x Buffer and water up to a final volume of 50 μl. The PCR was performed using a GeneAmp PCR system 9700 (PE Applied Biosystems) under the following conditions: 4 min at 94ºC, followed by 35 cycles of 30s at 94ºC, 30s at 50ºC and 2 min at 72ºC, finally an extension step of 7 min at 72ºC was performed. The reaction gave a PCR product of 287 bp including the start codon and the 5' untranslated region (UTR) and was used to design the specific primer cycaCD3εFW3. Under similar PCR conditions, cycaCD3εFW3 was used in combination with λgt10RV to extend the 3'-end of the sequence. The

obtained PCR product of 300 bp included the stop codon and the 3' UTR. The full-length coding sequence of 549 bp was confirmed using the specific primers cycaCD3εFW0 and cycaCD3εRV0.

To identify carp ZAP-70, first a forward and reverse primer were designed based on a known zebrafish sequence (NP_001018425) in areas showing the highest percentage of identity to human and mouse ZAP-70. RNA (1 μg) from whole thymus was used as template in a Reverse Transcriptase-PCR (RT-PCR) using the primers ZAP70FW1 in combination with ZAP70RV1 (Table 1). RT-PCR was performed using the SuperScript™ One-Step RT-PCR with Platinum® Taq kit (Invitrogen). Total RNA (722.1 ng/μl) was combined with 2x Reaction Mix, RNaseOUT™ (40 U/μl) (Invitrogen) primers (400 nM each) and water up to a final volume of 30 μl. The PCR was performed under the following conditions: 30 min at 50°C and 2 min at 95°C, followed by 25-45 cycles of 30 s at 94°C, 30 s at 50-55°C and 1-2 min at 72°C, finally an extension step of 7 min at 72°C was performed. Products were purified and 5 µl was used as template for a second PCR using nested primers ZAP70FW2 and ZAP70RV2. The obtained product showed the expected size of 634 bp.

To identify carp Lck, a forward and reverse primer were designed based on a known zebrafish sequence (NM_001001596) in areas showing the highest percentage of identity to human and mouse Lck. RNA (1 μg) from whole thymus was used as template in an RT-PCR using the primers LckFW3 in combination with LckRV1 (Table 1). The obtained product showed the expected size of 830 bp.

All amplified products were ligated into pGEM-Teasy vector and cloned in JM109 competent cells using the pGEM-T Easy kit (Promega) according to standard protocols. Positive clones were selected by blue-white colony screening on agar plates containing 50 μg/ml Ampicillin. At least 8 clones for each PCR product were selected for subsequent colony-PCR using T7 and SP6 plasmid-specific primers. A standard PCR program was performed, using the GoldStar® DNA polymerase. From each PCR product both strands were sequenced using the ABI Prism Big Dye Terminator Cycle Sequencing Ready Reaction kit (Applied Biosystems) and analysed using a 3730 DNA analyser. Nucleotide sequences were translated using the ExPASy translate tool (http://us.expasy.org/tools/dna.html) and aligned with Clustal W (http://www.ebi.ac.uk/clustalw) and BLAST software (http://www.ncbi.nlm.nih.gov/BLAST).

RNA isolation and cDNA synthesis

Total RNA was isolated from carp thymus or carp peripheral blood leukocytes (PBL), using the RNAeasy Mini Kit according to the manufacturer's (Qiagen) instructions, including on-column DNase treatment with the RNase-free DNase set and stored at -80°C until use. Prior to cDNA synthesis, to 0.25-1 μg total RNA, a second DNase treatment was performed using DNase I, Amplification Grade (Invitrogen). Synthesis of cDNA was

performed using random primers (300 ng) and Superscript™ III First Strand Synthesis Systems for RT-PCR (Invitrogen). A non-reverse transcriptase control was included for each sample. cDNA samples were further diluted 1:5 in nuclease-free water prior to RT-qPCR analysis.

Table 1 Primers used for identification of carp CD3ε, ZAP-70 and Lck cDNA

Primer	primers (5'→3')
λgt10.FW	TTGAGCAAGTTCAGCCTGGTTAAG
λgt10.RV	GGCTTATGAGTATTTCTTCCAGGG
CD3εRV4	VAHGCAGTTYTCACACACTTT
cycaCD3εFW3	AGCACACCTTCTACCTCAAA
cycaCD3εFW0	TTCAGGACGTTACACCATG
cycaCD3εRV0	AACAGCATCTATTTATTG
ZAP70FW1	CTCGGGACCTCCATCAT
ZAP70RV1	ACTGTTGTCATTCTATCCTGTC
ZAP70FW2	CGAGAGAGAGATGAAATGG
ZAP70RV2	GGTAGAGATGGGCATGAA
LckFW3	CCAAAAACCCTGGTGGCA
LckRV1	TGCTCCTGGTACTGTCCCTCTGT

Gene expression analysis by real-time quantitative PCR (RT-qPCR)

RT-qPCR using SYBR Green I technology was performed with Rotor-Gene™ 6000 (Corbett Research) and the Brilliant® SYBR® Green QPCR (Stratagene) as detection chemistry as described previously (24). Primers used for RT-qPCR are listed in Table 2. Fluorescence data from RT-qPCR experiments were analyzed using Rotor-Gene version 6.0.21 software and exported to Microsoft Excel. The

cycle threshold C_t for each sample and the reaction efficiencies (E) for each primer set were obtained upon Comparative Quantitation Analysis from the Rotor-Gene version 6.0.21 software. The relative expression ratio (R) of a target gene was calculated relative to the S11 protein of the 40S subunit as reference gene (32, 33).

Primary antibodies

Monoclonal mouse antibody WCI12 binds to the heavy chain of IgM on carp B cells (34, 35). Monoclonal mouse antibody TCL-BE8 binds to carp neutrophilic granulocytes (strong affinity), monocytes (low affinity) (36), and basophilic granulocytes (intermediate affinity; unpublished results). Monoclonal mouse antibody WCL15 strongly reacts with the cytoplasm of carp monocytes and macrophages in tissue sections (37, 38). On live cells WCL15 stains the surface of carp monocytes and macrophages and shows a weak cross-reactivity to thrombocytes (39). Monoclonal mouse antibody WCL6 recognizes a 90 kDa membrane molecule on carp thrombocytes (40). Monoclonal rabbit antibody anti-hZAP-70 recognizes human ZAP-70 and was purchased from Cell Signaling technology (Cat No: 99F2).

Affinity-purified polyclonal rabbit antibody anti-hCD3ε was purchased from Dako (Cat No

Table 2 Primers used for Real-Time quantitative PCR

Primer	FW primers (5'→3')	RV primers (5'→3')	Acc. no.
q40S	CCGTGGGTGACATCGTTACA	TCAGGACATTGAACCTCACTGTCT	AB012087
qCD3ε	TGAGTTGAGCGGTTTGACTG	TGGCAGCACAGAAGTAGATGA	-
qZAP70	GGAACAAGCCATCATTAGCC	GTCGTCTCTCACCCTCCTG	-
qLck	CAAGTGGACGGCACCTGA	GCAATCACCTCTGGGTTTGT	-

A0452). Polyclonal rabbit antibodies anti-carp CD4 (cCD4) and cCD8α were produced against synthetic peptides coupled to keyhole limpet hemocyanin (KLH), according to a 3-months standard protocol (Eurogentec). Affinity purification of rabbit IgG was performed against purified peptides and specificity assessed by ELISA (Eurogentec). For cCD4, amino acids 254-268 (PQGADNKVKAEKRE) were chosen for immunization. For cCD8α amino acids 79-93 (GKVSLAIQSFNKKTD), positioned in a region conserved between carp CD8α1 and CD8α2, were chosen for immunization. Both peptides were chosen in the extracellular region of the respective protein.

Purification of carp leukocyte subtypes

Fish were killed by an overdose of anaesthetic (0.3 g/l Tricaine Methane Sulfonate (TMS), Crescent Research Chemicals) in aquarium water buffered with 0.6 g/l sodium bicarbonate. Blood was collected by puncture of the caudal vein and immediately diluted 1:1 with carp RPMI (cRPMI-1640 (Gibco) adjusted to 280 mOsmol kg^{-1}) containing 50 IU of heparin (Leo Pharmaceutical products). Total peripheral blood leukocytes (PBL) were isolated by centrifugation on Ficoll-Paque™ Plus (Amersham Biosciences) as previously described (24). Thymus and head kidney were aseptically removed and a single cell suspension was obtained by forcing the tissue through a 100 µm nylon mesh. Total cell suspensions from thymus were layered on a 1.02, 1.06, 1.0838 g/ml discontinuous Percoll density gradient (Amersham Pharmacia

Biotech. AB) and cells at the interface between the 1.0838-1.06 g/ml gradient layers were collected and washed twice in cRPMI. Total cell suspensions from head kidney were layered on a 1.02, 1.06, 1.07, 1.0838 g/ml discontinuous Percoll density gradient and cells at the interface of each layer were collected, washed twice and used as primary source for a second purification step using Magnetic Activated Cell Sorting (MACS) of B cells (1.02-1.06 g/ml), macrophages (1.06-1.07 g/ml) and granulocytes (1.07-1.838 g/ml).

For MACS, cells (1 x 10^7/ml) were incubated for 30 min on ice with the primary antibodies WCI12, WCL15 or TCL-BE8 to specifically label B cells, macrophages and granulocytes, respectively. Cells were washed twice with MACS-buffer (0.5% BSA in cRPMI) and subsequently incubated for 30 min on ice with a 1:50 dilution of Phycoerythrin (PE)-conjugated goat-anti-mouse (GAM-PE) secondary antibody (Dako). Cells were extensively washed and incubated for 15 min at 4ºC with 10 µl/10^8 cells magnetic beads (anti-PE Microbeads, Miltenyi Biotec). Cells were washed, resuspended in MACS buffer and sorted on LS-MidiMACS Columns according to the manufacturer's instructions. Purity of the different carp leukocyte subtypes was assessed by flow cytometric analysis (Beckman Coulter, Epics XL-MCL, Miami, FL, USA).

Human Jurkat T cell line

For some experiments, the human Jurkat T cell line (ATCC: TIB-152), was used as positive control. Cells were cultured in RPMI-1640 supplemented with 25 mM HEPES, 10%

(v/v) Fetal Bovine Serum (FBS), L-Glutamin (2 mM), Penicillin-G (100 IU/ml) and Streptomycin sulphate (50 mg/l), and maintained at a cell density of 1-1.5 x 10^6 cells/ml.

Western blot

Carp thymocytes and magnetically-sorted B cells, macrophages and granulocytes were isolated as described above. Total cell lysates from carp leukocytes or human Jurkat cells were obtained by resuspending cell pellets in lysis buffer (20 μM Tris-Cl, pH 7.2, 100 μM NaCl, 1 μM EDTA, 0.5% (v/v) Triton X-100, 1 μM PMSF) at a concentration of 10 µl/ 2 x 10^6 cells. Lysates were homogenized on ice by 6-7 passages through a 22 gauge needle and subsequently incubated on ice for 15 min in lysis buffer to ensure complete lysis. Lysates were centrifuged at max speed (21000 x *g*) for 10 minutes at 4°C to pellet nuclei. Supernatants were carefully collected and protein concentration measured spectrophotometrically (NanoDrop® ND-1000, Labtech International Ltd.) at OD_{280nm}. Total cell lysates (10 µg) were resolved on a 10% SDS-PAGE and proteins transferred to nitrocellulose membranes (Protrans, Schleicher & Schuell, Bioscience GmbH). Membranes were incubated overnight at 4°C with a 1:1000 dilution of anti-hZAP-70 antibody with gentile agitation. Horseradish peroxidase (HRP)-conjugated goat-anti-rabbit antibody (1:2000; GAR-HRP, Dako) was used as secondary antibody. Proteins were visualized by chemiluminescence detection (Amersham, ECL detection system for Western blot) on X-ray films.

Flow cytometry

Carp PBL or carp thymocytes were adjusted to a concentration of 1 x 10^7 cells/ml in MACS-buffer. Cell suspensions (100 µl) were incubated on ice for 30 min with WCI12 (1:50), WCL15 (1:50), TCL-BE8 (1:50) or WCL6 (1:100). After washing, cells were incubated for 30 min on ice with a 1:50 dilution of GAM-PE as secondary antibody. For intracellular staining of ZAP-70 or CD3ε, cells were first permeabilized by incubation for 15 min on ice in Cytofix/Cytoperm buffer (BD Bioscience). After a washing step with 1x Perm/Wash buffer (BD Bioscience), cells were resuspended in the same buffer and incubated for 30 min on ice with anti-hZAP-70 or anti-hCD3ε (1:20). After washing, cells were incubated for 30 min on ice with fluorescein isothiocyanate (FITC)-conjugated swine-anti-rabbit antibody (1:20; SWAR-FITC, Dako) as secondary antibody. For double-staining, first the procedure for extracellular staining was performed, followed by permeabilization and intracellular staining. After extensive washing, fluorescence intensities of 10^4 events were acquired in log scale using a Beckman Coulter Epics XL-MCL flow cytometer.

Laser scanning microscopy

Cell surface and intracellular staining was performed as described above. After washing, cells were centrifuged for 5 min at 100 x *g* on poly-*L*-lysine coated glass slides (BDH Laboratory supplies) and subsequently fixed for 7 min in ice-cold 4% (w/v) paraformaldehyde in 100% ethanol solution. Slides were embedded in Vecta-Shield Mounting medium

(Vector laboratories) and cell fluorescence examined with a laser scanning microscope (LSM 510, Carl Zeiss, Germany). A FITC signal was excited with a 488 nm argon laser and detected using a band-pass filter (505-530 nm), whereas a PE signal was excited with a 543 nm helium-neon laser and detected using a long-pass filter (585 nm).

Immunohistochemistry

Cryosections (4-7 μm) of spleen tissue were mounted on poly-*L*-lysine-coated glass slides, air-dried for 30-60 min and incubated in a 0.3% H_2O_2 solution in methanol for 20 min to inactivate endogenous peroxidase. Following steps were performed at room temperature (rT) unless stated otherwise. Sections were washed for 5 min with PBS, then with distilled water and incubated for 10 min at 37°C in proteinase-K (Promega) solution (50 µg/ml in distilled water). Samples were fixed for 5 min at 4°C in 4% (w/v) paraformaldehyde followed by washing first for 10 min at 4°C and then for 7 min at rT in PBS-Triton (PBS-T, 150 mM NaCl, 2 mM KCl, 20 mM Na_2HPO_4, 2 mM KH_2PO_4, 0.1% (v/v) Triton X-100). A blocking solution of 5% normal goat serum (Dako) was then added and slides were incubated for 30 min. Primary antibodies WCI12 (1:50), anti-hCD3ε (1:50), anti-hZAP-70 (1:50), anti-cCD4 (1:10) or anti-cCD8α (1:10) were diluted in PBS-T and slides were incubated for 1h. After washing twice for 10 min in PBS-T, sections were incubated for 1h with GAR-HRP or GAM-AP (1:200 in PBS) as secondary antibody. For single-staining with GAR-HRP antibodies, sections were incubated for 10 min

in 0.05 M sodium acetate buffer, pH 5 and following addition of 0.4 mg/ml 3-amino-9-ethyl-carbazole (AEC; Sigma-Aldrich) for 25 min in 0.03% H_2O_2 in sodium acetate buffer. Rinsed sections (4x in distilled water) were embedded in Kaiser's glycerin gelatin (Merck). For single-staining with GAM-AP, sections were incubated for 10 min in AP-buffer (0.1 M Tris-Cl, 0.1 M NaCl, 0.05 M $MgCl_2$, pH 9.5) and then stained using AP-substrate (4.5 µl/ml nitro-blue-tetrazoleum and 3.5 µl/ml 5'-bromo-4'-chloro-3'-indolyl phosphatase [BCIP] all from Roche Applied Science) diluted in AP-buffer for 2-5 min. Rinsed sections (4x in distilled water) were embedded in Aquatext (Merk). For double-staining, sections were first stained for AP and then for AEC, rinsed in distilled water and embedded in Kaiser's glycerin gelatin. Sections treated identically but without the presence of the first antibody showed no staining.

Results

Carp CD3ε sequence analysis

Using a homology cloning approach a carp CD3ε cDNA sequence of 581 bp covering the complete full-length mRNA sequence was identified. The sequence encodes for a protein of 173 amino acids (Fig. 2) with a putative 20 aa leader peptide which upon cleavage would release a protein of about 17 kDa. Alignment of the translated carp sequence indicates 20-26% overall identity with other fish CD3ε sequences and 17-20% identity with mammalian CD3ε sequences. Particularly the transmembrane and cytoplasmatic regions showed a slightly higher degree of conservation with an overall identity

of 30-36%. Carp CD3ε presents an immunoglobulin (Ig) domain in the extracellular region and the cysteins required for the intrachain disulphide bond as well as the invariant tryptophan are appropriately located (see Fig. 2). The CXXCXE motif required for CD3ε heterodimerization present in the linker peptide following the Ig domain is conserved. The ITAM motif in the cytoplasmic region of carp CD3ε has an intervening sequence between two conserved tyrosine residues that is 10 instead of 7 amino acids long, resulting in an NXX-YXXL-(X)$_{10}$-YXXL ITAM sequence. No potential glycosylation sites were identified. A polyclonal rabbit antibody directed against the proline-rich sequence of the cytoplasmic region of human CD3ε (indicated by a box in the human sequence in Fig. 2) was used in this study based on the conservation of the corresponding region in the carp sequence.

```
                       Leader peptide                              Ig domain
Carp        ----MLLLSVMLVLLAAAVNPAQGQVIK-----------EIKEDSVILDCEA-EDATVKWFKDKTEDKEQTKTT----- 58
Pufferfish  MIVRALLCFAVLFLVAGQEEGQEQEQDKPG--------GVIFWETFVTMTCPR----DGKWFKDKKEVSE--GPA----- 61
Salmon      -MNRDGVYGGLVFLLLIMTS-----VEGGG--------DVSFWRTTVTLTCPD----KGDWYDNTIKMNEEESKE----- 57
Chicken     --MRCEVPLPLLGLLLCVVGAAAQGGQE--------EFAVEISGTTVTITCPS-SGDDIKWKP-DPALG--DNNK----- 61
Mouse       --MRWNTFWGILCLSLLAVGTCQDDAEN-------IEYKVSISGTSVELTCPLDSDENLKWEKNGQELP-QKHDK----- 65
Human       --MQSGTHWRVLGLCLLSVGVWGQDGNEEMGGITQTPYKVSISGTTVILTCPQYPGSEILWQHNDKNIGGDEDDKNIGSD 78
                      ::  *                            :      *  *  :  *                  *

                Ig domain                                Transmembrane region
Carp        ----FEAKAKQGVVEGVFTCEFSKTET-IQIKHTFYLKIKVCENCYELSG-LTGWGMFGDVLITGGVIIIIYFCAARNSD 132
Pufferfish  -----YAFEYD-NKKGRYHCTYDNSRYD------FYVQGKVCENCFELDGGFWGMIIAADMFLTVVVMVMVYKCAKKRSS 129
Salmon      ----IKMDYDESKKNVYQCKYLYDQYDTEKTTYQFYFKGKVCKDCYELNPTVVAGAIIGDLLVTGGVILIVYLRARKKSG 133
Chicken     ----YIIQNH--DSSPLTVSCTAGD------QEHTMYLNAKVCANCEELDTFTVVGIIAADLLITLGVLILVYYFSKNKKG 130
Mouse       --HLVLQDFSEVEDSGYYVCYTPAS----NKNTYLYLKARVCEYCVEVDLTAVAIIIIVDICITLGLLMVIYYWSKNRKA 139
Human       EDHLSLKEFSELEQSGYYVCYPRGSKP-EDANFYLYLRARVCENCMEMDVMSVATIVIVDICITGGLLLLVYYWSKNRKA 157
                            :*..  :**   * *:.            :   *:  :* :::::*  :   ...

                                ITAM motif
Carp        GPPK--------KASNPRSVNPPRPPNPDYAALDPKMRSGNALYAGLNK------ 173
Pufferfish  AALP-------RVP---KAGGRAPPLPSPDYEPLNPHTRS-QGTYSEVHP--KRMG 172
Salmon      PAAP-------QKPTSRSAGRGPPVVPSPDYEPLSVATRS-SDIYATTQTSTQRTG 181
Chicken     QSR-----AAAGSRPRAQKMQRPPPVPNPDYEPIRKGQR---DVYAGLEH--RGF- 175
Mouse       KAKPVTRGTGAGSRPRGQNKERPPPVPNPDYEPIRKGQR---DLYSGLNQ--RAV- 189
Human       KAKPVTRGAGAGGRQRGQNKERPPPVPNPDYEPIRKGQR---DLYSGLNQ--RRI- 207
                     .    .*  *.*** .:     *        *:  .
```

Figure 2. **Clustal W alignment of carp CD3ε with selected CD3ε proteins.** Regions corresponding to the putative leader peptide, Ig domain, transmembrane region and cytoplasmatic region including an ITAM motif are marked above the sequence alignment. Symbol (*) indicates identities and symbol (:) or (.) denotes similarities. Dashes indicate gaps used to maximize the alignment. Conserved cystein (C) and tryptophan (W) residues important for the folding of the Ig domain are shaded in grey; conserved tyrosines (Y) within the ITAM motif are also shaded in grey. The conserved CXXCXE motif possibly involved in CD3ε heterodimerization is indicated by a box. In the cytoplasmic region, the sequence of the peptide used for immunization and affinity purification of the anti-human CD3ε (Dako) used in the present study, is indicated by a box in the human sequence. GenBank accession nos: pufferfish (*Takifugu rubripes* **AB166799**) Atlantic salmon (*Salmo salar*, **ABO10202**); chicken (*Gallus gallus*, **NP_996787**); mouse (*Mus musculus*, **NM_007648**); human (*Homo sapiens*, **P07766**).

CHAPTER 8

137

Carp ZAP-70 sequence analysis

Using a homology cloning approach a partial carp ZAP-70 cDNA sequence of 606 bp spanning the N-terminal region of the protein (Fig. 3) was identified. The sequence encodes for a peptide of 183 amino acids containing almost the complete N-terminal Sh2-1 domain followed by a partial Sh2-2 domain. Based on the zebrafish ZAP-70 protein sequence, approximately 30 amino acids at the N-terminal

and 380 at the C-terminal still need to be identified of the carp sequence. Alignment of the translated carp sequence revealed a high identity (72%) to the human ZAP-70 and a very high identity of 90% to the zebrafish ZAP-70 sequence. Considering the overall sequence conservation of ZAP-70, in the present study we use an anti-hZAP-70 antibody directed against the N-terminal domain of the protein.

```
                                            Sh2-1 domain
                          _____
Carp       LFLLRQCLRSLGGYVLSLVWNLEFYHYSIEKQLNGTYCIAGGKPHCGPAELCEYYSKDPDGLMCTLRKPC 70
Zebrafish  LFLLRQCLRSLGGYVLSMIWNLDFYHYSIEKQLNGTYCIAGGKPHCGPAELCEYYSKDPDGLVCTLRKPC 103
Human      LFLLRQCLRSLGGYVLSLVHDVRFHHFPIERQLNGTYAIAGGKAHCGPAELCEFYSRDPDGLPCNLRKPC 103
           ****************::  ::  *:*:.**:*****.***** .********:**:***** *.*****

Carp       LRSADTQIKTGVFDSLRDNMLREYVRQTWHLEGEAMEQAIISQAPQLEKLIATTAHEKMPWFHGKIPRQE 140
Zebrafish  LRSPETEIRKGVFDNLRDNMLREYVRHTWKLEGDAMEQAIISQAPQLEKLIATTAHEKMPWFHGKIPRQE 172
Human      NRPSGLEPQPGVFDCLRDAMVRDYVRQTWKLEGEALEQAIISQAPQVEKLIATTAHERMPWYHSSLTREE 172
           *..  :  : **** *** *:*:***:**:.***:*:********** :********** :***:*..:.*:*:*
                                            Sh2-2 domain
                          _____
Carp       GERRLYSGSQPDGKFLVREREEFGTFALSLTYGKTVYHYQILHDK- 185
Zebrafish  GERRLYSGSQPDGKFLVRERDEMGTFALSVTYGKTVYHYQILRDKS 217
Human      AERKLYSGAQTDGKFLLRPRKEQGTYALSLIYGKTVYHYLISQDKA 217
           .**:****:*.*****:* *.* **:***: ******** * :**
```

Figure 3. **Clustal W alignment of carp ZAP-70 with zebrafish and human ZAP-70 proteins.** The partial sequence identified for carp ZAP-70 encodes for almost the entire N terminal region. The Src Homology-1 (Sh1) domain and part of the central Sh2 domain identified in this region are marked above the sequence alignment. GenBank accession nos: zebrafish (*Danio rerio*, **NP_001018425**); human (*Homo sapiens*, **NP_001070**). Numbers in the human and zebrafish sequence indicate the amino acids' position relative to the full-length molecule.

Carp Lck sequence analysis

Using a homology cloning approach a partial carp Lck cDNA sequence of 772 bp spanning the central region of the protein (Fig. 4) was identified. The sequence encodes for a peptide of 248 amino acids spanning almost completely the central protein tyrosine kinase catalytic (PTKc) domain. Tyrosine 394, important for Lck activation in the mammalian protein, is appropriately located in the carp sequence. Based on the known fish Lck protein sequence, approximately 225 amino acids at the N-terminal and 24 at the C-terminal still need to be identified of the carp sequence. Alignment

of the translated carp sequence indicates a high identity to the human (80%) and zebrafish (90%) Lck and very high sequence identity (96%) to Ginbuna crucian carp Lck. An affinity purified polyclonal rabbit antibody directed against the C terminal region of hLck was tested in the present study. Although in Western blot, the antibody recognizes a protein of the expected molecular weight, the reaction was much weaker than the reaction obtained with the anti-hZAP-70 antibody, therefore the anti-Lck antibody was not considered for further use.

Protein Tyrosine Kinase catalytic domain

```
Carp       QKPWWQDEWEVPRESLKLERRLGQGQFGEVVMGLYNNNRRVAIKNLKTGTMPISAFLAEANLMKTLQHPR 70
G.C.Carp   QKPWWQDEWEVPRESLKLERRLGQGQFGEVVMGLYNNNRRVAIKSLKTGTMSISAFLAEANLMKALQHPR 299
Zebrafish  QKPWWQDEWEVPRESLKLERRLGQGQFGEVVMGLYNNNRQVAIKSLKPGTMSISAFLAEANLMKSLQHPR 299
Human      QKPWWEDEWEVPRETLKLVERLGAGQFGEVVMGYYNGHTKVAVKSLKQGSMSPDAFLAEANLMKQLQHQR 299
           *****:*********:*** .*** ********* **.: :**:*.** *:*. .********** *** *

Carp       LVRLFAVVTQEPIYIITEYMENGSLVDFLKTPEGCAMPINTLIDMAAQVADGMAYIEQKNYIHRDLRAAN 140
G.C.Carp   LVRLFAVVTQEPIYIITEYMENGSLVDFLKTPEGCAIPINTLIDMAAQVADGMAYIEQKNYIHRDLRAAN 369
Zebrafish  LVRLFAVVTQEPIYIITEYMENGSLVDFLKTPEGSDIPINTLIDMAAQVAEGMAYVEQKNYIHRDLRAAN 369
Human      LVRLYAVVTQEPIYIITEYMENGSLVDFLKTPSGIKLTINKLLDMAAQIAEGMAFIEERNYIHRDLRAAN 369
           ****.:**********************.*   :.:**.*:*****:*:***::*:.***********
                                      394
Carp       ILVSDELICKIADFGLARLIENNE Y TAKEGAKFPIKWTAPEAINYGTFSIKSDVWSFGVLLTEIVTYGRI 210
G.C.Carp   ILVSDELICKIADFGLARLIENNE Y TAREGAKFPIKWTAPEAINYGTFSIKSDVWSFGVLLTEIVTYGRI 439
Zebrafish  ILVSHELTCKIADFGLARLIKNNE Y TAREGAKFPIKWTAPEAINYGTFSIKSDVWSFGVLLTEIVTYGRI 439
Human      ILVSDTLSCKIADFGLARLIEDNE Y TAREGAKFPIKWTAPEAINYGTFTIKSDVWSFGILLTEIVTHGRI 439
           ****. * *************:.:*****.*****************:********:*******:***

Carp       PYPGMTNPEVIANLERGYRMPCPDNCPEDLYDIMKHCW 248
G.C.Carp   PYPGMTNPEVIANLERGYRMPCPDNCPEDLYDIMKHCW 477
Zebrafish  PYPGMTNPEVIANLERGYRMPCPDNCPEALYNVMKHCW 477
Human      PYPGMTNPEVIQNLERGYRMVRPDNCPEELYQLMRLCW 477
           *********** ******** ****** **::*: **
```

Figure 4. **Clustal W alignment of carp Lck with selected fish and human Lck proteins.** The partial sequence identified for carp Lck encodes for almost the entire central Protein Tyrosine Kinase catalytic domain. Conservation of one of the activatory tyrosines (Y394) is indicated by a box. GenBank accession nos: Ginbuna crucian carp (*Carassius auratus langsdorfii*, **BAF56886**); zebrafish (*Danio rerio*, **NP_001001596**); human (*Homo sapiens*, **NP_001036236**). Numbers in the human zebrafish and Ginbuna crucian carp sequence indicate the amino acids' position relative to the full-length molecule.

CD3ε, ZAP-70 and Lck are highly expressed in carp thymocytes

To confirm the specificity of the newly identified CD3ε, ZAP-70 and Lck sequences to the carp T-cell-lineage, gene expression analysis was performed on purified thymocytes and sorted B lymphocytes, granulocytes and macrophages (Fig. 5) isolated from nine-month old carp. Magnetic sorting resulted in B cell and granulocyte populations of >90% purity and macrophage populations of 84% purity. No significant gene expression of CD3ε, ZAP-70 and Lck was observed in B cells or granulocytes whereas a low basal gene expression could be detected in macrophages, possibly owing to the presence of low numbers of contaminating T lymphocytes. Clearly, the highest gene expression for CD3ε, ZAP-70 and Lck was observed in thymocytes.
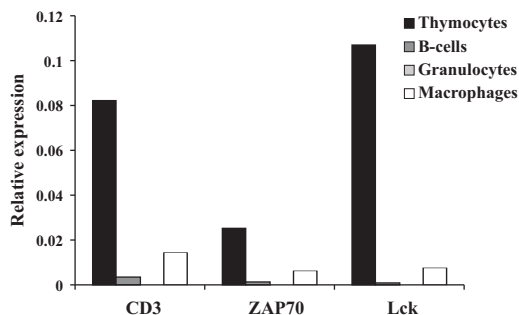
Figure 5. **Real-time quantitative PCR analysis of CD3ε, ZAP-70 and Lck in carp leukocytes.** Total thymocytes and MACS-sorted B cells, granulocytes and macrophages were purified as described in the material and methods. Gene expression was normalized relative to the S11 protein of the 40S subunit as a reference gene. Shown are the values of one experiment representative of three independent experiments.

Detection of cells from the T-cell lineage in the thymus of carp

In the present study, we used an antibody recognizing the proline-rich part of the cytoplasmic region of human CD3ε and an antibody recognizing the N-terminal region of the human ZAP-70 protein, to detect cells from the T-cell-lineage in carp. We based the use of these anti-human T-cell markers on the conservation of the relevant regions in the carp CD3ε and ZAP-70 protein sequences. We also produced and affinity purified polyclonal rabbit antibodies raised against selected peptides of the carp CD4 and CD8α protein sequence.

Immunohistochemical analysis of carp thymus showed a similar distribution of immunoreactivity for all tested antibodies (Fig. 6A). As indicated by the intensity of the staining, the highest density of CD3ε+, ZAP-70+, CD4+ and CD8α+ cells was observed in the cortical area. A clear demarcation between cortex and medulla could be observed, particularly after staining with the anti-CD8α antibody (Fig. 6A, lower-panel). Staining with anti-cCD4 revealed the presence of intensely stained groups of cells in the medullar region. The observed staining is in accordance with the general distribution of thymocytes described in mammals where immature (CD3ε+/ZAP-70+/CD4+/CD8+) T cells are found in the cortical region whereas mature (CD3ε+/ZAP-70+/CD4+ or CD3ε+/ZAP-70+/CD8+) T cells are found in the medulla before leaving the thymus (41).

Flow cytometric analysis of carp thymocytes using anti-hCD3ε and anti-hZAP-70 positively identified 80-90% of the total number of cells (Fig 6B), confirming the specificity of these two antibodies as markers for the T-cell-lineage in carp. In contrast, despite the reactivity of the anti-cCD4 and anti-cCD8α antibody in immunohistochemistry, these antibodies did not produce reliable staining patterns in flow cytometry. Our results identify the anti-hCD3ε and anti-hZAP-70 antibodies as reliable tools for the specific identification of cells belonging to the T-cell-lineage in carp, both in immunohistochemical applications on frozen tissue sections as well as flow cytometric applications on live cells. To confirm that the anti-hCD3ε and the anti-hZAP-70 (both raised in rabbits) unequivocally identify the same cell type, double staining using conjugated antibodies is planned.
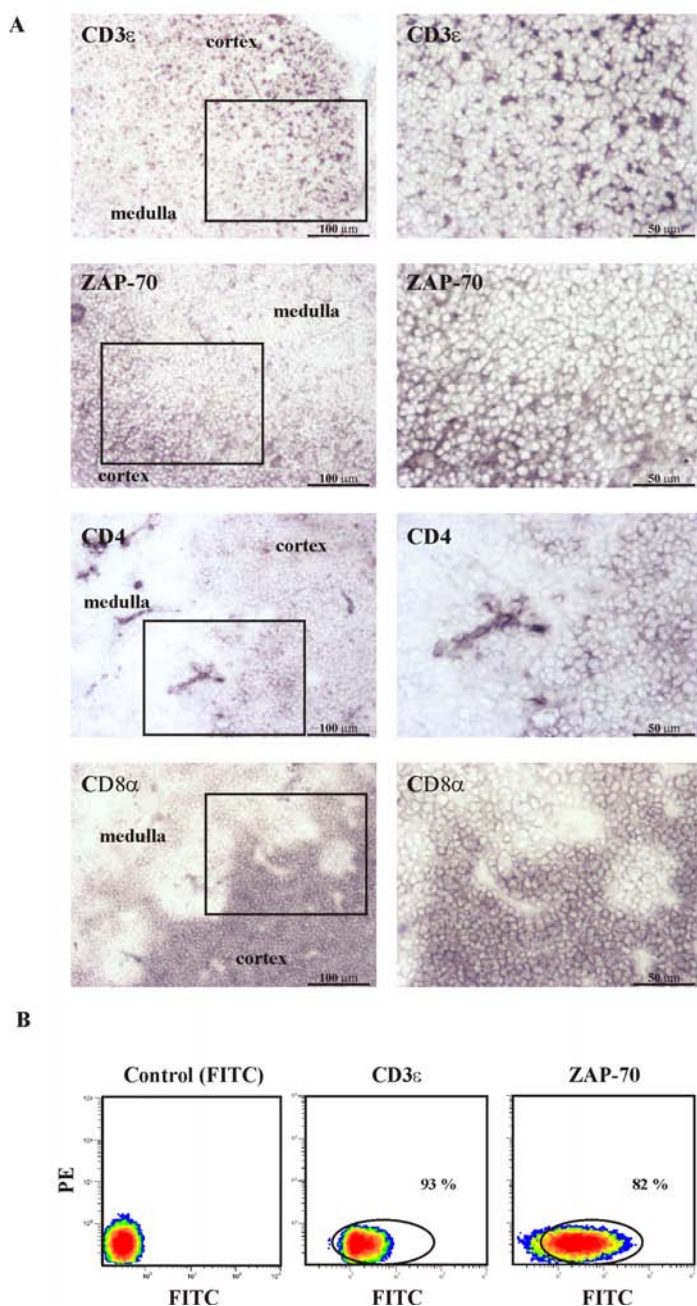
Figure 6. Identification of cells from the T-cell-lineage in carp thymus using anti-hCD3ε, anti-hZAP-70, anti-cCD8α and anti-cCD4 antibodies.
A) Immunohistochemistry. Cryosections of carp thymus stained with anti-hCD3ε, anti-hZAP-70, anti-cCD4 or anti-cCD8α antibodies are shown. On the left are low magnification images where the cortex and medulla are indicated and on the right are enlargements of the area indicated by the box. B) Flow cytometry. Density plots of total thymocytes, permeabilized and stained with anti-hCD3ε and anti-hZAP-70 using SWAR-FITC as secondary antibody. As a negative control, incubation with only the SWAR-FITC secondary antibody is shown on the left. Analysis revealed that both primary antibodies recognize 80-90% of carp thymocytes.

Detection of cells from the T-cell lineage in carp blood

Anti-hCD3ε and anti-hZAP-70 antibodies were used in combination with previously described antibodies that recognize carp B cells (WCI12), monocytes (WCL15), neutrophilic granulocytes (TCL-BE8) or thrombocytes (WCL6) to identify the relative percentage of PBL that belong to the T-cell-lineage.

Intracellular staining (CD3ε; ZAP-70) of carp PBL was performed along with cell surface staining (WCI12; WCL15; TCL-BE8; WCL6). Permeabilization for intracellular staining resulted in cross-reactivity of the anti-hCD3ε antibody with a subpopulation of B cells and some monocytes/macrophages (data not shown). In contrast, permeabilization for intracellular staining did not affect the specificity of the anti-hZAP-70 antibody and single-staining revealed the presence of about 5-15% ZAP-70+ cells in the blood of healthy carp (Fig. 7A, upper panel). Double staining confirmed the specificity of the ZAP-70 staining, revealing negligible cross-reactivity with other leukocyte cell types in the blood (Fig. 7A, lower panel).

Laser scanning microscopical analysis of carp PBL upon single- or double-staining with WCI12 (PE, red) and anti-hZAP-70 (FITC, green), confirmed the specificity of ZAP-70 to cells of the T-cell-lineage (Fig. 7B). As expected, staining with the anti-hZAP-70 antibody revealed intracellular staining of lymphocyte-like cells with a large nucleus and a thin rim of cytoplasm whereas staining with the anti-IgM antibody WCI12, revealed a typical surface staining with patches of IgM+ areas (42) on lymphocytes.

Western blot analysis using the anti-hZAP-70 antibody on total cell lysates of sorted leukocyte sub-populations confirmed the presence of a protein band with expected molecular weight of 70 kDa in carp thymocytes and human T cells, but not in other carp leukocyte cell types (Fig. 7C). All together, our results indicate the suitability of the anti-hZAP-70 antibody to serve as tool for immunohistochemical, flow cytometric and Western blot analysis of cells belonging to the T-cell-lineage in carp.
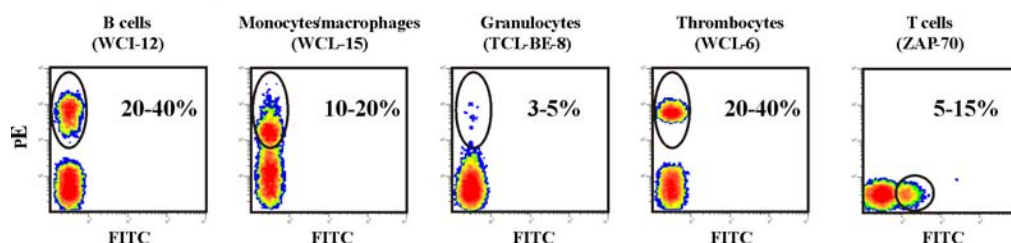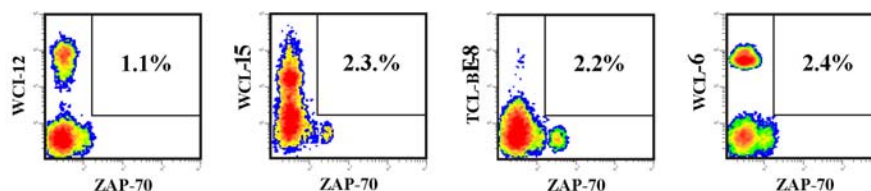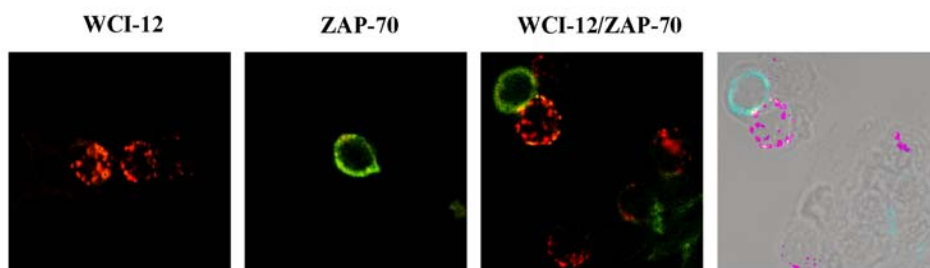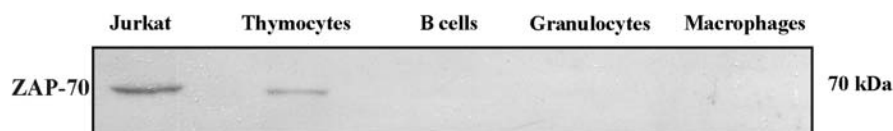
Figure 7.   **Identification of cells from the T-cell-lineage in carp using anti-hZAP-70 antibody.** A) Flow cytometry. Upper panel: cell surface staining for B cells (WCI12+), monocytes (WCL15+), granulocytes (TCL-BE-8+) and thrombocytes (WCL6+), using GAM-PE as secondary antibody, and intracellular staining for cells of the T-cell-lineage (ZAP-70+), using SWAR-FITC as secondary antibody. The range of positive cells (% of total PBL) in *n*=4 fish is indicated. Lower panel: cell surface staining followed by permeabilization and intracellular staining against ZAP-70. Percentage of double-positive cells is indicated. B) Laser scanning microscopy. Cytocentrifuge preparations of the cell populations shown in A), showing WCI12+ B cells and ZAP-70+ cells after single and double staining. Phase-contrast image is shown on the right. C) Western blot analysis. ZAP-70 protein expression in different carp leukocyte cell-types using anti-hZAP-70 antibody (1:1000) on total cell lysates (10 μg) from human Jurkat T cells, carp thymocytes, sorted B cells, granulocytes or macrophages, resolved on a 10% SDS-PAGE.

Distribution of T cells in spleen of *T. borreli*-infected carp

We have previously shown the presence of extremely enlarged B cell areas in spleen of carp heavily infected with *T. borreli* (28). The marked B cell proliferation may be explained by the polyclonal B cell activation typically associated with *T. borreli* infections (43). Owing to the lack of suitable T cell markers, the distribution and the involvement of T cells during the immune response of carp to *T. borreli* has not been investigated. We used the WCI12 antibody to specifically target carp B cells and both the anti-hCD3ε and anti-hZAP-70 antibodies to identify T cells in carp spleen during infection with *T. borreli* (Fig. 8).

In spleen from naïve, non-infected, carp only few and small B or T cell areas can be observed, particularly around small ellipsoids (Fig. 8A, left panel). During infection, not only enlarged B cell (WCI12+) but also enlarged T cell areas (CD3ε+ and ZAP-70+) can be observed in spleen (Fig. 8A, right panels). The location of B and T cell areas within the spleen overlapped in consecutive sections indicative of a co-localization of proliferating B cells and T cells during *T. borreli* infection.

Double-staining using WCI12 in combination with either anti-hCD3ε or anti-hZAP-70 confirmed specificity of the staining indicating the presence of intermingled single-positive WCI12 and single-positive CD3ε or ZAP-70 cells in the same area. In addition, the co-localization of B and T cell areas confirms the lack of a clear demarcation between B and T cell areas in the spleen of fish, particularly during an infection.

Discussion

The TCR complex consists of a single TCRαβ heterodimer associated with at least three CD3 dimers including γε, δε and ξξ and the CD4 or CD8 co-receptors. The protein tyrosine kinases Lck and ZAP-70 provide essential signals in the cascade of events which will finally lead to T cell signalling and activation. In the present study we report the cloning of a full-length mRNA sequence for carp CD3ε and partial mRNA sequences for carp Lck and ZAP-70. Only single transcripts were found for these newly described molecules. Duplicate copies for the constant region of carp TCRα (24, 44), CD8α and CD8β (24), but so far only a single copy for carp CD4 has been described (23). Two CD3ε isoforms have been reported for Japanese flounder (*Paralichthys olivaceus*) (20) and fugu (*Takifugu rubripes*) (45) and two isoforms of Lck have been reported for rainbow trout (*Oncorhynchus mykiss*) (46). Common carp is considered an allotetraploid species (47) and genes often occur in duplicated form in the genome. Thus, we expect that isoforms of several, if not all, molecules of the TCR complex could exist in duplicate copies in carp.
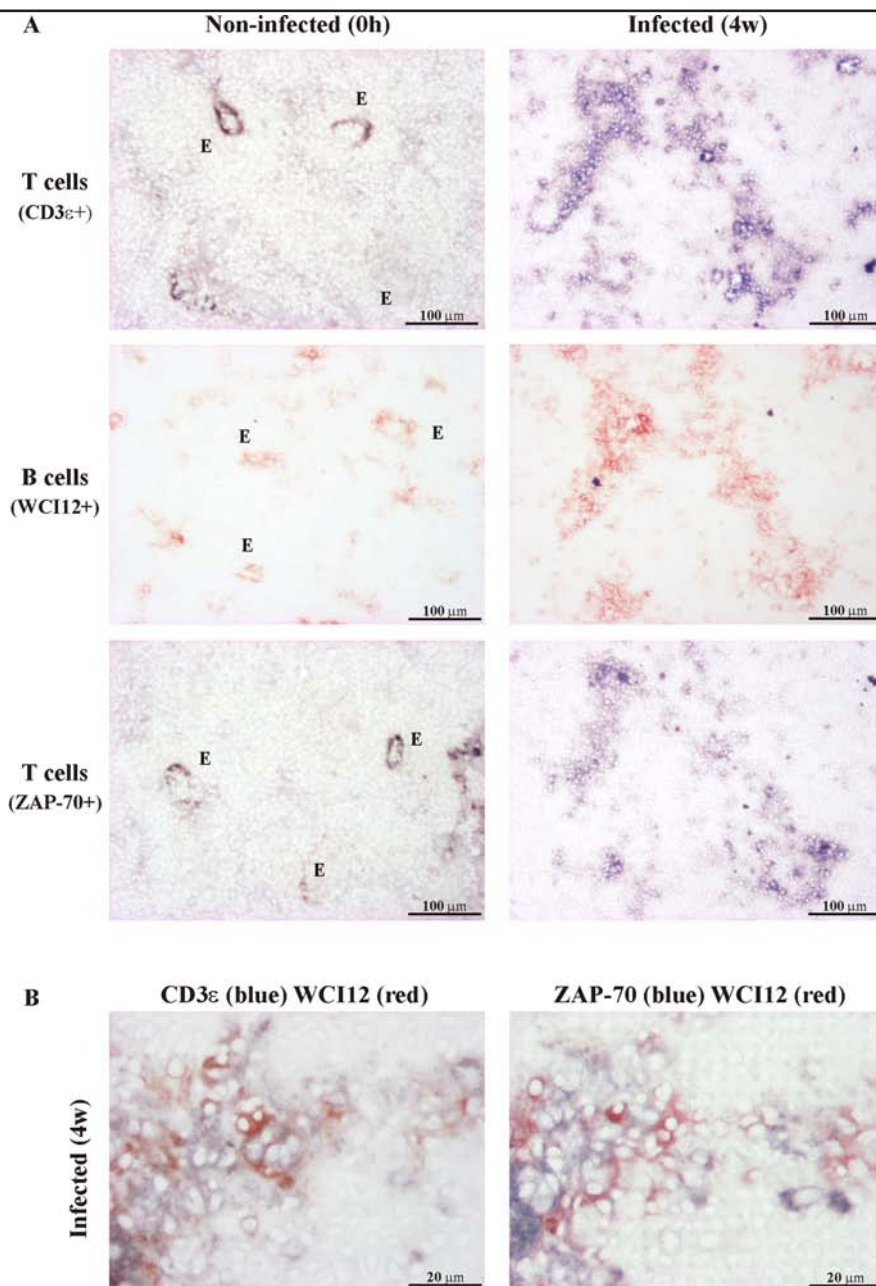
Figure 8. Distribution of B and T lymphocytes in spleen after infection with *T. borreli*. WCI12 antibody was used to specifically target carp B cells and both the anti-hCD3ε and anti-hZAP-70 antibodies were used to identify T cells in carp spleen. A) <u>Left panel</u>: cryosections (4-7 μm) of spleen from control fish stained with anti-hCD3ε, WCI12 or hZAP-70 antibodies revealing the presence of only few and small-sized B- (WCI12+, red) and T- (CD3ε+ and ZAP-70+, blue) cell areas. <u>Right panel</u>: consecutive sections from spleen of 4 weeks infected fish revealing the presence of co-localized enlarged B- and T-cell areas. B) Double-staining of consecutive sections from spleen of 4 weeks infected fish with WCI12 in combination with anti-hCD3e or anti-hZAP-70 antibody, revealing distinct B and T cells staining.

Despite the amount of genetic information on the TCR complex, the number of monoclonal antibodies (MAbs) available for the identification and functional characterization of T cells in fish is very limited. For example, MAbs that have been produced against recombinant rainbow trout TCRα and TCRβ were cross-reactive with other lymphocyte subpopulations and could not be used to specifically target T lymphocytes (2). Attempts to identify cross-reactive MAbs developed for use in mammalian immunology that would specifically recognize fish antigens also have been without much success. Of a panel of 213 antibodies directed against various human leukocyte surface antigens, none proved reliably cross-reactive to trout antigens (48). Another attempt with a panel of 377 MAbs directed against, among other, human CD antigens yielded only four MAbs that clearly reacted with trout PBL and two antibodies that reacted with carp PBL (4). The latter attempts emphasize the phylogenetic distance between warm- and cold-blooded vertebrates and confirm the generally low conservation of extracellular domains of cell surface molecules.

In the present study we selected two antibodies developed for use in mammalian immunology based not on the extracellular but on the intracellular epitopes recognized. The anti-hCD3ε antibody had previously been used also in other fish species (19, 21, 49) and in *Xenopus laevis* (22) whereas the anti-hZAP-70 antibody had not been considered before. In carp, the anti-hCD3ε antibody can reliably be used in immunohistochemical but not in flow cytometric assays where it was found to cross-react with a subpopulation of B cells and monocytes in the blood (not shown). In contrast, the anti-hZAP-70 specifically recognizes T lymphocytes in both immunohistochemistry and flow cytometry with negligible cross-reactivity. Western blot analysis confirmed recognition of a carp protein of expected molecular weight. Therefore, owing to the general high conservation of the fish ZAP-70s (zebrafish: NP_001018425; pufferfish: CAG00734) when compared to the mammalian homologues, the antibody used in this study will most likely be applicable to more fish species. A drawback concerning the use of this antibody, however, is the permeabilization step, which does not allow for immunopurification of live cells.

Upon TCR engagement, ZAP-70 is activated either by autophosphorylation or by phosphorylation by Lck (see Fig. 1). ZAP-70 phosphorylation, therefore, is one of the earliest signalling events and detection of phospho-ZAP-70 (pZAP-70) is commonly regarded a reliable marker for T cell activation (50). The combined use of anti-hZAP-70 and anti-pZAP-70 antibodies would not only allow for detection of changes in the distribution of T cells throughout the organism but also for detection of their activation state both, *in vitro* and *in vivo*. The latter possibility, focusing on the very early signalling events, rather than on downstream products such as IL-2 or on T cell proliferation, would allow for an unequivocal detection of activated T cells, at least *in vitro*. At present, we are therefore investigating the

CHAPTER 8

use of antibodies directed against phosphorylated tyrosines (Y) of ZAP-70, in particular Y319, as marker for activated T cells of carp.

In this study affinity purified rabbit antibodies directed against carp CD4 and CD8α were also produced. Antigenic epitopes present in the extracellular region of these molecules were selected for peptide synthesis and immunization. Both anti-cCD4 and anti-cCD8α were suitable for immunohistochemical analysis. Structural analysis of the carp thymus using a combination of the anti-hCD3ε, anti-hZAP-70, anti-cCD4 and anti-cCD8α antibodies revealed a conserved picture of the general distribution and development of carp thymocytes. The high cell density and intense staining observed in the thymic cortex with all antibodies, most likely indicates the presence of double-positive CD4+/CD8+ immature T cells (CD3ε+/ZAP-70+) in the cortical region. This is similar to what is generally observed in mammals and has also been observed in sea bass, using *in situ* hybridization to demonstrate staining for CD4 and CD8α in overlapping areas in the cortex, but not in the medulla (51). Despite the suitability for immuno histochemistry, both anti-cCD4 and anti-cCD8 did not show reactivity to live cells in flow cytometry. The epitopes chosen for immunization were selected on an extracellular region where no predicted glycosylation sites were found. However, it can not be excluded that neighbouring glycosylation sites might interfere with the accessibility of the antibody to the protein backbone.

New strategies for the production of antibodies suitable for T cell recognition have been finally developed. Most recently, Köllner and colleagues established a panel of MAbs which specifically recognize peripheral rainbow trout T cells (52). Magnetic sorting using one selected MAb confirmed the expression of TCRα and β, CD8α and β, CD4 and major histocompatibility class II genes in the purified lymphocyte population, indicating this MAb can be considered a pan-specific T cell marker. Key to their succes was the use of activated leukocytes from mixed leukocyte cultures for the immunization protocol in mice. Another successful and highly promising approach, used a retrovirus-mediated gene transfer system, resulting in rat MAbs recognizing two distinct populations of CD8α+ and CD4+ lymphocytes in Ginbuna crucian carp (*Carassius auratus langsdorfii*) (53). Although this species and the common carp are closely related fish species, these antibodies do not seem to recognize T cells of carp in flow cytometry (Nakanishi T, pers comm; and unpublished data).

We have previously shown that infections with *T. borreli* are characterized by polyclonal B cell activation as determined by ELISA on serum samples collected from infected fish (43). Immunohistochemical analysis showed the presence of extremely enlarged B cell areas in the spleen of infected fish (28). In the present study, the anti-hCD3ε and anti-hZAP were used to study T cell distribution in the spleen of *T. borreli*-infected carp. We could show the presence of both enlarged B cell and T cell areas and their co-localization in the

CHAPTER 8

spleen of infected fish. Double-staining revealed that B and T cells are intermingled to each other, with no clear distinction between a B or T cell zone, especially during infection. Changes in the typical distribution of B and T cells in the white pulp were observed in mice infected with *Plasmodium chabaudi chabaudi*, where B cells and T cells are also found intermingled to each other (54). Future differentiation between T cell subtype (Th or CTL) during *T. borreli* infection in fish, requires the development of anti-cCD4 and anti-cCD8α antibodies. The most recent successful attempts in rainbow trout and Ginbuna crucian carp hold a promise to comparative immunologists that the long-desired T cell-specific MAbs will soon become available. In addition, application of forward and reverse genetic approaches in zebrafish

(*Danio rerio*) also provides an elegant example of *in vivo* tracking of T cells. Transgenic zebrafish expressing GFP under the Lck promoter enabled the actual (real-time) visualization of T cell development, homing and hematopoietic origin (55-57). Exploitation and implementation of the zebrafish animal model alongside the carp animal model should rapidly burst the study of T cell function in fish as well as help to bridge the gap of knowledge between mammalian and comparative immunology.

Acknowledgements

References

1. Litman, G. W., and M. D. Cooper. 2007. Why study the evolution of immunity? *Nat Immunol* 8:547-548.

2. Jansson, E., K. O. Gronvik, A. Johannisson, K. Naslund, E. Westergren, and L. Pilström. 2003. Monoclonal antibodies to lymphocytes of rainbow trout (*Oncorhynchus mykiss*). *Fish Shellfish Immunol* 14:239-257.

3. Timmusk, S., E. Jansson, and L. Pilström. 2003. The generation of monoclonal antibodies by genetic immunisation: antibodies against trout TCRalpha and IgL isotypes. *Fish Shellfish Immunol* 14:187-206.

4. Fischer, U., and B. Köllner. 2007. Cross-reactivity of human leukocyte differentiation antigen monoclonal antibodies on carp and rainbow trout cells. *Vet Immunol Immunopathol* 119:142-155.

5. Scapigliati, G., M. Mazzini, L. Mastrolia, N. Romano, and L. Abelli. 1995. Production and characterisation of a monoclonal antibody against the thymocytes of the sea bass *Dicentrarchus labrax* (L.) (Teleostea, Percicthydae). *Fish Shellfish Immunol* 5:393-405.

6. Scapigliati, G., I. Boschi, E. Randelli, S. Picchietti, C. Bernini, and F. Buonocore. 2009. "In vitro" cell-mediated cytotoxic activities in the sea bass *Dicentrarchus labrax*, and immunopurification of cytotoxic leukocytes. In *11th Congress of the International Society of Developmental and Comparative Immunology*, Prague, Czech Republic.

7. Rombout, J. H. W. M., J. W. van de Wal, A. Companjen, N. Taverne, and A. J. Taverne-Thiele. 1997. Characterization of a T cell lineage marker in carp (*Cyprinus carpio* L.). *Dev Comp Immunol* 21:35-46.

8. Rombout, J. H. W. M., P. H. M. Joosten, M. Y. Engelsma, A. P. Vos, N. Taverne, and J. J. Taverne-Thiele. 1998. Indications for a distinct putative T cell population in mucosal tissue of carp (*Cyprinus carpio* L.). *Dev Comp Immunol* 22:63-77.

9. Huttenhuis, H. B. T., N. Romano, C. Van Oosterhoud, A. Taverne-Thiele, L. Mastrolia, W. B. Van Muiswinkel, and J. H. W. M. Rombout. 2006. The ontogeny of mucosal immune cells in common carp (*Cyprinus carpio* L.). *Anat Embryol* 211:19-29.

CHAPTER 8

10. Huttenhuis, H. B. T., M. O. Huising, T. van der Meulen, C. N. van Oosterhoud, N. A. Sanchez, A. J. Taverne-Thiele, H. W. Stroband, and J. H. W. M. Rombout. 2005. Rag expression identifies B and T cell lymphopoietic tissues during the development of common carp (*Cyprinus carpio*). *Dev Comp Immunol* 29:1033-1047.

11. Romano, N., A. J. Taverne-Thiele, M. Fanelli, M. R. Baldassini, L. Abelli, L. Mastrolia, W. B. Van Muiswinkel, and J. H. M. W. Rombout. 1999. Ontogeny of the thymus in a teleost fish, *Cyprinus carpio* L.: developing thymocytes in the epithelial microenvironment. *Dev Comp Immunol* 23:123-137.

12. Lam, S. H., H. L. Chua, Z. Gong, T. J. Lam, and Y. M. Sin. 2004. Development and maturation of the immune system in zebrafish, *Danio rerio*: a gene expression profiling, in situ hybridization and immunological study. *Dev Comp Immunol* 28:9-28.

13. Zapata, A., B. Diez, T. Cejalvo, C. Gutiérrez-de Frías, and A. Cortés. 2006. Ontogeny of the immune system of fish. *Fish Shellfish Immunol* 20:126-136.

14. Romano, N., F. Rossi, L. Abelli, E. Caccia, R. Piergentili, L. Mastrolia, E. Randelli, and F. Buonocore. 2007. Majority of TCRbeta+ T-lymphocytes located in thymus and midgut of the bony fish, *Dicentrarchus labrax* (L.). *Cell Tissue Res* 329:479-489.

15. Danilova, N., V. S. Hohman, F. Sacher, T. Ota, C. E. Willett, and L. A. Steiner. 2004. T cells and the thymus in developing zebrafish. *Dev Comp Immunol* 28:755-767.

16. Lam, S. H., H. L. Chua, Z. Gong, Z. Wen, T. J. Lam, and Y. M. Sin. 2002. Morphologic transformation of the thymus in developing zebrafish. *Dev Dynamics* 225:87-94.

17. Bowden, T. J., P. Cook, and J. H. W. M. Rombout. 2005. Development and function of the thymus in teleosts. *Fish Shellfish Immunol* 19:413-427.

18. Hoffmann, J. A., and J. M. Reichhart. 2002. Drosophila innate immunity: an evolutionary perspective. *Nat Immunol* 3:121-126.

19. Cook, M. T., R. N. Morrison, R. Wilkinson, B. F. Nowak, P. J. Hayball, and J. D. Hayball. 2001. A screen of mammalian antibodies on snapper (*Pagrus auratus*, Sparidae) peripheral blood leukocytes reveals cross reactivity of an anti-human CD3 antibody with a population of mIg- cells. *Dev Comp Immunol* 25:553-559.

20. Park, C. I., I. Hirono, J. Enomoto, B. H. Nam, and T. Aoki. 2001. Cloning of Japanese flounder *Paralichthys olivaceus* CD3 cDNA and gene, and analysis of its expression. *Immunogenetics* 53:130-135.

21. Bakke-McKellep, A. M., M. K. Frøystad, E. Lilleeng, F. Dapra, S. Refstie, K. Å, and T. Landsverk. 2007. Response to soy: T-cell-like reactivity in the intestine of Atlantic salmon, *Salmo salar* L. *J Fish Dis* 30:13-25.

22. Göbel, T. W. F., E. L. Meier, and L. Du Pasquier. 2000. Biochemical analysis of the *Xenopus laevis* TCR/CD3 complex supports the "stepwise evolution" model. *Eur J Immunol* 30:2775-2781.

23. Sun, X. F., N. Shang, W. Hu, Y. P. Wang, and Q. L. Guo. 2007. Molecular cloning and characterization of carp (*Cyprinus carpio* L.) CD8beta and CD4-like genes. *Fish Shellfish Immunol* 23:1242-1255.

24. Forlenza, M., J. D. de Carvalho Dias, T. Veselý, D. Pokorová, H. F. Savelkoul, and G. F. Wiegertjes. 2008. Transcription of signal-3 cytokines, IL-12 and IFNαβ, coincides with the timing of CD8αβ up-regulation during viral infection of common carp (*Cyprinus carpio* L). *Mol Immunol* 45:1531-1547.

25. Kazazi, F., J. M. Mathijs, P. Foley, and A. L. Cunningham. 1989. Variations in CD4 expression by human monocytes and macrophages and their relationships to infection with the human immunodeficiency virus. *J Gen Virol* 70 (Pt 10):2661-2672.

26. Chan, L. S. 2003. *Animal models of human inflammatory skin diseases*. CRC Press.

27. Amin, S., A. Parker, and J. Mann. 2008. ZAP70 in chronic lymphocytic leukaemia. *Int J Biochem Cell Biol* 40:1654-1658.

28. Forlenza, M., J. P. Scharsack, N. M. Kachamakova, A. J. Taverne-Thiele, J. H. W. M. Rombout, and G. F. Wiegertjes. 2008. Differential contribution of neutrophilic granulocytes and macrophages to nitrosative stress in a host-parasite animal model. *Mol Immunol* 45:3178-3189.

29. Irnazarow, I. 1995. Genetic variability of Polish and Hungarian carp lines. *Aquaculture Research* 129:215-219.

30. Steinhagen, D., P. Kruse, and W. Körting. 1989. The parasitemia of cloned *Trypanoplasma borreli* Laveran and Mesnil, 1901, in laboratory-infected common carp (*Cyprinus carpio* L.). *J Parasitol* 75:685-689.

31. van Erp, S. H., B. Dixon, F. Figueroa, E. Egberts, and R. J. M. Stet. 1996. Identification and characterization of a new major histocompatibility complex class I gene in carp (*Cyprinus carpio* L.). *Immunogenetics* 44:49-61.

32. Pfaffl, M. W. 2001. A new mathematical model for relative quantification in real-time RT-PCR. *Nucleic Acids Res* 29:e45.

33. Tichopad, A., M. Dilger, G. Schwarz, and M. W. Pfaffl. 2003. Standardized determination of real-time PCR efficiency from a single reaction set-up. *Nucleic Acids Res* 31:e122.

34. Secombes, C. J., J. J. van Groningen, and E. Egberts. 1983. Separation of lymphocyte subpopulations in carp *Cyprinus carpio* L. by monoclonal antibodies: immunohistochemical studies. *Immunology* 48:165-175.

35. Koumans-van Diepen, J. C. E., E. Egberts, B. R. Peixoto, N. Taverne, and J. H. W. M. Rombout. 1995. B cell and immunoglobulin heterogeneity in carp (*Cyprinus carpio* L); An immuno(cyto)chemical study. *Developmental & Comparative Immunology* 19:97-108.

36. Nakayasu, C., M. Omori, S. Hasegawa, O. Kurata, and N. Okamoto. 1998. Production of a monoclonal antibody for carp (*Cyprinus carpio* L.) phagocytic cells and separation of the cells. *Fish Shellfish Immunol* 8:91-100.

37. Weyts, F. A. A., J. H. W. M. Rombout, G. Flik, and B. M. L. Verburg-Van Kemenade. 1997. A common carp (*Cyprinus carpio* L.) leucocyte cell line shares morphological and functional characteristics with macrophages. *Fish Shellfish Immunol* 7:123-133.

38. Romano, N., S. Picchietti, J. J. Taverne-Thiele, N. Taverne, L. Abelli, L. Mastrolia, B. M. L. Verburg-van Kemenade, and J. H. W. M. Rombout. 1998. Distribution of macrophages during fish development: an immunohistochemical study in carp (*Cyprinus carpio*, L.). *Anat Embryol (Berl)* 198:31-41.

39. Romano, N., J. J. Taverne-Thiele, J. C. Van Maanen, and J. H. M. W. Rombout. 1997. Leucocyte subpopulations in developing carp (*Cyprinus carpio* L.): immunocytochemical studies. *Fish Shellfish Immunol* 7:439-453.

40. Rombout, J. H. W. M., J. C. E. Koumans-van Diepen, P. M. Emmer, J. J. Taverne-Thiele, and N. Taverne. 1996. Characterization of carp thrombocytes with specific monoclonal antibodies. *J Fish Biol* 49:521-531.

41. Rothenberg, E. V., J. E. Moore, and M. A. Yui. 2008. Launching the T-cell-lineage developmental programme. *Nat Rev Immunol* 8:9-21.

42. van Diepen, J. C. E., G. T. M. Wagenaar, and J. H. W. M. Rombout. 1991. Immunocytochemical detection of membrane antigens of carp leucocytes using light and electron microscopy. *Fish Shellfish Immunol* 1:47-57.

43. Saeij, J. P. J., B. J. de Vries, and G. F. Wiegertjes. 2003. The immune response of carp to *Trypanoplasma borreli*: kinetics of immune gene expression and polyclonal lymphocyte activation. *Dev Comp Immunol* 27:859-874.

44. Imai, E., J. Ishikawa, T. Moritomo, and M. Tomana. 2005. Characterisation of T cell antigen receptor α chain isotypes in the common carp. *Fish Shellfish Immunol* 19:205-216.

45. Araki, K., H. Suetake, K. Kikuchi, and Y. Suzuki. 2005. Characterization and expression analysis of CD3ε and CD3γ/δ in fugu, *Takifugu rubripes*. *Immunogenetics* 57:158-163.

46. Laing, K. J., S. Dutton, and J. D. Hansen. 2007. Molecular and biochemical analysis of rainbow trout LCK suggests a conserved mechanism for T-cell signaling in gnathostomes. *Mol Immunol* 44:2737-2748.

47. Zhang, Y., L. Liang, P. Jiang, D. Li, C. Lu, and X. Sun. 2008. Genome evolution trend of common carp (*Cyprinus carpio* L.) as revealed by the analysis of microsatellite loci in a gynogenetic family. *J Genet Genomics* 35:97-103.

48. Brodersen, R., F. Bijlsma, K. Gori, K. T. Jensen, W. Chen, J. Dominguez, K. Haverson, P. F. Moore, A. Saalmuller, D. Sachs, W. J. Slierendrecht, C. Stokes, O. Vainio, F. Zuckermann, and B. Aasted. 1998. Analysis of the immunological cross reactivities of 213 well characterized monoclonal antibodies with specificities against various leucocyte surface antigens of human and 11 animal species. *Vet Immunol Immunopathol* 64:1-13.

49. Park, C.-I., I. Hirono, and T. Aoki. 2005. Molecular characterization of the Japanese flounder, *Paralichthys olivaceus*, CD3ε and evolution of the CD3 cluster. *Dev Comp Immunol* 29:123-133.

50. Mustelin, T., and K. Taskén. 2003. Positive and negative regulation of T-cell activation through kinases and phosphatases. *Biochem. J.* 371:15-27.

51. Picchietti, S., L. Guerra, F. Buonocore, E. Randelli, A. M. Fausto, and L. Abelli. 2009. Lymphocyte differentiation in sea bass thymus: CD4 and CD8-alpha gene expression studies. *Fish Shellfish Immunol* 27:50-56.

52. Köllner, B. 2009. T-lymphocytes in rainbow trout: investigation with newly established T-cell specific monoclonal antibodies. In *11th Congress of the International Society of Developmental and Comparative Immunology*, Prague, Czech Republic. 23.

53. Toda, H., Y. Shibasaki, T. Koike, M. Ohtani, F. Takizawa, M. Ototake, T. Moritomo, and T. Nakanishi. 2009. Alloantigen-specific killing is mediated by CD8-positive T cells in fish. *Dev Comp Immunol* 33:646-652.

54. Achtman, A. H., M. Khan, I. C. MacLennan, and J. Langhorne. 2003. *Plasmodium chabaudi chabaudi* infection in mice induces strong B cell responses and striking but temporary changes in splenic cell distribution. *J Immunol* 171:317-324.

55. Langenau, D. M., A. A. Ferrando, D. Traver, J. L. Kutok, J. P. Hezel, J. P. Kanki, L. I. Zon, A. T. Look, and N. S. Trede. 2004. In vivo tracking of T cell development, ablation, and engraftment in transgenic zebrafish. *Proc Natl Acad Sci U S A* 101:7369-7374.

56. Traver, D., A. Winzeler, H. M. Stern, E. A. Mayhall, D. M. Langenau, J. L. Kutok, A. T. Look, and L. I. Zon. 2004. Effects of lethal irradiation in zebrafish and rescue by hematopoietic cell transplantation. *Blood* 104:1298-1305.

57. Langenau, D. M., and L. I. Zon. 2005. The zebrafish: a new model of T-cell and thymic development. *Nat Rev Immunol* 5:307-317.
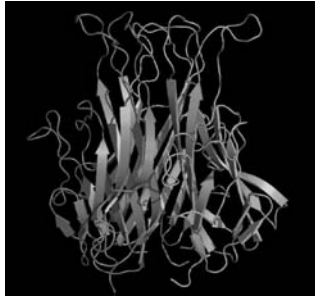
CHAPTER 8

CHAPTER 8

CHAPTER

9

Receptor-mediated and lectin-like activities of carp TNFα

Maria Forlenza, Stefan Magez, Jörn P. Scharsack,
Adrie Westphal, Huub F.J. Savelkoul and Geert F. Wiegertjes

CHAPTER 9

Receptor-Mediated and Lectin-Like Activities of Carp (*Cyprinus carpio*) TNF-α[1,2]

Maria Forlenza,* Stefan Magez,[†] Jörn P. Scharsack,[‡] Adrie Westphal,[§] Huub F. J. Savelkoul,* and Geert F. Wiegertjes[3]*

Functional characterization of TNF-α in species other than mammalian vertebrates is limited, and TNF-α has been studied in a limited number of fish species, primarily in vitro using recombinant proteins. Studies on TNF-α from different fish species so far pointed to several inconsistencies, in particular with respect to some receptor-mediated activities of fish TNF-α, such as the ability to directly activate phagocytes. In the present study a comprehensive analysis of in vitro as well as in vivo biological activities of two isoforms of carp TNF-α was performed. Our results show that carp TNF-α directly primes carp phagocytes and indirectly promotes typical receptor-mediated activities such as phagocyte activation by acting via endothelial cells. Additionally, for the first time in nonmammalian vertebrate species, the lectin-like activity of fish TNF-α homologs was investigated. Our results show an evolutionary conservation of function of this receptor-independent activity of TNF-α not only in cyprinid fish, but also in perciform and salmonid fish. The role of TNF-α in vivo, during infections of carp with the blood parasite *Trypanoplasma borreli*, was examined using three fundamentally different but complementary approaches: (1) inhibition of TNF-α expression, (2) overexpression of TNF-α, and (3) inhibition of shedding of membrane-bound TNF-α. Our results show that, also in fish, a tight regulation of TNF-α expression is important, since depletion or excess of TNF-α can make an important difference to survival of infection. Finally, we demonstrate a crucial protective role for membrane-bound TNF-α, which has a yet unexploited function in fish.   *The Journal of Immunology,* 2009, 183: 5319–5332.

Tumor necrosis factor-α is a pleiotropic cytokine and a major regulator of leukocyte trafficking and inflammation (1). Under most conditions monocytes/macrophages are the major producers of TNF-α, but in response to specific stimuli such as polyclonal activation, PMA, or LPS stimulation, also T and B lymphocytes, NK cells, endothelial cells, and other immune cells can produce TNF-α (2–6).

So far, TNF-α homologs have been identified only in the mammalian warm-blooded vertebrates. In birds, neither TNF-α nor lymphotoxin-α has been identified (7, 8). In amphibians, only very recently the first TNF-α sequence was published (9), with a limited functional characterization. In contrast, TNF-α homologs have been reported for at least 10 different teleost fish species (10–23)

*Cell Biology and Immunology Group, Wageningen Institute of Animal Sciences, Wageningen University, Wageningen, The Netherlands; [†]Unit of Cellular and Molecular Immunology, Vrije Universiteit Brussel, Brussels, Belgium, and Department of Molecular and Cellular Interactions, Institute for Biotechnology, Ghent, Belgium; [‡]Institute for Evolution and Biodiversity, Animal Evolutionary Ecology Group, University of Münster, Münster, Germany; and [§]Laboratory of Biochemistry, Department of Agrotechnology and Food Sciences, Wageningen University, Wageningen, The Netherlands

[3] Address correspondence and reprint requests to Dr. Geert F. Wiegertjes. Cell Biology and Immunology Group, Department of Animal Sciences, Wageningen University, P.O. Box 338, 6700 AH, Wageningen, The Netherlands. E-mail address: geert.wiegertjes@wur.nl

with two or sometimes three isoforms of TNF-α found in several fish species, including the common carp (*Cyprinus carpio*) (11, 13, 14, 16–18, 22). In vitro studies using recombinant proteins have shown that fish TNF-α is active at concentrations at least 1000 times higher than its mammalian counterpart (20–22, 24–27) and have evidenced crucial differences between TNF-α of cold- and warm-blooded vertebrates. Furthermore, activities of fish TNF-α appear species-specific in particular with respect to the ability of fish TNF-α to activate phagocytes directly. For example, both in rainbow trout (*Oncorhynchus mykiss*) (24) and goldfish (*Carassius auratus*) (22), TNF-α stimulates phagocyte activity in vitro, albeit at different concentrations. In contrast, seabream (*Sparus aurata*) TNF-α is a potent activator of endothelial cells but does not activate phagocytes directly (27). Instead, supernatant from seabream endothelial cells treated with TNF-α promoted the adhesion, migration, and activation of leukocytes. This is in line with receptor-mediated functions of TNF-α in mammalian vertebrates, where stimulation of endothelial cells with TNF-α increases the expression of adhesion molecules and the synthesis of chemotactic mediators such as IL-8. Thereby, TNF-α promotes leukocyte recruitment and activation and contributes to the inflammatory process. In the present study we show that carp (*C. carpio*) TNF-α primes but does not directly activate phagocytes and thereby promotes phagocyte activation, indirectly, via stimulation of endothelial cells.

TNF-α fulfills important functions in host-pathogen interactions and is required for protective immunity against intracellular bacteria and fungi but also against intracellular and extracellular protozoan parasites (28, 29). An additional, but perhaps less well-known activity of TNF-α, is its lectin-like activity first recognized in 1988 (30) when TNF-α was reported to directly interact with specific oligosaccharides through its lectin-like domain. The lectin domain is located at the top of the pyramid-shaped TNF-α molecule, also referred to as TIP domain, and is spatially and functionally distinct from the receptor binding region. TNF-α binds

through its lectin-like domain to mannose moieties present in the flagellar pocket of some African trypanosomes and can cause direct parasite lysis (31–34). The lectin-like activity of TNF-α, a yet unexamined receptor-independent function of fish TNF-α, was investigated in a trypanolytic assay in vitro. Our results clearly show that not only carp and zebrafish (*Danio rerio*) (both Cyprinidae), but also rainbow trout (Salmonidae) and seabream (Perciformes) TNF-α directly lyse *Trypanosoma brucei*, indicating that the lectin-like activity of TNF-α is evolutionary conserved.

Studies with TNF-α-deficient knockout mice, with transgenic mice overexpressing TNF-α, or studies administrating recombinant TNF-α all pointed out a dual role of TNF-α in immune protection as well as pathology (35). The "double-edged sword" role of TNF-α has most clearly been shown in studies on malaria and trypanosome infections where TNF-α was identified as a key mediator in both control of parasitemia as well as infection-associated pathology (28, 29, 36–38). In fish, due to a general lack of knockout and transgenic animals, the function of TNF-α in vivo is largely unknown. Only very recently, by the use of TNFR1 morphant zebrafish, TNF-α signaling has been shown to mediate resistance to mycobacteria by inhibiting bacterial growth and preventing macrophage death (39). To further investigate the in vivo role played by TNF-α with respect to protection or infection-associated pathology, we used a natural host-parasite infection model. Experimental infection of carp with the extracellular blood parasite *Trypanoplasma borreli* (Kinetoplastida) presents most of the pathological features associated with trypanosome infections in mammalian vertebrates such as anemia, splenomegaly, polyclonal B cell activation, as well as extremely elevated serum nitrite levels and associated tissue nitration (40–44). Similarly, *T. borreli* infection of carp can be treated with the human anti-trypanosome drug melarsoprol (Arsobal) (44). In the present study we show that inhibition of TNF-α gene expression in *T. borreli*-infected carp treated with the TNF-α inhibitor pentoxifylline results in extremely high parasitemia and increased mortality, whereas overexpression of TNF-α by injection of plasmid DNA leads to increased mortality, possibly owing to an exacerbation of the inflammatory response. Our results indicate a functional conservation in fish of the dual role of TNF-α in control of parasitemia and in infection-associated pathology.

TNF-α is present as a soluble and membrane-bound (mTNF-α)[4] form, with both exhibiting unique and overlapping activities. While soluble TNF-α mainly signals via TNFRI (p55), mTNF-α is the prime activating ligand of TNFR2 (p75) (45). Membrane-bound TNF-α has been shown to be involved in several biological activities, such as cytotoxicity, polyclonal activation of B cells, induction of IL-10 by monocytes, induction of chemokines, and ICAM-1 expression on endothelial cells (46–48). mTNF-α has been implicated in the control of *Listeria monocytogenes* (49), mycobacterial infection (50, 51), and possibly in the pathogenesis of experimental cerebral malaria (52). In the present study, we used an inhibitor of TNF-α-converting enzyme (TACE) to investigate the contribution of mTNF-α to the clearance of *T. borreli* in infected carp. In vitro, treatment of LPS-stimulated carp leukocytes with TACE inhibitor increased the number of cells bearing TNF-α on their surface. In vivo, fish treated with the TACE inhibitor were fully protected and cleared the parasite within days after treatment. Additionally, splenomegaly, plasma nitrite levels, and tissue nitration were all considerably reduced in fish treated with the TACE inhibitor, suggesting a so far unrecognized protective role for membrane-bound TNF-α in fish.

Materials and Methods

Animals

European common carp (*Cyprinus carpio carpio* L.) were bred and raised in the central fish facility at Wageningen University, The Netherlands, at 23°C in recirculating UV-treated tap water and fed pelleted dry food (Trouvit; Nutreco) daily. R3xR8 carp, which are the offspring of a cross between fish of Hungarian origin (R8 strain) and of Polish origin (R3 strain), were used (53). All experiments were performed with the approval of the animal experimental committee of Wageningen University.

Cell isolation

Fish were killed by an overdose of anesthetic (0.3 g/L tricaine methane sulfonate; Crescent Research Chemicals) in aquarium water buffered with 0.6 g/L sodium bicarbonate (Sigma-Aldrich). PBL, head kidney leukocytes (HKL), or enriched phagocyte fractions (macrophages and neutrophilic granulocytes) were isolated as described previously (54, 55). After isolation, cells were adjusted to the appropriate concentration with carp complete RPMI 1640 medium (cRPMI Invitrogen) adjusted to 280 mOsmol/kg, supplemented with 1.5% (v/v) heat inactivated-pooled carp serum, 2 mM L-glutamine, 100 U/ml penicillin G, and 50 mg/ml streptomycin sulfate).

Isolation of cardiac endothelial cells (EC) was performed as published (56, 57) with some modifications. Briefly, hearts from 9- to 12-mo-old carp were aseptically removed and transferred to 20 ml of ice-cold cRPMI supplemented with 5 IU/ml heparin (Leo Pharmaceutical Products). All subsequent steps were performed at room temperature. Excess blood was removed by slowly injecting into the atrium 10 ml of perfusion buffer (56) supplemented with 5 IU/ml heparin. Atria were dissected and several incisions were made to ensure complete access of the following buffers. Atria were incubated by shaking at 250 rpm for 30 min in carp PBS (cPBS, 150 mM NaCl, 2 mM KCl, 20 mM Na_2HPO_4, 2 mM KH_2PO_4) for 5 min in cPBS containing 0.5 mg/ml trypsin and 0.1 mg/ml EDTA and for 30 min in 0.7% saline solution containing 0.5 mg/ml collagenase and 0.7 mg/ml $CaCl_2$. After each incubation step, cells were centrifuged for 5 min at $400 \times g$. After collagenase treatment, the suspension was transferred to a sterile petri dish and flushed 5–10 times through the jet of a 10-ml syringe. Large fragments were discarded by sedimentation at $1 \times g$ for 8–10 min. The resulting cell suspension was centrifuged for 5 min at $400 \times g$ and cell pellets were resuspended in complete EC medium (RPMI 1640 supplemented with 10% FCS, 2 mM L-glutamine, 100 U/ml penicillin G, 50 mg/ml streptomycin sulfate, and 50 μg/ml gentamicin). The cell suspension obtained from $n = 4$ atria was seeded in two collagen type I-coated 6-well plates or two 24-well plates (Greiner, catalog nos. 657950 and 662950) and incubated at 27°C in a humidified atmosphere of 5% CO_2 to allow cells to adhere. After 24–48 h, cell debris and nonadherent cells were removed by washing twice with complete EC medium and then cultures were left undisturbed.

Parasites

T. borreli was cloned and characterized Steinhagen et al. (58) and maintained by syringe passage through carp following i.p. injection with 1×10^4 parasites/fish. Parasitemia was monitored using a Bürker counting chamber after dilution of blood 1/1 in RPMI 1649 medium adjusted to 280 mOsmol/kg containing 50 IU/ml of heparin. For parasite isolation, blood was collected from heavily infected carp and, after centrifugation, *T. borreli* were collected from the buffy coat and purified on a 1×12-cm ion-exchange column chromatography using DEAE cellulose (DE-52; Whatman International) (59). After isolation, parasites were harvested by centrifugation and resuspended in fresh complete HML medium (60) supplemented with 5% pooled carp serum, L-glutamine (2 mM), penicillin G (100 IU/ml), and streptomycin sulfate (50 mg/L)).

Bacterial expression constructs

For bacterial expression of soluble TNF-α, the sequence corresponding to the mature peptide of carp TNF-α1 (accession no. AJ311800, aa 77–237) or TNF-α2 (accession no. AJ311801, aa 70–231) was amplified by standard PCR using a proofreading *Taq* polymerase (Expand high-fidelity *Taq* polymerase; Roche) and cDNA from LPS-stimulated HKL as template. All primers used for cloning are listed in Table I. PCR products were directly cloned into pQE-30UA plasmid (Qiagen) downstream of the sequence

CHAPTER 9

Table I. *Primers used for TNF-α cloning in bacterial or eukaryotic plasmid*

Primer	Sequence $5' \rightarrow 3'^a$
pQETNF1_FW	ctttcaaaagcaaatgtc
pQETNF2_FW	ctttcaaaagaaaatgtc
pQETNF_RV	taaagcaaacaccccaaa
IRES_*Eco*RI_TNF1_FW	aagagaattcctttcaaaagcaaatgtc
IRES_*Eco*RI_TNF2_FW	aagagaattcctttcaaaag+aaaatgtc
IRES_*Bam*HI_TNF RV	agaggggatcctcataaagcaaacaccccaa
*Xho*I_TGFleader_FW	cggacgctcgagatgagggtggagagtttatta
*Eco*RIHisLeader_RV	ctccaggaattcgtgatggtgatggtgatgtgc tccgctatagtgcacaaatccc

coding for a 6× histidine tag. The primers used for the amplification were pQETNF1_FW or pQETNF2_FW in combination with pQETNF_RV.

Eukaryotic expression constructs

For eukaryotic expression of soluble TNF-α1 or TNF-α2, the mature peptides (excluding the TNF-α leader peptide and transmembrane sequence) were cloned in the pIRES-EGFP plasmid (Promega), downstream of the leader peptide region of the carp TGFβ (AF136947). The transmembrane region was removed to favor direct TNF-α secretion. The TGFβ leader peptide was inserted upstream of the mature TNF-α peptide to increase the rate of TNF-α secretion, as the use of a TGFβ leader peptide has been previously shown to effectively increase protein secretion in carp cells (61). TNF-α1 or TNF-α2 sequences were amplified as described above using IRES_*Eco*RI_TNF1_FW or IRES_*Eco*RI_TNF2_FW in combination with IRES_*Bam*HI_TNF_RV (see Table I). The nucleotide sequence encoding for the leader peptide region of the carp TGFβ was amplified using *Xho*I_TGFleader_FW and *Eco*RIHisLeader_RV, with part of the RV primers containing the sequence encoding for a 6× histidine tag. The leader sequence was first cloned into the *Xho*I site of the pIRES-EGFP plasmid, followed by restriction and ligation of the TNF-α1 or TNF-α2 sequence between the *Eco*RI site, downstream of the leader-His sequence, and the *Bam*HI site of the pIRES-EGFP plasmid. All constructs were transformed into M15 competent *Escherichia coli* cells, and positive clones were selected on agar plates containing ampicillin (100 μg/ml) and kanamicin (25 μg/ml). At least eight clones for each construct were sequenced. Expression of mature carp TNF-α was confirmed by Western blot analysis of supernatants from transfected *Epithelioma papulosum cyprini* (EPC) cells (62) using an anti-histidine Ab (Qiagen).

Recombinant carp TNF-α

Transformed *E. coli* M15 cells were grown on agar plates supplemented with antibiotics (100 μg/ml ampicillin and 25 μg/ml kanamicin) overnight at 37°C. One single colony was transferred to 20 ml of Luria-Bertani medium (1% (w/v) tryptone, 0.5% (w/v) yeast extract, 0.5% (w/v) NaCl (pH 7.5)) supplemented with antibiotic and grown overnight at 37°C with shaking. The overnight culture was transferred to 1 liter of prewarmed TB medium (tryptone 2.4% (w/v), yeast extract 1.2% (w/v), NaCl 0.5% (w/v), glycerol 4% (v/v) (pH 7.5)) and incubated at 30°C with shaking. At OD_{600} of 0.6–0.8, protein production was induced with 1 mM isopropyl β-D-thiogalactoside and the culture was incubated for a further 4 h at 30°C. Bacterial pellets were collected by centrifugation at 5270 × g for 15 min at 4°C and stored at −80°C until use. Proteins were purified under native conditions and all steps were conducted at 4°C unless stated otherwise. Bacterial pellets from 1-liter culture were resuspended in 20–40 ml of lysis buffer (LB; 50 mM Tris-Cl (pH 7.5), 500 mM NaCl, 5 mM $MgCl_2$, 10 mM imidazole, 10 mM 2-ME, 10% glycerol (v/v), 0.1% Triton X-114 (v/v)) supplemented with protease inhibitor cocktail (Sigma-Aldrich, catalog no. P8849) and lysozyme (1 mg/ml; Merck) and the suspension was incubated for 30 min on ice. Lysates were sonicated and subsequently centrifuged at 10,000 × g for 20 min at 4°C. Supernatants were collected and combined with 500 μl (for TNF-α1) or 750 μl (for TNF-α2) of Ni-NTA matrix (Qiagen). Samples were incubated for 30 min at 4°C while rotating and subsequently loaded on a 12-ml Poly-Prep chromatography column (Bio-Rad, catalog no. 7311550). All washing steps were performed under the following conditions: 300 × g for 4.5 min at 4°C. Columns were washed five times with 5 ml of wash buffer A (LB containing 20 mM imidazole), five times with 5 ml of wash buffer B (LB containing 30 mM imidazole), three times with 5 ml of wash buffer C (LB containing 50 mM imidazole, without Triton X-114), once with 5 ml of wash buffer D (LB containing 100 mM imidazole, without Triton X-114), and three times with 5 ml of wash buffer E

(500 mM NaCl, 2 mM KCl, 20 mM Na_2HPO_4, 2 mM KH_2PO_4, 100 mM imidazole). After an empty centrifugation step, proteins were eluted in elution buffer (wash buffer E containing 250 mM imidazole). Eluted proteins were subsequently dialyzed against cPBS, and endotoxins were measured by end-point chromogenic *Limulus* amebocyte lysate test (Charles River Laboratories). If necessary, further removal of endotoxin was achieved by Triton X-114 phase separation (63). All preparations contained <0.015 EU/ml. Unless stated otherwise, heat-treated TNF-α samples were used as negative control in all stimulation assays.

Western blot

To confirm overexpression of carp TNF-α in plasmid-injected fish, ~100 mg of tissue collected from the injection site was resuspended in 1 ml of RIPA lysis buffer (50 mM Tris-HCl (pH 7.4), 1% Nonidet P-40, 0.25% sodium deoxycholate, 150 mM NaCl, 1 mM EDTA, 1 mM PMSF, and protease inhibitor cocktail (Sigma-Aldrich, catalog no. P8849) and homogenized on ice by sonication (3 min, on for 30 s, off for 30 s, power 5, duty 30%). Lysates were cleared by centrifugation at 21,000 × g for 20 min at 4°C. Supernatants were carefully collected and 25 μl was resolved on a 12.5% SDS-PAGE. Proteins were transferred to nitrocellulose membranes (Protran; Schleicher & Schuell BioScience) and incubated overnight at 4°C with a 1/2000 dilution of affinity-purified polyclonal rabbit-anti-cTNFα Ab with gentile agitation. HRP-conjugated goat-anti-rabbit Ab (1/2000; Dako) was used as secondary Ab. Proteins were visualized by chemiluminescence detection (ECL detection system for Western blot; Amersham Biosciences) on x-ray films.

Affinity-purified polyclonal rabbit IgG anti-carp TNF-α1 or anti-TNF-α2 was produced by immunization of rabbits with purified bacterial recombinant TNF-α, according to a 3-mo standard protocol (Eurogentec). Affinity-purified IgG recognized both TNF-α1 and TNF-α2. Anti-TNF-α Abs were used for subsequent protein detection.

Cell stimulation

PBL, HKL, or enriched phagocyte fractions were resuspended in complete medium at a concentration of 1×10^7 cells/ml and 100 μl was transferred to 96-well plates. Cells were incubated overnight at 27°C in a humidified atmosphere of 5% CO_2. The following day cells were stimulated with various concentration of TNF-α, in the presence or absence of LPS in a final volume of 200 μl.

EC were cultured in 24-well plates until confluent and subsequently stimulated with various concentrations of TNF-α in a final volume of 500 μl. After 4 h cells were harvested for gene expression analysis. Alternatively, EC were cultured in 6-well plates in complete EC medium until confluent. The day before stimulation the medium was replaced with complete cRPMI containing 1.5% pooled carp serum, and cells were subsequently stimulated with 1 μg/ml TNF-α in a final volume of 1.5 ml. After 24 h cell supernatants were collected and cleared through a 0.45-μm filter. Supernatants were used immediately or stored at −80°C until use.

RNA isolation and cDNA synthesis

Total RNA was isolated from spleen, PBL, or enriched phagocyte fractions using the RNeasy Mini Kit according to the manufacturer's instructions, including an on-column DNase treatment with the RNase-free DNase set (Qiagen), and stored at −80°C until use. Before cDNA synthesis, to 0.25–1 μg of total RNA, a second DNase treatment was performed using DNase I, amplification grade (Invitrogen). Synthesis of cDNA was performed using SuperScript III first-strand synthesis systems for RT-PCR (Invitrogen) using random primers. A nonreverse transcriptase control was included for each sample. cDNA samples were further diluted 1/5 in nuclease-free water before real-time quantitative PCR analysis.

Gene expression analysis

Real-time quantitative PCR using SYBR Green I technology was performed with Rotor-Gene 6000 (Corbett Research) and the Brilliant SYBR Green quantitative PCR (Stratagene) as detection chemistry as described previously (55). Primers used for real-time quantitative PCR are listed in Table II. Fluorescence data from real-time quantitative PCR experiments were analyzed using Rotor-Gene version 6.0.21 software and exported to Microsoft Excel. The cycle threshold (C_t) for each sample and the reaction efficiencies (E) for each primer set were obtained upon comparative quantitation analysis from the Rotor-Gene version 6.0.21 software. The relative expression ratio (R) of a target gene was calculated based on the E and C_t deviation of sample vs control (64, 65), and it was expressed relative to the S11 protein of the 40S subunit as reference gene.

Table II. *Primers used for quantitative real-time PCR analysis*

Primer	Sequence 5′ → 3′	Accession No.
q40S.FW1	ccgtgggtgacatcgttaca	AB012087
q40S.RV1	tcaggacattgaacctcactgtct	
qTNFa1_FW	gagcttcacgaggactaatagacagt	AJ311800
qTNFa1_RV	ctgcggtaagggcagcaatc	
qTNFa2_FW	cggcacgaggagaaaccgagc	AJ311801
qTNFa2_RV	catcgttgtgtctgttagtaagttc	
qIL_10_FW	cgccagcataaagaactcgt	AB110780
qIL-10_RV	tgccaaatactgctcgatgt	
qIL_1β_FW	aaggaggccagtggctctgt	CCA245635
qIL-1β_RV	cctgaagaaggaggctgtca	
qiNOS_FW	aacaggtctgaaagggaatcca	AJ242906
qiNOS_RV	cattatctctcatgtccagagtctcttct	
qCXCa_FW	ctgggattcctgaccattggt	AJ421443
qCXCa_RV	gttggctctctgtttcaatgca	
qIL1RI_FW	acgccaccaagagccttttta	AJ843873
qIL1RI_RV	gcagcccatatttggtcaga	
qsele_FW	ggaaagaataatgaagactgtgtgg	GQ231486
qsele_RV	caggatgccgtgtagcagag	

Respiratory burst assay

Enriched phagocyte fractions (1×10^6) were stimulated for 1 h at 27°C in a humidified atmosphere of 5% CO_2 with increasing concentrations of recombinant TNF-α in the presence of 0.1 μg/ml dihydrorhodamine (DHR; Sigma-Aldrich). In all set-ups, PMA (Sigma-Aldrich) was added 15 min before measurement at a final concentration of 0.05 μg/ml. Each treatment was conducted in quadruplicate. Cells were analyzed by flow cytometry in the presence of 1 μg/ml propidium iodide to exclude necrotic cells. Forward scatter and side scatter characteristics of 1×10^4 events were acquired in linear mode and fluorescence intensities were acquired at log scale using a Beckman Coulter Epics XL-MCL flow cytometer.

Phagocytosis assay

Heat-killed, formalin-fixed bacteria (*Staphylococcus aureus*; Pansorbin cells standardized; Calbiochem/EMD Biosciences, catalog no. 507861) were incubated overnight with 5 μg/ml FITC in carbonate/bicarbonate buffer (pH 9.4) at room temperature, while rotating and protected from light. Excess FITC was removed by washing five times in cPBS, and bacteria were resuspended in cRPMI and were ready to use in the phagocytosis assay.

Total HKL (0.5×10^6) were transferred to flow cytometry tubes and stimulated for 30 min at 27°C in a humidified atmosphere of 5% CO_2 with increasing concentrations of recombinant carp TNF-α in the presence of FITC-labeled bacteria (5×10^6). Each treatment was conducted in quadruplicate. Phagocytosis was stopped by placing the tubes on ice and by adding 800 μl of ice-cold 1.5% paraformaldehyde. Two-hundred microliters of cell suspension was combined with 200 μl of cPBS containing 1.5% PFA and 200 μg/ml trypan blue and measured by flow cytometry as described above. Live cell gating excluded free bacteria from the measurement.

NO assay

Total HKL (1×10^6) were stimulated with various concentrations of TNF-α in the presence or absence of LPS (20 μg/ml). Each treatment was conducted in triplicate. After 72 h of incubation at 27°C in a humidified atmosphere of 5% CO_2, 75 μl of cell culture supernatant was combined with 100 μl of 1% (w/v) sulfanilamide in 2.5% (v/v) phosphoric acid and 100 μl of 0.1% (w/v) *N*-naphthyl-ethylenediamine in 2.5% (v/v) phosphoric acid. Absorbance values at 540 nm were acquired and nitrite concentration was measured using a sodium nitrite standard curve. In plasma samples, total nitrite plus nitrate was quantified as previously described (44) using a nitrite/nitrate colorimetric method (Roche Diagnostics, catalog no. 1746081) according to the manufacturer's instruction.

Migration assay

Cell migration was analyzed using a 10-well transmigration chamber (Neuroprobe, catalog no. AA10) as described previously (66). Total HKL (4×10^6) were layered in the upper well of a transmigration chamber and TNF-α-treated EC supernatants were layered in the lower well. The upper and lower wells were separated by a polyvinylpyrrolidone-pretreated polycarbonate filter with 3-μm pores. Pooled carp serum (at 10%) was used as positive control, and EC supernatants stimulated with heat-treated TNF-α served as negative controls. After 3 h cells were harvested and an absolute cell count was performed by flow cytometry, as described previously (44).

Three-dimensional modeling of carp TNF-α

The structure of mouse TNF-α with a resolution of 1.41 Å (Protein Data Bank entry 2tnf) was used as a template to model the carp TNF-α1 and TNF-α2 with the program MODELLER (version 9v5) (67, 68) using the consistent valence force field (69). The models were verified after several rounds of sequence alignment adjustments and energy minimization. Stereochemical quality of the homology models was assessed using the program PROCHECK (70). Protein folding quality was verified using the program PROSAII (71), which independently evaluates the compatibility of each residue to its environment.

Trypanolysis assay

Trypanolysis assay was performed as described previously (32). Briefly, AnTat1.1 *T. brucei* parasites were purified on a DE-52 ion-exchange column and resuspended to a concentration of 2×10^6 parasites/ml in PSG (PBS (pH 8.0) supplemented with 0.1% glucose). One hundred microliters of parasite suspension was combined with recombinant TNF-α or with TNF-α preincubated for 30 min with increasing concentration of *N,N′*-diacetylchitobiose (Sigma-Aldrich, catalog no. D1523) and then incubated at 30°C. Percentage cell death was calculated by light microscopy counts of remaining parasites after 4 h of incubation. Recombinant rainbow trout TNF-α (accession no. NM_001124357) was provided by Dr. J. Zou (Department of Zoology, University of Aberdeen, Aberdeen, U.K.) and recombinant zebrafish (accession no. NM_212859) and seabream (accession no. AJ413189) TNF-α were provided by Dr. F. Roca (Department of Cell Biology and Histology, University of Murcia, Murcia, Spain).

Inhibition of TNF-α expression in vivo

Nine-month-old carp (weighing 65 ± 0.3 g) were infected with 1×10^4 *T. borreli* per fish. Starting at 1 wk after infection, and for a period of 4 wk, fish (n = 11) received a daily dose (i.p.) of pentoxifylline (PTX; Sigma-Aldrich, catalog no. P1784) of 50 mg/ml dissolved in 100 μl cPBS. PBS-injected fish (n = 11) served as infected control, and noninfected fish (n = 5) injected with PTX only (same concentration, same volume) served as negative control for adverse side effects due to PTX administration. In a parallel experiment, spleen tissue from n = 5 fish from each group was collected to confirm inhibition of TNF-α expression in PTX-treated fish.

Overexpression of TNF-α in vivo

Six-month-old carp (n = 77, weighing 16 ± 0.2 g) were infected with 1×10^4 *T. borreli* per fish; at the same time, fish received two i.m. injections in the dorsal muscle of 25 μl of PBS containing plasmid DNA: fish were divided over seven groups (n = 11) and injected with a high (640 ng/μl) or low dose (64 ng/μl) of plasmid DNA encoding either TNF-α1 or TNF-α2 (pIRES-TNF-α1-EGFP or pIRES-TNF-α2-EGFP) or with equivalent doses of a mixture of the two plasmids. Control fish received the equivalent of a high dose of empty plasmid (pIRES-EGFP). To confirm overexpression of carp TNF-α in plasmid-injected fish, muscle tissue from the injection site was collected from n = 3 fish from each group at 48 h after injection and used for TNF-α detection by Western blot.

Overexpression of mTNFα in vivo

Nine-month-old carp (weighing 70 ± 2.2 g) were infected with 1×10^4 *T. borreli* per fish. After 2.5 wk when parasitemia levels reached 2×10^6 parasites/ml of blood, fish (n = 9) received three consecutive daily injections of 100 μl (i.p.) of TACE inhibitor (PKF242-484, 10 mg/ml). PKF242–484 was provided by Dr. A. Trifilieff and was synthesized at the Novartis Institute for BioMedical Research, Basel, Switzerland. As PKF242–484 was shown to inhibit various matrix metalloproteinases, FN-439 (10 mg/ml, 100 μl, i.p.), a broad-range matrix metalloproteinase inhibitor that has no activity on TACE, was used as negative control (72, 73). After 3 days parasitemia was measured and plasma collected for subsequent measurement of nitrite levels. Spleen tissues were collected and snap-frozen in liquid nitrogen for subsequent histological analysis.

In a parallel in vitro experiment, head kidney leukocytes were stimulated with LPS (50 μg/ml) in the presence or absence of PKF242-hyphen]484 (50 μM). At various time points after stimulation, cells were collected and washed once in cold cRPMI medium. To remove any receptor-bound soluble TNF-α, cells were first acid-treated as described previously (74) and subsequently analyzed by flow cytometry. Surface-bound TNF-α was detected using affinity-purified rabbit-anti-carp TNF-α IgG.

Immunohistochemistry

For the detection of nitrotyrosine, anti-nitrotyrosine rabbit polyclonal immunoaffinity-purified IgG (Bio-connect; Upstate Biotechnology, catalog

FIGURE 1. Real-time quantitative PCR analysis of gene expression in spleen after in vivo infection with *T. borreli*. Fish (9 mo old, weighing 160 ± 20 g) were infected with 1×10^4 parasites per fish. At time point 0 h, $n = 5$ control fish and at various time points after infection, $n = 5$ infected and $n = 3$ noninfected fish were sacrificed. Parasitemia was monitored during infection and is shown in the upper right plot. Gene expression was normalized relative to the 40S ribosomal protein S11 as internal reference gene and expressed relative to noninfected fish at time point 0. Values are given as means and SD. *, Significant difference relative to noninfected fish at the same time point. Note the difference in fold change (*y*-axis) between the genes.
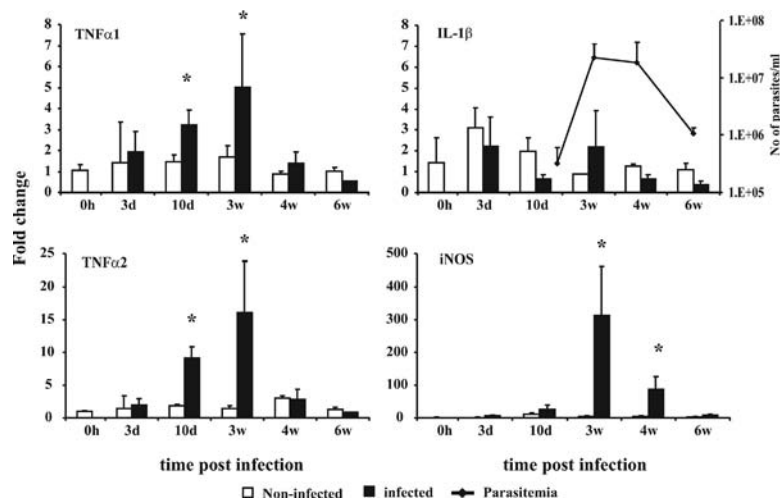
no. 06-284) was used. Cryosections (7 μm) of spleen tissue were mounted on poly-L-lysine-coated glass slides (BDH Laboratory Supplies) and treated as described previously (44) Anti-nitrotyrosine Ab was used in a 1/20 dilution and alkaline phosphatase-conjugated goat-anti-mouse Ab (Dako) was used in a 1/200 dilution.

Statistical analysis

For gene expression analysis, relative expression ratios (R) were calculated as described. Transformed ($\ln(R)$) values were used for statistical analysis in SPSS software (15.0). Significant differences ($p < 0.05$) were determined by independent sample Student's t test for the in vitro gene expression study and by a two-way ANOVA followed by a Sidak's test for the in vivo gene expression study. A one-way ANOVA followed by a Sidak's test was used for the migration and respiratory burst studies.

Results

TNF-α mRNA is up-regulated by T. borreli *in vivo*

One of the typical signs associated with *T. borreli* infections is splenomegaly, and we therefore focused on the spleen to study the kinetics of TNF-α gene expression in vivo by real-time quantitative PCR (Fig. 1). Two isoforms of carp TNF-α (TNF-α1 and TNF-α2) were identified previously (14) and will be referred to as TNF-α when differences between the two isoforms are not relevant. TNF-α2 fold change in gene expression was consistently higher than the fold change observed for TNF-α1. This difference can be explained by the dissimilar basal expression of the two genes in carp PBL, where TNF-α1 is ~50-fold more expressed than TNF-α2. Hence, TNF-α2, although being expressed very low at the basal level, is up-regulated to a larger extent than TNF-α1, possibly leading to a comparable protein expression. At peak levels of parasitemia, both TNF-α1 and TNF-α2 were up-regulated in spleen from *T. borreli*-infected fish, concomitantly with the peak of expression of inducible NO synthase (iNOS), but not IL-1β (Fig. 1).

TNF-α fails to directly activate carp phagocytes

Recombinant TNF-α1 and TNF-α2 (Fig. 2) were produced in a bacterial system and the biological activity was initially tested in vitro with respect to the ability of recombinant carp TNF-α to promote classical proinflammatory activities in carp phagocytes. Throughout the study, heat-treated recombinant carp TNF-α was used as a negative control. Stimulation with various concentrations

of recombinant TNF-α1 and TNF-α2 resulted in only a moderate up-regulation of proinflammatory molecules (Fig. 3, *A* and *B*). Both TNF-α1 and TNF-α2 failed to induce the production of oxygen (DHR oxidation, Fig. 3, *C* and *D*) and nitrogen (nitrite) radicals (Fig. 3, *E* and *F*), as well as phagocytosis in carp phagocytes (Fig. 3, *G* and *H*). Longer or shorter incubation times with carp TNF-α also failed to promote phagocyte activity under the condition tested (data not shown). Additionally, carp TNF-α was produced in two eukaryotic systems: in insect cells and in EPC cells
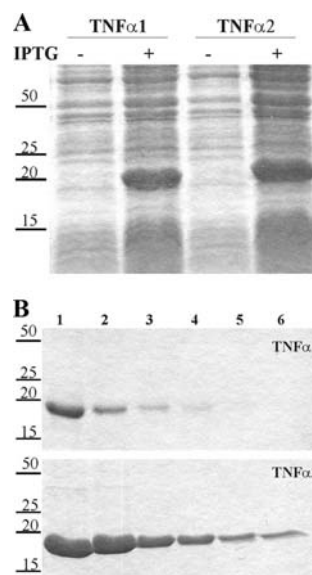
FIGURE 2. Expression and purification of carp TNF-α1 and TNF-α2. *A*, Total bacterial cell lysates from noninduced ($-$) and isopropyl β-D-thiogalactoside (IPTG)-induced ($+$) cultures and (*B*) elution fractions (*lanes 1–6*) of purified proteins were analyzed on 12.5% SDS-PAGE and visualized by Coomassie brilliant blue staining.
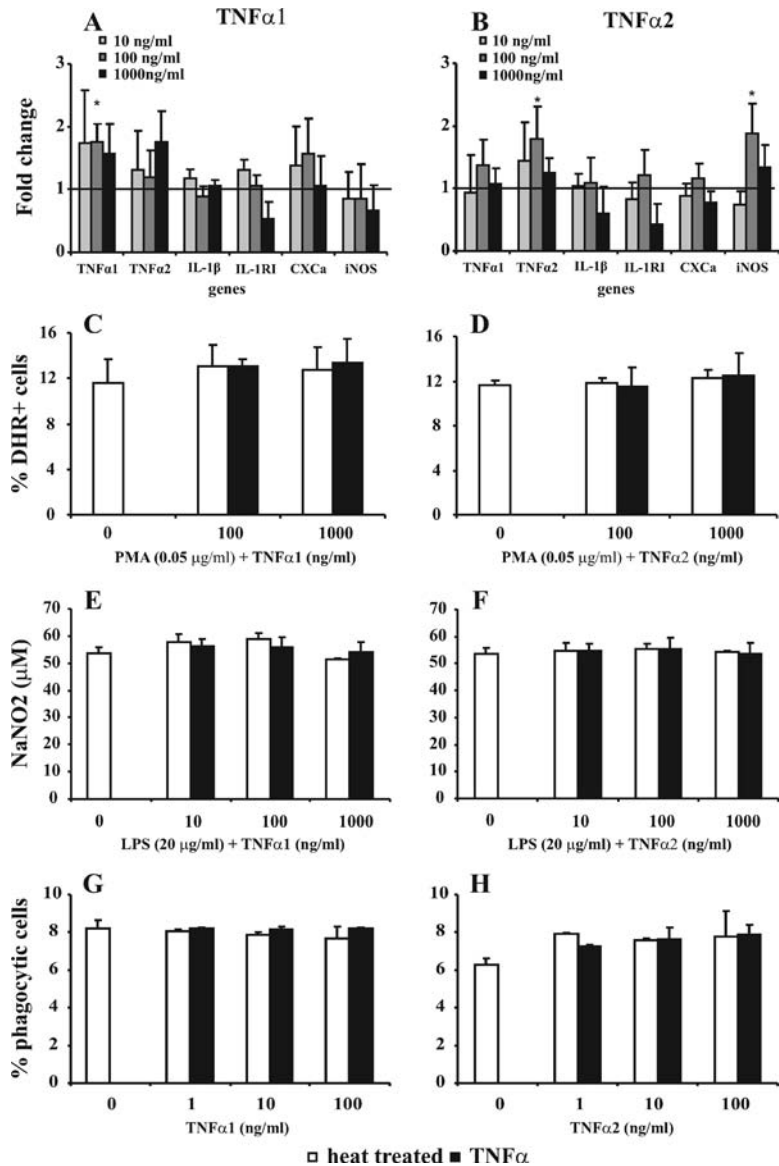
FIGURE 3. Effects of recombinant carp TNF-α on phagocytes: *A* and *B*, Real-time quantitative PCR analysis of gene expression. Phagocytes (1 × 10⁶) were stimulated for 3 h with the indicated concentrations of recombinant carp TNF-α1 and TNF-α2. 40S was used as internal reference gene, and expression was normalized against the respective heat-treated control. *C* and *D*, Respiratory burst activity (DHR oxidation). Phagocytes (1 × 10⁶) were stimulated with increasing concentration of native or heat-treated TNF-α. Respiratory burst activity was measured fluorometrically after 1 h. *E* and *F*, NO production. Total HKL (1 × 10⁶) were stimulated with a suboptimal LPS concentration (20 μg/ml) in the presence or absence of increasing concentrations of native or heat-treated TNF-α. After 72 h supernatants were collected and nitrite concentrations measured by Griess reaction. *G* and *H*, Percentage of phagocytosis. Total HKL (0.5 × 10⁶) were stimulated with FITC-labeled bacteria (5 × 10⁶) in the presence or absence of increasing concentrations of native or heat-treated TNF-α. Percentage of phagocytosis was determined fluorometrically after 30 min.

(62). Recombinant carp TNF-α, affinity purified from insect cell supernatants or TNF-α-containing supernatants from transfected EPC also failed to promote phagocyte activity (data not shown).

TNF-α indirectly promotes migration of leukocytes via activation of endothelial cells

Next, the ability of recombinant TNF-α to stimulate carp EC was analyzed. TNF-α1 and TNF-α2 were both able to promote the expression of several proinflammatory genes, CXCa (a fish chemokine with IL-8 characteristics), and adhesion molecules in EC (Fig. 4*A*). TNF-α2 was more potent than TNF-α1 in promoting gene expression. iNOS gene expression was present at low basal level ($R = 0.0045$, relative to reference gene) in carp EC and could be up-regulated after stimulation, only with TNF-α2. Additionally, based on homology sequencing, we identified a partial sequence of carp P-selectin (Sele, accession no. GQ231486) with extremely high ($R = 1.395$, relative to reference gene) basal gene expression in EC.

Given the up-regulation of chemokines and adhesion molecules in EC after stimulation with TNF-α, the ability of supernatants from TNF-α-treated EC to promote leukocyte migration was investigated. Supernatants collected from EC treated with either TNF-α1 or TNF-α2 were able to promote leukocyte migration (Fig. 4*B*), whereas recombinant TNF-α alone did not. In line with
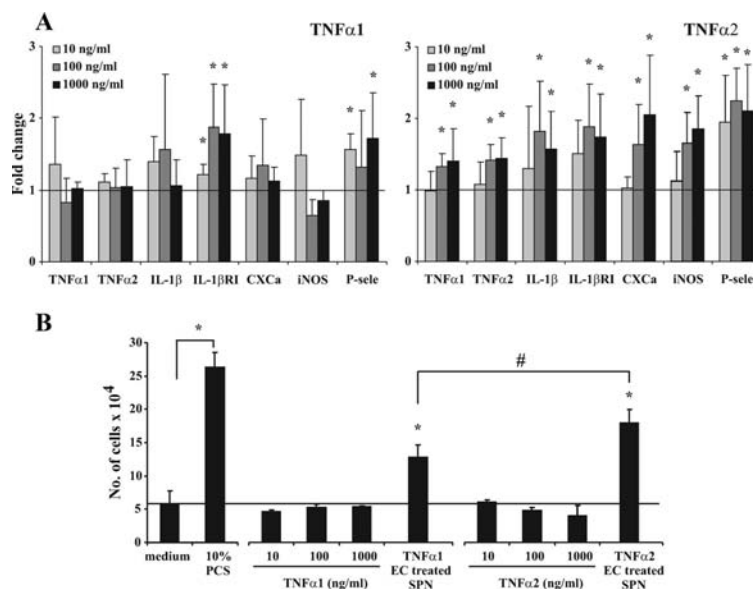
FIGURE 4. Effects of recombinant carp TNF-α on EC. *A*, Real-time quantitative PCR analysis of gene expression. Endothelial cells were cultured in 24-well plates until confluent and then stimulated for 4 h with the indicated concentrations of carp TNF-α1 and TNF-α2. Gene expression was normalized relative to the 40S ribosomal protein S11 as internal reference gene and was expressed relative to the respective heat-treated control. Values are given as means and SD ($n = 4$). *, Statistical differences relative to the heat-treated control. *B*, Migration of leukocytes. Total HKL (4×10^6) were layered on the upper well of a transmigration chamber, and migration toward TNF-α alone or toward supernatants from TNF-α-treated EC was recorded after 3 h. Pooled carp serum (10%) was used as positive control and complete cRPMI as negative control. The total number of cells that migrated toward supernatants from EC stimulated with native TNF-α was corrected for the number of cells that migrated toward supernatants from EC stimulated with heat-treated TNF-α. *, Significant differences relative to the medium control or to supernatants form samples stimulated with the respective heat-treated control; #, significant differences between supernatants treated with TNF-α1 and TNF-α2. P-sele indicates carp P-selectin; SPN, supernatant.

the difference observed at the gene expression level, TNF-α2-treated supernatants were more potent than TNF-α1-treated supernatants in promoting leukocyte migration.

TNF-α directly primes and indirectly promotes phagocyte activation by acting on endothelial cells

To investigate the indirect activation of phagocytes by carp TNF-α, supernatants from TNF-α-treated EC were used to promote the production of oxygen radicals (DHR oxidation) in carp phagocytes (Fig. 5). Clearly, increased DHR oxidation was observed in granulocytes (Fig. 5A, gate B) in samples incubated for 30–60 min with supernatants from TNF-α-treated EC (Fig. 5, *A* and *B*, gray bars). Preincubation of phagocytes for as short as 10 min with carp TNF-α1 or TNF-α2 resulted in a more rapid (15 min) DHR oxidation of granulocytes (Fig. 5, *A* and *B*, black bars). Preincubation with TNF-α2 resulted in a higher production of oxygen radicals than did preincubation with TNF-α1. The difference in oxidation of DHR in phagocytes prestimulated, or not, with TNF-α was less pronounced after 30 min. However, after 60 min, oxidation of DHR in prestimulated cells was significantly lower than in non-prestimulated phagocytes, with a greater effect visible in TNF-α1-prestimulated cells (compare gray and black bars in Fig. 5B). This indicates that although carp TNF-α was not able to directly promote the production of oxygen radicals in phagocytes, TNF-α can prime phagocytes to respond faster to EC-derived mediators.

Lectin-like activity of carp TNF-α

Carp TNF-α is homologous to mammalian TNF-α and presents many conserved structural features of its mammalian counterpart

(14). We produced a putative three-dimensional model based on the crystal structure of mouse TNF-α (75), confirming that also carp TNF-α might exist as a homotrimer, with each subunit consisting of anti-parallel β-sheets organized in a "jelly-roll" motif with a pyramid shape (Fig. 6). Mammalian TNF-α has a lectin domain located at the top of the pyramid-shaped molecule also referred to as TIP domain. Carp TNF-α has a conserved three-dimensional structure clearly identifying a TIP domain (Fig. 6A). More detailed analysis of the three-dimensional structure and of the primary sequence corresponding to the TIP region evidenced considerable differences between TNF-α1 and TNF-α2 (Fig. 6, *B* and *C*).

We investigated whether the lectin-like activity ascribed to mammalian TNF-α, and known to act through its TIP domain (31, 32), would be conserved in the homologous carp TNF-α molecule. The ability of carp TNF-α1 and TNF-α2 to kill the bloodstream form of *T. brucei* (AnTat 1.1 clone) was investigated in a trypanolytic assay. Both TNF-α1 and TNF-α2 killed *T. brucei* in a dose- and time-dependent manner (data not shown) where, maximally, 1 μg/ml carp TNF-α killed 100% of parasites within 4 h (Fig. 7, *A* and *B*). Trypanolytic activity of carp TNF-α against *T. brucei* could be blocked by preincubation with increasing concentrations of *N,N'*-diacetylchitobiose (Fig. 7, *A* and *B*), confirming that TNF-α activity acted via a lectin-like interaction. In parasite cultures incubated with TNF-α1, *N,N'*-diacetylchitobiose completely blocked TNF-α1 activity at concentrations >1 ng/ml, whereas in cultures incubated with TNF-α2 even the highest concentration of *N,N'*-diacetylchitobiose could not completely block TNF-α2 activity. Such a difference could be due to the dissimilarities observed in the
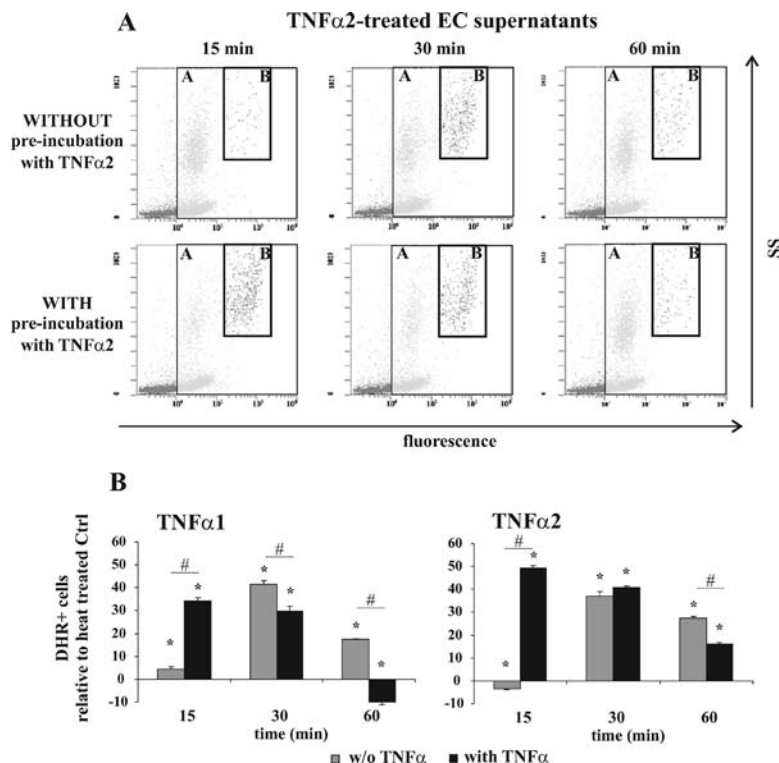
FIGURE 5. Activation of phagocytes by supernatants from TNF-α-treated EC. Carp phagocytes (1×10^6) were incubated for the indicated time with supernatants collected from TNF-α-treated EC in the presence of DHR (0.1 μg/ml). Alternatively, cells were first preincubated for 10 min with 1 μg/ml carp TNF-α1 or TNF-α2. For the last 15 min, PMA was added to the culture and fluorescence values of 10^4 events were acquired fluorometrically. *A*, Representative scatter dot plot of phagocytes stimulated with TNF-α2-treated EC supernatants. Cells were directly incubated with TNF-α2-treated EC supernatants (*upper panel*) or pretreated with TNF-α2 and subsequently stimulated with the respective supernatant (*lower panel*). Gate A indicates total DHR$^+$ cells and gate B indicates a granulocyte subpopulation with increased fluorescence intensity. *B*, Positive cells in gate B in phagocyte cultures directly stimulated with EC supernatants (gray bars) or preincubated with TNF-α and subsequently stimulated with the respective supernatant (black bars). Measurements were performed in quadruplicate. Values are given as means and SD. ∗, Significant differences with respect to supernatant from EC stimulated with heat-treated TNF-α; #, significant differences between prestimulated and non-prestimulated phagocytes. Shown is one representative experiment of two independent experiments performed.

TIP region. Collectively, these results indicate that both isoforms of carp TNF-α have lectin-like activities and that TNF-α2 might have a stronger activity than TNF-α1.

Evolutionary conservation of the lectin-like activity of fish TNF-α

To investigate whether the lectin-like activity would be limited to carp TNF-α only, we investigated the trypanolytic activity of TNF-α from zebrafish (both Cyprinidae) but also from two more distantly related fish species, seabream (Perciformes) and rainbow trout (Salmonidae). All investigated TNF-α were effective in killing *T. brucei* at concentrations and time comparable to that observed for carp TNF-α (Fig. 7*C*), further confirming that the lectin-like activity is highly conserved.

TNF-α is essential to control parasitemia

We investigated the role of TNF-α in vivo particularly with respect to fish survival and control of parasitemia. Starting at 1 wk postinfection, infected fish received a daily dose of PTX, a TNF-α inhibitor that acts at the transcriptional level (14, 76). Fish injected

with PTX showed lower survival and higher parasitemia at all time points after infection when compared with the infected control group (Fig. 8, *A* and *B*), indicating that TNF-α is critically involved in parasitemia control. Reduced TNF-α, but not iNOS, gene expression was observed in spleen from infected fish treated with PTX, but not in PBS-injected fish infected with *T. borreli* (Fig. 8*C*). Noninfected PTX-injected fish did not show any side effects due to PTX administration (data not shown).

Overexpression of TNF-α is detrimental to the host

A recombinant plasmid expressing TNF-α1 or TNF-α2 was constructed to investigate the immunomodulatory activity of excess TNF-α during in vivo *T. borreli* infection. Fish treated with various doses of recombinant plasmid encoding either TNF-α1 or TNF-α2 all showed lower survival than the infected control group, with the group injected with a high dose of TNF-α2 plasmid showing the lowest survival (Fig. 8*D*). Despite the clear effect on survival, parasitemia was not significantly affected. For clarity, only the parasitemia curve of the group injected with a high dose of TNF-α2 plasmid is shown (Fig. 8*E*). TNF-α plasmid-injected fish
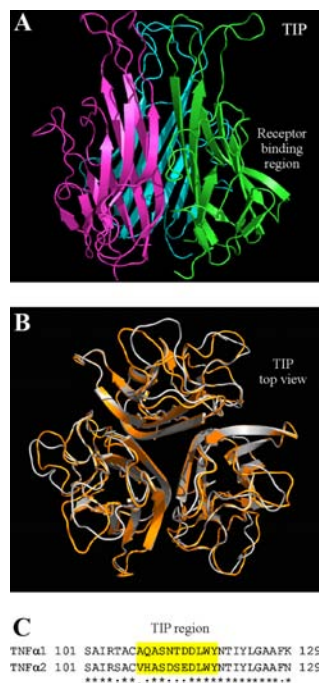
FIGURE 6. Three-dimensional analysis of carp TNF-α. *A,* Side view of carp TNF-α1 with the individual monomers shown in magenta, blue, and green. At the top of the pyramid-shaped molecule is the TIP domain. *B,* Top view of superimposed TNF-α1 (orange) and TNF-α2 (gray) trimeric molecules showing the different orientation of the loops forming the TIP domain in each of the two molecules. *C,* ClustalW alignment of the amino acid portion corresponding to the TIP region of TNF-α1 and TNF-α2. Despite the high similarity in the surrounding region, the TIP region (yellow) shows a considerable degree of variation.

showed high TNF-α protein expression in muscle tissue at the injection site as detected by Western blot (Fig. 8*F*). Parallel experiments performed by i.p. injection of high and low doses of recombinant carp TNF-α1 and TNF-α2 showed similar results, where all groups treated with TNF-α had lower survival than did the infected control group (data not shown).

Membrane-bound TNF-α is crucial for full protection of the host

An inhibitor of TACE was used in vivo during *T. borreli* infection to prevent TNF-α shedding, thereby increasing mTNF-α levels (73). About 2.5 wk (18 days) after infection fish reached a parasitemia of 2×10^6 parasites/ml of blood and received TACE inhibitor. After 3 days of treatment only, in all fish treated with the TACE inhibitor, complete clearance of the parasite was observed, while in fish treated with a general matrix metalloproteinase inhibitor, which has no effect on TACE, parasitemia progressed normally (Fig. 8, *G* and *H*). In vitro, stimulation of carp leukocytes with LPS in the presence of the TACE inhibitor significantly increased the number of positive cells with detectable surface-bound TNF-α in a time-dependent manner (Fig. 8*I*). Additionally, fish treated with the TACE inhibitor displayed extremely reduced spleen size as compared with the control group (data not shown). Neither the TACE inhibitor nor the control compound showed direct parasite toxicity in vitro in a concentration range from 0.2 to
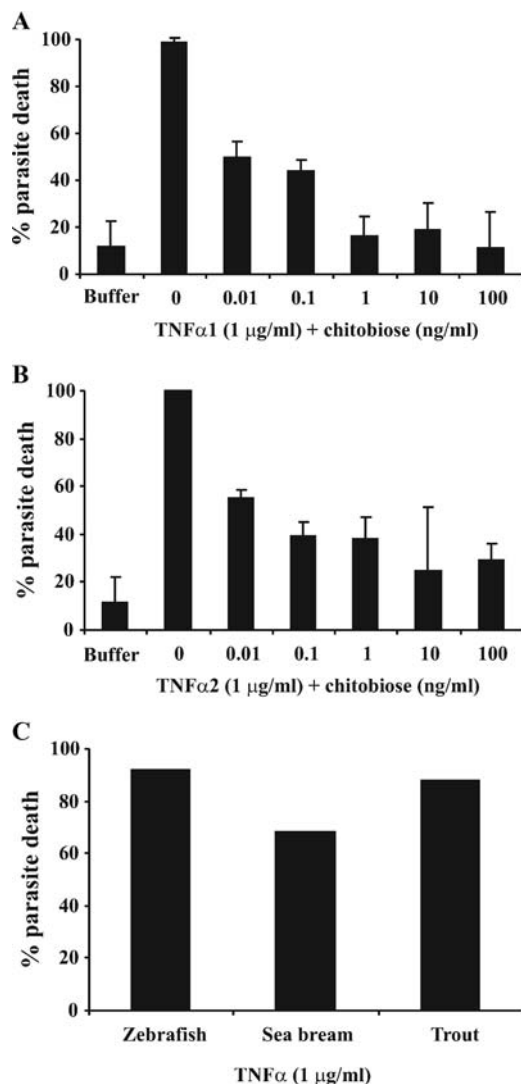
FIGURE 7. Lysis of bloodstream forms of *T. brucei* by fish TNF-α. Freshly isolated parasites (2×10^6/ml) were incubated in PSG (pH 8.0) with TNF-α (1 μg/ml) for 4 h at 37°C. Parasites were incubated with carp TNF-α1 (*A*) or carp TNF-α2 (*B*) alone or after preincubation with increasing concentrations of *N,N′*-diacetylchitobiose or (*C*) with zebrafish, seabream, or trout.

100 μM (data not shown). The effects of the TACE inhibitor on parasitemia and spleen size led us to investigate whether other parameters generally associated with pathology of infection, such as plasma nitrite levels and tissue nitration, would also be affected. As expected, plasma nitrite levels were strongly reduced, although not significantly owing to high variation between individuals, in fish treated with the TACE inhibitor (Fig. 9A). Tissue nitration, as measured by immunohistochemistry using an anti-nitrotyrosine Ab (44), was also reduced by treatment with TACE inhibitor, as indicated by the lower nitrotyrosine staining in the spleen of treated fish (Fig. 9*B*).
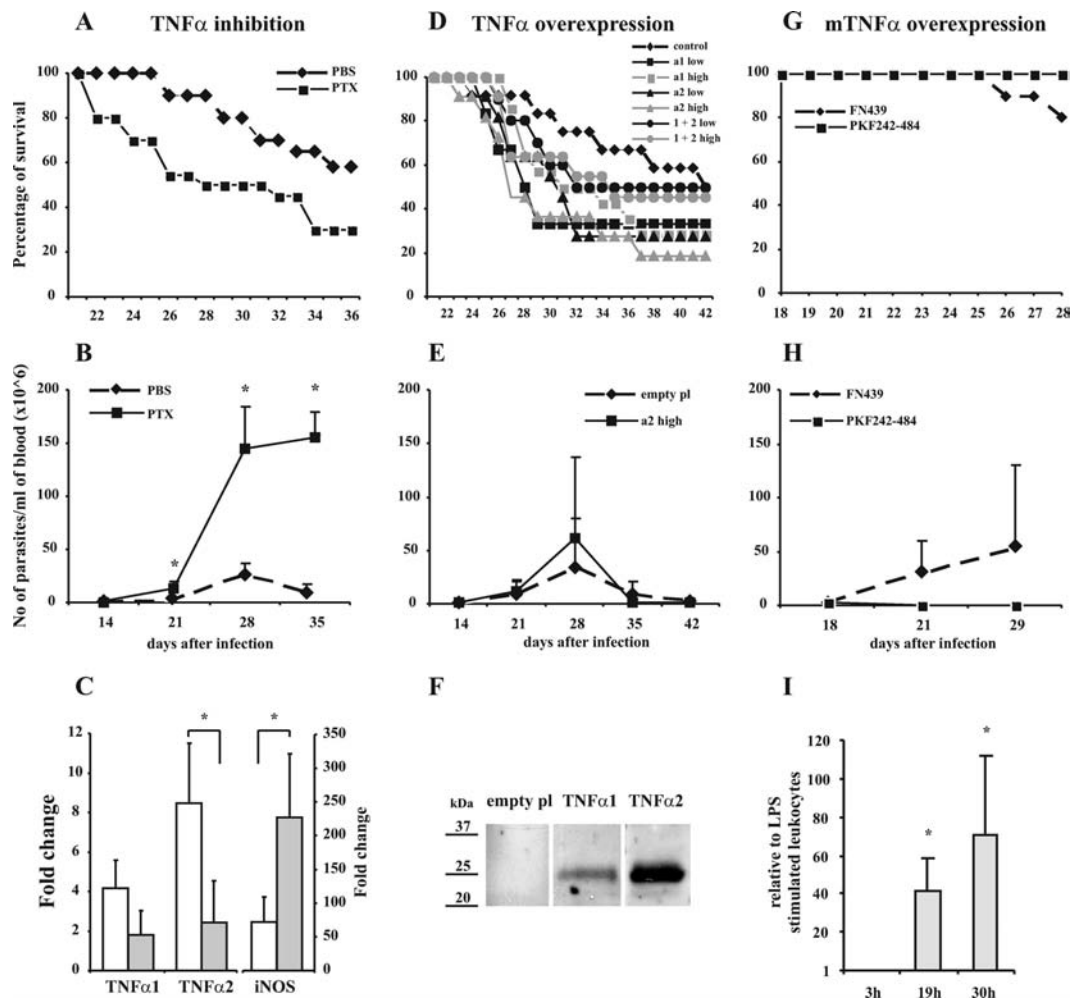
FIGURE 8. Immunomodulation by soluble and mTNF-α during *T. borreli* infection in vivo. At time 0 fish were infected i.p. with 10^4 parasites. Mortality (*top panels*) and parasitemia (*middle panels*) were monitored. Control experiments are shown in the *lower panels*. A–C, Inhibition of TNF-α expression by PTX administration. A and B, Mortality and parasitemia in infected fish. Starting 1 wk after infection, fish ($n = 12$) received a daily dose of PTX (50 mg/kg) or PBS. C, TNF-α and iNOS gene expression (quantitative RT-PCR) in spleen of nontreated and PTX-treated infected fish. Spleen from $n = 5$ fish was collected at 24 days postinfection. Shown are expression data relative to the noninfected fish at the same time point. Note that for clarity, fold changes of TNF-α1 and TNF-α2 are indicated on the left axis and iNOS of the right axis. D–F, Overexpression of TNF-α by recombinant plasmid DNA administration. D and E, Mortality and parasitemia in infected fish. At time 0, fish ($n = 11$) were injected i.m. with 25 μl of PBS containing a high dose (10 μg/10 g), a low dose (1 μg/10 g), or a mixture of the two of plasmid encoding for carp TNF-α1 (a1) or TNF-α2 (a2). Fish injected with a high dose of empty plasmid served as infected negative control. F, TNF-α protein expression at the injection site in muscle of plasmid-injected fish. Muscle from fish injected with the empty plasmid or with a high dose of plasmid encoding for TNF-α1 and TNF-α2 was collected for protein expression analysis. Carp TNF-α was detected using an affinity-purified rabbit anti-carp TNF-α IgG and HRP-conjugated goat-anti-rabbit IgG as secondary Ab by Western blot. Shown are the results from one fish out of $n = 3$ tested showing similar results. G–I, Overexpression of mTNF-α by administration of TACE inhibitor. G and H, Mortality and parasitemia in infected fish. After 18 days, when parasitemia reached $\sim 2 \times 10^6$ parasites/ml of blood, fish ($n = 9$) received three consecutive daily injections of the TACE inhibitor (PKF242-484, 10 mg/ml) or equivalent doses of the control compound (FN439). Values are given as mean ± SD of at least $n = 7$ measurements. *, Significant differences with respect to the infected control group. I, Relative increase of the number of cells bearing surface-bound TNF-α. Carp leukocytes were stimulated in triplicate wells with LPS (50 μg/ml) in the presence of PKF242-484 (50 μM) and values are expressed relative to leukocytes stimulated with LPS only. Shown are results from one representative experiment out of three performed independently.

Discussion

To date, TNF-α homologs have been identified in mammalian vertebrates, one amphibian species (*Xenopus laevis*) (9), and several teleost species (10–23) but not in birds (7, 8). Although TNF-α has been identified in several teleost fish species its biological activities and role particularly during infections are largely unknown. In fish, a limited number of functional studies have been performed (20–22, 24–27), mostly using recombinant TNF-α in vitro, and
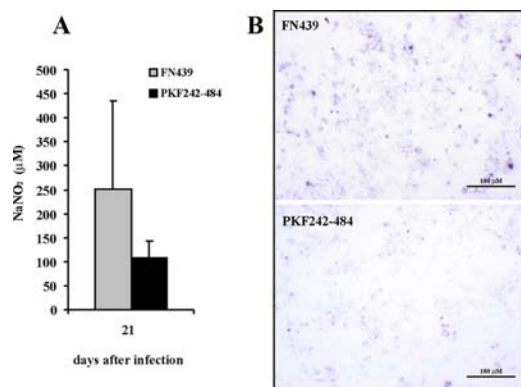
FIGURE 9. Plasma nitrite levels and tissue nitration in *T. borreli*-infected fish treated with TACE inhibitor. At time 0 fish were infected i.p. with 10^4 parasites. After 18 days, when parasitemia reached $\sim 2 \times 10^6$ parasites/ml of blood, fish ($n = 9$) received three consecutive daily injections of the TACE inhibitor (PKF242-484, 10 mg/ml) or equivalent doses of the control compound (FN439). At 21 days (3 days after treatment) plasma and spleen tissue samples were collected. *A*, Plasma nitrite levels. *B*, Anti-nitrotyrosine immunoreactivity (purple). Incubation of anti-nitrotyrosine Ab with a solution of 10 mM 3-nitrotyrosine completely abrogated the reaction (not shown).

results point out several inconsistencies particularly with respect to some receptor-mediated activities of fish TNF-α, such as the ability of fish TNF-α to directly activate phagocytes. In the present study, carp TNF-α directly stimulated the expression of proinflammatory cytokines, chemokines, and adhesion molecules in endothelial cells but not in phagocytes, and supernatants from TNF-α-treated endothelial cells were able to promote leukocyte migration and respiratory burst activity. Interestingly, although TNF-α failed to directly stimulate the production of nitrogen and oxygen radicals, TNF-α-primed phagocytes were able to respond faster to TNF-α-induced mediators from endothelial cells. Our findings are in line with a recent study in zebrafish embryos on mycobacterial pathogenesis using a TNFR1 knock-down approach (39). In this study, both control and TNFR1 morphant embryos displayed iNOS staining that colocalized with a subset of infected macrophages, suggesting that TNF-α signaling is not required for iNOS expression. In the same study, where the authors showed that TNF-α is not required for tuberculous granuloma formation but does maintain granuloma integrity, macrophage trafficking across epithelial and endothelial barriers was shown to be independent from TNF-α signaling. Another study in zebrafish (77), however, did show a role for TNF-α signaling in neutrophil influx into the intestine in response to proinflammatory stimuli induced by LPS. Most recently, a study in seabream (27) showed that endothelial cells, more than phagocytes, might be the primary target of fish TNF-α, suggesting that TNF-α is primarily involved in the recruitment of phagocytes to inflammatory sites rather than in the direct activation of phagocytes.

Besides the numerous receptor-dependent activities exerted by TNF-α, at least one receptor-independent activity, that is, the lectin-like recognition of specific oligosaccharides, has been described. In mammals, TNF-α has been shown to directly bind to the variant specific glycoprotein present in the flagellar pocket of some African trypanosomes and to cause direct lysis (31–34). An invertebrate functional analog of mammalian TNF-α, named coelomic cytolytic factor (CCF-1), has been described in the earth-

worm *Eisenia foetida foetida* (78). CCF-1 has been shown to exert lectin-like activities similar to mammalian TNF-α and is able to directly lyse *T. brucei* and *Trypanosoma cruzi* in vitro (79, 80). However, despite the functional similarities based on their lectin-like activity, CCF-1 and mammalian TNF-α do not share any sequence similarity and are not homologous genes, indicating a convergent evolution of function of two genetically unrelated cytokines (79). In the present study, the lectin-like activity of fish TNF-α homologs was investigated and results showed an evolutionary conservation of function of this receptor-independent activity of TNF-α not only in cyprinid fish, but also in salmonids and perciforms. To our knowledge this is the first report of lectin-like activities of TNF-α homologs in lower vertebrate species.

The conservation of the lectin-like activity of TNF-α among different fish species is opposed to the differences between fish species with regard to the receptor-dependent proinflammatory functions of TNF-α (24, 25, 22, 27), most of which have been studied in vitro. The role played by fish TNF-α during immune responses in vivo is largely unknown owing to the lack of suitable knockout or transgenic animal models. In the present study, we examined the role of TNF-α in vivo using three fundamentally different but complementary approaches: (1) inhibition of TNF-α expression, (2) overexpression of TNF-α, and (3) inhibition of mTNF-α shedding.

Inhibition of TNF-α gene expression during *T. borreli* infections was achieved by administration of PTX. PTX-treated fish showed impaired TNF-α but not iNOS gene expression and high plasma nitrite levels with kinetics corresponding to parasitemia (our unpublished data), indicating that parasite-derived components but not TNF-α directly contribute to the high nitrite levels typically associated with *T. borreli* infections. This is in line with our in vitro results showing that carp TNF-α did not induce NO production in phagocytes and corresponds to findings in TNFR1 morphant zebrafish embryos displaying normal iNOS staining during mycobacterium infections (39). Results showed that TNF-α is essential to control parasitemia since PTX-treated fish showed extremely high parasitemia numbers and succumbed faster to the infection. In mice, a crucial role for TNF-α in parasitemia control has been described in several studies on African trypanosomes where TNF-α-deficient mice show severely shortened survival times and fail to control parasitemia (36, 81, 82). The mechanisms underlining TNF-α activity are diverse and parasite species-specific. In *T. congolense* infections, TNFRI (TNFp55) signaling and soluble TNF-α have been shown to be crucial for NO-mediated parasite killing (82). In *T. brucei* infections, parasite control is independent from NO and it is TNF-α that might play a central role owing to its possible direct trypanolytic effects (32). In carp, the mechanisms by which TNF-α might contribute to the control of parasite load remain to be investigated. Although a direct lytic effect of carp TNF-α on *T. borreli* could not be detected in vitro (data not shown), the possibility that TNF-α might directly interact with *T. borreli* in vivo through a lectin-like interaction cannot be excluded. Independent of the exact mechanism involved, our results indicate that also in fish, TNF-α deficiency can make a difference in survival to parasitic infections.

Overexpression of carp TNF-α during *T. borreli* infections was achieved by i.m. injection of DNA plasmid encoding for carp TNF-α. Fish overexpressing TNF-α, regardless of the dose or isoform, all succumbed faster to the infection than did the control group, indicating that excess of TNF-α is detrimental to the host. Our results are in line with studies in mice showing that overexpression of TNF-α in vivo during malaria or *T. cruzi* infections

result in increased mortality (29). In fact, as opposed to its beneficial effects on parasiteamia control, TNF-α has also been implicated in the immunosuppression and immunopathology typically associated with protozoan infections (29, 38). In our study, the adverse effects observed after administration of carp TNF-α could not be ascribed to increased parasitemia or plasma nitrite levels (data not shown). In contrast, treated fish were able to control the parasite load, since parasitemia decreased during the late phase of infection in treated as well as control fish. We have previously shown that Abs and complement are the main mechanisms responsible for parasite control and clearance of *T. borreli* (41), and the present results suggest that TNF-α does not interfere with this process. However, excess of TNF-α might directly contribute to pathology possibly through an exacerbation of the inflammatory response.

Inhibition of mTNF-α shedding during *T. borreli* infections was achieved by administration of an inhibitor of TACE. The compound used in this study (PFK242-484) has previously been shown to effectively reduce the inflammatory response associated with intestinal ischemia and reperfusion by inhibiting the production of soluble TNF-α (73). PFK242-484 has inhibitory effects not only on TACE but also on other matrix metalloproteinases (72); therefore, also in our study, FN439, a general matrix metalloproteinase inhibitor that has no effect on TACE was used as negative control. TNF-α is active not only as soluble but also as membrane-bound molecules, with both exerting unique and overlapping activities. mTNF-α has been reported to play a role during *L. monocytogenes* and mycobacterial infections (49–51), while in *T. congolense* infections soluble but not mTNF-α was necessary to control infection (82). In fish, the role of mTNF-α has not been investigated except for our preliminary studies. The TACE inhibitor was used in the period immediately before the peak of TNF-α transcription and to the peak of parasitemia, and results show that mTNF-α is a determining factor in protection since fish treated with the TACE inhibitor had extremely reduced splenomegaly and cleared the parasites within a period as short as 3 days. Although we cannot exclude that also in fish TACE might be involved in the shedding of other molecules besides TNF-α (83), given the clear involvement of TNF-α during *T. borreli* infections, the implications of increased levels of mTNF-α must have a great impact on the immune response to this parasite. The mechanisms responsible for the protective effects mediated by mTNF-α are unknown at present and could be several: (1) mTNF-α, similar to soluble TNF-α, might directly interact with the parasite through the lectin-like domain and cause direct parasite lysis. This mechanism does not provide the most likely explanation, however, because TNF-α-mediated trypanolysis of African trypanosomes requires accumulation in the endocytotic vesicles (34), and it seems unlikely that mTNF-α would be as easily endocytosed by the parasite as soluble TNF-α. (2) At the time of treatment, parasite-specific Abs are already present (data not shown) and TNF-α has almost reached maximum mRNA levels (this study). Thus, Abs present on leukocytes (via binding to Fc receptors) or on the parasite itself (opsonization) together with the high levels of mTNF-α on leukocytes might lead to a tight adhesion of the parasite to the surface of effector cells. In this context, mTNF-α would contribute to adhesion more than to direct lysis of the parasite. Ab-dependent cell-mediated cytotoxicity by IgM "armed" NK-like cells, as has been described for the channel catfish (*Ictalurus punctatus*) (84), potentially could play a role in this mechanism. In mice infected with *T. congolense*, parasitaemia is effectively cleared by macrophage/neutrophil-derived soluble TNF but not mTNF-α, as well as by intact TNFR1 signaling, which induces trypanolytic NO (82). This contrasts with our results in two ways: in our infection model

mTNF-α does seem crucial for protection, and NO is not trypanolytic for *T. borreli* (44). (3) mTNF-α itself can mediate a "bidirectional signal" (85) whereby mTNF-α alone, independent from Abs, might act as receptor upon interaction with the parasite and transmit positive and/or negative feedback signals into the bearing cell. At present, we cannot firmly exclude nor confirm any of the above-mentioned mechanisms without extensive experimentation. Without doubt our results provide clear evidence for a yet unexploited functional role for membrane-bound TNF-α in fish that warrants further investigation.

Throughout this study we analyzed the biological activity of two isoforms of carp TNF-α. The most obvious difference was detected at the transcription level where TNF-α2, although expressed at very low levels, could be up-regulated to a greater extent than TNF-α1, both in vitro and in vivo. In general, recombinant TNF-α2 was more potent than TNF-α1 in promoting endothelial cell activation based on gene expression and on the ability of TNF-α-treated endothelial cell supernatant to promote leukocyte migration. In vivo, overexpression of TNF-α led to a lower survival in all groups, whereas fish injected with a high dose of plasmid encoding for TNF-α2 had the lowest survival and succumbed faster to the infection. Three-dimensional analysis of carp TNF-α showed major differences between the two isoforms, particularly in the region corresponding to the TIP domain. With regard to the lectin-like activity of TNF-α, at maximum concentrations, TNF-α1 and TNF-α2 were equally effective in killing *T. brucei* in vitro, whereas TNF-α2, in the presence of N,N'-diacetylchitobiose, constantly showed a slightly higher trypanolytic activity than did TNF-α1. Carp (14, 16), rainbow trout (13), goldfish (22), and zebrafish (17) all have multiple copies of TNF-α. At present, the evolutionary relationship between these TNF-α family members is not resolved (86). A recent study using the zebrafish *ducttrip* (*dtp*) mutant phenotype model showed the involvement of zebrafish TNF-α, but not TNF-β, in hepatic steatosis and liver degeneration (87). Our results show that both carp TNF-α isoforms examined in this study are biologically active. Further characterization of the biological relevance of the differences between TNF-α1 and TNF-α2 would require identification of the TNF-α receptors in carp.

Collectively, this study provides a comprehensive analysis, not only in vitro but also in vivo, of the biological activities of TNF-α in one fish species. Our data provide important insights in the functional conservation of TNF-α activities in teleost fish and point out similarities but also differences not only between mammals and fish, but also among different fish species. For the first time the lectin-like activity of TNF-α homologs in vertebrate species other than mammals has been investigated. Additionally, we provide evidence that, also in fish, a tight regulation of TNF-α expression is important, because depletion or excess of TNF-α can make an important difference to survival of infection. Finally, we propose a crucial protective role for mTNF-α, a yet unexploited function of TNF-α in fish.

Acknowledgments

Disclosures

The authors have no financial conflicts of interest.

References

1. Grell, M., and P. Scheurich. 1997. Tumor necrosis factor. In *Growth Factors and Cytokines in Health and Disease*, Vol. 2B. D. LeRoith and C. Bondy, eds. JAI press, Greenwich, pp. 669–726.

2. Peters, P. M., J. R. Ortaldo, M. R. Shalaby, L. P. Svedersky, G. E. Nedwin, T. S. Bringman, P. E. Hass, B. B. Aggarwal, R. B. Herberman, D. V. Goeddel, et al. 1986. Natural killer-sensitive targets stimulate production of TNF-α but not TNF-β (lymphotoxin) by highly purified human peripheral blood large granular lymphocytes. *J. Immunol.* 137: 2592–2598.

3. Cuturi, M. C., M. Murphy, M. P. Costa-Giomi, R. Weinmann, B. Perussia, and G. Trinchieri. 1987. Independent regulation of tumor necrosis factor and lymphotoxin production by human peripheral blood lymphocytes. *J. Exp. Med.* 165: 1581–1594.

4. Sung, S. S., J. M. Bjorndahl, C. Y. Wang, H. T. Kao, and S. M. Fu. 1988. Production of tumor necrosis factor/cachectin by human T cell lines and peripheral blood T lymphocytes stimulated by phorbol myristate acetate and anti-CD3 antibody. *J. Exp. Med.* 167: 937–953.

5. Andersson, U., G. Adolf, M. Dohlsten, G. Moller, and H. O. Sjogren. 1989. Characterization of individual tumor necrosis factor α- and β-producing cells after polyclonal T cell activation. *J. Immunol. Methods* 123: 233–240.

6. Chan, E. L., S. B. Haudek, B. P. Giroir, and J. T. Murphy. 2001. Human coronary endothelial cell activation by endotoxin is characterized by NF-κB activation and TNF-α synthesis. *Shock* 16: 349–354.

7. Takimoto, T., K. Takahashi, K. Sato, and Y. Akiba. 2005. Molecular cloning and functional characterizations of chicken TL1A. *Dev. Comp. Immunol.* 29: 895–905.

8. Takimoto, T., K. Sato, Y. Akiba, and K. Takahashi. 2008. Role of chicken TL1A on inflammatory responses and partial characterization of its receptor. *J. Immunol.* 180: 8327–8332.

9. Mawaribuchi, S., K. Tamura, S. Okano, S. Takayama, Y. Yaoita, T. Shiba, N. Takamatsu, and M. Ito. 2008. Tumor necrosis factor-α attenuates thyroid hormone-induced apoptosis in vascular endothelial cell line XLgoo established from *Xenopus* tadpole tails. *Endocrinology* 149: 3379–3389.

10. Hirono, I., B. H. Nam, T. Kurobe, and T. Aoki. 2000. Molecular cloning, characterization, and expression of TNF cDNA and gene from Japanese flounder *Paralychthys olivaceus*. *J. Immunol.* 165: 4423–4427.

11. Laing, K. J., T. Wang, J. Zou, J. Holland, S. Hong, N. Bols, I. Hirono, T. Aoki, and C. J. Secombes. 2001. Cloning and expression analysis of rainbow trout *Oncorhynchus mykiss* tumour necrosis factor-α. *Eur J. Biochem.* 268: 1315–1322.

12. Garcia-Castillo, J., P. Pelegrin, V. Mulero, and J. Meseguer. 2002. Molecular cloning and expression analysis of tumor necrosis factor α from a marine fish reveal its constitutive expression and ubiquitous nature. *Immunogenetics* 54: 200–207.

13. Zou, J., T. Wang, I. Hirono, T. Aoki, H. Inagawa, T. Honda, G. I. Soma, M. Ototake, T. Nakanishi, A. E. Ellis, and C. J. Secombes. 2002. Differential expression of two tumor necrosis factor genes in rainbow trout, *Oncorhynchus mykiss*. *Dev. Comp. Immunol.* 26: 161–172.

14. Saeij, J. P., R. J. Stet, B. J. de Vries, W. B. van Muiswinkel, and G. F. Wiegertjes. 2003. Molecular and functional characterization of carp TNF: a link between TNF polymorphism and trypanotolerance? *Dev. Comp. Immunol.* 27: 29–41.

15. Zou, J., C. J. Secombes, S. Long, N. Miller, L. W. Clem, and V. G. Chinchar. 2003. Molecular identification and expression analysis of tumor necrosis factor in channel catfish (*Ictalurus punctatus*). *Dev. Comp. Immunol.* 27: 845–858.

16. Savan, R., and M. Sakai. 2004. Presence of multiple isoforms of TNF-α in carp (*Cyprinus carpio* L.): genomic and expression analysis. *Fish Shellfish Immunol.* 17: 87–94.

17. Savan, R., T. Kono, D. Igawa, and M. Sakai. 2005. A novel tumor necrosis factor (TNF) gene present in tandem with the TNF-α gene on the same chromosome in teleosts. *Immunogenetics* 57: 140–150.

18. Haugland, Ø., I. S. Mercy, K. Romøren, J. Torgersen, and Ø. Evensen. 2007. Differential expression profiles and gene structure of two tumor necrosis factor-α variants in Atlantic salmon (*Salmo salar* L.). *Mol. Immunol.* 44: 1652–1663.

19. Nascimento, D. S., P. J. B. Pereira, M. I. R. Reis, A. do Vale, J. Zou, M. T. Silva, C. J. Secombes, and N. M. S. dos Santos. 2007. Molecular cloning and expression analysis of sea bass (*Dicentrarchus labrax* L.) tumor necrosis factor-α (TNF-α). *Fish Shellfish Immunol.* 23: 701–710.

20. Ordas, M. C., M. M. Costa, F. J. Roca, G. Lopez-Castejon, V. Mulero, J. Meseguer, A. Figueras, and B. Novoa. 2007. Turbot TNFα gene: molecular characterization and biological activity of the recombinant protein. *Mol. Immunol.* 44: 389–400.

21. Xiao, J., Z. C. Zhou, C. Chen, W. L. Huo, Z. X. Yin, S. P. Weng, S. M. Chan, X. Q. Yu, and J. G. He. 2007. Tumor necrosis factor-α gene from mandarin fish, *Siniperca chuatsi*: molecular cloning, cytotoxicity analysis and expression profile. *Mol. Immunol.* 44: 3615–3622.

22. Grayfer, L., J. G. Walsh, and M. Belosevic. 2008. Characterization and functional analysis of goldfish (*Carassius auratus* L.) tumor necrosis factor-α. *Dev. Comp. Immunol.* 32: 532–543.

23. Covello, J. M., S. Bird, R. N. Morrison, S. C. Battaglene, C. J. Secombes, and B. F. Nowak. 2009. Cloning and expression analysis of three striped trumpeter (*Latris lineata*) pro-inflammatory cytokines, TNF-α, IL-1β and IL-8, in response to infection by the ectoparasitic, *Chondracanthus goldsmidi*. *Fish Shellfish Immunol.* 26: 773–786.

24. Zou, J., S. Peddie, G. Scapigliati, Y. Zhang, N. C. Bols, A. E. Ellis, and C. J. Secombes. 2003. Functional characterisation of the recombinant tumor necrosis factors in rainbow trout, *Oncorhynchus mykiss*. *Dev. Comp. Immunol.* 27: 813–822.

25. García-Castillo, J., E. Chaves-Pozo, P. Olivares, P. Pelegín, J. Meseguer, and V. Mulero. 2004. The tumor necrosis factor-α of the bony fish seabream exhibits the in vivo proinflammatory and proliferative activities of its mammalian counterparts, yet it functions in a species-specific manner. *Cell. Mol. Life Sci.* 61: 1331–1340.

26. Hino, K., O. Nakamura, Y. Yoshiura, H. Suetake, Y. Suzuki, and T. Watanabe. 2006. TNF induces the growth of thymocytes in rainbow trout. *Dev. Comp. Immunol.* 30: 639–647.

27. Roca, F. J., I. Mulero, A. Lopez-Munoz, M. P. Sepulcre, S. A. Renshaw, J. Meseguer, and V. Mulero. 2008. Evolution of the inflammatory response in vertebrates: fish TNF-α is a powerful activator of endothelial cells but hardly activates phagocytes. *J. Immunol.* 181: 5071–5081.

28. Pfeffer, K. 2003. Biological functions of tumor necrosis factor cytokines and their receptors. *Cytokine Growth Factor Rev.* 14: 185–191.

29. Clark, I. A. 2007. How TNF was recognized as a key mechanism of disease. *Cytokine Growth Factor Rev.* 18: 335–343.

30. Sherblom, A. P., J. M. Decker, and A. V. Muchmore. 1988. The lectin-like interaction between recombinant tumor necrosis factor and uromodulin. *J. Biol. Chem.* 263: 5418–5424.

31. Lucas, R., S. Magez, R. De Leys, L. Fransen, J. P. Scheerlinck, M. Rampelberg, E. Sablon, and P. De Baetselier. 1994. Mapping the lectin-like activity of tumor necrosis factor. *Science* 263: 814–817.

32. Magez, S., M. Geuskens, A. Beschin, H. del Favero, H. Verschueren, R. Lucas, E. Pays, and P. de Baetselier. 1997. Specific uptake of tumor necrosis factor-α is involved in growth control of *Trypanosoma brucei*. *J. Cell Biol.* 137: 715–727.

33. Daulouede, S., B. Bouteille, D. Moynet, P. De Baetselier, P. Courtois, J. L. Lemesre, A. Buguet, R. Cespuglio, and P. Vincendeau. 2001. Human macrophage tumor necrosis factor (TNF)-α production induced by *Trypanosoma brucei gambiense* and the role of TNF-α in parasite control. *J. Infect. Dis.* 183: 988–991.

34. Magez, S., M. Radwanska, B. Stijlemans, H. V. Xong, E. Pays, and P. De Baetselier. 2001. A conserved flagellar pocket exposed high mannose moiety is used by African trypanosomes as a host cytokine binding molecule. *J. Biol. Chem.* 276: 33458–33464.

35. Aggarwal, B. B. 2003. Signalling pathways of the TNF superfamily: a double-edged sword. *Nat. Rev. Immunol.* 3: 745–756.

36. Magez, S., M. Radwanska, A. Beschin, K. Sekikawa, and P. De Baetselier. 1999. Tumor necrosis factor α is a key mediator in the regulation of experimental *Trypanosoma brucei* infections. *Infect. Immun.* 67: 3128–3132.

37. Magez, S., C. Truyens, M. Merimi, M. Radwanska, B. Stijlemans, P. Brouckaert, F. Brombacher, E. Pays, and P. de Baetselier. 2004. P75 tumor necrosis factor-receptor shedding occurs as a protective host response during African trypanosomiasis. *J. Infect. Dis.* 189: 527–539.

38. Antoine-Moussiaux, N., S. Magez, and D. Desmecht. 2008. Contributions of experimental mouse models to the understanding of African trypanosomiasis. *Trends Parasitol.* 24: 411–418.

39. Clay, H., H. E. Volkman, and L. Ramakrishnan. 2008. Tumor necrosis factor signaling mediates resistance to mycobacteria by inhibiting bacterial growth and macrophage death. *Immunity* 29: 283–294.

40. Saeij, J. P., W. B. Van Muiswinkel, A. Groeneveld, and G. F. Wiegertjes. 2002. Immune modulation by fish kinetoplastid parasites: a role for nitric oxide. *Parasitology* 124: 77–86.

41. Saeij, J. P., B. J. de Vries, and G. F. Wiegertjes. 2003. The immune response of carp to *Trypanoplasma borreli*: kinetics of immune gene expression and polyclonal lymphocyte activation. *Dev. Comp. Immunol.* 27: 859–874.

42. Saeij, J. P., J. P., W. B. van Muiswinkel, M. van der Meent, C. Amaral, and G. F. Wiegertjes. 2003. Different capacities of carp leukocytes to encounter nitric oxide-mediated stress: a role for the intracellular reduced glutathione pool. *Dev. Comp. Immunol.* 27: 555–568.

43. Scharsack, J. P., D. Steinhagen, C. Kleczka, J. O. Schmidt, W. Körting, R. D. Michael, W. Leibold, and H. J. Schuberth. 2003. The haemoflagellate *Trypanoplasma borreli* induces the production of nitric oxide, which is associated with modulation of carp (*Cyprinus carpio* L.) leucocyte functions. *Fish Shellfish Immunol.* 14: 207–222.

44. Forlenza, M., J. P. Scharsack, N. M. Kachamakova, A. J. Taverne-Thiele, J. H. Rombout, and G. F. Wiegertjes. 2008. Differential contribution of neutrophilic granulocytes and macrophages to nitrosative stress in a host-parasite animal model. *Mol. Immunol.* 45: 3178–3189.

45. Grell, M., E. Douni, H. Wajant, M. Lohden, M. Clauss, B. Maxeiner, S. Georgopoulos, W. Lesslauer, G. Kollias, K. Pfizenmaier, and P. Scheurich. 1995. The transmembrane form of tumor necrosis factor is the prime activating ligand of the 80 kDa tumor necrosis factor receptor. *Cell* 83: 793–802.

46. Decker, T., M. L. Lohmann-Matthes, and G. E. Gifford. 1987. Cell-associated tumor necrosis factor (TNF) as a killing mechanism of activated cytotoxic macrophages. *J. Immunol.* 138: 957–962.

47. Higuchi, M., K. Nagasawa, T. Horiuchi, M. Oike, Y. Ito, M. Yasukawa, and Y. Niho. 1997. Membrane tumor necrosis factor-α (TNF-α) expressed on HTLV-I-infected T cells mediates a costimulatory signal for B cell activation: characterization of membrane TNF-α. *Clin. Immunol. Immunopathol.* 82: 133–140.

48. Xu, J., A. K. Chakrabarti, J. L. Tan, L. Ge, A. Gambotto, and N. L. Vujanovic. 2007. Essential role of the TNF-TNFR2 cognate interaction in mouse dendritic cell-natural killer cell crosstalk. *Blood* 109: 3333–3341.

49. Torres, D., L. Janot, V. F. Quesniaux, S. I. Grivennikov, I. Maillet, J. D. Sedgwick, B. Ryffel, and F. Erard. 2005. Membrane tumor necrosis factor confers partial protection to *Listeria* infection. *Am. J. Pathol.* 167: 1677–1687.

50. Fremond, C., N. Allie, I. Dambuza, S. I. Grivennikov, V. Yeremeev, V. F. Quesniaux, M. Jacobs, and B. Ryffel. 2005. Membrane TNF confers protection to acute mycobacterial infection. *Respir. Res.* 6: 136.

51. Allie, N., L. Alexopoulou, V. J. Quesniaux, L. Fick, K. Kranidioti, G. Kollias, B. Ryffel, and M. Jacobs. 2008. Protective role of membrane tumour necrosis factor in the host's resistance to mycobacterial infection. *Immunology* 125: 522–534.

52. Lucas, R., P. Juillard, E. Decoster, M. Redard, D. Burger, Y. Donati, C. Giroud, C. Monso-Hinard, T. De Kesel, W. A. Buurman, et al. 1997. Crucial role of tumor necrosis factor (TNF) receptor 2 and membrane-bound TNF in experimental cerebral malaria. *Eur. J. Immunol.* 27: 1719–1725.

53. Irnazarow, I. 1995. Genetic variability of Polish and Hungarian carp lines. *Aquaculture* 129: 215–219.

54. Kemenade, B., A. Groeneveld, B. Rens, and J. Rombout. 1994. Characterization of macrophages and neutrophilic granulocytes from the pronephros of carp (*Cyprinus carpio*). *J. Exp. Biol.* 187: 143–158.

55. Forlenza, M., P. D. Walker, B. J. de Vries, S. E. Wendelaar Bonga, and G. F. Wiegertjes. 2008. Transcriptional analysis of the common carp (*Cyprinus carpio* L.) immune response to the fish louse *Argulus japonicus* Thiele (Crustacea: Branchiura). *Fish Shellfish Immunol.* 25: 76–83.

56. Farrell, A. P. 1987. Coronary flow in a perfused rainbow trout heart. *J. Exp. Biol.* 129: 107–123.

57. Koren, C. W., B. Sveinbjornsson, and B. Smedsrod. 1997. Isolation and culture of endocardial endothelial cells from Atlantic salmon (*Salmo salar*) and Atlantic cod (*Gadus morhua*). *Cell Tissue Res.* 290: 89–99.

58. Steinhagen, D., P. Kruse, and W. Körting. 1989. The parasitemia of cloned *Trypanoplasma borreli* Laveran and Mesnil, 1901, in laboratory-infected common carp (*Cyprinus carpio* L.). *J. Parasitol.* 75: 685–689.

59. Overath, P., J. Ruoff, Y.-D. Stierhof, J. Haag, H. Tichy, I. Dyková, and J. Lom. 1998. Cultivation of bloodstream forms of *Trypanosoma carassii*, a common parasite of freshwater fish. *Parasitol. Res.* 84: 343–347.

60. Steinhagen, D., W. Hedderich, A. Skouras, J. P. Scharsack, J. Schuberth, W. Leibold, and W. Körting. 2000. In vitro cultivation of *Trypanoplasma borreli* (Protozoa: Kinetoplastida), a parasite from the blood of common carp *Cyprinus carpio. Dis. Aquat. Org.* 41: 195–201.

61. Collet, B., and C. J. Secombes. 2005. Construction and analysis of a secreting expression vector for fish cells. *Vaccine* 23: 1534–1539.

62. Fijan, N., D. Sulimanovic, M. Bearzotti, D. Muzinic, L. O. Zwillenberg, S. Chilmonczyk, J. F. Vautherot, and P. de kinkelin. 1983. Some properties of the *Epitherlioma papulosum cyprini* (EPC) cell line from carp *cyprinus carpio. Ann. Virol.* (*Institue Pasteur*) 134: 207–220.

63. Liu, S., R. Tobias, S. McClure, G. Styba, Q. Shi, and G. Jackowski. 1997. Removal of endotoxin from recombinant protein preparations. *Clin. Biochem.* 30: 455–463.

64. Pfaffl, M. W. 2001. A new mathematical model for relative quantification in real-time RT-PCR. *Nucleic Acids Res.* 29: e45.

65. Tichopad, A., M. Dilger, G. Schwarz, and M. W. Pfaffl. 2003. Standardized determination of real-time PCR efficiency from a single reaction set-up. *Nucleic Acids Res.* 31: e122.

66. Gonzalez, S. F., M. O. Huising, R. Stakauskas, M. Forlenza, B. M. Lidy Verburg-van Kemenade, K. Buchmann, M. E. Nielsen, and G. F. Wiegertjes. 2007. Real-time gene expression analysis in carp (*Cyprinus carpio* L.) skin: inflammatory responses to injury mimicking infection with ectoparasites. *Dev. Comp. Immunol.* 31: 244–254.

67. Sali, A., and T. L. Blundell. 1993. Comparative protein modelling by satisfaction of spatial restraints. *J. Mol. Biol.* 234: 779–815.

68. Eswar, N., B. John, N. Mirkovic, A. Fiser, V. A. Ilyin, U. Pieper, A. C. Stuart, M. A. Marti-Renom, M. S. Madhusudhan, B. Yerkovich, and A. Sali. 2003. Tools for comparative protein structure modeling and analysis. *Nucleic Acids Res.* 31: 3375–3380.

69. Dauber-Osguthorpe, P., V. A. Roberts, D. J. Osguthorpe, J. Wolff, M. Genest, and A. T. Hagler. 1988. Structure and energetics of ligand binding to proteins: *Escherichia coli* dihydrofolate reductase-trimethoprim, a drug-receptor system. *Proteins* 4: 31–47.

70. Laskowski, R. A., M. W. Macarthur, D. S. Moss, and J. M. Thornton. 1993. PROCHECK: a program to check the stereochemical quality of protein structures. *J. Appl. Crystallogr.* 26: 283–291.

71. Sippl, M. J. 1993. Recognition of errors in three-dimensional structures of proteins. *Proteins* 17: 355–362.

72. Kottirsch, G., G. Koch, R. Feifel, and U. Neumann. 2002. Beta-aryl-succinic acid hydroxamates as dual inhibitors of matrix metalloproteinases and tumor necrosis factor alpha converting enzyme. *J. Med. Chem.* 45: 2289–2293.

73. Souza, D. G., F. L. Ferreira, C. T. Fagundes, F. A. Amaral, A. T. Vieira, R. A. Lisboa, M. V. Andrade, A. Trifilieff, and M. M. Teixeira. 2007. Effects of PKF242-484 and PKF241-466, novel dual inhibitors of TNF-α converting enzyme and matrix metalloproteinases, in a model of intestinal reperfusion injury in mice. *Eur. J. Pharmacol.* 571: 72–80.

74. Van Ommen, R., A. E. Vredendaal, and H. F. Savelkoul. 1994. Secondary IgE responses in vivo are predominantly generated via γ1ε-double positive B cells. *Scand. J. Immunol.* 40: 491–501.

75. Baeyens, K. J., H. L. De Bondt, A. Raeymaekers, W. Fiers, and C. J. De Ranter. 1999. The structure of mouse tumour-necrosis factor at 1.4 Å resolution: towards modulation of its selectivity and trimerization. *Acta Crystallogr. D Biol. Crystallogr.* 55: 772–778.

76. Doherty, G. M., J. C. Jensen, H. R. Alexander, C. M. Buresh, and J. A. Norton. 1991. Pentoxifylline suppression of tumor necrosis factor gene transcription. *Surgery* 110: 192–198.

77. Bates, J. M., J. Akerlund, E. Mittge, and K. Guillemin. 2007. Intestinal alkaline phosphatase detoxifies lipopolysaccharide and prevents inflammation in zebrafish in response to the gut microbiota. *Cell Host Microbe* 2: 371–382.

78. Beschin, A., M. Bilej, F. Hanssens, J. Raymakers, E. Van Dyck, H. Revets, L. Brys, J. Gomez, P. De Baetselier, and M. Timmermans. 1998. Identification and cloning of a glucan- and lipopolysaccharide-binding protein from *Eisenia foetida* earthworm involved in the activation of prophenoloxidase cascade. *J. Biol. Chem.* 273: 24948–24954.

79. Beschin, A., M. Bilej, L. Brys, E. Torreele, R. Lucas, S. Magez, and P. De Baetselier. 1999. Convergent evolution of cytokines. *Nature* 400: 627–628.

80. Olivares Fontt, E., A. Beschin, E. Van Dijck, V. Vercruysse, M. Bilej, R. Lucas, P. De Baetselier, and B. Vray. 2002. *Trypanosoma cruzi* is lysed by coelomic cytolytic factor-1, an invertebrate analogue of tumor necrosis factor, and induces phenoloxidase activity in the coelomic fluid of *Eisenia foetida foetida. Dev. Comp. Immunol.* 26: 27–34.

81. Iraqi, F., K. Sekikawa, J. Rowlands, and A. Teale. 2001. Susceptibility of tumour necrosis factor-α genetically deficient mice to *Trypanosoma congolense* infection. *Parasite Immunol.* 23: 445–451.

82. Magez, S., M. Radwanska, M. Drennan, L. Fick, T. N. Baral, N. Allie, M. Jacobs, S. Nedospasov, F. Brombacher, B. Ryffel, and P. De Baetselier. 2007. Tumor necrosis factor (TNF) receptor-1 (TNFp55) signal transduction and macrophage-derived soluble TNF are crucial for nitric oxide-mediated *Trypanosoma congolense* parasite killing. *J. Infect. Dis.* 196: 954–962.

83. Moss, M. L., L. Sklair-Tavron, and R. Nudelman. 2008. Drug insight: tumor necrosis factor-converting enzyme as a pharmaceutical target for rheumatoid arthritis. *Nat. Clin. Pract. Rheumatol.* 4: 300–309.

84. Shen, L., T. B. Stuge, J. P. Evenhuis, E. Bengtén, M. Wilson, V. G. Chinchar, L. W. Clem, and N. W. Miller. 2003. Channel catfish NK-like cells are armed with IgM via a putative FcμR. *Dev. Comp. Immunol.* 27: 699–714.

85. Eissner, G., W. Kolch, and P. Scheurich. 2004. Ligands working as receptors: reverse signaling by members of the TNF superfamily enhance the plasticity of the immune system. *Cytokine Growth Factor Rev.* 15: 353–366.

86. Glenney, G. W., and G. D. Wiens. 2007. Early diversification of the TNF superfamily in teleosts: genomic characterization and expression analysis. *J. Immunol.* 178: 7955–7973.

87. Matthews, R. P., K. Lorent, R. Manoral-Mobias, Y. Huang, W. Gong, I. V. Murray, I. A. Blair, and M. Pack. 2009. TNFα-dependent hepatic steatosis and liver degeneration caused by mutation of zebrafish *S*-adenosylhomocysteine hydrolase. *Development* 136: 865–875.

CHAPTER

10
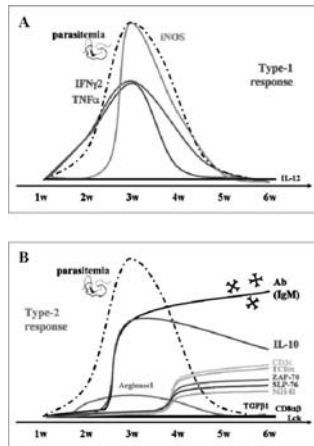
General Discussion

Maria Forlenza

Fish are the oldest vertebrate group that possesses all basic elements of the innate and adaptive immune system of higher vertebrates. The initial recognition of pathogens by molecules and cells of the innate immune system will ultimately lead to the development of an adaptive immune response characterized by specificity and memory formation. Specificity and memory are fundamental to vaccination, the best known and most successful application of immunological principles to human and animal health, including fish. This means that a fundamental interest in the evolution of immune mechanisms and, consequently, a detailed understanding of the fish immune system is essential for the correct implementation of prophylactic strategies, such as vaccination, in daily aquaculture practice. In this context, the use of natural (homologous) infection models is particularly relevant. A true understanding of relevant protective mechanisms, as well as kinetics of immune activation, can be achieved only by triggering the immune system with the appropriate stimulus. In this chapter we integrate the results obtained by the molecular and cellular analysis of the *Trypanoplasma borreli* infection model of carp and discuss the progress made on the understanding of the immune response to this parasite.

Nitric oxide: friend or foe?

There is no doubt that *the* most typical feature of *T. borreli* infections of carp is the induction of extremely high levels of nitric oxide (NO). As extensively discussed in this thesis, this parasite infection model provides a clear example of how an evolutionary established balance between parasite virulence and effectiveness of the immune response is required for both parasite persistence and host survival. Although, during the early stages of infection, NO can assist the host to gain time by reducing parasite motility, the NO-inducing ability of *T. borreli* clearly is an adaptation strategy of the parasite to induce immunosuppression and evade the host's immune system, without a direct negative effect on the parasite itself.

Noteworthy is the observation that *Trypanosoma carassii* (Kinetoplastida, Trypanosomatida), another natural parasite of carp, clearly does not induce NO, neither *in vitro* (1) nor *in vivo* (2, 3). We investigated the effects of NO donors (SNAP and GSNO) *in vitro* on the viability of this parasite and found that NO was highly trypanotoxic to *T. carassii* (Figure 1), which is in contrast to what was observed for *T. borreli* (*cf*. Fig. 7A, chapter 6). This experiment shows how related parasites, that can even share a common environment during mixed infections in a common host (2, 4), can opt for different
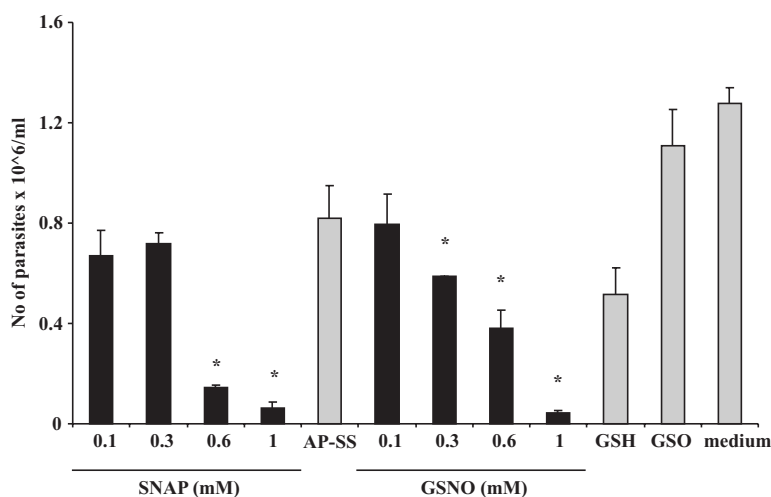
Figure 1. **Effects of NO donors on *Trypanosoma carassii* viability *in vitro*.** Freshly isolated parasites (clone K1, (5)) were seeded out at a density of 1×10^5 cells/well and incubated in the presence of different concentrations of NO donors, SNAP or GSNO, or with 1 mM of the respective control substances AP-SS or GSH and GSO. After 24h, parasite viability was measured microscopically by counting the number of viable parasites using a Bürker counting chamber. Data are expressed as absolute number of parasites per well. Values represent means and SD of triplicate wells of one representative experiment out of three independent experiments with similar results. Symbol (*), indicates significant differences relative to the respective control substance. Abbreviations: SNAP: S-nitroso-N-acetyl-D,L-penicillamine; AP-SS: N-acetyl-D,L-penicillamine disulphide; GSNO: S-nitroso-glutathion; GSH: reduced form of glutathione; GSO: oxidized form of glutathione.

adaptation strategies. Most likely *T. carassii*, differently from *T. borreli*, does not induce radical production in the host because apparently, the parasite itself did not develop an affective anti-oxidant system that would prevent its own damage. *T. carassii* rather chose a strategy where persistence (low parasitemia for a longer period of time) in the host provides the best chance of transmission to another host (6).

The fact that *T. borreli* induces high levels of NO must signify that this parasite evolved an effective anti-oxidant system which allows for protection against nitrosative damage. Although, so far, we have not been able to identify the components specifically involved in the anti-oxidant system of *T. borreli*, given the susceptibility of this parasite to the human anti-trypanosome drug, Arsobal, the trypanothione system represents the most plausible candidate. Although the effectivity of Arsobal against *T. carassii* has not been investigated yet, we have no reasons to believe the trypanothione system would not be present in *T. carassii* as well. However, qualitative or quantitative differences in trypanothione activity between *T. borreli* and *T. carassii* might account for the observed differences in

susceptibility to radicals between these two parasites. Physical barriers or additional anti-oxidant enzymes present in *T. borreli* only, might allow this parasite to tolerate better the high NO concentrations generated during infection (1, 4, 7).

Elevated nitric oxide production or serum nitrate/nitrite levels have also been associated with natural trypanosome infections of human and cattle and with experimental infections of mice. Whether NO was directly involved in parasitemia control, or in mediating immunosuppression, was strictly dependent on the animal species under investigation. Whereas experimental (non-homologous) murine infections with *T. congolense* clearly point towards a role for NO in both parasitemia control and immunosuppression (8), natural *T. congolense* infections of cattle indicates that NO is not involved in either of the two aspects (9, 10). In fact, in contrast to the mouse model, the capacity of bovine macrophages to produce NO is actually down-regulated in infected cattle. These apparently contrasting findings underline the importance of homologous infection models for the evaluation and extrapolation of experimental data to natural situations.

A question highly relevant to the understanding of the mechanisms leading to the high production of NO in the *T. borreli*-carp model is: *what triggers the production of NO?* Three possible mechanisms of NO induction which are not necessarily mutually exclusive will be touched upon: 1) direct stimulation of pattern recognition receptors (PRRs) by parasite components, 2) modification of host's proteins that would act as 'danger signals' and 3) indirect stimulation by induction of host cytokines such as TNFα and IFNγ. The latter mechanism will be more extensively dealt with later in this discussion.

The first mechanism is based on the fact that the innate immune system makes use of PRRs such as the Toll-like receptors (TLRs) to sense conserved molecular structures of invading pathogens (11) (12). TLRs are type I transmembrane proteins containing leucine-rich repeat motifs important for the recognition of pathogen associated molecular patterns (PAMPs). TLR2, at least in mammalian vertebrates, not only senses bacterial membrane components but also glycosyl-phosphatidyl-inositol (GPI) anchors from parasites (13, 14). Ongoing research in our laboratory is investigating the possibility that surface components of *T. borreli*, possibly GPI-anchors, would signal via TLR2 to induce NO in carp macrophages. TLR2 is one of the surface receptors implicated in macrophage activation typically leading to increased NO production (15). Preliminary data suggest that, indeed, supernatants from phosphatidylinositol-specific phospholipase C (PI-PLC)-treated parasites can up-regulate TLR2 gene expression in carp macrophages (C.M.S. Ribeiro, personal communication). Since also *T. carassii* has mucin-like GPI-anchored surface proteins (16),

future experiments will have to point out whether GPI anchors from *T. borreli* have a stronger capacity to stimulate PRR such as TLR2, leading to a higher production of NO in carp macrophages.

The second mechanism by which parasites can skew the immune response of the host towards an increased production of NO is the modification or degradation of self-derived components. Modified host proteins or degradation products can then act as 'alarmins' delivering a 'danger signal' to host immune cells, such as macrophages. Transferrin (Tf) cleavage products have been shown to induce NO production in goldfish (17) and carp (18) macrophages. In fact, digestion of Tf by elastase results in a 31 amino acid peptide derived from the N2 sub-domain of the Tf N-lobe, named TMAP. This fragment has been shown to induce chemotaxis, nitric oxide and TNFα secretion in different macrophage populations (19). It is well established that trypanosomes (*T. brucei*) need iron for growth and are dependent on the availability of Tf-bound iron for their survival (20). Trypanosomes can internalize Tf-bound iron *via* the flagellar pocket using specific Tf receptors (TfR) (21, 22). Once internalized, the Tf-TfR complex is transported to the lysosome where iron is released from Tf at acidic pH and Tf is proteolytically degraded. The resulting cleavage products are released to the circulation while the iron remains parasite-associated (23). We recently identified a *T. borreli*-specific cysteine proteinase and have shown that the activated recombinant enzyme digests carp Tf at acidic pH (24). At this moment, it remains to be proven whether TMAP-like peptides are present among the cleavage products most probably released also by *T. borreli*, and whether these fragments contribute to the induction of NO observed during infections.

We studied tissue tyrosine nitration as a marker of immunological activity resulting from increased NO production, by using an anti-nitrotyrosine antibody in combination with carp leukocyte sub-type specific monoclonal antibodies. This study revealed that not only macrophages but also carp neutrophilic granulocytes strongly contributed to *in vivo* tissue nitration, most likely through both, a peroxynitrite- and a myeloperoxidase-mediated mechanism. In humans, neutrophilic granulocytes constitute the major type of blood leukocytes, which does not seem to hold true for the blood of healthy carp. Although human neutrophils have been assigned a critical role in innate immunity through their phagocytosing capacity and release of various anti-microbial substances, they secrete lower amounts of cytokines than CD14^{+} monocytes (25). Fish neutrophils have been reported to possess a longer functional half-life than mammalian neutrophils (26), which may point at a different functional role for neutrophils of fish. Certainly, in *T. borreli*-infected carp,

neutrophilic granulocytes contribute to the production of nitric oxide and to tissue-associated pathology, possibly even to a larger extent than macrophages.

Regulation of nitric oxide production by cytokines: IFNγ and TNFα

As discussed above, it is likely that parasite components as well as modified host proteins directly stimulate PRRs on innate immune cells and trigger NO production. In addition, a modulating role for several cytokines, among which IFNγ and TNFα, should certainly be considered as third mechanism of NO induction. The importance of IFNγ signaling for the induction of TNFα and NO has been confirmed in numerous studies on African trypanosomiasis of mammals (8, 27-33). Presentation of parasite antigens by MHC-II can stimulate Th1 cells to secrete IFNγ that triggers the development of classically activated macrophages, which in turn produce a second signal, namely TNFα. The combination of IFNγ and TNFα signaling will then lead to the induction of iNOS expression in these macrophages. During experimental infections of mice with *T. congolense*, especially, the IFNγ-dependent NO production by classically activated macrophages is fundamental for parasite killing. Despite the well-documented trypanotoxic effects of NO *in vitro* (34), during experimental infections of mice with *T. brucei*, TNFα more than NO seems to be involved in parasite control (27, 28). In fact, TNFα has been shown to exert direct trypanotoxic effects against *T. brucei*, but not *T. congolense* (35, 36).

In our study, we reported an up-regulation of two isoforms of TNFα (TNFα1 and TNFα2) in spleen of *T. borreli*-infected carp, but we also concluded that carp TNFα might *not* be the major contributing factor to the production of high NO levels. Direct stimulation of carp macrophages with TNFα *in vitro* did not result in iNOS up-regulation, nor in increased NO production in macrophage culture supernatants. Furthermore, *in vivo* inhibition of TNFα gene expression by administration of a TNFα inhibitor (PTX) also did not influence iNOS gene expression. These findings excluded a direct effect of TNFα on the production of NO and suggest that parasite components or signaling factors other than TNFα should be responsible for the high induction of NO in *T. borreli*-infected carp.

In the mouse studies mentioned above, IFNγ-dependent activation of macrophages was essential for NO production during trypanosome infections. In carp, only very recently two IFNγ genes were reported and IFNγ2 was shown to share high structural and functional similarity with IFNγ from mammalian vertebrates (37). IFNγ2 gene expression was induced upon *in vitro* stimulation of carp leukocytes and mature thymocytes with the T cell mitogen PHA. Furthermore, recombinant carp IFNγ2 alone, or in combination with LPS, was shown

to induce iNOS gene expression and NO production in the supernatant of carp phagocytes (38). A preliminary study of IFNγ2 gene expression in *T. borreli*-infected carp, although only measured at one time point (3 weeks) post infection (p.i.), suggested the involvement of IFNγ2 during infection. We therefore analyzed the kinetics of IFNγ2 gene expression during the entire period of *T. borreli* infection and compared these results to the kinetics of gene expression of TNFα2, iNOS and IL-10 (Fig. 2). Both IFNγ2 and TNFα2 gene expression were significantly up-regulated already before the peak of parasitemia, increased to reach a maximum at 3 w.p.i. concomitantly with the peak of parasitemia (lower-right plot) and returned to control levels at 4 w.p.i. (TNFα2) or later (IFNγ2). The kinetics of iNOS gene expression followed a similar pattern. The kinetics of the IL-10 gene expression will be discussed later in this chapter.
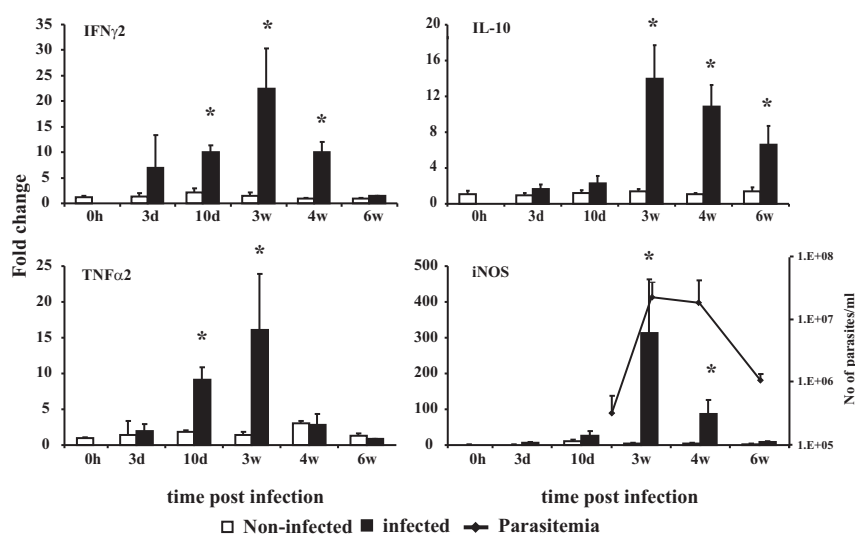
Figure 2. **Real-time quantitative PCR analysis of IFNγ2, IL-10, TNFα and iNOS gene expression in spleen after *in vivo* infection with *T. borreli*.** Fish (9-months-old, weighing 160 ± 20 g) were infected with 1×10^4 parasites/fish. At time point 0h, $n=5$ control fish and at various time points after infection, $n=5$ infected and $n=3$ non-infected fish were sacrificed. Parasitemia was monitored during infection and is shown in the upper right plot. Gene expression was normalized relative to the 40S ribosomal protein S11 as internal reference gene and expressed relative to non-infected fish at time point zero. Values are given as mean and SD. Symbol (*) indicates a significant difference relative to non-infected fish at the same time point. Note the difference in fold change (Y-axis) between the different genes. TNFα2 and iNOS gene expression are similar to figure 1 of chapter 9 and reported only to facilitate comparison.

Taken together, we hypothesize that upon infection with *T. borreli*, parasite antigens via MHC-II stimulate T cells to secrete IFNγ which triggers a classical activation of macrophages that, as a second signal, produce TNFα. Although TNFα does not seem to drive the expression of iNOS, the high production of NO certainly does correlate with a typical classical activation of macrophages. Furthermore, the ability of TNFα to activate endothelial cells (EEC) cannot be disregarded. In fact, production of TNFα by activated macrophages might stimulate EEC to secrete chemokines and promote leukocyte extravasation to the tissue, thereby contributing to the inflammation observed in peripheral organs. NO has been shown a potent vasodilatating agent in zebrafish (39), therefore high levels of NO in the blood might favor the extravasation of *T. borreli* to the tissue. This hypothesis is in accordance with the observation that *T. borreli* can penetrate peripheral organs during the late stages of infection, whereas *T. carassii*, which does not induce NO (1), is a 'hematic' parasite that is found exclusively in the blood circulation.

The present availability of recombinant carp TNFα as well as recombinant carp IFNγ, and availability of specific antibodies against TNFα and IFNγ provide new tools that will certainly contribute to a further elucidation of the role played by these two cytokines during infection with *T. borreli*. This infection model, because of the typically high NO response, seems extremely suitable for investigations on IFNγ-mediated activation of macrophages.

Regulation of nitric oxide production by cytokines: IL-10

In general, in a host-parasite relationship, both host and parasite are balancing their impact on the immune response to not only guarantee survival of the host but also to support persistence of the parasite. As discussed above, an early immune response driven by IFNγ and by the potential trypanocidal molecules TNFα and NO is essential to limit initial parasite replication. However, for a successful resolution of the infection and for parasite clearance, the production of specific antibodies, limitation of immune-mediated damage and,ultimately the generation of an anti-inflammatory immune response is essential (40). Fundamental to this switch is the anti-inflammatory cytokine IL-10 (28, 30, 41, 42). Studies with mammalian trypanosomes show that in the absence of a switch from an inflammatory to an anti-inflammatory response, the host succumbs to infection owing to an uncontrolled IFNγ production and inflammation-induced lesions (27, 28, 43).

The sequence for carp IL-10 has been described (44), and studies using the recombinant protein are presently ongoing. Investigation of the kinetics of IL-10 gene expression during *T. borreli* infection (Fig. 2) clearly shows a prolonged up-regulation of IL-10 in comparison

with the gene expression profiles of IFNγ, TNFα2 and iNOS. The kinetics of IL-10 gene expression correlates with the kinetics of antibody production, decreased parasitemia and reduced tissue nitration. This suggests a role for IL-10, in carp, in the down-regulation of the early inflammatory response and possibly also in the switch towards an anti-inflammatory response, as it will be more extensively discussed in the next section.

We also investigated the kinetics of gene expression in a carp strain (E4E5xR3R8) highly susceptible to *T. borreli* (45) (Fig. 3). To appreciate the difference in susceptibility; these carp were infected with 10 rather than with the usual 10^4 parasites per fish. In this carp strain, typically, all individuals reach parasitemia levels of $>10^7$ parasites/ml after 4-5 weeks and are unable to control parasitemia, that eventually leads to death. In contrast to what is usually observed in relatively resistant carp (R3xR8; Fig. 2), in highly susceptible carp IL-10 transcription was up-regulated prior to the peak of pro-inflammatory molecules and parasitemia. In addition, the level of TNFα gene expression was low in these carp.
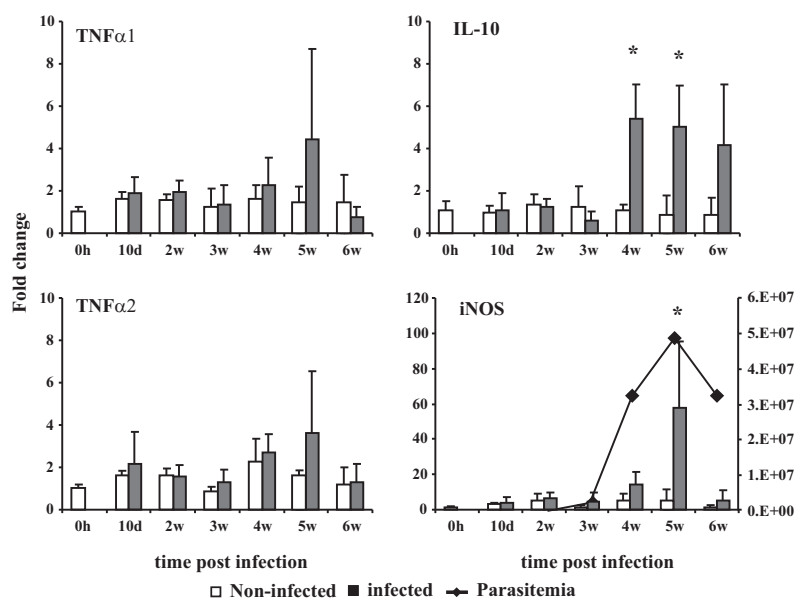
Figure 3. **Gene expression analysis in highly susceptible carp infected with *T. borreli*.** Real-time quantitative PCR analysis of gene expression in spleen from E4E5xR3R8 carp. Fish (9-months-old, weighing 170 ± 30 g) were infected with 10 parasites/fish. Data are presented as described in the legend of figure 2.

In African trypanosomiasis, IL-10 has been shown to exert a detrimental effect by mediating immunosuppression (46-48), but also to be beneficial by controlling excessive lethal release of cytokines such as IFNγ and TNFα (49-51). Although we have no conclusive evidence that IL-10 alone might be responsible for the high susceptibility of the particular (E4E5xR3R8) carp strain, the difference in the kinetics of IL-10 gene expression between relatively resistant and susceptible carp is striking. Our data suggests that an early presence of IL-10 during infection with *T. borreli* could induce a state of immunosuppression and, possibly, prevent the onset of an early inflammatory response important for parasite control.

Kinetics of type-1 and type-2 immune responses during *T. borreli* infections

In mammals, type-1 inflammatory responses are characterized by the development of (IFNγ-dependent-) classically activated macrophages and the subsequent production of reactive oxygen species, NO, IL-12 and TNFα by these cells. Type-2 anti-inflammatory responses, typically antagonize type-1 responses, and are driven by the development of (IL-4/IL-13- or IL-10-dependent-) alternatively activated macrophages and by the production of regulatory molecules such as TGFβ or IL-10 by these cells. The cytokine environment created by these differentially activated macrophages will determine the progression towards a cellular or a humoral response (52). Type-1 responses commonly are associated with intracellular pathogens (bacteria or viruses), whereas type-2 responses are associated with extracellular parasites (helminths or protoza). During infection, *adaptation* is an essential element of the host-parasite relationship. Extreme modulation or immunosuppression of the immune response by the parasite leads to unwanted death of the host or to overreactions of the immune system. Uncontrolled type-1 immune reactions may lead to an exacerbation of the inflammatory response, whereas uncontrolled type-2 immune responses may lead to immunosuppression.

A good example of a strict requirement for a balanced type-1/type-2 immune response is provided by experimental infection of mice with African trypanosomes (53-55). In these infections, a type-1 cytokine environment and classical macrophage activation in the early stage of infection is required, enabling mice to control the first peak of parasitemia. Thereafter, a switch to a type-2 cytokine environment triggering alternative macrophage activation is essential to enable B cell maturation for antibody production and trypanotolerance in the chronic phase of infection.
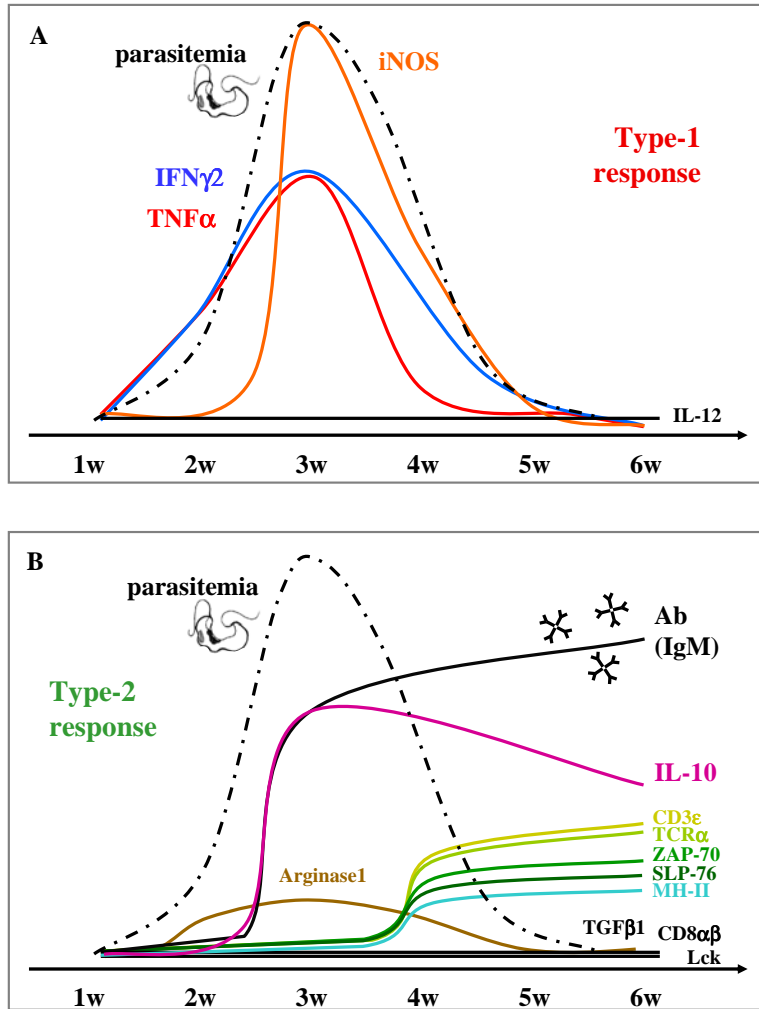
Figure 4. **Kinetics of Type-1 and Type-2 immune responses in carp during *T. borreli* infections.** A summary of the kinetics of expression of genes associated with type-1 (A) or type-2 (B) immune responses measured in spleen of infected fish is presented. During the type-1 response up-regulation of IFNγ2 in the presence of parasite antigens favors the development of classically activated macrophages (caMF) which in turn will increase their expression of TNFα and iNOS. IL-12, another cytokine associated with the development of caMF, was not up-regulated at any time during *T. borreli* infection. Starting at 3 weeks post infection (w.p.i.) up-regulation of IL-10, concomitantly with the generation of opsonizing parasite-specific antibodies, creates the optimal environment for the development of regulatory macrophages and the onset of a type-2 response. Regulatory macrophages will contribute to the down regulation of pro-inflammatory mediators, which is first observed at 4 w.p.i. and will favor the development of an adaptive humoral immune response. TGFβ does not seem to play a role in the regulatory phase of the response. A marginal up-regulation of T-cell-lineage-specific markers is observed during the late stages of infection indicative of an adaptive T cell response. Antibodies, in combination with complement (not shown) will finally determine the resolution of the infection.

We have previously shown that carp macrophages can polarize into innate and classically activated macrophages, based on the differential activity of iNOS and arginase, respectively (2, 3). Innate activation can be induced by a microbial trigger alone (*i.e.* LPS, parasite components), whereas classical activation is induced by a microbial trigger in combination with IFNγ (56, 57). As summarized in Fig. 4A, TNFα expression and without doubt NO production are typical of the early phase of *T. borreli*. Given the recently described activity of goldfish (58) and carp IFNγ (38) to induce NO in macrophages *in vitro*, and our present data on the early kinetics of IFNγ gene expression simultaneously with the presence of parasite antigens *in vivo*, we believe a prototypical classical macrophage activation occurs during *T. borreli* infection of carp.

Before we can analyze whether a type-2 anti-inflammatory response occurs during the later stages of *T. borreli* infections, some recent views have to be considered. The name originally given to macrophages that developed in the presence of IL-4 was 'alternatively' activated. However, this name implies that this would be the only other (alternative) way of macrophage activation. More recently, a new classification based on three fundamental macrophage activities important for maintaining homeostasis has been proposed. These activities are host defense, wound healing and immune regulation (57). Classically activated macrophages are associated with host defense and require IFNγ, as described above. Wound healing macrophages develop in the presence of IL-4 and IL-13 and exhibit arginase activity in response to tissue injury, or following an innate or an adaptive immune response. Regulatory macrophages can arise during the late stages of adaptive immune responses and are triggered by microbial agents and immune complexes (opsonized pathogens) but also by prostaglandins and phagocytosis of apoptotic cells, and are characterized but the production of high levels of the anti-inflammatory cytokine IL-10.

Two IL-4/13 loci have been described for teleost fish, although at this moment it is unclear whether the teleost IL-4/13 genes are orthologous to either IL-4 or IL-13, or whether these mammalian genes separated later in evolution (Ohtani et al, 2008: Immunogenetics 60: 383-397). As shown in Fig. 4B, arginase gene expression was only marginally up-regulated during infection and arginase activity in cyclicAMP-stimulated head kidney leukocytes isolated at various time points after *T. borreli* infection was not increased (2). Thus, based on the absence of increased arginase activity we conclude that wound-healing macrophages do *not* play an important role in the resolution of *T. borreli* infections. Identification of carp IL-4/IL-13 or identification of markers for wound-healing macrophages, such as chitinase-like protein YM1 or resistin-like molecule-α (RELMα)

(reviewed in (57)), should help to corroborate this hypothesis in the future. In contrast, our data do support the involvement of regulatory macrophages during later stages of the immune response to *T. borreli*, as shown by a profound up-regulation of IL-10, the presence of opsonized parasites which might act as activating immune complexes and the production of *T. borreli*-specific antibodies (Fig. 4B). Taken together, we conclude that a type-2 anti-inflammatory immune response occurs during the last phase of *T. borreli* infection, and that the down-regulation of the inflammatory response (IFNγ, TNFα, iNOS) is driven by the production of IL-10 by regulatory macrophages.

Kinetics of the adaptive immune response to *T. borreli*

The main mechanism suggested to control infections of mammals with African trypanosomes is the final production of parasite-specific antibodies, although most of the actual mechanisms are still under debate. African trypanosomes, however, have developed a very clever strategy particularly effective in evading the humoral immune response *i.e.* antigenic variation of their variant surface glycoprotein (VSG) (59, 60). By periodically changing their VSGs, trypanosome are initially not recognized by antibodies against VSG epitopes displayed on the former surface coat. New variant antigenic types (VATs) carry on the infection, whereas trypanosomes expressing the former coat are destroyed. Not only the production, but also the isotype of VSG-specific antibodies is crucial. In *T. brucei* and *T. evansi* infections opsonizing IgM, but in *T. congolense* infections opsonizing IgG is required to reduce the number of circulating parasites. A clear role for complement-mediated lysis could not be ascertained for trypanosome infections in mammals (61, 62). In *T. congolense* infections, IgG also facilitates antibody-mediated phagocytosis of opsonized parasites by Kupffer cells in the liver.

The humoral response to *T. borreli* is well documented. The production of *T. borreli*-specific (IgM) antibodies (45, 63), *T. borreli*-unrelated antibodies indicative of polyclonal B cell activation (45) and the presence of enlarged B cell areas in the spleen (7) have all been observed. There is no evidence that antigenic variation might occur also in *T. borreli* and therefore it cannot be a contributing factor to the large B cell proliferation. *T. borreli* infections are not characterized by a chronic phase, and fish that survive infections are protected upon re-infection. Classical complement activation plays a major role in protection against *T. borreli* and the importance of antibody-dependent complement-mediated lysis has been shown both *in vitro* (45) and *in vivo* (chapter 7). We have no evidence that (opsonised) *T. borreli* would be cleared in large numbers by macrophages in

the carp liver although occasionally, evidence of phagocytosed parasites can be noted in peripheral organs such as head kidney and liver (Fig. 5.) Previously, elimination of resident macrophages from the peritoneal cavity and liver, by intraperitoneal injection of clodronate-liposomes, was shown to render carp susceptible to opportunistic bacteria but not to *T. borreli* (64). This suggests that phagocytosis of *T. borreli* in the liver might not play a major role in parasite clearance. However, we do have clear indications that immune regulation and activation does take place in liver of infected fish. Cytokines found to be up-regulated in spleen, the organ of choice for most of the gene expression studies in this thesis, were also highly up-regulated in liver. In addition, IL-1β gene expression did not increase in spleen but did increase in liver (data not shown). Other genes including iNOS (7), several complement factors (chapter 7) and α2-macroglobulin (65) were also up-regulated in liver of infected carp. Possibly, liver macrophages isolated during the peak of parasitemia and incubated *in vitro* with opsonized parasites could phagocytose, reduce parasite motility or viability but also produce NO and maybe mediate antibody-dependent cell-mediated cytotoxicity. Certainly, the immune regulation and activation noted in liver of *T. borreli*-infect fish warrants a closer investigation of the liver in our infection model.
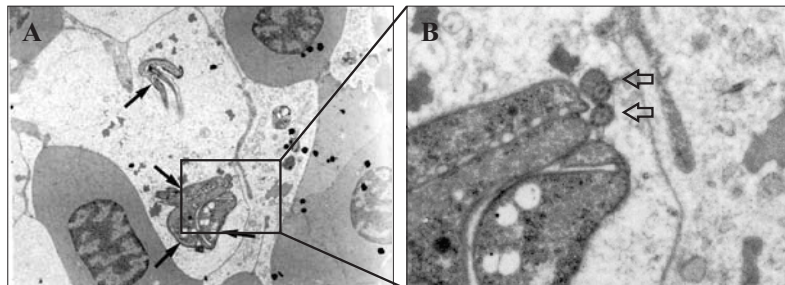
Figure 5.   Phagocytosis of *T. borreli* by tissue macrophages. Electron microscopy picture of *T. borreli* phagocytosed by a macrophage in head kidney of infected carp. A) Black arrows indicate the presence of 4 parasites in the cytoplasm of the macrophage. B) Enlarged view of the area boxed in figure A. Open arrows indicate the position of the basal bodies (similar to centrioles) identifying the position of the two flagella of *T. borreli*. (Magnification: 4400x)

During infection with *T. borreli* several T-cell-related genes are up-regulated, especially during the late phase of infection (Fig. 4B). We have also shown both a marked B and T cell proliferation in the spleen of infected fish. In trypanosome infections of mammals, T cell-dependent as well as T cell-independent mechanisms of B cell activation have been reported. The mechanisms underlining the B and T cell proliferation during *T. borreli*

infections are still unknown. Possibly, mitogenic parasite antigens or the presence of putative superantigens could be responsible for this pronounced lymphocyte activation, although to date substantial evidence in favor of this hypothesis is not available. Owing to a lack of suitable tools for their investigation, the functional T cell response to *T. borreli* is still poorly characterized. Only very recently, a system was optimized where carp kidney hematopoietic cells, co-cultured with a layer of feeder cells, proliferated and, after several passages, differentiated in cells belonging to the T cell-lineage as assessed by gene expression of GATA3, Lck and TCRβ (66). This system will certainly aid to the study of *T. borreli*-specific T cells responses, at least *in vitro*.

African trypanosomiasis is characterised by a state of general immunosuppression, well documented in *T. brucei*-infected mice and *T. congolense*-infected cattle (reviewed in (67)). During *T. congolense* infections, immunosuppression was found to occur primarily in the spleen and affects both humoral and cellular responses. Immunosuppression generally increases with progression of infection and it appears that both suppressor macrophages as well as antigen-specific suppressor T cells are responsible for the immunosuppressive effects. Also during *T. borreli* infections, immunosuppression can be observed as the inability to re-stimulate, *ex vivo*, cells isolated during the inflammatory phase of the infection (data not shown). Whether this suppression is mediated primarily by NO, macrophages, T cells, or by a combination of all will be the subject of further investigation. No doubt, modulation of adaptive reactions by ensuring immunosuppression of several components of the host humoral and cellular response, allows parasites to gain essential time to survive in the individual host, ensuring propagation within the population.

Future perspectives

Zebrafish and carp: non-identical twins

As argued in the introduction to this thesis, high quality infection models of inbred mouse strains have helped to pave the way for much of modern immunology. Although comparative immunology has profited to a great extent from the recent genome initiatives, advancement of fish immunology is still delayed by the use of several, phylogenetically distant, fish species as well as by the lack of inbred fish line and a limited set of reagents. Shared use of zebrafish as a common experimental animal besides selected fish species would certainly bring a much-needed higher level of standardization between different research laboratories. While zebrafish research initially centered on mutagenesis screens,

more recent years brought sophisticated reverse genetic methods such as morpholino knock-down or targeting induced local lesions in genomes (TILLING, see also Table 1). In addition, transgenic zebrafish have been developed and microarrays are now available to characterize gene experession on a near genome-wide scale. This suggests a meaningful interaction between zebrafish and aquacultural research should now be possible, although it is good to realize that zebrafish, in fact, is less closely related to most fishes of aquacultural interest (e.g. salmonids, sea bass, sea bream, cod, flatfishes) than those fish are among themselves (68). The only exception is carp, which is the most commonly cultured food-fish on the planet and is not only in the same Superorder but also in the same Family as zebrafish. Where zebrafish offers the advantage of a well-recognized low-cost animal model of vertebrate biology, the common carp, because of its large size, offers for example, the advantage of large numbers of leukocytes ($> 10^7$) for *in vitro* assays. Combination of the genetically tractable but small-sized zebrafish with the large-sized common carp would create a very strong combination of animal models that could address disease-related questions relevant to aquaculture such as vaccination, being based on increased understanding of fundamental immune mechanisms in comparative immunology.

The zebrafish genome has been sequenced and its annotation is continuously improved, gene microarrays and insertional mutants are commercially available, all of which are strong, mostly technical, arguments in favor of using the zebrafish as a model for animal physiology and development (Table 1). In addition, zebrafish is now gaining value as a model system also for immunological questions, not only for fish but also for mammals, particularly because of the ease of using embryonic stages to examine the development of immunity. External fertilization and small, transparent embryos allow for easy and non-invasive *in vivo* live-immaging observation up to the subcellular level. The translucency of the zebrafish embryos has facilitated the detection of fluorescently tagged transgenes and the monitoring of reporter gene activity. Similar to other teleosts, zebrafish are capable of adaptive immune reactions but the adaptive immune response requires several weeks to develop. This is often used as an argument to exclusively study innate immune responses in zebrafish, during the initial few days after fertilization. It is important to keep in mind, however, the limitation of studies in embryos only which creates an experimental and often unnatural division between innate and acquired immune responses that studies in adults do not suffer from. For that reason, the use of not only embryos but also adults in immunological studies using zebrafish should be strongly encouraged.

Table 1.   Common techniques used in zebrafish research

Technique	Description
FISH	Fluorescent in situ hybridization on whole-mount zebrafish embryos allows for simultaneous localization of gene expression patterns of two genes within the same embryo, permitting identification of colocalized expression within single cells
Microinjection of morpholino oligomers, preventing mRNA translation of targeted transcripts	Morpholinos are short oligomer sequences whose backbone is chemically modified, rendering them resistant to degradation by nucleases. This gene-specific knockdown antisense technology has proven to be a powerful tool for altering gene products and functions in zebrafish larvae. Knock-down is transient so the technique is not applicable to adult zebrafish.
Genetic screens	The method of choice for identifying genes with essential functions. Chemical mutagenesis can be used to generate loss-of-function phenotypes. Most mutants carry chemical (*N*-ethyl-*N*-nitrosourea; ENU)-induced mutations. Upon establishment of random mutant zebrafish lines, positional cloning can help to characterize the gene responsible for the stable phenotype.
TILLING	Targeting Induced Local Lesions IN Genomes (TILLING) is an important means by which mutations in specific genes of interest can be quickly identified and studied. The technique is effective to isolate mutants with defined mutations, and therefore can identify stable knock-out genotypes.
Injection of plasmid DNA	Can generate stable transgenics. Can be used to image spatiotemporal expression of fluorescent transgenes such as GFP in various organs and tissues.
Microarrays	Reflect a set of all mRNA transcripts actively being expressed at a given time-point following infection. Useful for transcriptome studies of infected animals.

One of the strongest observations made in this thesis was the crucial protective role for membrane TNFα (mTNFα) against infection of carp with *T. borreli*. In mammals, TNFα is first transported to the membrane and then cleaved by the TNFα converting enzyme TACE, to release soluble TNFα (sTNFα). Studies in fish have concentrated on *in vitro* activities of sTNFα and the presence and function of mTNFα was not considered so far. Interestingly, in experimental infection of mice with *Mycobacterium tuberculosis*, mTNFα has been shown sufficient to provide acute, but not long-term, control of infection (69, 70). In tuberculosis, mycobacteria are phagocytosed by macrophages that are modified by persistent cytokine signals (IFNγ) and that then recruit additional cells to form granulomas that eventually contain the infection. Of particular interest with respect to the elucidation of the protective mechanism mediated by mTNFα, is the natural infection model of zebrafish with *M. marinum*, a model for tuberculosis (71, 72). Using live *M. marinum*-infected embryos, loss of TNFα signaling was shown to cause increased mortality (73). TNFα was not required for tuberculous granuloma formation, but maintained granuloma integrity indirectly by restricting mycobacterial growth within macrophages and preventing their necrosis. Although these studies were performed in zebrafish embryos, limiting conclusions to innate

immunity, a recent microarray study showed a large overlap of expression signatures between infected embryos and adults, confirming the importance of innate immunity in mycobacterial infection (74). The high applicability of the zebrafish-*M. marinum* model and the fact that mTNFα can be sufficient to provide acute control of mycobacterial infection in mice, suggests that mycobacterial infection of zebrafish can be a good model to study mTNFα functions in fish.

We have shown that in carp, administration of a TACE-inhibitor *in vivo*, in the period preceding the peak of parasitemia, was sufficient to confer full protection against *T. borreli* infection. *In vitro*, we could also show that incubation of LPS-stimulated carp leukocytes with TACE inhibitor resulted in a significant increase of surface-bound TNFα. However, the cell types expressing mTNFα and the mechanisms underlining the protective effects observed during *T. borreli* infection are unknown. Zebrafish macrophages express TNFα, but Pu.1 morphant embryos lacking macrophages also express TNFα, indicating that other cell types beside macrophages can produce TNFα (75). The use of transgenic zebrafish expressing cell-lineage-specific fluorescent markers could help to elucidate the cell type(s) expressing mTNFα. In addition, the use of antibodies specifically recognizing carp B cells, granulocytes, macrophages, thrombocytes, immature thymocytes and mucosal T cells (76-79) could be a complementary tool to study the cellular source of mTNFα. Combination of the two animal model systems will certainly shed light on the role of mTNFα in fish.

For studies on mTNFα signaling, the *M. marinum* infection model of zebrafish certainly should be informative. The kinetics of granuloma formation are well characterized (71) and the importance of TNFα signaling through TNFα-receptor-1 (TNFR1) has already been demonstrated in this model (73). However, the question whether TNFR1-signaling is triggered by sTNFα or mTNFα has not been addressed. Application of a TACE inhibitor during *M. marinum* infection of zebrafish should help to investigate whether, similar to what has been observed in mice infected with M. *tuberculosis* (2, 3), mTNFα plays a role in cell migration, granuloma formation and control of infection, especially during the early phase of infection. In addition, a reverse genetic approach by administration of morpholinos directed against TNFR1 or TNFR2 in combination with a TACE inhibitor will reveal whether mTNFα signals preferentially via one TNFR in particular, or via both receptors. Signaling by mTNFα through binding of the TNFR is often associated with activation of NK (80, 81) and T cells (82) as well as macrophages (83) and the induction of cytotoxic activities. The rapid clearance of parasites observed during *T. borreli* infections can only be consistent with the involvement of cytotoxic mechanisms. In this respect, the zebrafish

model could provide crucial information to clarify receptor-mediated signaling of mTNFα and be instrumental for the development of future strategies such as production of anti-TNFR antibodies and recombinant soluble TNFR, or application of specific inhibitors of mTNFα or TNFR signaling with the aim to understand the mechanism of mTNFα-mediated protection during *T. borreli* infection.

An additional signaling mechanism described for mTNFα in mammals is 'reverse signaling' or 'bidirectional signaling' whereby the ligand acts as a receptor (84). In this process, cellular signals are transduced by the membrane-bound ligand upon interaction with a soluble or transmembrane receptor. Several members of the TNFα family, including mTNFα, have been shown to deliver an intracellular signal through a casein kinase 1 (CKI) motif (SX_2S) present in the cytoplasmic domain. In mammals, reverse signaling by members of the TNFα family described for B and T cells is generally of a stimulatory nature (85, 86), whereas for monocytes mainly inhibitory effects were observed (87, 88), indicating a differential role of this type of signal in adaptive and innate immunity. A putative CKI motif (SX_3S) could be identified in the cytoplasmic region of TNFα of several fish species, including carp and zebrafish (personal observation, data not shown). In fish TNFα, three but not two, intervening amino acids separate the two serine residues and at least one acid residue (required for optimal CKI activity) is present upstream of the N-terminal serine. At present, fourteen CK isoforms are annotated in the zebrafish database (data not shown), therefore all components required for the investigation of 'reverse signaling' by mTNFα are present, at least in zebrafish.

The drive to use zebrafish as animal model of vertebrate biology has primarily come from a fundamental interest in the evolution of immunity and developmental biology, however, the wish to address the use of adult zebrafish as animal model for studies in aquatic biology and life sciences is increasing. State-of-the-art techniques developed at technological zebrafish platforms, in combination with immunological research on closely related but larger sized carp will stimulate the development of a sustainable, environmentally and welfare-friendly aquaculture in the 21st century. It will do so by stimulating fundamental but strategic research in aquatic biology and life sciences.

References

1. Saeij, J. P., W. B. Van Muiswinkel, A. Groeneveld, and G. F. Wiegertjes. 2002. Immune modulation by fish kinetoplastid parasites: a role for nitric oxide. *Parasitology* 124:77-86.
2. Joerink, M., M. Forlenza, C. M. S. Ribeiro, B. J. de Vries, H. F. J. Savelkoul, and G. F. Wiegertjes. 2006. Differential macrophage polarisation during parasitic infections in common carp (*Cyprinus carpio* L.). *Fish Shellfish Immunol* 21:561-571.
3. Joerink, M., C. M. S. Ribeiro, R. J. M. Stet, T. Hermsen, H. F. J. Savelkoul, and G. F. Wiegertjes. 2006. Head kidney-derived macrophages of common carp (*Cyprinus carpio* L.) show plasticity and functional polarization upon differential stimulation. *J Immunol* 177:61-69.
4. Joerink, M., A. Groeneveld, B. Ducro, H. F. J. Savelkoul, and G. F. Wiegertjes. 2007. Mixed infection with *Trypanoplasma borreli* and *Trypanosoma carassii* induces protection: involvement of cross-reactive antibodies. *Dev Comp Immunol* 31:903-915.
5. Overath, P., J. Ruoff, Y. D. Stierhof, J. Haag, H. Tichy, I. Dykova, and J. Lom. 1998. Cultivation of bloodstream forms of *Trypanosoma carassii*, a common parasite of freshwater fish. *Parasitol Res* 84:343-347.
6. Wiegertjes, G. F., M. Forlenza, M. Joerink, and J. P. Scharsack. 2005. Parasite infections revisited. *Dev Comp Immunol* 29:749-758.
7. Forlenza, M., J. P. Scharsack, N. M. Kachamakova, A. J. Taverne-Thiele, J. H. W. M. Rombout, and G. F. Wiegertjes. 2008. Differential contribution of neutrophilic granulocytes and macrophages to nitrosative stress in a host-parasite animal model. *Mol Immunol* 45:3178-3189.
8. Magez, S., M. Radwanska, M. Drennan, L. Fick, T. N. Baral, F. Brombacher, and P. De Baetselier. 2006. Interferon-gamma and nitric oxide in combination with antibodies are key protective host immune factors during *Trypanosoma congolense* Tc13 Infections. *J Infect Dis* 193:1575-1583.
9. Taylor, K., V. Lutje, and B. Mertens. 1996. Nitric oxide synthesis is depressed in Bos indicus cattle infected with *Trypanosoma congolense* and *Trypanosoma vivax* and does not mediate T-cell suppression. *Infect Immun* 64:4115-4122.
10. Taylor, K. A. 1998. Immune responses of cattle to African trypanosomes: protective or pathogenic? *Int J Parasitol* 28:219-240.
11. Medzhitov, R. 2001. Toll-like receptors and innate immunity. *Nat Rev Immunol* 1:135-145.
12. Takeda, K., and S. Akira. 2005. Toll-like receptors in innate immunity. *Int Immunol* 17:1-14.
13. Campos, M. A., I. C. Almeida, O. Takeuchi, S. Akira, E. P. Valente, D. O. Procopio, L. R. Travassos, J. A. Smith, D. T. Golenbock, and R. T. Gazzinelli. 2001. Activation of Toll-like receptor-2 by glycosylphosphatidylinositol anchors from a protozoan parasite. *J Immunol* 167:416-423.
14. Debierre-Grockiego, F., M. A. Campos, N. Azzouz, J. Schmidt, U. Bieker, M. G. Resende, D. S. Mansur, R. Weingart, R. R. Schmidt, D. T. Golenbock, R. T. Gazzinelli, and R. T. Schwarz. 2007. Activation of TLR2 and TLR4 by glycosylphosphatidylinositols derived from Toxoplasma gondii. *J Immunol* 179:1129-1137.
15. Benoit, M., B. Desnues, and J. L. Mege. 2008. Macrophage polarization in bacterial infections. *J Immunol* 181:3733-3739.
16. Lischke, A., C. Klein, Y. D. Stierhof, M. Hempel, A. Mehlert, I. C. Almeida, M. A. Ferguson, and P. Overath. 2000. Isolation and characterization of glycosylphosphatidylinositol-anchored, mucin-like surface glycoproteins from bloodstream forms of the freshwater-fish parasite *Trypanosoma carassii*. *Biochem J* 345 Pt 3:693-700.
17. Stafford, J. L., N. F. Neumann, and M. Belosevic. 2001. Products of proteolytic cleavage of transferrin induce nitric oxide response of goldfish macrophages. *Dev Comp Immunol* 25:101-115.
18. Jurecka, P., I. Irnazarow, J. L. Stafford, A. Ruszczyk, N. Taverne, M. Belosevic, H. F. J. Savelkoul, and G. F. Wiegertjes. 2009. The induction of nitric oxide response of carp macrophages by transferrin is influenced by the allelic diversity of the molecule. *Fish Shellfish Immunol* 26:632-638.
19. Haddad, G., and M. Belosevic. 2009. Transferrin-derived synthetic peptide induces highly conserved pro-inflammatory responses of macrophages. *Mol Immunol* 46:576-586.
20. Schell, D., N. K. Borowy, and P. Overath. 1991. Transferrin is a growth factor for the bloodstream form of *Trypanosoma brucei*. *Parasitol Res* 77:558-560.
21. Steverding, D. 2000. The transferrin receptor of Trypanosoma brucei. *Parasitol Int* 48:191-198.
22. Henri, G. A. M. v. L., K. Rudo, M. m. Rainer, E. Markus, R. Bas ter, and B. Piet. 2005. Trypanosomes change their transferrin receptor expression to allow effective uptake of host transferrin. *Mol Microbiol* 58:151-165.
23. Grab, D. J., C. W. Wells, M. K. Shaw, P. Webster, and D. C. Russo. 1992. Endocytosed transferrin in African trypanosomes is delivered to lysosomes and may not be recycled. *Eur J Cell Biol* 59:398-404.

24. Ruszczyk, A., M. Forlenza, M. Joerink, C. M. S. Ribeiro, P. Jurecka, and G. F. Wiegertjes. 2008. *Trypanoplasma borreli* cysteine proteinase activities support a conservation of function with respect to digestion of host proteins in common carp. *Dev Comp Immunol* 32:1348-1361.

25. Smedman, C., B. Gardlund, K. Nihlmark, P. Gille-Johnson, J. Andersson, and S. Paulie. 2009. ELISpot analysis of LPS-stimulated leukocytes: human granulocytes selectively secrete IL-8, MIP-1beta and TNF-alpha. *J Immunol Methods* 346:1-8.

26. Lamas, J., and A. E. Ellis. 1994. Atlantic salmon (*Salmo salar*) neutrophil responses to *Aeromonas salmonicida*. *Fish Shellfish Immunol* 4:201-219.

27. Antoine-Moussiaux, N., S. Magez, and D. Desmecht. 2008. Contributions of experimental mouse models to the understanding of African trypanosomiasis. *Trends Parasitol* 24:411-418.

28. Stijlemans, B., M. Guilliams, G. Raes, A. Beschin, S. Magez, and P. De Baetselier. 2007. African trypanosomosis: from immune escape and immunopathology to immune intervention. *Vet Parasitol* 148:3-13.

29. Magez, S., M. Radwanska, M. Drennan, L. Fick, T. N. Baral, N. Allie, M. Jacobs, S. Nedospasov, F. Brombacher, B. Ryffel, and P. De Baetselier. 2007. Tumor necrosis factor (TNF) receptor-1 (TNFp55) signal transduction and macrophage-derived soluble TNF are crucial for nitric oxide-mediated *Trypanosoma congolense* parasite killing. *J Infect Dis* 196:954-962.

30. Namangala, B., P. De Baetselier, and A. Beschin. 2009. Both Type-I and Type-II Responses Contribute to Murine Trypanotolerance. *J Vet Med Sci* 71:313-318.

31. Yoshihara, K., A. Morris, F. Iraqi, and J. Naessens. 2007. Cytokine mRNA profiles in bovine macrophages stimulated with *Trypanosoma congolense*. *J Vet Med Sci* 69:421-423.

32. Vincendeau, P., and B. Bouteille. 2006. Immunology and immunopathology of African trypanosomiasis. *Anais da Academia Brasileira de Ciências* 78:645-665.

33. MacLean, L., M. Odiit, and Jeremy M. Sternberg. 2001. nitric oxide and cytokine synthesis in human african trypanosomiasis. *J Infect Dis* 184:1086-1090.

34. Vincendeau, P., S. Daulouede, B. Veyret, M. L. Darde, B. Bouteille, and J. L. Lemesre. 1992. Nitric oxide-mediated cytostatic activity on *Trypanosoma brucei gambiense* and *Trypanosoma brucei brucei*. *Exp Parasitol* 75:353-360.

35. Lucas, R., S. Magez, R. De Leys, L. Fransen, J. P. Scheerlinck, M. Rampelberg, E. Sablon, and P. De Baetselier. 1994. Mapping the lectin-like activity of tumor necrosis factor. *Science* 263:814-817.

36. Magez, S., M. Geuskens, A. Beschin, H. del Favero, H. Verschueren, R. Lucas, E. Pays, and P. de Baetselier. 1997. Specific uptake of tumor necrosis factor-alpha is involved in growth control of *Trypanosoma brucei*. *J Cell Biol* 137:715-727.

37. Stolte, E. H., H. F. J. Savelkoul, G. Wiegertjes, G. Flik, and B. M. L. Verburg-van Kemenade. 2008. Differential expression of two interferon-gamma genes in common carp (*Cyprinus carpio* L.). *Dev Comp Immunol* 32:1467-1481.

38. Verburg-van Kemenade, B. M. L., E. H. Stolte, J. A. Arts, E. Tijhaar, G. F. Wiegertjes, G. Flik, and H. F. J. Savelkoul. 2009. A genuine T-lymphocyte associated role for IFNγ-2 in carp (*Cyprinus carpio* L.). In *11th Congress of the International Society of Developmental and Comparative Immunology*, Prague, Czech Republic. p 71.

39. Fritsche, R., T. Schwerte, and B. Pelster. 2000. Nitric oxide and vascular reactivity in developing zebrafish, Danio rerio. *Am J Physiol Regul Integr Comp Physiol* 279:R2200-2207.

40. Belkaid, Y. 2007. Regulatory T cells and infection: a dangerous necessity. *Nat Rev Immunol* 7:875-888.

41. Noël, W., G. Hassanzadeh, G. Raes, B. Namangala, I. Daems, L. Brys, F. Brombacher, P. D. Baetselier, and A. Beschin. 2002. Infection stage-dependent modulation of macrophage activation in *Trypanosoma congolense*-resistant and -susceptible mice. *Infect Immun* 70:6180-6187.

42. Namangala, B., W. Noel, P. De Baetselier, L. Brys, and A. Beschin. 2001. Relative contribution of interferon-gamma and interleukin-10 to resistance to murine African trypanosomosis. *J Infect Dis* 183:1794-1800.

43. Magez, S., M. Radwanska, B. Stijlemans, H. V. Xong, E. Pays, and P. De Baetselier. 2001. A conserved flagellar pocket exposed high mannose moiety is used by African trypanosomes as a host cytokine binding molecule. *J Biol Chem* 276:33458-33464.

44. Ram, S., I. Daisuke, and S. Masahiro. 2003. Cloning, characterization and expression analysis of interleukin-10 from the common carp, *Cyprinus carpio* L. *European Journal of Biochemistry* 270:4647-4654.

45. Saeij, J. P., B. J. de Vries, and G. F. Wiegertjes. 2003. The immune response of carp to *Trypanoplasma borreli*: kinetics of immune gene expression and polyclonal lymphocyte activation. *Dev Comp Immunol* 27:859-874.

46. Uzonna, J. E., R. S. Kaushik, Y. Zhang, J. R. Gordon, and H. Tabel. 1998. Experimental murine *Trypanosoma congolense* infections. II. Role of splenic adherent CD3+Thy1.2+ TCR-alpha beta- gamma delta- CD4+8- and CD3+Thy1.2+ TCR-alpha beta- gamma delta- CD4-8- cells in the production of IL-4, IL-10, and IFN-gamma and in trypanosome-elicited immunosuppression. *J Immunol* 161:6189-6197.

47. Uzonna, J. E., R. S. Kaushik, J. R. Gordon, and H. Tabel. 1998. Immunoregulation in experimental murine *Trypanosoma congolense* infection: anti-IL-10 antibodies reverse trypanosome-mediated suppression of lymphocyte proliferation in vitro and moderately prolong the lifespan of genetically susceptible BALB/c mice. *Parasite Immunol* 20:293-302.

48. Shi, M. Q., G. J. Wei, and H. Tabel. 2007. *Trypanosoma congolense* infections: MHC class II-restricted immune responses mediate either protection or disease, depending on IL-10 function. *Parasite Immunol* 29:107-111.

49. Guilliams, M., G. Oldenhove, W. Noel, M. Herin, L. Brys, P. Loi, V. Flamand, M. Moser, P. De Baetselier, and A. Beschin. 2007. African trypanosomiasis: naturally occurring regulatory T cells favor trypanotolerance by limiting pathology associated with sustained type 1 inflammation. *J Immunol* 179:2748-2757.

50. Shi, M., G. Wei, W. Pan, and H. Tabel. 2006. Experimental African trypanosomiasis: a subset of pathogenic, IFN-gamma-producing, MHC class II-restricted CD4+ T cells mediates early mortality in highly susceptible mice. *J Immunol* 176:1724-1732.

51. Shi, M., W. Pan, and H. Tabel. 2003. Experimental African trypanosomiasis: IFN-gamma mediates early mortality. *Eur J Immunol* 33:108-118.

52. Martinez, F. O., A. Sica, A. Mantovani, and M. Locati. 2008. Macrophage activation and polarization. *Front Biosci* 13:453-461.

53. Baetselier, P. D., B. Namangala, W. Noël, L. Brys, E. Pays, and A. Beschin. 2001. Alternative versus classical macrophage activation during experimental African trypanosomosis. *Int J Parasitol* 31:574-586.

54. Noël, W., G. Raes, G. Hassanzadeh Ghassabeh, P. De Baetselier, and A. Beschin. 2004. Alternatively activated macrophages during parasite infections. *Trends Parasitol* 20:126-133.

55. Raes, G., A. Beschin, G. H. Ghassabeh, and P. De Baetselier. 2007. Alternatively activated macrophages in protozoan infections. *Curr Opinion Immunol* 19:454-459.

56. Martinez, F. O., L. Helming, and S. Gordon. 2009. Alternative activation of macrophages: an immunologic functional perspective. *Annu Rev Immunol* 27:451-483.

57. Mosser, D. M., and J. P. Edwards. 2008. Exploring the full spectrum of macrophage activation. *Nat Rev Immunol* 8:958-969.

58. Grayfer, L., and M. Belosevic. 2009. Molecular characterization, expression and functional analysis of goldfish (*Carassius aurutus* L.) interferon gamma. *Dev Comp Immunol* 33:235-246.

59. Antia, R., M. A. Nowak, and R. M. Anderson. 1996. Antigenic variation and the within-host dynamics of parasites. *Proc Natl Acad Sci U S A* 93:985-989.

60. Cross, G. A. 1996. Antigenic variation in trypanosomes: secrets surface slowly. *Bioessays* 18:283-291.

61. Baral, T. N., P. De Baetselier, F. Brombacher, and S. Magez. 2007. Control of *Trypanosoma evansi* infection is IgM mediated and does not require a type I inflammatory response. *J Infect Dis* 195:1513-1520.

62. Macaskill, J. A., P. H. Holmes, D. D. Whitelaw, I. McConnell, F. W. Jennings, and G. M. Urquhart. 1980. Immunological clearance of 75Se-labelled *Trypanosoma brucei* in mice. II. Mechanisms in immune animals. *Immunology* 40:629-635.

63. Wiegertjes, G. F., A. Groeneveld, and W. B. van Muiswinkel. 1995. Genetic variation in susceptibility to *Trypanoplasma borreli* infection in common carp (*Cyprinus carpio* L.). *Vet Immunol Immunopathol* 47:153-161.

64. Saeij, J. P., A. Groeneveld, N. Van Rooijen, O. L. Haenen, and G. F. Wiegertjes. 2003. Minor effect of depletion of resident macrophages from peritoneal cavity on resistance of common carp *Cyprinus carpio* to blood flagellates. *DAO* 57:67-75.

65. Onara, D. F., M. Forlenza, S. F. Gonzalez, K. Ł. Rakus, A. Pilarczyk, I. Irnazarow, and G. F. Wiegertjes. 2008. Differential transcription of multiple forms of alpha-2-macroglobulin in carp (*Cyprinus carpio*) infected with parasites. *Dev Comp Immunol* 32:339-347.

66. Katakura, F., F. Takizawa, M. Yoshida, T. Yamaguchi, K. Araki, M. Tomana, M. Nakao, T. Moritomo, and T. Nakanishi. 2009. Co-culture of carp (*Cyprinus carpio*) kidney haematopoietic cells with feeder cells resulting in long-term proliferation of T-cell lineages. *Veterinary Immunology and Immunopathology* In Press, Corrected Proof.

67. Tabel, H., G. Wei, and M. Shi. 2008. T cells and immunopathogenesis of experimental African trypanosomiasis. *Immunol Rev* 225:128-139.

68. Dahm, R., and R. Geisler. 2006. Learning from small fry: the zebrafish as a genetic model organism for aquaculture fish species. *Mar Biotechnol (NY)* 8:329-345.

69. Saunders, B. M., S. Tran, S. Ruuls, J. D. Sedgwick, H. Briscoe, and W. J. Britton. 2005. Transmembrane TNF is sufficient to initiate cell migration and granuloma formation and provide acute, but not long-term, control of *Mycobacterium tuberculosis* infection. *J Immunol* 174:4852-4859.

70. Fremond, C., N. Allie, I. Dambuza, S. I. Grivennikov, V. Yeremeev, V. F. Quesniaux, M. Jacobs, and B. Ryffel. 2005. Membrane TNF confers protection to acute mycobacterial infection. *Respir Res* 6:136.

71. Tobin, D. M., and L. Ramakrishnan. 2008. Comparative pathogenesis of *Mycobacterium marinum* and *Mycobacterium tuberculosis*. *Cellular Microbiology* 10:1027-1039.

72. Davis, J. M., and L. Ramakrishnan. 2009. The role of the granuloma in expansion and dissemination of early tuberculous infection. *Cell* 136:37-49.

73. Clay, H., H. E. Volkman, and L. Ramakrishnan. 2008. Tumor necrosis factor signaling mediates resistance to mycobacteria by inhibiting bacterial growth and macrophage death. *Immunity* 29:283-294.

74. van der Sar, A. M., H. P. Spaink, A. Zakrzewska, W. Bitter, and A. H. Meijer. 2009. Specificity of the zebrafish host transcriptome response to acute and chronic mycobacterial infection and the role of innate and adaptive immune components. *Mol Immunol* 46:2317-2332.

75. Clay, H., J. M. Davis, D. Beery, A. Huttenlocher, S. E. Lyons, and L. Ramakrishnan. 2007. Dichotomous role of the macrophage in early *Mycobacterium marinum* infection of the zebrafish. *Cell Host Microbe* 2:29-39.

76. Romano, N., J. J. Taverne-Thiele, J. C. Van Maanen, and J. H. M. W. Rombout. 1997. Leucocyte subpopulations in developing carp (*Cyprinus carpio* L.): immunocytochemical studies. *Fish Shellfish Immunol* 7:439-453.

77. Rombout, J. H. W. M., P. H. M. Joosten, M. Y. Engelsma, A. P. Vos, N. Taverne, and J. J. Taverne-Thiele. 1998. Indications for a distinct putative T cell population in mucosal tissue of carp (*Cyprinus carpio* L.). *Dev Comp Immunol* 22:63-77.

78. Secombes, C. J., J. J. van Groningen, and E. Egberts. 1983. Separation of lymphocyte subpopulations in carp *Cyprinus carpio* L. by monoclonal antibodies: immunohistochemical studies. *Immunology* 48:165-175.

79. van Diepen, J. C. E., G. T. M. Wagenaar, and J. H. W. M. Rombout. 1991. Immunocytochemical detection of membrane antigens of carp leucocytes using light and electron microscopy. *Fish Shellfish Immunol* 1:47-57.

80. Gersende, C., D. Yves, A. Jean-Pierre, M. Giovanni, H. Nathalie, B. Aline, M. Anthony, B. Jean-Yves, and J. Pascale. 1999. Human NK cells constitutively express membrane TNF-α (mTNFα) and present mTNFα-dependent cytotoxic activity. *Eur J Immunol* 29:3588-3595.

81. Xu, J., A. K. Chakrabarti, J. L. Tan, L. Ge, A. Gambotto, and N. L. Vujanovic. 2007. Essential role of the TNF-TNFR2 cognate interaction in mouse dendritic cell-natural killer cell crosstalk. *Blood* 109:3333-3341.

82. Georgopoulos, S., D. Plows, and G. Kollias. 1996. Transmembrane TNF is sufficient to induce localized tissue toxicity and chronic inflammatory arthritis in transgenic mice. *J Inflamm* 46:86-97.

83. Decker, T., M. L. Lohmann-Matthes, and G. E. Gifford. 1987. Cell-associated tumor necrosis factor (TNF) as a killing mechanism of activated cytotoxic macrophages. *J Immunol* 138:957-962.

84. Eissner, G., W. Kolch, and P. Scheurich. 2004. Ligands working as receptors: reverse signaling by members of the TNF superfamily enhance the plasticity of the immune system. *Cytok Growth Factor Rev* 15:353-366.

85. Harashima, S., T. Horiuchi, N. Hatta, C. Morita, M. Higuchi, T. Sawabe, H. Tsukamoto, T. Tahira, K. Hayashi, S. Fujita, and Y. Niho. 2001. Outside-to-inside signal through the membrane TNF-alpha induces E-selectin (CD62E) expression on activated human CD4+ T cells. *J Immunol* 166:130-136.

86. Suzuki, I., and P. J. Fink. 1998. Maximal proliferation of cytotoxic T lymphocytes requires reverse signaling through Fas ligand. *J Exp Med* 187:123-128.

87. Eissner, G., S. Kirchner, H. Lindner, W. Kolch, P. Janosch, M. Grell, P. Scheurich, R. Andreesen, and E. Holler. 2000. Reverse signaling through transmembrane TNF confers resistance to lipopolysaccharide in human monocytes and macrophages. *J Immunol* 164:6193-6198.

88. Lugering, A., M. Schmidt, N. Lugering, H. G. Pauels, W. Domschke, and T. Kucharzik. 2001. Infliximab induces apoptosis in monocytes from patients with chronic active Crohn's disease by using a caspase-dependent pathway. *Gastroenterology* 121:1145-1157.

English summary

Parasitism is a form of symbiotic relationship in which the parasite benefits while the host is harmed. In general, all living organisms can be hosts and can house microparasites (viruses, bacteria, fungi and protozoan) or macroparasites (helminths, arthropods and other metazoan), depending on the size of the host. In this thesis, we have studied three fundamentally different but natural (homologous) infection models of common carp (*Cyprinus carpio*). These included macroparasitic infection with the ectoparasite *Argulus japonicus* (arthropod) and microparasitic infections with spring viraemia of carp virus (SVCV) or *Trypanoplasma borreli* (protozoa). The *first* aim of the research described in this thesis was to develop both molecular and cellular tools to be implemented in the characterization of the innate and adaptive immune response of carp to infections. The *second* aim of this thesis was to integrate molecular and cellular approaches to investigate the immune response of carp to infections, taking into account the nature of the pathogen. In the second part of this thesis, we focused on one model in particular, *i.e.* infections with the extracellular blood parasite *T. borreli* (Parabodonida; Kinetoplastida).

In this thesis, we first reviewed the arguments in favor of studying experimental infection models to help reveal basic mechanisms in immunology (**chapter 1**) and argued that parasite infections in particular deserve more attention as model systems in comparative immunology. Over the last decade tremendous advances have been made in the field of comparative immunology especially owing to the progress made with molecular techniques and to the implementation of molecular approaches otherwise exclusive to mammalian immunology. These advancements included open access to genome information on a number of fish species including two pufferfish species (*Fugu rubripes, Tetraodon nigroviridis*), three-spined stickleback (*Gasterosteus aculeatus)*, medaka (*Oryzias latipes*) and zebrafish (*Danio rerio*), a close relative of carp, but also access to forward and reverse genetic approaches for studies on the development of immunity.

The combination of an increased amount of gene information and the development of a highly sensitive and accurate method to measure gene expression in real-time, has further pushed forward comparative immunology. Real Time-quantitative PCR (RT-qPCR) analysis has become the method of choice for quantitative and accurate measurement of mRNA expression levels. Indeed, RT-qPCR has been extensively used for the gene expression studies in this thesis and the most recent views on relative and absolute quantitation methods relevant for the analysis of gene expression data are discussed in **chapter 2**.

RT-qPCR was used to monitor the kinetics of immune gene expression during the immune response of carp to the macroparasite *A. japonicus* (**chapter 3**). Up-regulation of gene expression in the skin, of the chemokine CXCa, and to a lesser extent of the chemokine receptor CXCR1 and the cytokine tumor necrosis factor alpha (TNFα), proved to be a good indicator of parasite-induced skin damage and to correlate well with the increased number of neutrophilic granulocytes that migrated to the site of inflammation. In addition, we demonstrated that non-infected control skin samples isolated from infected fish should be considered for gene expression studies as suitable autologous controls.

Using a similar molecular approach, we proceeded with the gene expression analysis of selected immune genes during infection of carp with spring viraemia of carp virus (SVCV; *Rhabdoviridae*) (**chapter 4**). SVCV causes a severe infection of carp kept in aquaculture, with high mortalities especially at reduced water temperatures during spring. In this chapter, using a homology cloning approach, we reported the identification of cytotoxic T cell markers CD8α and CD8β, each present in duplicate copies in carp. RT-qPCR analysis pointed out the importance of interleukin-12, a cytokine with a crucial role

in the development of an effective cytotoxic T cell (CTL) response. Naïve CD8$^+$ T cells are activated by antigen (signal 1) and CD28 costimulation (signal 2) to undergo cell division, but programming for survival, effector function and memory requires a third signal that can be provided by IL-12 and/or type I interferons (IFN). The co-ordinated timing of expression of CD8 T cell markers and of IL-12 and type I IFN observed in chapter 4 provides evidence for an evolutionary conservation of function for these molecules to act as signal 3 cytokines during CTL activation in SVCV-infected carp.

Protection against SVC can be achieved by DNA vaccination, a prophylactic strategy that has proven particularly effective in fish. Although successful, DNA vaccination of carp against SVCV did not reach the high protection levels commonly observed for other rhabdoviruses. With this in mind, we proceeded with the characterization of the immune response of carp to DNA vaccination (**chapter 5**) using a recombinant plasmid encoding for the G protein of SVCV (SVCV-G). Common to all DNA vaccination studies is the early up-regulation of type I IFN-induced genes such as Mx (myxovirus resistance gene). Carp Mx1 cDNA was first identified in this study and indeed, carp Mx1 gene expression was up-regulated in fish that received the vaccine plasmid, but also in carp that received the empty plasmid only, possibly owing to the presence of stimulatory CpG motifs in the plasmid backbone. DNA vaccination against SVCV was successful but suboptimal, with a relative percent survival (RPS) of 66.7% and thus showed potential for further improvement. To this end, based on the results obtained in **chapter 4**, we report the construction of a recombinant plasmid encoding for a fused carp IL-12 heterodimer and discuss the possibility to co-administer carp IL-12 along with the SVCV-G DNA vaccine to serve as immunoadjuvant. All together, the data presented in **chapter 4** and **5** provide a good example of how the homologous infection model with SVCV allows for the extrapolation of experimental data towards a practical implementation of prophylactic strategies such as DNA vaccination, in aquaculture.

The *second* aim of the research described in this thesis was to investigate the balance between the immune response of the host to infection with *T. borreli*, and evasion strategies of the parasite itself. Infections with *T. borreli*, are typically characterized by the extreme (>100 fold) up-regulation of inducible nitric oxide synthase (iNOS) gene expression and by the presence of elevated serum nitrite levels. Consequently, tyrosine nitration dramatically increased in tissues from parasite-infected fish (**chapter 6**). Tyrosine nitration is considered a hallmark for nitrosative stress caused by the release of reactive oxygen and nitrogen species by activated leukocytes at sites of inflammation. The combined use of an anti-nitrotyrosine antibody with carp leukocyte sub-type specific monoclonal antibodies revealed that carp neutrophilic granulocytes strongly contributed to *in vivo* tissue nitration most likely through both, a peroxynitrite- and a myeloperoxidase-mediated mechanism. Conversely, fish macrophages, by restricting the presence of radicals and enzymes to their intraphagosomal compartment, contributed to a much lesser extent to *in vivo* tissue nitration. By the use of antibodies directed against carp B cells we could also investigated the B cell response in tissue of infected fish. Evident was the presence of enlarged B cell areas in correspondence of nitrated areas and the marked B cell proliferation in the spleen of infected fish. Our results are in line with previous reports describing polyclonal B cell activation and the production of antibodies against *T. borreli*-specific and *T. borreli*-unrelated antigens during infections.

The effects of nitrosative stress on the parasite itself (**chapter 6**) were different. *In vivo* nitration of *T. borreli* was limited, if not absent, despite the presence of parasites in highly nitrated tissue areas. We noted that only peroxynitrite, but not nitric oxide (NO) exerted strong cytotoxicity on the parasite *in vitro*. Treatment with Arsobal, a human anti-trypanosome drug which directly interferes with the parasite-specific trypanothione anti-oxidant system, immediately decreased viability of *T. borreli*. Clearance of surface-bound antibodies is one evasion mechanism that allows trypanosomes

to use their swimming movement to cause surface-bound antibodies to accumulate at the posterior end of the parasite, be internalized *via* the flagellar pocket and be degraded. Since high levels of NO lead to extensive tissue nitration in carp but did not seem to affect viability of *T. borreli*, we initially considered the high NO levels a parasite-driven evasion mechanism leading to immunosuppression. However, the induction of NO particularly during the early phase of *T. borreli* infections should be re-considered an effective part of the host immune response as demonstrated in **chapter 7**. We showed that at low NO concentrations *T. borreli* is able to rapidly remove surface-bound IgM. At moderate to high NO concentrations, however, surface-antibody clearance is hindered and IgM concentrations on the membrane of the parasites increase thereby favoring antibody-dependent complement-mediated parasite lysis.

In this thesis, we completed the missing information on the carp TCR complex by cloning TCR(α) and CD8($\alpha\beta$) (**chapter 4**) as well as CD3(ε), Lck and ZAP-70 (**chapter 8**). The T cell receptor (TCR) complex consists of a single TCR$\alpha\beta$ heterodimer associated with at least three CD3 dimers including $\gamma\varepsilon$, $\delta\varepsilon$ and $\xi\xi$ and includes the CD4 or CD8 co-receptors. The protein tyrosine kinases Lck and ZAP-70 provide essential signals in a cascade of events which will finally lead to T cell signalling and activation. Despite the rapid advancements on genetic information, making available the sequence coding for most of the components of the TCR complex, the number of antibodies available for the identification of T cells in carp is limited. Commercially available antibodies directed against a highly conserved prolin-rich region in the cytoplasmic tail of hCD3ε, the N-terminal region of ZAP-70 and the C-terminal region of Lck were tested for their ability to specifically recognize carp T cells. The anti-hZAP-70 antibody in particular, recognized carp T cells in both immunohistochemistry and flow cytometry and a 70 kDa protein by Western blot analysis. Owing to the high conservation of the relevant epitope, the anti-hZAP-70 antibody will most likely be applicable as a pan-T cell marker also to other fish species. Two antibodies directed against selected antigenic epitopes present in the extracellular region of carp CD4 and CD8α were raised in rabbits. Immunohistological analysis, using a combination of the anti-hCD3ε, anti-hZAP-70, anti-cCD4 and anti-cCD8α antibodies revealed a conserved picture of the structure of carp thymus. Despite their suitability for immunohistochemistry, both anti-cCD4 and anti-cCD8 did not show immunoreactivity to live T cells in flow cytometry and new immunization strategies are required to obtain monoclonal antibodies specifically recognizing carp CD4+ and CD8+ T cells. The anti-hCD3ε and anti-hZAP-70 were further selected to study T cell distribution in the spleen of *T. borreli*-infected carp with the aim to complement the information obtained in **chapter 6** on the B cell response to *T. borreli*. We showed the presence of not only enlarged B cell but also enlarged T cell areas in the spleen of infected fish. Double staining revealed that B and T cells lie intermingled to each other, with no clear distinction between a B or T cell zone, especially during infection. Despite the striking structural and functional similarity between the fish and mammalian thymus, the difference in cell distribution and organization in the spleen of fish was evident, leaving open a fundamental question concerning antigen presentation and the interaction between antigen presenting cells and cells of the adaptive immune system.

Upon RT-qPCR analysis, the up-regulation of both isoforms of carp TNFα (TNFα1 and TNFα2) in spleen of infected fish, drew our attention especially when considering the central role occupied by this cytokine in the immune system and more specifically in the immune response to trypanosome infections in mammals. Therefore, in the last part of this thesis (**chapter 9**), the biological activities of carp TNFα were studied both invitro and *in vivo*. Recombinant carp TNFα failed to directly stimulate typical receptor dependent activities of carp phagocytes such as the production of nitrogen and oxygen radicals. TNFα signaling, thus, could not explain the high NO induction observed in response to *T. borreli*. Recombinant carp TNFα did stimulate endothelial cells to increase expression of pro-inflammatory

cytokines, chemokines and adhesion molecules and TNFα-induced mediators from these cells stimulated the production of radicals in carp phagocytes directly but also when phagocytes were primed with TNFα. In addition, our results showed an evolutionary conservation of the receptor-independent lectin-like activity of TNFα. The role of TNFα *in vivo* during *T. borreli* infection was examined using three fundamentally different but complementary approaches: i) inhibition of TNFα gene expression, ii) overexpression of TNFα and iii) inhibition of shedding of membrane-bound TNFα (mTNFα). Our results showed a strict requirement for a tight regulation of TNFα expression during parasitic infection, since depletion or excess of TNFα made an important difference to survival. We demonstrated a crucial protective role for mTNFα, with a yet unexploited function in fish. The work described in **chapter 9** showed how a natural infection model has been instrumental to the understanding of the biological function of TNFα in carp. The availability of the *T. borreli* infection model proved fundamental for the *in vivo* approach which goes beyond the conventional *in vitro* investigation of biological activities of recombinant proteins. **Chapter 10** integrated the progress made in the understanding of the protective immune response of carp to infections, with particular attention to the *T. borreli* infection model. Future perspectives concerning the exploitation and implementation of other animal models such as zebrafish, alongside the carp animal model, were discussed.

Samenvatting

Parasitisme is een vorm van symbiotische relatie waarbij de parasiet profiteert ten nadele van de gastheer. In principe kunnen alle levende organismen functioneren als gastheer. Afhankelijk van hun grootte zijn ze gastheer van microparasieten (virussen, bacteriën, schimmels en andere eencelligen) of van macroparasieten (wormen, geleedpotigen en andere meercelligen). In dit proefschrift hebben we drie fundamenteel verschillende, maar allemaal natuurlijke (homologe) infecties van de gewone karper (*Cyprinus carpio*) bestudeerd. Dit waren een macroparasitaire infectie met de huidparasiet *Argulus japonicus* (geleedpotige) en microparasitaire infecties met *spring viraemia of carp virus* (SVCV) en *Trypanoplasma borreli* (eencelligen). De eerste doelstelling van het onderzoek zoals beschreven in dit proefschrift was het ontwikkelen van zowel moleculaire als cellulaire methoden die gebruikt konden worden voor een karakterisering van het aangeboren en verworven afweersysteem van de karper. De tweede doelstelling van dit proefschrift was het integreren van deze moleculaire en cellulaire methoden in het immunologisch onderzoek naar de afweer tegen een ziekteverwekker, maar ook in het onderzoek naar effecten op de ziekteverwekker zelf. In het tweede deel van dit proefschrift hebben we ons met name gericht op het infectiemodel met de extracellulaire bloedparasiet *T. borreli* (Parabonida; Kinetoplastida).

In dit proefschrift hebben we eerst gekeken naar argumenten voor het gebruik van experimentele infecties als onderzoeksmodel voor studies aan fundamentele mechanismes binnen de immunologie. In **hoofdstuk 1** hebben we beargumenteerd dat met name infecties met macroparasieten meer aandacht verdienen als experimenteel onderzoeksmodel in de vergelijkende immunologie. De tijdens het laatste decennium geboekte vooruitgang op het gebied van de vergelijkende immunologie is vooral te danken aan de progressie in een aantal moleculaire benaderingen die voorheen nog exclusief tot het terrein van de zoogdierimmunologie behoorden. Tot deze benaderingen behoren het verkrijgen van genoominformatie voor een aantal vissoorten waaronder twee kogelvis soorten (*Fugu rubripes*, *Tetraodon nigroviridis*), de driedoornige stekelbaars (*Gasterosteus aculeatus*), het rijstvisje (*Oryzias latipes*) én de nauw aan de karper verwante zebravis (*Danio rerio*), maar ook toegang tot 'forward' en 'reverse' genetische benaderingen voor studies aan de ontwikkeling van het afweersysteem. De vergaande genoominformatie in combinatie met de ontwikkeling van een zeer gevoelige methode voor het meten van genexpressie door middel van PCR in de tijd ('real time quantitative PCR'), heeft de ontwikkeling van de discipline 'Vergelijkende immunologie' sterk gestimuleerd. RT-qPCR analyse is de methode bij uitstek geworden voor accurate metingen van mRNA niveaus. In dit proefschrift is de RT-qPCR methode dan ook veelvuldig gebruikt voor genexpressie studies en de meest recente inzichten en de aan deze techniek gerelateerde rekenmethoden zijn bediscussieerd in **hoofdstuk 2**. In dit proefschrift is de RT-qPCR methode bijvoorbeeld gebruikt om de kinetiek in expressie van immuun genen te volgen tijdens de afweerrespons van de karper tegen de macroparasiet *A. japonicus* (**hoofdstuk 3**). Het bleek dat toename van genexpressie in de huid van met name het chemokine CXCa, en in mindere mate van de chemokine receptor CXCR1 en het cytokine tumor necrose factor alfa (TNFα), goede indicatoren waren van door de parasiet veroorzaakte huidbeschadiging. De toename in genexpressie kwam goed overeen met het toegenomen aantal neutrofiele granulocyten dat migreerde naar de plaats van ontsteking. Ook konden we aantonen dat huidmonsters, weliswaar genomen van geïnfecteerde vissen maar dan op niet-geïnfecteerde plekken op de huid, uitermate goed dienst kunnen doen als autologe controles.

Gebruik makend van een vergelijkende moleculaire aanpak zoals homologe klonering, zijn we verder gegaan met de genexpressie analyse van geselecteerde immuun genen tijdens infectie van de

karper met het virus SVCV (*Rhabdovirideae*) (**hoofdstuk 4**). SVCV is de oorzaak van een ernstige infectie van met name in de aquacultuur gehouden karpers met soms hoge sterfte, gerelateerd aan een lage watertemperatuur in de lente en wordt daarom in het Nederlands ook wel voorjaarsviremie genoemd. In dit hoofdstuk meldden we de identificatie van merkers voor de cytotoxische T cel: CD8α and CD8β, beiden als twee kopieën aanwezig in het transcriptoom van de karper. Onze RT-qPCR analyse liet het belang zien van interleukine-12, een cytokine met een cruciale rol in de ontwikkeling van een effectieve cytotoxische T cel (CTL) respons. Naïve CD8+ T cellen worden geactiveerd door antigeen (signaal 1) en costimulatie middels CD28 (signaal 2) om daarna tot celdeling over te gaan. Echter, de programmering van deze cellen voor overleving, effector functies en geheugenvorming heeft een derde signaal nodig, geleverd door IL-12 en/of een type I interferon (IFN) cytokine. Zoals beschreven in hoofdstuk 4 komen de genen voor CD8 en de genen voor IL-12 en type I IFN op hetzelfde tijdstip tot expressie. Dit kan als bewijs gezien worden voor een evolutionair geconserveerde rol van deze moleculen als signaal 3 cytokine tijdens de activatie van CTL in door SVCV geïnfecteerde karpers.

Bescherming tegen SVCV kan bereikt worden door middel van DNA vaccinatie, een profylactische strategie met bewezen effectiviteit in vissen. Hoewel succesvol, gaf DNA vaccinatie van de karper tegen SVCV niet het hoge beschermingsniveau dat normatiler gevonden wordt voor andere rhabdovirussen. Daarom hebben we de immuunresponsen van de karper na DNA vaccinatie in meer detail bestudeert (**hoofdstuk 5**), waarbij we gebruik gemaakt hebben van een recombinant plasmide dat codeert voor het G eiwit van SVCV (SVCV-G). Gebruikelijk voor alle DNA vaccinatie studies is de vroege opregulatie van type I IFN geïnduceerde genen zoals Mx ('myxovirus resistance gene'). De sequentie van het cDNA voor Mx1 van de karper was nog niet eerder beschreven. De expressie van dit gen bleek inderdaad opgereguleerd in vissen behandeld met het vaccin plasmide, maar ook in karpers behandeld met het lege controle plasmide, mogelijk door de aanwezigheid van CpG motieven in de plasmide zelf. DNA vaccinatie tegen SVCV bleek succesvol maar suboptimaal met een relatief overlevingspercentage van 66.7% en biedt dus mogelijkheden voor verdere verbetering. Met name de resultaten beschreven in hoofdstuk 4 leidden tot de constructie van een recombinant plasmide dat codeert voor een IL-12 heterodimeer en in hoofdstuk 5 hebben we vervolgens de mogelijkheid bediscussieerd om karper IL-12 toe te dienen als immuno-adjuvant tegelijk met het SVCV-G DNA vaccin. Samengevat zijn de **hoofdstukken 4** en **5** een goed voorbeeld van hoe belangrijk een homoloog infectiemodel zoals voorjaarsviremie kan zijn voor een extrapolatie van experimentele data naar een praktische toepassing van profylactische strategieën zoals DNA vaccinatie in de aquacultuur.

Het tweede doel van het onderzoek zoals beschreven in dit proefschrift was het bestuderen van de balans tussen het afweersysteem van de gastheer en de parasiet *T. borreli*, alsook ontwijkingstrategieën van de parasiet zelf. Infecties met *T. borreli* worden gekenmerkt door een extreme opregulatie (>100 keer) van het geïnduceerde stikstofmonoxide synthase ('iNOS') gen en door de aanwezigheid van verhoogde nitriet waarden in het serum van de karper. Als gevolg hiervan vindt er een dramatische verhoging plaats van tyrosine nitratie in het weefsel van vissen geïnfecteerd met de parasiet (**hoofdstuk 6**). Tyrosine nitratie kan worden beschouwd als een kenmerk van nitrosatieve stress, veroorzaakt door de afgifte van zuurstof en stikstof radicalen door geactiveerde leukocyten op de plaats van een ontsteking. Door een anti-nitrotyrosine antilichaam te combineren met monoklonale antilichamen specifiek voor bepaalde subtypes leukocyten konden we laten zien dat in de karper vooral neutrofiele granulocyten sterk bijdragen aan de nitratie *in vivo*, waarschijnlijk via een peroxynitriet- en een myeloperoxidase-gemedieerd mechanisme. Macrofagen daarentegen, beperken de aanwezigheid van radicalen en enzymen tot het fagosoom, waardoor zij een minder grote bijdrage leveren aan *in vivo* nitratie. Door gebruik te maken van antilichamen specifiek voor B lymfocyten van de karper konden we ook deze respons onderzoeken in het weefsel van geïnfecteerde vissen. Wat opviel was de proliferatie van B

cellen in de milt van geïnfecteerde vissen en de aanwezigheid van vergrote B cel gebieden binnen een genitreerde omgeving. Onze resultaten komen overeen met eerdere publicaties over een polyklonale B cel stimulatie en de productie van *T. borreli*-specifieke maar ook aspecifieke antilichamen gedurende infecties met *T. borreli*.

Het effect van nitrosatieve stress op de parasiet zelf (**hoofdstuk 6**) bleek verschillend van de hierboven beschreven effecten op karper leukocyten. *In vivo* bleef de nitratie van *T. borreli* zelf beperkt, of was zelfs afwezig, ondanks het feit dat de parasieten veelvuldig aanwezig waren in sterk genitreerde gebieden. *In vitro* zagen we dat alleen peroxynitriet, maar niet stikstofmonoxide (NO) een sterk cytotoxisch effect op de parasiet had. Behandeling met Arsobal, een humaan anti-trypanosoom geneesmiddel dat het anti-oxidant systeem van deze parasieten (trypanothion) verstoort, had onmiddellijk een negatief effect op de de levensvatbaarheid van *T. borreli*. Trypanosomen hebben een strategie waarmee ze het immuunsysteem kunnen ontwijken, waarbij ze oppervlakgebonden antilichamen verwijderen. Door gebruik te maken van hun zwembeweging hopen oppervlakgebonden antilichamen zich op aan het posterieure einde van de parasiet om te worden opgenomen in de zak waarin de flagel zich bevindt en daarna te worden afgebroken. Eerder zagen we dat hoge NO waardes leiden tot een sterke toename van nitratie van het weefsel, maar niet tot een verminderde levensvatbaarheid van de *T. borreli* parasiet zelf. Daarom beschouwden we in eerste instantie de hoge NO waardes als een parasietgestuurde ontwijkingstrategie die leidt tot onderdrukking van het afweersysteem. Echter, zoals aangetoond in **hoofdstuk 7,** zou met name de vroege NO inductie tijdens *T. borreli* infecties beschouwd moeten worden als een effectief deel van de immuunreacties van de gastheer. In hoofdstuk 7 lieten we zien dat bij lage NO concentraties *T. borreli* nog in staat is om in snel tempo oppervlakgebonden IgM te verwijderen. Maar bij middelmatig tot hoge NO concentraties wordt het verwijderen van oppervlakgebonden antilichamen verhinderd en neemt de IgM concentratie op het membraan van de parasiet toe, waardoor de antilichaam-afhankelijke complement-gemediëerde lysis van de parasiet wordt verhoogd.

In dit proefschrift hebben we de informatie die nog ontbrak aan het karper TCR complex aangevuld door de T cel receptor genen TCR(α) en CD8($\alpha\beta$) (**hoofdstuk 4**) en CD3(ϵ), Lck en ZAP-70 te kloneren (**hoofdstuk 8**). Het TCR complex bestaat uit een enkele TCR$\alpha\beta$ heterodimeer geassocieerd met minstens drie CD3 dimeren waaronder $\gamma\epsilon$, $\delta\epsilon$ en $\xi\xi$ en omvat de CD4 en CD8 coreceptoren. De eiwit tyrosine kinases Lck en ZAP-70 geven belangrijke signalen door in de cascade van gebeurtenissen die uiteindelijk leiden tot T cel activatie. Ondanks de recente toename in de beschikbare genetische informatie voor wat betreft het merendeel van de componenten van het TCR complex, is het aantal beschikbare antilichamen voor de identificatie van T cellen in de karper nog steeds sterk gelimiteerd. Wij testten een aantal commercieel beschikbare antilichamen gericht tegen de sterk geconserveerde proline-rijke regio in het cytoplasmatische deel van hCD3ϵ, in de N-terminale regio van ZAP-70 en in de C-terminale regio van Lck op geschiktheid voor het herkennen van karper T cellen. Het anti-hZAP-70 antilichaam herkende karper T cellen in zowel immunohistochemie en flow cytometrie en reageerde met een eiwit van 70 kDa in Western blot analyse. Dankzij de sterke evolutionaire conservering van het relevante epitoop, zal het anti-hZAP-70 antilichaam hoogst waarschijnlijk ook toepasbaar zijn voor andere vissoorten als een algemene T-cel marker. Twee nieuwe antilichamen werden opgewekt in konijnen tegen geselecteerde antigen epitopen in het extracellulaire gebied van zowel karper CD4 en CD8α. Immunohistologische analyse, gebruikmakend van een combinatie van anti-hCD3ϵ, anti-hZAP-70, anti-cCD4 en anti-cCD8α antilichamen, liet een geconserveerd beeld zien van de thymus van de karper. Ondanks hun bruikbaarheid voor immunohistochemie, lieten de anti-cCD4 en anti-cCD8 konijnen antilichamen geen reactiviteit zien voor T cellen in de flow cytometer. Daarom zijn nieuwe immunisatie strategieën nodig om monoklonale antilichamen te verkrijgen die wel specifiek CD4+ en CD8+ T cellen van de karper kunnen herkennen. De anti-hCD3ϵ en anti-hZAP-70 werden gebruikt om

de distributie van T cellen te bestuderen in de milt van *T. borreli* geïnfecteerde karpers met als doel meer informatie te krijgen over de in **hoofdstuk 6** gerapporteerde B cel respons tegen *T. borreli*. We konden laten zien dat in de milt van geïnfecteerde vissen niet alleen de B cel maar ook de T cel gebieden toenamen in grootte. Dubbelkleuring liet zien dat, met name tijdens infectie, de B en T cellen door elkaar lagen, zonder duidelijk onderscheid tussen een B en T cel zone. Ondanks het geconserveerde beeld voor de thymus van de karper, was het verschil in distributie en organisatie van de leukocyten in de milt opvallend. Dit vraagt om nader onderzoek met betrekking tot antigen presentatie en de interactie tussen antigen presenterende cellen en cellen van het verworven immuunsysteem van de karper.

De door RT-qPCR analyse waargenomen opregulatie van beide vormen van het cytokine tumor necrose factor alfa (TNFα1 en TNFα2) in de milt van geïnfecteerde karpers trok de aandacht, vooral omdat dit cytokine zo'n centrale rol inneemt binnen het immuunsysteem, met name in de afweer tegen trypanosoom infecties van zoogdieren. Daarom hebben we in het laatste deel van dit proefschrift (**hoofdstuk 9**) de biologische activiteiten van karper TNFα nog eens nader bestudeerd, zowel *in vitro* als *in vivo*. Recombinant karper TNFα kon niet de typisch receptorafhankelijke activiteit van karper fagocyten, zoals de productie van stikstof en zuurstof radicalen, stimuleren. Verhoogde concentraties van TNFα vormen dus geen verklaring voor de hoge concentraties aan stikstof radicalen tijdens infectie met *T. borreli*. Recombinant karper TNFα kon wel de genexpressie in endotheelcellen stimuleren van pro-inflammatoire cytokines, van chemokines en van adhesie moleculen. Als endotheelcellen gestimuleerd werden met TNFα dan kon het supernatant van deze cellen de productie van radicalen stimuleren in karper fagocyten, vooral als deze fagocyten vooraf gestimuleerd werden met TNFα. Tevens konden we een evolutionaire conservering laten zien van de receptoronafhankelijke 'lectine' activiteit van TNFα. De rol van TNFα *in vivo* tijdens *T. borreli* infectie werd bestudeerd middels drie fundamenteel verschillende, maar complementaire benaderingen: i) inhibitie van TNFα genexpressie, ii) overexpressie van TNFα en iii) inhibitie van 'shedding' van membraangebonden TNFα. In dit hoofdstuk konden we laten zien hoe belangrijk het is dat TNFα genexpressie nauwkeurig gereguleerd wordt tijdens een parasitaire infectie; de aanwezigheid van te weinig maar ook overmaat TNFα had een grote invloed op de overleving van de gastheer. Verder toonden we aan dat mTNFα een cruciaal beschermende rol heeft, met een nog niet in vissen benutte functie. Het werk in **hoofdstuk 9** laat zien hoe belangrijk een natuurlijke infectie kan zijn voor het beter begrijpen van de biologische functie van TNFα in de karper. De beschikbaarheid over het *T. borreli* infectiemodel bleek essentieel voor de *in vivo* benadering, waarbij we verder konden gaan dan de conventionele benadering met *in vitro* onderzoek naar de biologische activiteit van recombinante eiwitten. In **hoofdstuk 10** is getracht de opgedane kennis van de beschermende immuunresponsen tegen met name *T. borreli* te integreren tot één geheel. Als laatste zijn de toekomstperspectieven van andere diermodellen zoals de zebravis, naast die van de karper, bediscussieerd.

Acknowledgments

enthusiasm and for the great collaboration that has started. Thank you also for being so sportive when Spain won over Italy at the European Football Championship, *that* was a tough evening. I know you are now a full-time father but do not even consider skipping the Fish Workshop! **Fran**, thank you for your help with the TNF, it would have been nice to have you in our group but I am sure we will have plenty of occasions to collaborate and keep in touch. **Niels,** if I now like also viruses so much it is definitely thank to you!! The enthusiasm and dedication you show in your work, in your presentations and in all discussions we had, really made me think to the way *I* want to contribute to fish immunology. Together with you, Thomas and Dasa a very nice collaboration has started which I really hope will last for long. So I guess you won't get rid of me too soon, ci vediamo presto ;-) **Miki**, it took some time but we did manage to write a paper together and I am so proud of it. Thank you for being open, for sharing your sequences and for your enthusiasm about our future collaborations. See you in Fukuoka in 2012! **Stefan**, thank you so much for the crucial help with the TNFα paper, one of the happiest days of my PhD was indeed when you told me that the trypanolysis assay was working!!! It was also nice to finally be able to talk 'in parasite terms' with somebody who knew about it and is in love with these little creatures as much as I am ;-) Talking and working with you has inspired me since the beginning and now, at the end of my PhD, I have so many ideas and I really hope I will get the chance to develop them; maybe in collaboration with you and maybe who knows, you might start liking fish trypanosomes as well ;-) **Uwe** and **Bernd**, thank you for your enthusiasm, for your support, for being open, willing to share and collaborate. Uwe, after all your explanations at the Fish Workshop I finally think I have understood the cytotoxicity test ;-) Bernd I really hope your new tricks will make a difference to make antibodies against T cells in fish, so I am really looking forward to work on it together ;-) Thank you to all product specialists of **Westburg** who greatly contributed to the set up of the RQ-PCR in our lab, and in particular to **Monique** and **Albert**, thank you for your patience for the billions of questions and for your great professionalism. **Sjo**, thank you for always being available for a quick question on EPC, endothelial cells, media… and for being willing to help whenever is possible. Who knows, maybe one day we can try again with IL-10 ;-)

Work would not be fun if you do not meet funny people! A special thank therefore goes to some (ex-)colleagues, who I can certainly call friends! **The Danish delegation!** Be sure that if they kick me out of The Netherlands I'll come to Denmark!!! **Michael**, the macho-man. Thank you for the fruitful discussion especially about the *Argulus* experiment. A meeting or a conference without you is not the same, so I hope we will manage to keep the collaboration strong. Thank you also for all the fun, the exquisite dinners, dinner in the dark, dancing and for being one of the few who understands that also women like having muscles and driving fast cars ;-) **Thomas**, thank you for all your smiles, the fun, the dinners, the dances and for coping with Michael ;-) Although you left the 'fish world' I still know where to find you ;-). **Jeannette**, one of the most beautiful women I know! (I guess I can say that even if I am a woman, right?) ;-) You know I have a lot to thank you but I guess simple words would not be enough. Whenever you run out of stroopwafels just ring a bell and I'll get them to you. **Katja**, every time I drink a glass of water you can be sure I think about you ;-) Thank you for the great after-IMAQUANIM-meetings drinks, chats and laughs ;-) Thank you for coming over to my house and for the moral support during the last period while writing my thesis, a nice energy-power e-mail was always welcome!

Of course I cannot forget to thank the many people who have directly or indirectly contributed to this thesis just by simply having supported me in different ways in my life outside work. **Pim**, my sbm, we know each other since so long and we are still learning about the other. You are an incredible man! I have learnt a lot and I have changed a lot since I met you, hopefully for the better ;-) Thank you for your (infinite) patience, for the many fights we have, and for the many advices (maybe I should have followed more of those). Thank you for sharing your music and your paintings with me, for letting me help with the Painted Dogs association and for turning every visit to a museum into a great, pleasant

List of publications

M. Forlenza, S. Magez, J.P. Scharsack, A.H. Westphal, H.F.J. Savelkoul and G.F. Wiegertjes. **2009.** Receptor-dependent and Lectin-like activity of carp TNFα. *Journal of Immunology,* 2009 **183**, 5319–5332.

M. Forlenza, M. Nakao, I. Wibowo, M. Joerink, J.A.J. Arts, H. F.J. Savelkoul and G.F. Wiegertjes **2009.** Nitric oxide hinders antibody clearance from the surface of *Trypanoplasma borreli* and increases susceptibility to complement-mediated lysis. *In Press in Molecular Immunology.*

M. Forlenza, T. Kaiser, H.F.J. Savelkoul and G.F. Wiegertjes. **2009**. The use of Real-Time quantitative PCR (RT-qPCR) for the analysis of cytokine mRNA levels. To be published in *Cytokine Protocols* (Methods in Molecular Biology), Marc De Ley (Editor), 2009. Humana Press Inc.

P. Jurecka, I. Irnazarow, A.H. Westphal, **M. Forlenza**, J.A.J. Arts, H.F. Savelkoul and G.F. Wiegertjes. **2009**. Allelic discrimination, three-dimensional analysis and gene expression of multiple transferrin alleles of common carp (*Cyprinus carpio* L.). *Fish Shellfish Immunol* **26**, 573-581.

K.Ł. Rakus, I. Irnazarow, **M. Forlenza**, R.J.M. Stet, H.F.J. Savelkoul and G.F. Wiegertjes. **2009**. Classical crosses of common carp (*Cyprinus carpio* L.) show co-segregation of antibody response with major histocompatibility class II B genes. *Fish Shellfish Immunol* **26**, 352-358.

M. Forlenza, J.D. de Carvalho Dias, T. Veselý, D. Pokorová, H.F.J. Savelkoul and G.F. Wiegertjes. **2008**. Transcription of signal-3 cytokines, IL-12 and IFNαβ, coincides with the timing of CD8αβ up-regulation during viral infection of common carp (*Cyprinus carpio* L). *Mol Immunol* **45**, 1531-1547.

M. Forlenza, J.P. Scharsack, N.M. Kachamakova, A.J. Taverne-Thiele, J.H.W.M. Rombout and G.F. Wiegertjes. **2008**. Differential contribution of neutrophilic granulocytes and macrophages to nitrosative stress in a host-parasite animal model. *Mol Immunol* **45**, 3178-3189.

M. Forlenza, P.D. Walker, B.J. de Vries, S.E. Wendelaar Bonga and G.F. Wiegertjes. **2008**. Transcriptional analysis of the common carp (*Cyprinus carpio* L.) immune response to the fish louse *Argulus japonicus* Thiele (Crustacea: Branchiura). *Fish Shellfish Immunol* **25**, 76-83.

D.F. Onara, **M. Forlenza**, S.F. Gonzalez, K.Ł. Rakus, A. Pilarczyk, I. Irnazarow and G.F. Wiegertjes. **2008**. Differential transcription of multiple forms of alpha-2-macroglobulin in carp (*Cyprinus carpio*) infected with parasites. *Dev Comp Immunol* **32**, 339-347.

A. Ruszczyk, **M. Forlenza**, M. Joerink, C.M.S. Ribeiro, P. Jurecka and G.F. Wiegertjes. **2008**. *Trypanoplasma borreli* cysteine proteinase activities support a conservation of function with respect to digestion of host proteins in common carp. *Dev Comp Immunol* **32**, 1348-1361.

A. Ruszczyk, **M. Forlenza**, H.F.J. Savelkoul and G.F. Wiegertjes. **2008**. Molecular cloning and functional characterisation of a cathepsin L-like proteinase from the fish kinetoplastid parasite *Trypanosoma carassii*. *Fish Shellfish Immunol* **24**, 205-214.

S.F. Gonzalez, M.O. Huising, R. Stakauskas, **M. Forlenza**, B.M.L. Verburg-van Kemenade, K. Buchmann, M.E. Nielsen and G.F. Wiegertjes. **2007**. Real-time gene expression analysis in carp (*Cyprinus carpio* L.) skin: inflammatory responses to injury mimicking infection with ectoparasites. *Dev Comp Immunol* **31**, 244-254.

M. Joerink, **M. Forlenza**, C.M.S. Ribeiro, B.J. de Vries, H.F.J. Savelkoul and G.F. Wiegertjes. **2006**. Differential macrophage polarisation during parasitic infections in common carp (*Cyprinus carpio* L.). *Fish Shellfish Immunol* **21**, 561-571.

F. Buonocore, **M. Forlenza**, E. Randelli, S. Benedetti, P. Bossu, S. Meloni, C.J. Secombes, M. Mazzini and G. Scapigliati. **2005**. Biological activity of sea bass (*Dicentrarchus labrax* L.) recombinant interleukin-1β. *Mar Biotechnol (NY)* **7**, 609-617.

G.F. Wiegertjes, **M. Forlenza**, M. Joerink and J.P. Scharsack. **2005**. Parasite infections revisited. *Dev Comp Immunol* **29**, 749-758.

F. Buonocore, M. Mazzini, **M. Forlenza**, E. Randelli, C.J. Secombes, J. Zou and G. Scapigliati. **2004**. Expression in Escherichia coli and purification of sea bass (*Dicentrarchus labrax*) interleukin 1β, a possible immunoadjuvant in aquaculture. *Mar Biotechnol (NY)* **6**, 53-59.

Curriculum Vitae

I, Maria Forlenza, was born in Rome on 20 November 1978. In 1997, after graduating at the Scientific Gymnasium "La Farnesina" in Rome, I started my study in Biology at the University of Viterbo, La Tuscia (Italy). During the last two years of the study I performed my master thesis at the laboratory of Prof. Giuseppe Scapigliati and Dr. Francesco Buonocore on a project entitled: "Cloning and expression analysis of recombinant sea bass (Dicentrarchus labrax) Interleukin-1β". I graduated cum laude in July 2002. In September 2002, I started as PhD student at the Cell Biology & Immunology Group of Wageningen University, The Netherlands on a project entitled 'The immune response of carp (Cyprinus carpio) to parasitic and viral infections', under supervision of dr. Geert Wiegertjes and Prof. Huub Savelkoul. From 2002 till 2005, I was enrolled in a European, Marie Curie Research Training Network entitled 'Integrated approach to the innate immune response to parasites in fish (PARITY)'. Starting 2005 until present, I am enrolled in another European, Integrated Research Project 'Immunity of aquacultured animals (IMAQUANIM)'.

Contact address: maria.forlenza@wur.nl

Training and Supervision Plan

The Basic Package

WIAS Introduction Course, Wageningen, The Netherlands	2003
Horizon Debating course, Wageningen, The Netherlands	2003

Subtotal Basic Package   **3 credits***

Scientific Exposure

International conferences

EAFP, Malta	2003
ISDCI, St Andrews, Scotland, UK	2003
First international symposium on quantitative PCR, Freising, Germany	2004
EAFP, Copenhagen, Denmark	2005
ISDCI, Charleston, USA,	2006
NOFFI, Stirking, Scotland, UK	2007
ISDCI, Prague, Czech Rep.	2009

Seminars and workshops

NVVI, Veldhoven, The Netherlands	2002
WIAS seminar Trypanosomes: host-parasite interaction in the genomics era, Wageningen, The Netherlands	2002
NVVI, Noordwijkerhout, The Netherlands	2003
qPCR Seminar Experimental design and data analysis, Leusden, The Netherlands	2003
NVVI, Maastricht, The Netherlands	2004
First GeNeYousS Symposium, Utrecht, The Netherlands	2004
NVVI, Soesterberg, The Netherlands	2005
WIAS seminar Macrophage polarisation, Wageningen, The Netherlands	2006
WIAS seminar Immune responses to viruses, Wageningen, The Netherlands	2006
WIAS seminar Corticosteroid receptors in common carp, Wageningen, The Netherlands	2008
WIAS seminar Multidisciplinary study of allergy, Wageningen, The Netherlands	2008
WIAS seminar Fishing for Immunity, Wageningen, The Netherlands	2008

Poster Presentations

Innate immune responses to parasites in carp, Veldhoven, (NVVI)	2002
Role of Nitric Oxide in the immune response to 'tryps' in carp, St. Andrews (ISDCI),	2003

Oral Presentations

Functional characterization of carp leukocytes, Malta (EAFP)	2003
(Anti)-inflammatory response of carp to parasite infections, Copenhagen (EAFP)	2005
Experiences with Quantitative PCR for monitoring carp cytokines, Copenhagen (EAFP)	2005
Cytokine expression profile after Typanosomes infection in carp. Westburg user's meeting, Leusden	2005
Interleukin-10: Let's have a closer look at it, Charleston (ISDCI)	2006
Differential contribution of neutrophilic granulocytes and macrophages, Prague (ISDCI),	2009
TNFalpha: a double-edged sword, Prague (ISDCI)	2009

Subtotal Scientific Exposure   **22 credits***

In-Depth Studies

Advanced statistics course, Wageningen, The Netherlands	2002
Fish Immunology Workshop, Wageningen, The Netherlands	2003
SCOFDA Fish Diseases Workshop, Copenhagen, Denmark	2003
RNAi technique and application in viral diseases (WIAS)Wageningen, The Netherlands	2004
Fish Vaccination Workshop, Wageningen, The Netherlands	2004
QPCR workshop, Corbett Research user meeting, Leusden, The Netherlands	2005
RQ-PCR -users meeting Leusden, The Netherlands	2005
Recent Advancements in Immunological methods for fish immunology, Stirling, Scotland, UK	2007
ELISA: basic understanding and trouble shooting (WIAS), Wageningen, The Netherlands	2007
Subtotal In-Depth Studies	**7 credits***

Professional Skills Support Courses

Use of Laboratory Animals, Utrecht, The Netherlands	2003
Working with EndNote, Wageningen UR Library, Wageningen, The Netherlands	2003
Presentation skills, Wageningen, The Netherlands	2003
Techniques for Writing and Presenting a Scientific Paper, Wageningen, The Netherlands	2005
Subtotal Professional Skills Support Courses	**5 credits***

Didactic Skills Training

Supervising practicals and excursions

practicals Comparative Immunology	2006
practicals Comparative Immunology	2007
practicals Human & Veterinary Immunology	2008
Subtotal supervising practicals and excursions	**6 credits***

Supervising theses

11 major MSc	2002-2008
3 minor MSc theses	2002-2008
Subtotal Supervising theses	**27 credits***

Management Skills Training

Organisation of seminars and courses

Co-organization International Fish Workshops	2003-2008
Subtotal organisation of seminars and courses	**12 credits***
Total number of credit points	**82 credits***

Herewith the WIAS Graduate School declares that the PhD candidate has complied with the educational requirements set by the Educattional Committee of WIAS.

* A credit point represents a normative study load of 28 hours of study.

Stupid questions do exist:

a stupid question is the one you ask
without having thought about the possible answer yourself

Maria